The Lipopeptide Antibiotic Daptomycin: Its Interaction With Calcium And Membranes And The Effects Of Membrane Lipid Composition On Its Activity

by

Robert Mackay Taylor

A thesis
presented to the University of Waterloo
in fulfillment of the
thesis requirement for the degree of
Doctor of Philosophy
in
Chemistry

Waterloo, Ontario, Canada, 2018

Examining Committee Membership

The following served on the Examining Committee for this thesis. The decision of the Examining Committee is by majority vote.

External Examiner	Dr. Richard M. Epand, PhD. Professor Emeritus, McMaster University Biochemistry and Biomedical Sciences
Supervisor	Dr. Scott D. Taylor, PhD. Professor, University of Waterloo Chemistry
Internal Member	Dr. Michael Palmer, PhD. M.D., Dr. habil Associate Professor, University of Waterloo Chemistry
Internal-external Member	Dr. Zoya Leonenko, PhD. Professor, University of Waterloo Physics and Astronomy
Other Member(s)	Dr. Thorsten Dieckmann, PhD. Associate Professor, University of Waterloo Associate Chair (Graduate Studies and Research) Chemistry
	Dr. John Honek, PhD. Professor, University of Waterloo Chemistry

Author's Declaration

I hereby declare that I am the sole author of this thesis. This is a true copy of the thesis, including any required final revisions, as accepted by my examiners.

I understand that my thesis may be made electronically available to the public.

Abstract

Daptomycin (Dap) is a calcium-dependent cyclic lipodepsipeptide antibiotic used clinically to treat infections with pathogenic Gram-positive bacteria, including methicillin-resistant *Staphylococcus aureus* (MRSA). It targets the cell membrane, which must contain phosphatidylglycerol (PG) for activity. Although Dap was discovered over 30 years ago, its mechanism of action is still debated among researchers. Many action mechanisms have been proposed for Dap. The mechanism that has garnered the most attention involves Dap oligomerization in the cell membrane resulting in the formation of cation-selective pores, which lead to membrane depolarization and cell death. To further investigate this proposed mechanism of action, I here studied the interaction of Dap with calcium, the activity and pore-forming abilities of a Dap dimer, and the effects of membrane lipid composition on Dap-membrane interactions and pore formation.

The stoichiometry of calcium to Dap in the presence of liposomes and how calcium concentration affects Dap oligomerization and membrane insertion was investigated using fluorescence spectroscopy and isothermal titration calorimetry. It was shown that Dap interacts with liposomes in two sequential calcium-binding events. The binding of the first calcium ion is suggested to cause oligomer formation of Dap in the membrane. The binding of a second calcium ion is suggested to cause a deeper insertion of this oligomer, followed, potentially, by translocation into the inner leaflet, ultimately forming a functional pore.

The effect of Dap pre-oligomerization on antibacterial activity was studied via the synthesis and characterization of a Dap dimer. The dimer was prepared by connecting the *N*-termini of two Dap monomers via an octadecanedioate linker. It was anticipated that the dimer would decrease the entropic cost associated with oligomer formation. This would promote oligomer formation, thereby enhancing its activity. In contrast to expectation, the activity of the dimer was greatly reduced on vegetative cells yet was able to form cation-selective pores in liposomes. On bacterial L-forms, which lack a cell wall, dimer activity was close to that of the monomer. This suggests that the dimer was unable to cross the cell wall of vegetative cells, thus highlighting the role of the cell wall in Dap resistance.

The effect of lipid acyl chain composition on Dap's ability to interact with, oligomerize, and form pores in membranes was examined. Dap was found to insert into and form oligomers on phosphatidylcholine (PC)/PG liposomes containing either dimyristoyl (DMPC/DMPG), dioleyl

(DOPC/DOPG) or dipalmitoleoyl (POPC/POPG) acyl chains. DMPC/DMPG lipids were found to support pore formation, while DOPC/DOPG and POPC/POPG lipids did not support pore formation. Only 1-5% of an added oleoyl chained lipid, regardless of head group, was necessary to prevent pore formation in liposomes containing dimyristoyl acyl chains. Permeabilization was regained when the molar concentration of Dap surpassed the molar concentration of the dioleoyl chained lipid present. This indicates a near-stoichiometric dose-response interaction of a dioleoyl chained lipid, DOPC, to Dap.

The reason for the reduced permeabilization of Dap on DOPC/DOPG lipids was further investigated. Experiments indicated that the acyl chain unsaturation of dioleoyl chained lipids alone is not sufficient for the inhibitory effect of DOPC/DOPG lipids on Dap; thus, the greater length of oleoyl relative to myristoyl acyl groups appears to be important. Moreover, the inhibitory effect cannot be overcome by extending the *N*-terminal acyl residue of Dap itself. Overall, the findings in this thesis provide substantial new detail on the mode of action of Dap. They also shed light on mechanisms of bacterial resistance to Dap, and they help to reconcile some of the conflicting findings on Dap activity that were obtained with model membranes differing in lipid composition.

Acknowledgements

I wish to express my deepest gratitude and appreciation to my supervisor Dr. Scott D. Taylor and mentor and committee member Dr. Michael Palmer. From day one of this journey, Dr. Scott Taylor has demonstrated the focus and drive needed in research. His constant guidance, support and discussions throughout my degree have been extremely appreciated. Although on paper Dr. Michael Palmer is a committee member of mine, I will always treat him as a supervisor to me. Dr. Palmer is an exceptionally intelligent person, in regards to research, science as a whole and the world outside the lab. I will always be eternally grateful for his support, humbleness, constant reassurance and guidance throughout my time here. Both Dr. Taylor and Dr. Palmer are curious gentlemen that are pushing science and the world of Daptomycin forward. I will always be eternally grateful for being a part of each of their labs.

I wish to express gratitude to my committee members, Dr. Thorsten Dieckmann and Dr. John Honek, for their guidance and discussions throughout this degree.

I would like to thank my external examiner, Dr. Richard Epand, and my internal-external examiner, Dr. Zoya Leonenko for their acceptance to read and edit this thesis and for their valuable comments and suggestions.

Thank you to my family for their endless support and help throughout my career at the University of Waterloo. Thank you to my significant other, Victoria. She has and always will be there for me and love me through it all. Her support and love for me helped me get through when times were tough.

Thank you to Dr. John Honek and Anton van der Ven for being the mentors I needed during my undergraduate studies. Their mentorship lead me to a path in research. Their guidance, understanding and fun-loving attitude made me understand the joys and hard work required of research.

Thank you to my peers throughout my studies within Dr. Michael Palmer's and Dr. Scott Taylor's laboratories, namely (in no particular order): David Beriashvili, Braden Kralt, Brad Scott, Dr. Chuda Lohani, Dr. Tiahua Zhang, Jacob Soley, Michael Noden, Eric Brefo-Mensah, Bowen Zheng.

Dedication

To my loved ones…

Table of Contents

List of Figures

List of Tables

List of Abbreviations

3-D	Three Dimensional
14C-Dap	Daptomycin with a myristoyl acyl tail
A5	A54145-Factor D
AFM	Atomic Force Microscopy
ATP	Adenosine tri-phosphate
B. subtilis	*Bacillus subtilis*
BOC	*Tert*-butyloxycarbonyl protecting group
CAMPs	Cationic Antimicrobial Peptides
$CaCl_2$	Calcium chloride
CAP	Community Acquired Pneumonia
CAT domain	Condensation-Adenylation-Thiolation domain
CCCP	Carbonyl Cyanide *m*-Chlorophenyl Hydrazine
CD	Circular Dichroism
CDA	Calcium dependent antibiotic
CL	Cardiolipin
Dab	Diaminobutyric acid
Dap	Daptomycin
DAPA	Diaminopropionic acid
DHPC	Diheptanoylphosphatidylcholine
$DISC_3$	3,3' – Dipropylthiadicarbocyanine iodide
DMF	Dimethylformamide
DMPC	1,2-dimyristoyl-*sn*-glycero-3-phosphatidylcholine
DMPG	1,2-dimyristoyl-*sn*-glycero-3-phosphatidy-(1'-rac-glycerol)
DNA	Deoxy-ribonucleic acid
DOPC	1,2-dioleoyl-*sn*-glycero-3-phosphatidylcholine
DOPG	1,2-dioleoyl-*sn*-glycero-3-phosphatidy-(1'-rac-glycerol)
DPH	Diphenylhexatriene
DSC	Differential Scanning Calorimetry

DSPC	Distearoylphosphatidylcholine
DXDG	Aspartate-X-Aspartate-Glycine
E. faecalis	*Enterococcus faecalis*
E. faecilium	*Enterococcus faecilium*
EDTA	Ethylenediaminetetraacetic acid
FDA	Food and Drug Administration
Fmoc	Fluorenylmethyloxycarbonyl chloride
^{19}F-NMR	Fluorine – Nuclear Magnetic Resonance
FRET	Fluorescence Resonance Energy Transfer
GUV	Giant Unilamellar Vesicle
HEPES	4-(2-hydroxyethyl)-1-piperazineethanesulfonic acid
HPLC	High Performance Liquid Chromatography
ICP-OES	Inductively Coupled Plasma-Atomic Emission Spectroscopy
ITC	Isothermal Titration Calorimetry
LB broth	Luria-Bertani broth
LPS	Lipopolysacharide
LTA	Lipoteichoic acid
LUV	Large Unilamellar Vesicle
Lysyl-PG	Lysyl-phosphatidylglycerol
MD	Molecular Dynamics
MES	2-(*N*-morpholino)ethanesulfonic acid
MHB	Mueller Hinton Broth
MIC	Minimum Inhibitory Concentration
MLV	Multiple Lamellar Vesicles
MRSA	Methicillin resistant *Staphylococcus aureus*
MSM	Magnesium chloride, sucrose, maleic acid
MSSA	Methicillin susceptible *Staphylococcus aureus*
NaCl	Sodium chloride
NBD	4-nitrobenzoxadiazole
NMR	Nuclear Magnetic Resonance
NOE	Nuclear Overhauser Effect
NRPS	Non-Ribosomal Peptide Synthetase

PBFI	4,4′-[1,4,10,13-tetraoxa-7,16-diazacyclooctadecane-7,16-diylbis(5-methoxy-6,2-benzofurandiyl)]bis-1,3-benzenedicarboxylic acid
PC	Phosphatidylcholine
PE	Phosphatidylethanolamine
PG	Phosphatidylglycerol
POPC	1-palmitoyl-2-oleoyl-sn-glycero-3-phosphocholine
POPG	1-palmitoyl-2-oleoyl-sn-glycero-3-phospho-(1'-rac-glycerol)
Py-A54145	Pyrene labeled A54145-Factor D
RNA	Ribonucleic Acid
S. aureus	*Staphylococcus aureus*
S. pneumoniae	*Streptomyces pneumoniae*
SAR	Structure Activity Relationship
SBFI	4,4'-[1,4,10-trioxa-7,13-diazacyclopentadecane-7,13-diylbis(5-methoxy-6,2-benzofurandiyl)]bis-1,3-Benzenedicarboxylic acid
SEM	Scanning Electron Microscopy
SPPS	Solid Phase Peptide Synthesis
SUV	Small Unilamellar Vesicles
TE domain	Thioesterase domain
TEM	Transmission Electron Microscopy
TFA	Trifluoroacetic Acid
T_m	Transition temperature
TMCL	1',3'-bis[1,2-dimyristoyl-*sn*-glycero-3-phospho]-*sn*-glycerol (sodium salt)
TOCL	1',3'-bis[1,2-dioleoyl-*sn*-glycero-3-phospho]-*sn*-glycerol (sodium salt)
Val	Valinomycin
VISA	Vancomycin-intermediate *Staphylococcus aureus*
VRE	Vancomycin resistant *Enterococci*
WHO	World Health Organization
ΔH	Reaction heat
14:1 PC	1,2-dimyristoleoyl-*sn*-glycero-3-phosphocholine

Chapter 1

Introduction

The use of antibacterial agents to treat life-threatening conditions can be dated back to the time of the Egyptians who used clay and mold to treat anything from pain to disease[1]. Over the next several thousand years the use of antibacterial agents improved but their identity and mode of action was unknown. It was not until the early 1670's that the world was introduced to microbes. Two centuries later, the connection between microbes and disease was made and antibacterial discovery became a pursuit based, at least to some degree, on science. The discovery of penicillin in the 1920's, and its used in the 1940's, revolutionized medicine, and from that point forward, antibiotics have continued to have a dramatic impact on human health and well-being[2].

In the late 1940's the United Nations created the World Health Organization (WHO), a specialized agency that is concerned with international public health[3]. In the late 1970's the first list of essential medicines was produced by WHO, which contains the medications considered to be the most effective and safe to meet the most important needs in a health care system[4]. Many medicines on this list are antibiotics. Unfortunately, due in part to the overuse of antibiotics, some bacteria have developed resistance[5,6]. This has brought about the rise of "super bugs," i.e. bacteria that are resistant to just about every antibiotic available[7]. One such super bug is termed methicillin resistant *Staphylococcus aureus* (MRSA)[7], classified by WHO as a serious infectious pathogen.

To combat these super bugs, the WHO created a list of several so-called last resort antibiotics. The idea was that these antibiotics would only be used when other more commonly used antibiotics were ineffective. An important and widely used last resort antibiotic, particularly in the treatment of MRSA, is Daptomycin[8–10]. Daptomycin (Dap) was first approved by the FDA in the USA, in 2003, for treating complicated skin and skin structure infections, particularly caused by MRSA and vancomycin-resistant *enterococci* (VRE)[11,12]. Although resistance is still rare for this potent antibiotic, it has been observed in several clinical isolates[13]. Although determining Dap's

mechanism of action has been a focus for many researchers for several decades, its mechanism of action is still incompletely understood. Knowing Dap's mode of action could facilitate the development of Dap analogs that are active against Dap-resistant bacteria. The work presented in this thesis is directed to obtaining a better understanding of Dap's action mechanism.

1.1 Antibiotics

Antibiotics have been the forefront of medicine for almost a century. In the early 1900's, Paul Ehrlich believed that antibiotics could become a "magic bullet" that directly targeted an infection, killing the cell[14]. He then led an exhaustive chemical screening program to discover compounds with antibacterial properties. This work culminated in the discovery of the antibacterial, salvarsan (arsphenamine)[15]. In the 1920's, Alexander Fleming discovered the well-known antibiotic penicillin[2,16]. Penicillin was the first antibiotic to be widely adopted around the world in a very short period of time. Since the 1930's, many antibiotics have been created synthetically, like salvarsan, or discovered, like penicillin[17]. A timeline of these discoveries is highlighted in Figure 1.1.

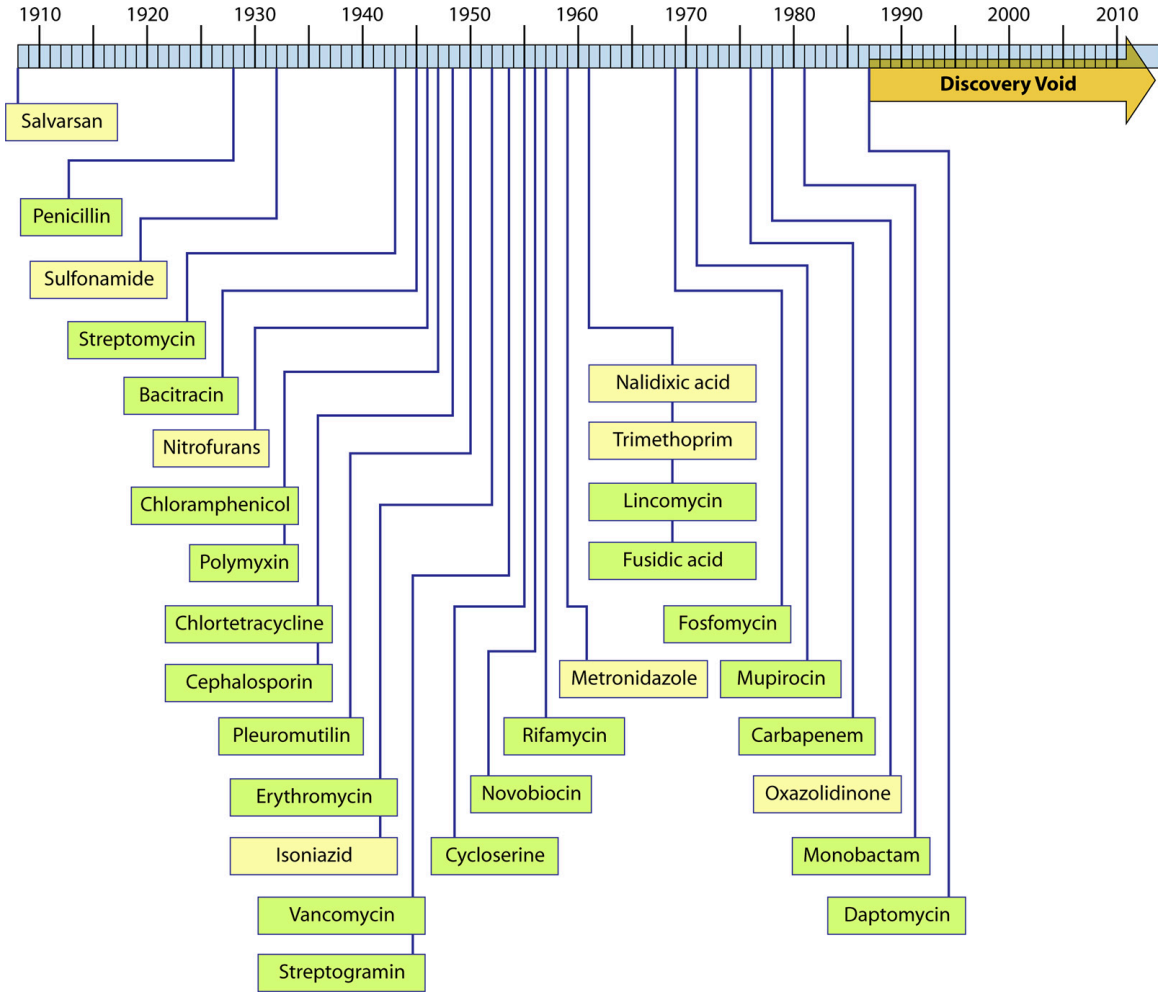

Figure 1.1 The history of discovered antibacterials from the initial discovery of salvarsan to Daptomcyin[17]. Each box represents a new antibiotic class. The green boxes indicate natural compounds isolated from soil microorganisms (fungi or bacteria), whereas the yellow boxes indicate synthetic compounds. The figure was used with permission.

As seen in Figure 1.1, antibacterial discovery was extremely fruitful from the early 1940's to the 1960's. These years have been termed the "Golden Era" of antibiotic development. The discovery and synthesis of antibacterials slowed down considerably after the discovery of Dap, in the late 1980's. This period of time is called the "Discovery Void," as very few new or improved antibiotics have been created or discovered since the 1980s. This is mainly due to the high cost of drug development, which has deterred pharmaceutical companies from developing new antibiotics, since these are not as profitable as other classes of drugs[17]. DiMasi, *et al.* pointed out that average cost of getting a drug approved to market from 1979 to 1991, effectively doubled, to a value of

approximately 230 million dollars[18]. By 2010, the total cost has risen to over one billion dollars, with the time required to pass all clinical trials increasing to almost 15 years[19].

Interestingly, many of the antibiotics discovered over the past hundred years have been obtained from the same host organism, *Streptomyces spp*.[20] The reason for this has been suggested to be due to the sheer number of species and versatility that this organism has, combined with their high metabolite production rate[20]. A shortened list to give an idea of this is shown in Table 1.1. Bacteria are constantly in competition for resources. Due to the large number of *Streptomyces* species, and the fact that most of these species require similar growth conditions, these bacteria have developed an array of defence mechanisms (antibiotics)[21].

Host Microorganism	*Antibiotic*
Bacteria	
Streptomyces spp.	Chloroamphenicol
	Erythromycin
	Neomycin
	Nystatin
	Rifampicin
	Streptomycin
	Tetracyclines
	Vancomycin
	Daptomycin
Bacillus spp.	Bacitracin
	Polymyxins
Micromonospora spp.	Gentamicin
Fungi	
Penicillium spp.	Griseofulvin
	Penicillin
Cephalosporium spp.	Cephalosporins

Table 1.1 Several important antibiotics are outlined in regards to the host microorganism that produces them. As can be seen, *Streptomyces spp*. is a powerhouse of antibiotic discovery.

Although many antibiotic classes exist, the last decade has seen the largest drop in antibiotic discovery. This reduced rate of antibiotic discovery has become a very growing concern. Antibiotics are used widely across the world without caution. This selects for the mutations in bacteria that results in resistance to even the most potent last resort antibiotics. This highlights the need for the synthesis of new and improved antibiotics to counter this ever-growing threat to human health.

1.2 Mechanisms of Action and Resistance of Antibiotics

Understanding the molecular mechanisms of action of antibiotics, as well as of bacterial resistance to them, will facilitate a rational approach to the design of antibiotics with improved activity. The major targets include the cell wall, protein synthesis, DNA/RNA, and the cell membrane. This section will outline these targets and how bacteria become resistant to the antibiotics used.

1.2.1 Cell Wall

The cell wall is the structural barrier in bacteria that protects the cytosol from the external environment. The cell wall structures of Gram-negative and Gram-positive bacteria, as well as mycobacteria are illustrated in Figure 1.2 below.

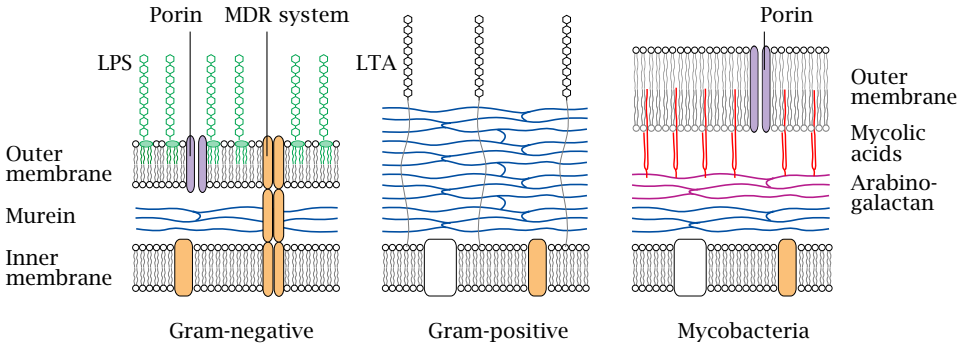

Figure 1.2 The cell wall and membrane of Gram-negative, Gram-positive and Mycobacteria[16]. Each cell type contains an inner membrane, but otherwise is entirely varied. Gram-negative bacteria contain a thin peptidoglycan layer, with a second outer membrane. This outer membrane contains lipopolysaccharides (LPS). Gram-positive bacteria contain only an inner membrane, thick peptidoglycan layer and lipoteichoic acid (LTA) groups stemming from the membrane. This figure was used with permission.

Antibiotics that disrupt the cell wall usually do so by inhibiting peptidoglycan synthesis, at several different steps[22]. Peptidoglycan synthesis is a complex process as outline in Figure 1.3.

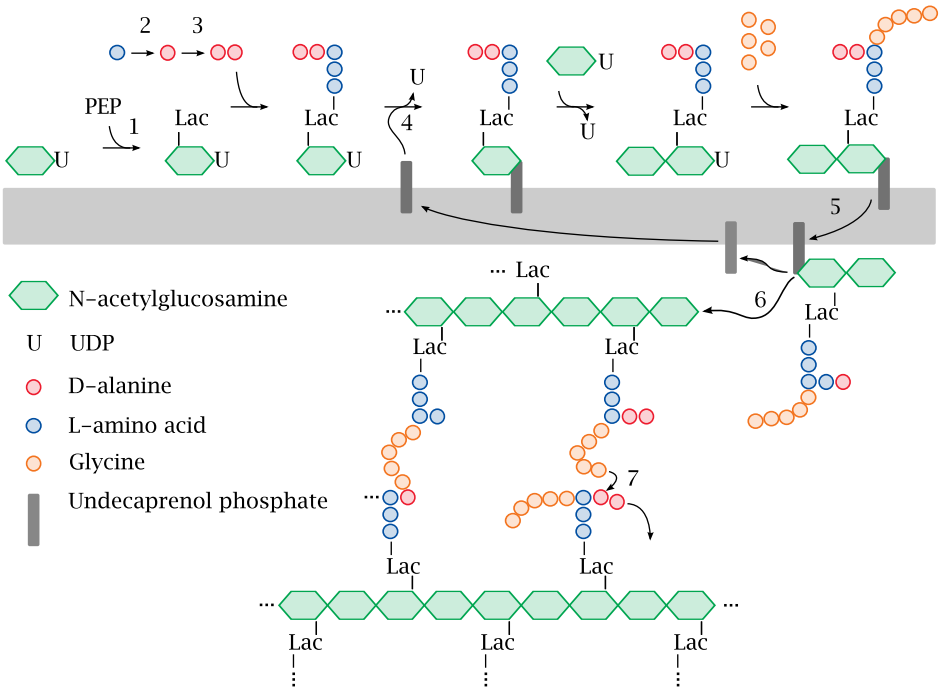

Figure 1.3 Synthesis of peptidoglycan from N-acetylglucosamine to crosslinking of lipid II containing chains[16]. 1: An enolpyruvyltransferase, MurA, catalyzes the reaction between phosphoenolpyruvate (PEP) to a UDP attached N-acetylglucosamine. This reaction supplies the substrate with a lactate (Lac) moiety. 2: Alanine racemase converts a L-alanine to the D configuration. 3: A pentapeptide consisting of L and D – alanine residues is attached to the Lac group on N-acetylglucosamine. 4: This building block is then transferred to undecaprenol phosphate within the membrane with the dislodgment of UDP. This process creates a membrane bound building block that is named, Lipid I. Lipid I is then extended, with a glycosyltranserase (MurG), with a second N-acetylglucosamine moiety producing Lipid II. 5: Lipid II is then flipped from the inner membrane to the outer membrane. 6: Lipid II building blocks are then connected in unison through reaction with a transglycosylase. 7: A transpeptidase enzyme finally crosslinks the Lipid II linked building blocks by displacing a D-alanine. This figure was used with permission.

Several antibiotics that disrupt this process include: β-lactams (penicillin, methicillin, ampicillin, etc.), vancomycin, bacitracin, laspartomycin, fosfomycin and cycloserine[22]. β-lactams and vancomycin interact directly with the transpeptidase reaction. Vancomycin specifically binds to the D-alanine dipeptide of lipid II[16], a key intermediate that is formed during the synthesis of the bacterial cell wall. Disrupting the transpeptidase reaction prevents the cross-linking of lipid II, resulting in the disruption of the structural integrity of the cell wall[23,24]. Fosfomycin has been found to inhibit step 1 of Figure 1.3 and cycloserine inhibits steps 2-3, with bacitracin interacting directly with undecaprenol phosphate, preventing the flipping of lipid II to outer leaflet[25–27]. The inhibition of most other steps in this process leads to the interruption of lipid II production; therefore the cell wall components are

never formed[25,26,28,29]. A common resistance mechanism is the chemical modification of the target or the inhibitor. This includes ring opening for fosfomycin and β-lactams[5], mutations in the enzymes that these antibiotics bind to and in the case of bacitracin, over-expression of undecaprenol phosphate, a lipid involved in the flipping of lipid II from the inner to outer leaflet of bacterial memrbanes[27].

1.2.2 Protein Synthesis

The protein synthesis machinery is a common target shared by many antibiotics. Bacterial ribosomes (Figure 1.4) have a 50S subunit and a smaller 30S subunit[30].

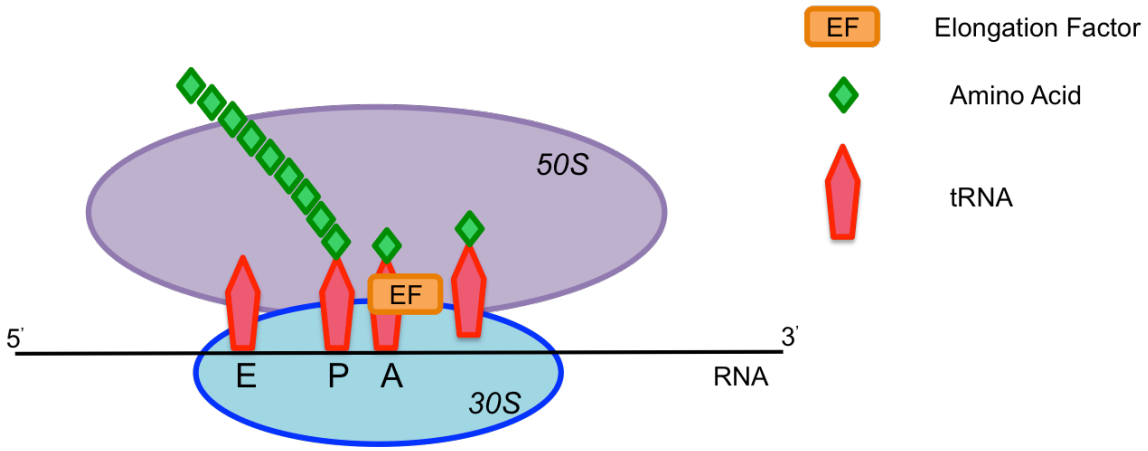

Figure 1.4 Transcription of a messenger RNA strand into a polypeptide chain. An amino acid bound to its specific tRNA binds to the RNA strand, at the aminoacyl (A) site. At this site an elongation factor protein binds, and the tRNA is transitioned into the peptidyl (P) site. A peptidyl transferase then links the incoming amino acid to the growing chain. This reaction then forces the tRNA to enter the exit (E) site, leaving the RNA strand.

There are many structural differences between bacterial and eukaryotic ribosomes, with many antibiotics specifically targeting the smaller, simpler bacterial form[16]. Examples of antibiotics that target this process include: streptomycin, gentamycin, chloramphenicol, erythromycin, chlortetracycline and linezolid. Most of these antibiotics target the 23S ribosomal RNA elongation factor, which is part of the larger 50S subunit, preventing amino acid elongation[31–33]. This factor contains a peptidyl transferase site needed for elongating the incoming peptide with amino acids. Streptomycin and gentamycin more specifically prevent the reading of the incoming RNA strand, binding the 30S subunit[31]. The most common resistance mechanism involves the bacterial mutation of the 23S elongation factor, thereby preventing the antibiotic from binding[33].

1.2.3 DNA/RNA

Another target of antibiotics is the inhibition of the synthesis of DNA or RNA. DNA and RNA are normally replicated with a DNA-polymerase or a DNA-dependent RNA-polymerase[34]. A DNA gyrase is important in DNA repair and assisting polymerases to open up the double stranded helix, facilitating polymerase binding[35,36]. Common antibiotics that interfere with this process include: rifampicin, metronidazole, nalidixic acid, novobiocin and ciprofloxacin. Rifampicin specifically interacts with the DNA-dependent RNA-polymerase, preventing this polymerase from binding[37]. Nalidixic acid, novobiocin and ciprofloxacin interact directly with DNA gyrase, preventing DNA repair and transcription[35,36]. A common resistance mechanism to these antibiotics is the mutation of the enzymes they target, mainly either the polymerase or DNA gyrase.

1.2.4 Cell Membranes

The cell membrane is made of mainly proteins and lipids, but the specifics and percentages of these components are dependent on the bacterial species[16,38]. The majority of lipids found in bacterial membranes are phospholipids. Antibiotics that target the cell membrane function by either affecting the membrane potential or by dislodging and/ore inactivating proteins (or macromolecules) attached to the membrane[39]. Dislodging or binding to proteins/macromolecules bound to the cytoplasmic membrane can disrupt cell wall synthesis and proper efflux of compounds. Antibiotics that disrupt membrane potential do so by forming a pore or lesion in the membrane, which results in loss of ions across the membrane. The enzyme ATPase drives ATP production, which is dependent on the cell membrane potential. A loss of ions will destroy the cell membrane potential, therefore stopping the production of ATP, and therefore most other functions of the cell[40]. Several antibiotics that target the cytosolic membrane include polymyxin, nisin and Dap[41,42]. Polymyxin's mechanism of action involves the binding and dislodging of lipopolysaccharides (LPS), found on the outer membrane of Gram-negative bacteria[43]. Nisin has been observed to cause a loss of membrane potential but also an inhibition of cell wall synthesis[44]. In the case of Dap, many mechanisms have been proposed. One such proposal is the loss of membrane potential[40,45,46]. Resistance to these types of antibiotics includes modification of the cell membrane, mainly the lipoteichoic (LTA) groups of Gram-positive or LPS groups of Gram-negative bacteria[39]. LTA groups, as shown in Figure 1.2, are anchored to the cell membrane but likely span the entirety of the cell wall. Modifications to LTA could be affecting the ability of antibiotics, for example Dap, to traverse the cell wall, preventing its interaction with the

cytoplasmic membrane[47]. Another common mechanism of resistance involves the alteration of the membrane lipid composition, preventing certain antibiotics from properly inserting into the membrane[48].

1.3 Daptomycin

Daptomycin (Dap) is a cyclic lipodepsipeptide used to treat serious skin infections caused by Gram-positive bacteria, including methicillin-resistant *Staphylococcus aureus* (MRSA) and vancomycin-resistant *enterococci* (VRE)[9,11,12,40,48–58]. Dap is a last resort antibiotic, meaning it should be used only when necessary. Widespread resistance has not yet been observed[59]. Dap is part of the A21978C class of antibiotics. This class, consisting of Dap, A54145 and the so-called calcium-dependent antibiotic (CDA) are shown in Figure 1.5. They have other certain conserved features, which will be discussed in Section 1.3.1. This class of antibiotics contains a cyclic macrolactone ring enclosed by an ester bond. These lipopeptides also contain exocyclic portions connected to different fatty acyl chains. Dap is currently the only clinically used antibiotic of this class[12].

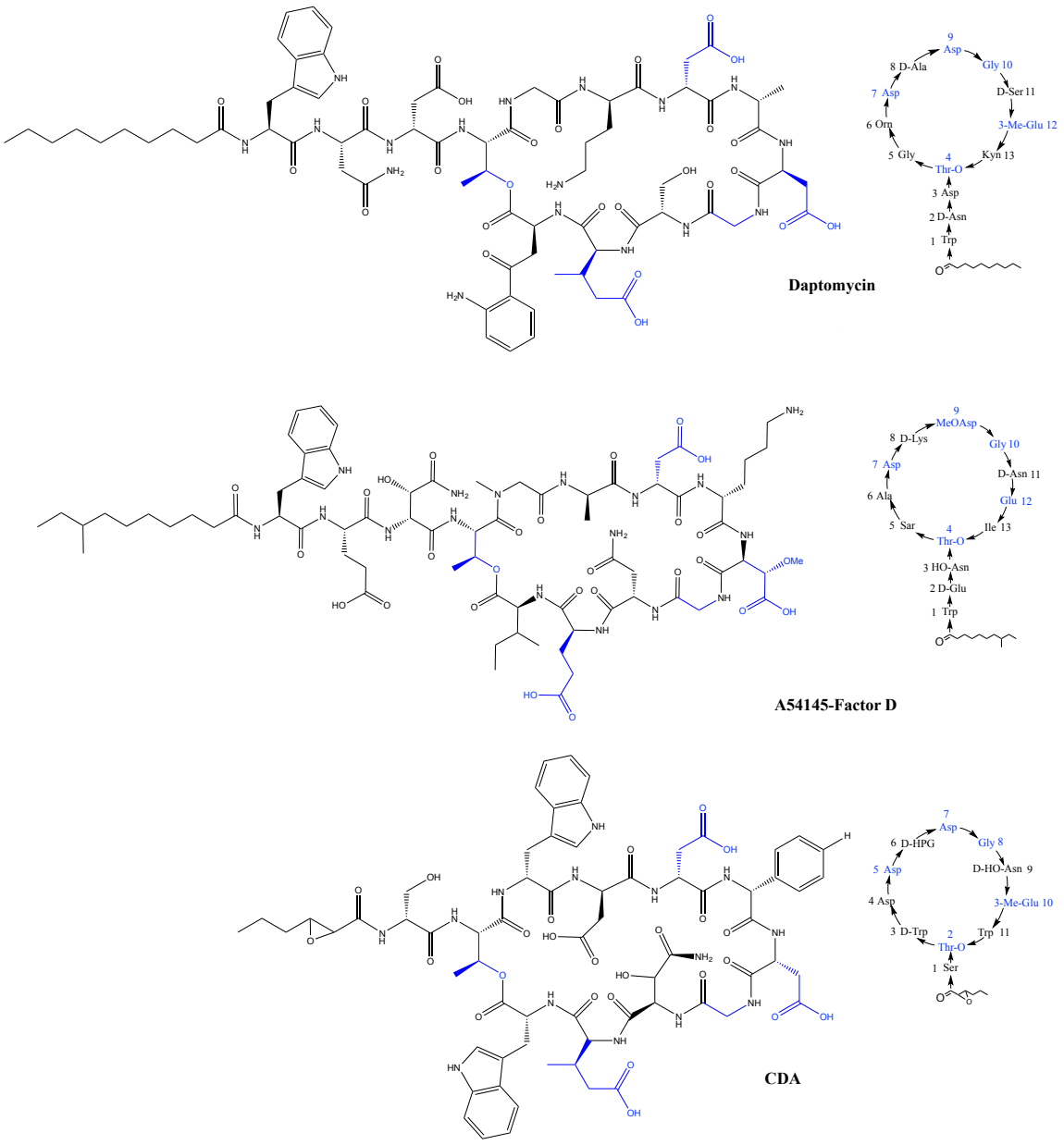

Figure 1.5 The structures of Daptomycin, A54145-Factor D and CDA. Each lipopeptide has a ten amino acid membered cyclic portion. The cyclic region is closed by a depsi bond between the conserved threonine residue and the thirteenth amino acid. The other conserved amino acids are shown in blue. Each amino acid has a glutamate residue in position 12 and a conserved DXDG, calcium-binding sequence.

Dap was first discovered by researchers at Eli Lily© in the early 1980's in cultures of the bacterium *Streptomyces roseosporus*[9,60]. In 1985, Eli Lily© began studies on Dap, attempting to determine the proper dose regimen for clinical use. They later abandoned this work due to mycopathy

in phase II clinical trials. In 1997, Cubist Inc.© (recently purchased by Merck & Co.©) acquired the rights and continued clinical trials, adjusting the dose[61]. They determined that the mycopathic effects observed by Eli Lily© could be diminished if the dose was lowered[61]. Dap was approved by the FDA in 2003, in USA and Europe, for the treatment of complicated skin and skin-structure conditions, particularly methicillin-susceptible *S. aureus* (MSSA) and MRSA[11,40]. In 2006, Dap was approved for use in the treatment of bacteremia causing right-sided endocartitis, due to MSSA or MRSA[12]. The dose regimen for Dap involves a 4 mg/kg injection daily for MRSA and 6 mg/kg daily for bacteremia[61]. The increased dosage used for bacteremia has been shown to decrease the emergence of resistance, in *S. aureus* strains[62]. Dap, having a lipophilic tail, binds to proteins[63] (mainly albumin in the blood) decreasing its overall free concentration, when exposed to the pathogenic bacteria. This proten binding is dependent on the concentration of Dap used, ranging from 4-8 mg/kg[63]. Carpenter, *et al*. showed that the half-life of Dap is ~8-9 hours with a maximal plasma concentration of 57.8 μg/mL (4 mg/kg dose) and 98.6 μg/mL (6 mg/kg dose)[63]. Dvorchik, *et al.* further stated that the plasma concentration decreases quickly over time, with only ~20 μg/mL Dap, 12 hours after administration[64].

Interestingly, Dap has been found to be inactive against community-acquired *pneumoniae* caused by *Streptococcus pneumoniae*. This is thought to be due to a sequestering of Dap by pulmonary surfactant[65]. Dap has also been shown recently in increase the compressibility of lung surfactant, which may facilitate further sequestration of the antibiotic[66]. Pulmonary surfactant contains a higher percentage, compared to all other mammalian lipid membranes, of phosphatidylglycerol (PG), a required lipid for Dap action. Dap interacts with the high PG content of the lung surfactant, thus preventing its interaction with *S. pneumoniae*[65]. Efforts have been made to improve Dap's activity within lung surfactant[67–69]. One approach is through the study of A54145, which is active in pulmonary surfactant, but is too toxic to be used clinically[10,70,71]. Investigating the similarities and differences between Dap and A54145 might lead to compounds that combine the favourable traits of both. An example of this was shown by Nguyen, *et al.* with the creation of hybrid analogs, discussed in Section 1.5.1[72].

1.3.1 Structure of A21978C Antibiotics

As stated previously, Dap, A54145 and CDA are cyclic lipodepsipeptides. The "depsi" in this name refers to the ester bond linkage found within the macrocyclic core. They all have a conserved

aspartate-X-aspartate-glycine (DXDG) sequence[9,11,50,52,57]. This sequence is also found in the EF hand motif of many proteins that bind calcium[11,68,72,73]. This conserved feature could explain the dependence of these antibiotics to calcium, suggesting each lipopeptide has a conserved mechanism of action.

Dap contains a 10 amino acid-membered macrolactone ring that is closed by an ester bond between threonine4 and kynurenine13[57,74]. It also has a 3 amino acid exocyclic portion, where the terminal amino acid, tryptophan1, is attached to a decanoyl tail. Dap contains six non-proteinogenic amino acids, including three D-amino acids: ornithine, kynurenine, (2S,3R)-3-methylglutamate, D-serine, D-alanine and D-asparagine are highlighted in red in Figure 1.6.

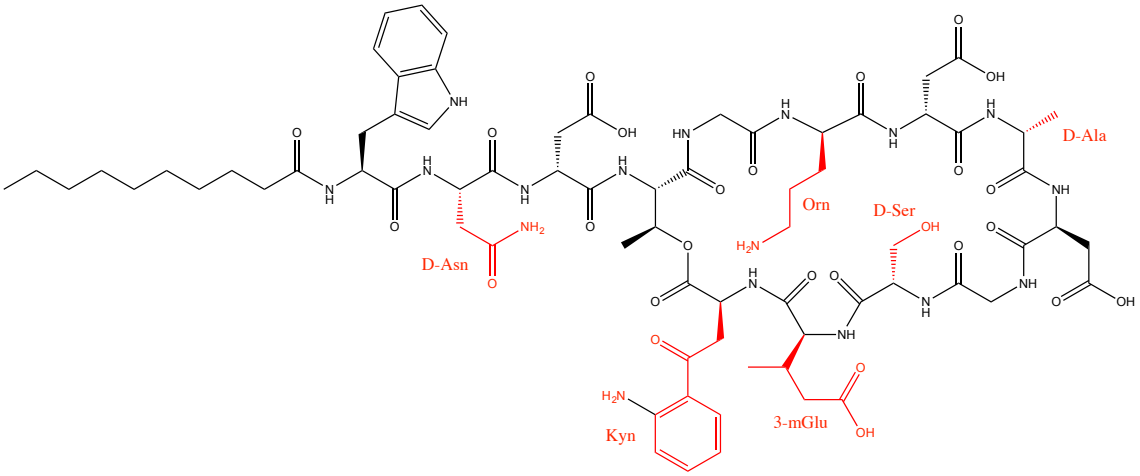

Figure 1.6 The non-proteinogenic amino acids found in Daptomycin. These non-proteinogenic amino acids are highlighted in red.

The A54145 family of antibiotics all have the same general core structure[9,10,71]. Boeck, *et al.* isolated eight different factors of A54145 that differ, mainly in the fatty acyl tail moiety[70]. From this work, it was determined that A54145-Factor D (A5, Figure 1.5) had comparable activity to Dap against *S. aureus* strains. A5 contains an 8-methyldecanoyl tail, varying slightly from Dap's decanoyl moiety. A5 was used in this thesis, since it has been determined that this factor of A54145 has the lowest toxicity to activity ratio, of this class. That being said, A5 is still too toxic to be used clinically and has lower activity *in vivo* compared to the clinically used vancomycin[57,67,72].

When comparing the physiochemical properties of Dap and A5, both are found to have several amino acids with ionizable side chains, shown in red (cationic) and blue (anionic) in Figure 1.7.

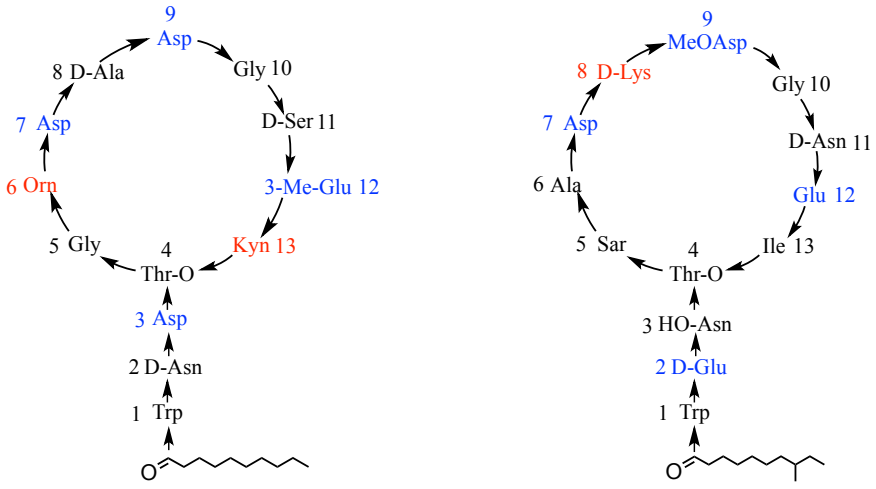

Daptomycin **A54145-Factor D**

Figure 1.7 Conserved amino acids found with Daptomycin and A54145-Factor D. The anionic amino acids are highlighted in blue within each lipopeptide. The cationic amino acids are highlighted in red. As can be seen, the ionic amino acids are highly conserved between the two calcium dependent antibiotics.

In the case of Dap, the pKa's of each of the ionizable amino acids have been determined through several methods, including NMR spectroscopy, ultraviolet spectrophotometry and potentiometric titration[75]. The pKa's of these groups are shown in Table 1.2.

	Amino acid	pKa
Cationic residues	kynurenine13	0.8-1.3
	ornithine6	10.7
Anionic residues	aspartate3	4.3
	aspartate7	1.0
	aspartate9	3.8
	3-methylglutamate12	4.6

Table 1.2 The pKa's for the ionic residues found within Daptomycin, determined through varying methods mentioned previously.

All of the ionizable amino acids, except kynurenine13, will be bear a single positive or negative charge at physiological pH. Therefore, Dap will have an overall charge of -3 at pH 7.4, with no calcium bound. As seen in Table 1.2, the pKa of aspartate7 is unexpectedly lower than the other aspartates within Dap, though the reason for this is not clear[75]. The same set of experiments has not been done on A5; however; it is likely that A5 also has an overall charge of -3 at pH 7.4, since the DXDG motif is conserved between Dap and A5, which suggests that both lipopeptides would interact with calcium similarly.

Dap and A5 also contain one or more fluorophore(s). Dap contains both kynurenine and tryptophan, whereas A5 only contains the latter. The fluorescence emission spectrum of tryptophan overlaps the absorption spectrum of kynurenine[76]. Therefore, when studying Dap using fluorescence spectroscopy, exciting the tryptophan residue will result in fluorescence resonance energy transfer (FRET) to kynurenine[76], and only the fluorescence of the kynurenine residue will be observed. The fluorescence properties of Dap and A5 are explained in more detail in Section 1.6.

1.3.2 Biosynthesis

The A21978C class of calcium-dependent antibiotics are produced by their host organisms through several non-ribosomal peptide synthetases (NRPSs)[11,57,77,78]. In the case of Dap the host organism is *Staphylococcus roseosporus*[11], for A5 it is *Staphylococcus fradiae*[72]. Each organism uses separate NRPS modules, as outlined in Figure 1.8.

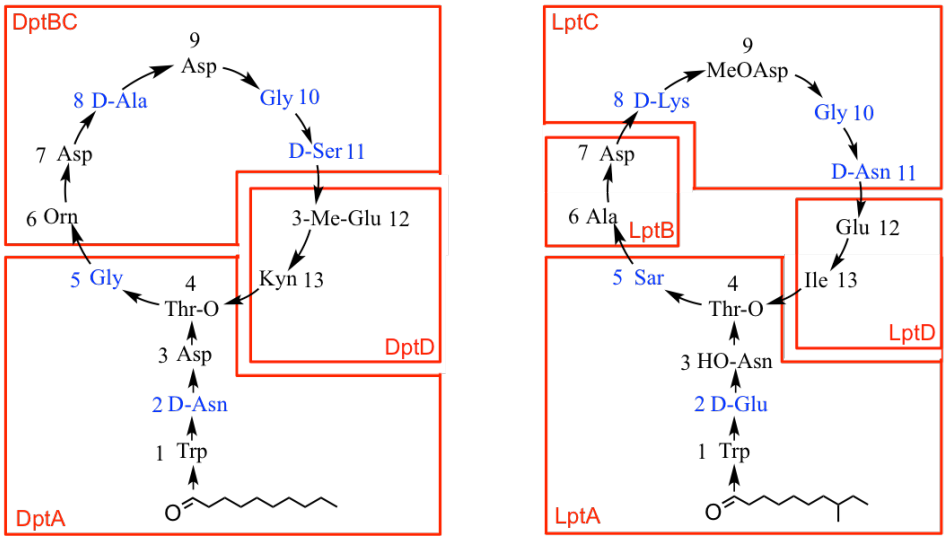

Daptomycin **A54145-Factor D**

Figure 1.8 The NRPS enzymes found in the biosynthetic pathways of Dap and A5. Three multifunctional enzymes, DptA, DptBC and DptD control the biosynthesis of Dap. Dpt D contains the thioesterase domain necessary for cyclization and release of the peptide. Four enzymes, LptA, LptB, LptC and LptD that work in the same manner as Dap's enzymes, carry out the biosynthesis of A5. Figure was adapted from Miao, *et al*.[71]

The syntheses of Dap and A5 are similar, whereby modules, each of which has a condensation-adenylation-thiolation (CAT) domain, incorporate an amino acid. There is also an optional epimerization (E) domain. In the case of Dap (Figure 1.9), three large, multifunctional enzymes, DptA, DptBC and DptD, govern the assembly[11,40,72,77,79]. A module called DptE initiates the synthesis by activating decanoic acid in an ATP-dependent manner. The activated decanoic acid is then transferred to a module called DptF. The *N*-terminus of the C-domain of the DptA initiation module then catalyzes the condensation between the enzyme-bound decanoyl tail and tryptophan. After this initial condensation, the peptide chain is elongated by linearly operating NRPSs: DptA, DptBC, and DptD. Once the peptide chain has been completed, it encounters the thioesterase (TE) domain, which is located in DptD. This TE domain directs the intramolecular attack of the hydroxyl group of threonine on the enzyme-O-TE oxoester intermediate, which leads to the release of the cyclic lipopeptide.

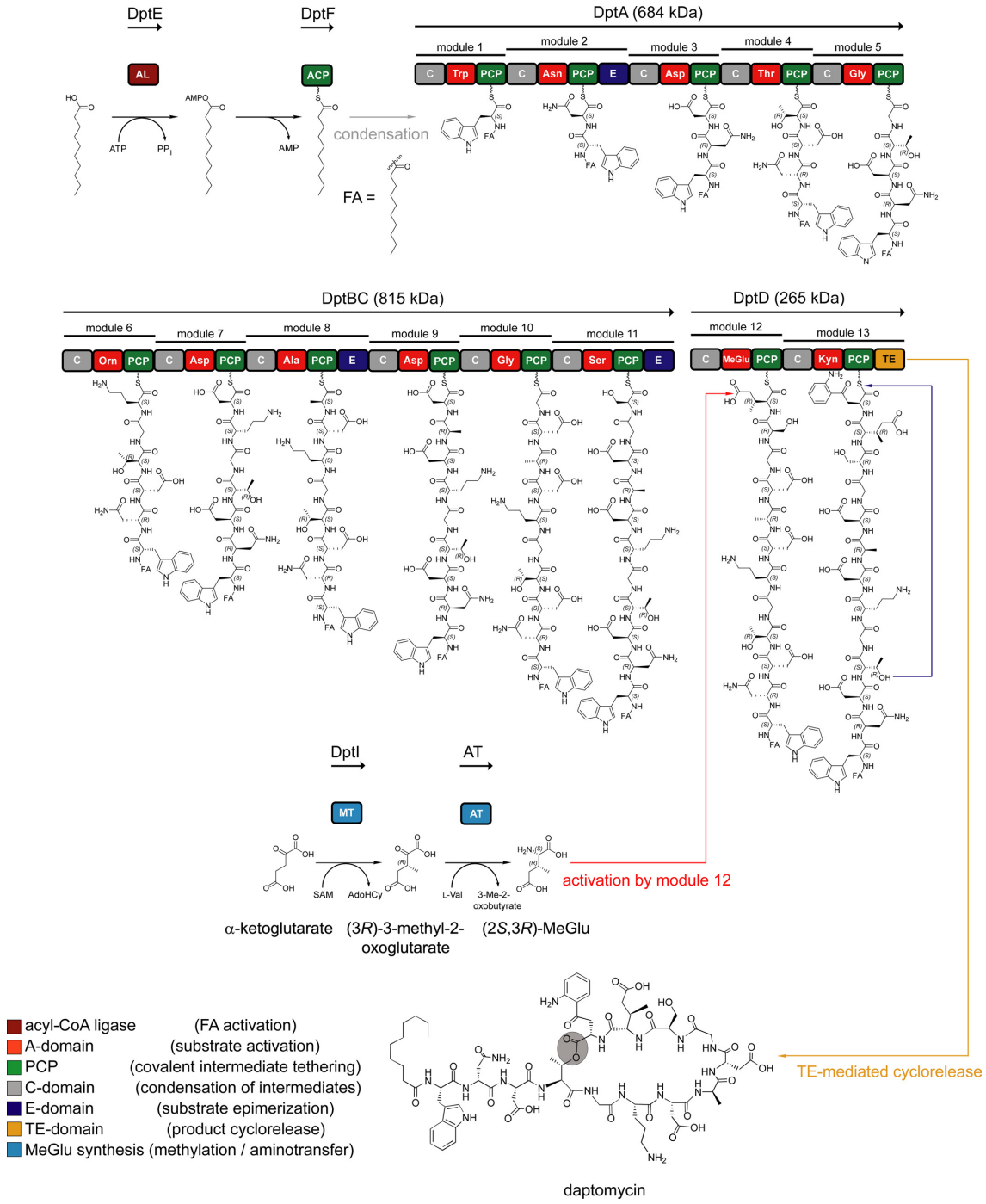

Figure 1.9 The biosynthesis of Dap, that occurs through three separate NRPSs[77]. Each amino acid is added to the growing peptide chain through a conserved C-A-T/PCP domain. This domain mediates condensation, adenylation and thiolation. There can also be an epimerization (E) domain present. The amino acids are first adenylated by the A domain and then attached to the T domain on the same module. The C domain bridges the first amino acid with the second through formation of a peptide bond. Three large enzymes carry out the synthesis of Dap (DptA, DptBC and DptD). Each enzyme

contains multiple C-A-T modules, with additional domains as necessary. The DptF module is attached to the proper acyl tails, which is added initially to DptA. The thioesterase domain (TE), cyclizes and released the lipopeptide. The figure was used with permission.

1.4 Three-Dimensional Structure of Daptomycin

One property that has not been addressed so far is the three-dimensional (3-D) structure of Dap. Knowing the 3-D structure both in solution and within the membrane would assist in determining Dap's mechanism of action. Dap occurs mainly in three forms: free in solution with and without calcium bound and in a membrane with calcium bound.

Several researchers have studied the structure of apo-Dap (no calcium bound). Unfortunately, all of these researchers differ on their conclusions. Dap, at physiological pH 7.4 has a -3 charge[40]. The anionic residues repel one another, preventing Dap aggregation even at millimolar concentrations[75]. When the pH is lowered, Dap losses some of these negative charges, which results in aggregation, even at sub-millimolar concentrations[80,81]. Hancock and coworkers determined the structure of apo-Dap by NMR, in solution at a concentration of 2 mM at pH 6.6[82]. At this pH, the charge of Dap is still -3, and so aggregation was not occurring. What they concluded was a lack of a preferential structure for Dap, although an averaged model of the structure exhibited two bends at aspartate7 and aspartate9, and a highly variable region around glycine5[82]. Rotondi, *et al.* also utilized NMR to determine the structure of Dap at 1.9 mM, pH 5.3[81]. Under these conditions, aggregation is unlikely to occur. These researchers concluded that Dap did have a preferential structure. The macrocycle adopted a hairpin-loop like structure[81]. A type II beta-turn[83] was found near D-alanine8 and aspartate9. There was a second hairpin loop with a beta turn at threonine4 and kynurenine13. The hydrophobic portions of Dap (tryptophan, kynurenine, and the decanoyl tail) were clustered at one end of the hairpin loop, with the polar amino acids at the other. In another study, Ball, *et al.* determined the NMR structure using a 0.8 mM solution of Dap at pH 5.0[80]. At this acidic pH, aggregation will be more likely to occur[75]. Ball, *et al.* also observed a low energy structure. They stated that Dap was mostly fully extended, but with sharper turns in the structure near D-alanine8 and glycine10/D-serine11[80]. The R-groups of the amino acids were solvent exposed, showing a preferential side chain orientation. They stated that, overall, the amino acids were orientated randomly and that the anionic amino acids would not be close enough to bind a calcium ion.

Hancock and coworkers also attempted to determine the structure of calcium-bound Dap (holo-Dap), by NMR[82]. They used 2 mM Dap, in the presence of 5 mM Ca^{2+} at pH 6.6. They noted only a small degree of line broadening, suggesting minimal aggregation. Their structure of holo-Dap was more defined than their structure of apo-Dap. Several medium and long range Nuclear Overhauser Effects (NOEs), such as between aspartate3 and alanine8, were observed. Only sequential NOEs were found for apo-Dap[82]. On the basis of these medium and long range NOEs, they concluded that the cyclic ring of Dap was less circular and that the side chain of aspartate3 was underneath the ring. They also concluded that a calcium-binding site might be found between aspartate3 and aspartate7. The data also suggested that a significant change in the re-alignment of the hydrophobic portions of Dap, to external solvent, had occurred upon calcium binding. They, therefore, further concluded that Dap must undergo a large conformational change upon the binding of calcium[82]. However, later work by Rotondi, *et al.* showed that the concentration of Dap used by Hancock was high enough, with the added calcium ions, to induce aggregation[81]. They suggested that some or all of Hancock's measured medium and long range NOEs, which were key pieces of information leading to Hancock's determined structure, might have arisen from intermolecular interactions rather than intermolecular ones.

The Hancock laboratory therefore reexamined their finding[84]. From molecular dynamic (MD) simulations, it was concluded that the previously reported NOE restraints were intermolecular and should not have been included during structure refinement. Overall, they concluded that the structure of holo-Dap did not differ from their calcium-free strcuture[84]. No calcium-binding site was evident in the refined structure. They then utilized circular dichroism (CD) to show that Dap only exhibited minor changes in solution, upon the addition of calcium. Ball, *et al.* further showed, using NMR, that the structure of holo-Dap (0.8 mM at pH 5.0 with one molar equivalent of calcium) was very similar to apo-Dap[80].

Straus, *et al.* reported the NMR structure of Dap bound to diheptanoylphosphatidylcholine (DHPC) micelles in the presence of calcium[85]. They used a 2 mM Dap solution at pH 6.7, to which they added 5 mM Ca^{2+} and titrated in ~ 100 mM DHPC (1:50 ratio). The found that it resembled the structure that they reported for apo-Dap. They then speculated that Dap experiences only minor conformational rearrangements when binding to these model membranes. Although this finding is interesting, it must be taken lightly as these lipid membranes, are not an accurate model to mimic

susceptible lipid membranes, due mainly to the lack of phosphatidylglycerol (PG), which is necessary for Dap activity (See Section 1.7.1)[86,87].

Although the structure of Dap is still elusive, it would be helpful to examine the structure of another calcium-dependent antibiotic. So far only one class of calcium-dependent antibiotics, the A21978C class, has been discussed. A second class of these antibiotics includes, but is not limited to, tsushimycin, amphomycin and laspartomycin. This group differs from the A2198C class in several ways, one of which is the replacement of the depsi bond with an amide linkage. Nevertheless, as shown in Figure 1.10, there are conserved portions within each class of the calcium-dependent antibiotics, including the DXDG motif. Studying this other class could shed light onto the structure of Dap in solution.

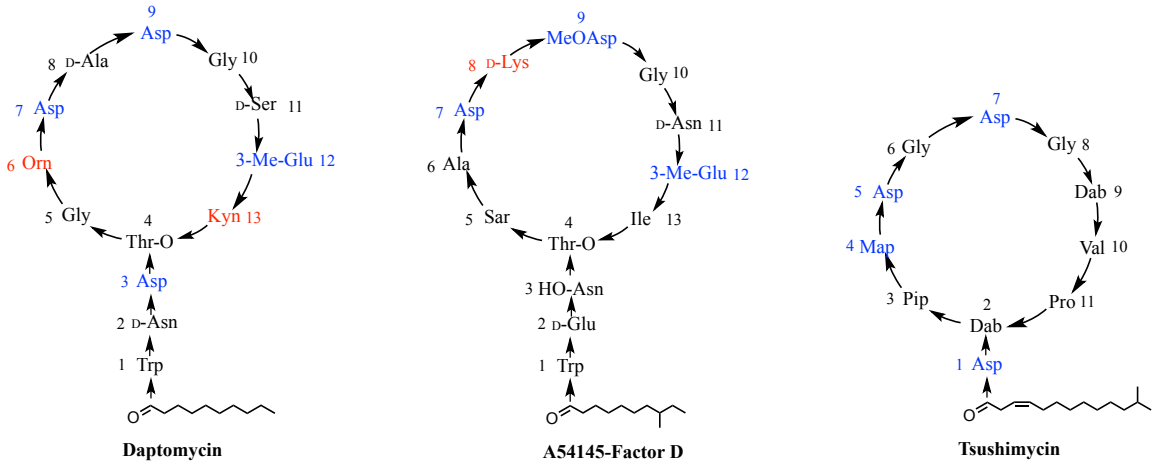

Figure 1.10 The conserved residues between calcium-dependent antibiotics. Daptomycin, A54145-Factor D and tsushimycin are shown from left to right. As seen, there is considerable similarity between the lipopeptides. The conserved amino acids are shown in blue, which correspond to the anionic residues. The amino acids highlight in red show the cationic residues found in Dap and A5. For tsushimycin there are three unnatural amino acids, pipecolinic acid (Pip), β-methylaspartate (Map) and 2,3-diaminobutyric acid (Dab).

The X-ray crystal structure of tsushimycin has been reported at 1.0 Å resolution (Figure 1.11)[88]. The antibiotic has a saddle like structure where a calcium ion is bound in the middle, interacting with two acidic residues (aspartate1 and aspartate5), four carbonyl atoms (diaminobutyric acid (Dab)2, glycine6, glycine8 and valine10) and a water molecule. The antibiotic forms a dimer whose subunits are linked by hydrogen bonds between aspartate7 of one monomer and Dab9 of another. The carboxyl groups of aspartate7 and aspartate1 interact with additional calcium. There is a

tunnel found in the center of the dimer, large enough to fit a phospholipid molecule. The antibiotic's charged groups point outwards while the hydrophobic regions point internally.

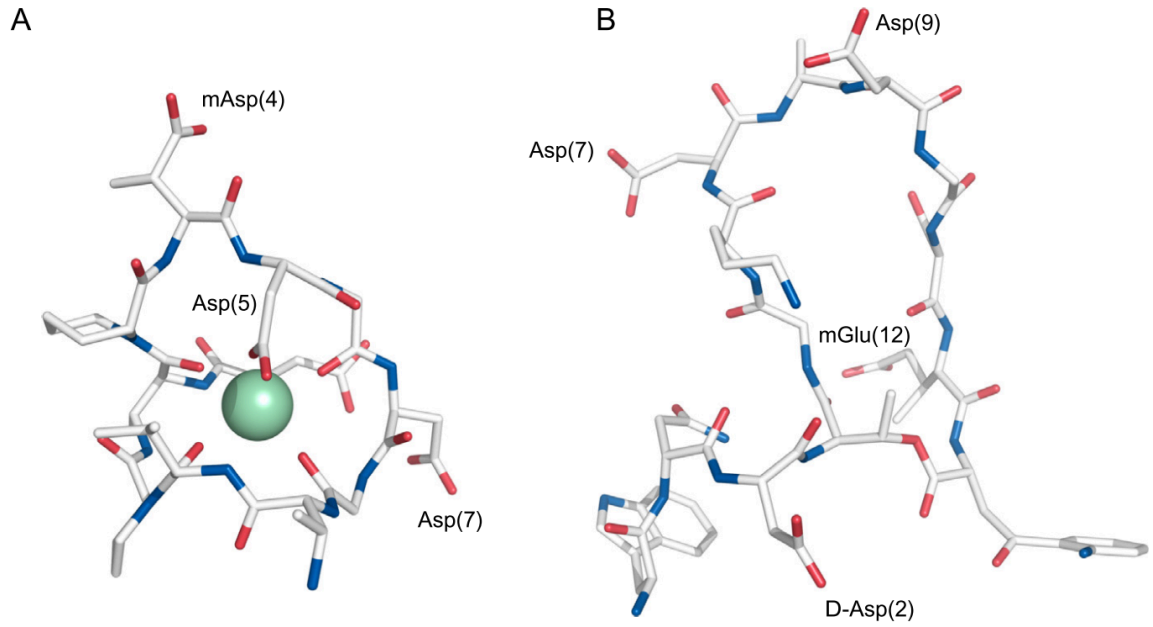

Figure 1.11 The crystal structure of tsushimycin and the H-NMR generated structure of Dap[40]. A: The structure of tsushimycin shows a Ca^{2+} ion coordinated by an asparate5 residue[88]. Additional calcium ions that bridge dimers of tsushimycin are not shown in image. B: Ball, *et al.* reported the structure of Dap in a calcium free environment[80]. This structure is more loosely fitted than tsushimycin, with the anionic residues on opposing sides of the ring. No calcium-binding site was observed. For both structures, the acyl tail has been removed from the presented image. Figure was taken from Taylor, *et al.*[40] with permission.

As discussed above, the amino acid sequence of Dap is different from tsushimycin, however; there are several conserved features[40]. The aspartate1 and aspartate5 of tsushimycin, which bind calcium, are conserved in Dap as aspartate3 and aspartate7. This suggests that these residues are also crucial for Dap-Ca^{2+} interaction. That being said, aspartate3 of Dap has been replaced with D-asparagine, the amino acid found natively in tsushimycin, at this position. This replacement causes only a fourfold reduction on Dap's activity (Section 1.5)[67], suggesting aspartate3 is not essential to activity. The Dab9 residue of tsushimycin has been shown to be the determining factor of dimer formation[88].

In summary, this section showed that the 3-D structure of Dap has yet to be determined with certainty. Apo-Dap appears to be highly flexible in solution. Dap does not appear to undergo major

conformational changes when bound to calcium in solution or within DHPC membranes. Although the crystal structure of tsushimycin implicates certain residues important in the calcium binding of Dap, there is still no certainty regarding the structure when bound to susceptible membranes.

1.5 Structure-Activity Relationships

Daptomycin is currently used clinically as a last resort antibiotic against serious skin infections. Unfortunately, resistance to Dap has been already been observed in some clinical studies[9,11,12,59,89]. To combat this growing resistance new and improved analogs of Dap must be created. The synthesis of new analogs of Dap has been reported in the literature. The methods that have been used to create these analogs and the activity of these analogs are outlined in this section.

1.5.1 The Biosynthetic Approach to Preparing Dap and A5 Analogs

As mentioned in Section 1.3, Dap is naturally produced by *Streptomyces roseosporus* via non-ribosomally, site-directed mutagenesis[52]. Since Dap is made non-ribosomaly, mutagenesis/over-expression is not a suitable approach to produce new Dap analogs. This feature forced scientists to investigate other options. One option is to utilize combinatorial biosynthesis[10,52,67,90,91]. In this approach, entire modules responsible for the incorporation of individual amino acids are swapped with NRPS systems encoding other lipopeptides, in particular A5 or CDA.

Cubist Inc.© has investigated this combinatorial approach to prepare analogs of Dap and A5. Using this approach they reported the preparation of 40 Dap and A5 analogs shown in Table 1.3. Cubist Inc.©'s objective was to prepare non-toxic hybrids of Dap and A5 that were active in the presence of lung surfactant.

compound[a]	amino acid at position listed[b]									*S. aureus* MIC (μg/mL)[c]		
	2	3	5	6	8	9	11	12	13	− surf	+ surf	ratio (+/−)
daptomycin	D-Asn	Asp	Gly	Orn	D-Ala	Asp	D-Ser	3mGlu	Kyn	0.5	64	128
CB-181,220	D-Asn	Asp	Gly	Orn	D-Ala	Asp	D-Ser	3mGlu	Kyn	0.5	64	128
CB-182,098	D-Asn	Asp	Gly	Orn	D-Ala	Asp	D-Ser	3mGlu	***Trp***	1	32	32
CB-182,107	D-Asn	Asp	Gly	Orn	D-Ala	Asp	D-Ser	3mGlu	***Ile***	2	8	4
CB-182,106	D-Asn	Asp	Gly	Orn	D-Ala	Asp	D-Ser	3mGlu	***Val***	4	8	2
A21978C1(Asn13)	D-Asn	Asp	Gly	Orn	D-Ala	Asp	D-Ser	3mGlu	***Asn***	128	ND	ND
CB-182,130	D-Asn	Asp	Gly	Orn	D-Ala	Asp	D-Ser	***Glu***	Kyn	8	16	2
CB-182,166	D-Asn	Asp	Gly	Orn	D-Ala	Asp	***D-Ala***	3mGlu	Kyn	1	16	16
CB-182,290	D-Asn	Asp	Gly	Orn	D-Ala	Asp	***D-Asn***	3mGlu	Kyn	1	16	16
CB-182,123	D-Asn	Asp	Gly	Orn	***D-Ser***	Asp	D-Ser	3mGlu	Kyn	1	32	32
CB-182,257	D-Asn	Asp	Gly	Orn	***D-Asn***	Asp	D-Ser	3mGlu	Kyn	8	ND	ND
CB-182,286	D-Asn	Asp	Gly	Orn	D-Ala	Asp	***D-Asn***	3mGlu	***Ile***	4	ND	ND
CB-182,251	D-Asn	Asp	Gly	Orn	D-Ala	Asp	***D-Asn***	***Glu***	Kyn	32	ND	ND
CB-182,263	D-Asn	Asp	Gly	Orn	***D-Asn***	Asp	D-Ser	3mGlu	***Ile***	16	ND	ND
CB-182,269	D-Asn	Asp	Gly	Orn	***D-Asn***	Asp	D-Ser	***Glu***	Kyn	128	ND	ND
CB-182,296	D-Asn	Asp	Gly	Orn	***D-Lys***	Asp	***D-Asn***	3mGlu	Kyn	1	32	32
A54145E	D-Glu	hAsn	Sar	Ala	D-Lys	moAsp	D-Asn	3mGlu	Ile	1	32	32
A54145D	D-Glu	hAsn	Sar	Ala	D-Lys	moAsp	D-Asn	***Glu***	Ile	2	4	2
CB-182,548	D-Glu	hAsn	Sar	Ala	D-Lys	moAsp	***D-Ala***	3mGlu	Ile	1	16	16
CB-182,332	D-Glu	hAsn	Sar	Ala	D-Lys	moAsp	***D-Ser***	3mGlu	Ile	2	16	8
CB-182,443	D-Glu	hAsn	Sar	Ala	D-Lys	***Asp***	D-Asn	3mGlu	Ile	2	4	2
CB-182,571	D-Glu	hAsn	Sar	Ala	***D-Ala***	moAsp	D-Asn	3mGlu	Ile	1	32	32
CB-182,549	D-Glu	hAsn	Sar	Ala	***D-Ser***	moAsp	D-Asn	3mGlu	Ile	1	16	16
CB-182,510	D-Glu	hAsn	Sar	Ala	***D-Asn***	moAsp	D-Asn	3mGlu	Ile	8	64	8
CB-182,363	D-Glu	***Asn***	Sar	Ala	D-Lys	moAsp	D-Asn	3mGlu	Ile	2	16	8
CB-182,575	***D-Asn***	hAsn	Sar	Ala	D-Lys	moAsp	D-Asn	3mGlu	Ile	2	4	2
CB-183,296	D-Glu	hAsn	Sar	Ala	D-Lys	moAsp	D-Asn	***Glu***	***Kyn***	1	2	2
CB-182,509	D-Glu	hAsn	Sar	Ala	D-Lys	moAsp	***D-Ala***	***Glu***	Ile	8	16	2
CB-182,336	D-Glu	hAsn	Sar	Ala	D-Lys	moAsp	***D-Ser***	***Glu***	Ile	64	128	2
CB-182,350	D-Glu	hAsn	Sar	Ala	D-Lys	***hAsp***	D-Asn	***Glu***	Ile	8	16	2
CB-182,333	D-Glu	hAsn	Sar	Ala	D-Lys	***Asp***	D-Asn	***Glu***	Ile	32	64	2
CB-182,567	D-Glu	hAsn	Sar	Ala	***D-Ala***	moAsp	D-Asn	***Glu***	Ile	4	8	2
CB-182,532	D-Glu	hAsn	Sar	Ala	***D-Ser***	moAsp	D-Asn	***Glu***	Ile	8	8	1
CB-182,531	D-Glu	hAsn	Sar	Ala	***D-Asn***	moAsp	D-Asn	***Glu***	Ile	16	16	1
CB-182,391	D-Glu	hAsn	***Gly***	Ala	D-Lys	moAsp	D-Asn	***Glu***	Ile	16	32	2
CB-182,325	D-Glu	***Asn***	Sar	Ala	D-Lys	moAsp	D-Asn	***Glu***	Ile	32	32	1
CB-182,444	***D-Asn***	hAsn	Sar	Ala	D-Lys	moAsp	D-Asn	***Glu***	Ile	8	8	1
CB-182,597	D-Glu	***Asn***	Sar	Ala	D-Lys	***hAsp***	D-Asn	3mGlu	Ile	1	16	16
CB-182,390	D-Glu	***Asn***	Sar	Ala	D-Lys	***Asp***	D-Asn	3mGlu	Ile	2	2	1
CB-182,561	***D-Asn***	***Asp***	Sar	Ala	D-Lys	moAsp	D-Asn	3mGlu	Ile	1	2	2
CB-182,349	D-Glu	***Asn***	Sar	Ala	D-Lys	***hAsp***	D-Asn	***Glu***	Ile	32	64	2
CB-182,348	D-Glu	***Asn***	Sar	Ala	D-Lys	***Asp***	D-Asn	***Glu***	Ile	16	32	2
CB-182,560	***D-Asn***	***Asp***	Sar	Ala	D-Lys	moAsp	D-Asn	***Glu***	Ile	8	16	2

Table 1.3 Dap and A5 analogs created through combinatorial biosynthesis[67]. The analogs above A54145D are more similar to Dap, the one below are more similar to A54145. The MICs are reported both in the presence and absence of lung surfactant. [a]Dap contains a decanoyl residue, all other lipopeptides contain an *anteiso*-undecanoyl chain. [b]Amino acid changes are shown in bold italics. [c]MICs against *S. aureus* were determined in the presence of 1% lung surfactant. Reprinted with permission from Baltz, R. H. *Am. Chem. Soc. – Synth. Biol.* 2014, *3*, 748-758. Copywright 2014, American Chemical Society.

As shown in Table 1.3, it is clear that the combinatorial biosynthetic approach has been fruitful in synthesizing new Dap derivatives. Some interesting trends were observed with these analogs. When kynurenine 13 was replaced with more hydrophobic residues (tryptophan, isoleucine

or valine) the activity in lung surfactant increased but the activity without surfactant decreased. This suggests that the kynurenine is likely interacting more with PG in the membrane than the other amino acids tested. An interchange of kynurenine13 for asparagine eliminated activity, suggesting that a non-polar residue is necessary at this position. Replacing 3-methylglutamate with glutamate significantly reduced the activity, but the relative effect of surfactant was lowered. Positions 12 and 13 when substituted together increase activity in surfactant but have an increased MIC value without surfactant. Substituting D-serine with D-alanine or D-asparagine slightly increased activity in surfactant with minimal change the MICs without surfactant, suggesting that the D-serine residue is likely not vital for Dap action.

Although the use of combinatorial biosynthesis is a powerful tool for the discovery of new analogs of Dap, there are several shortcomings that make this approach less useful[92]. The *S. roseosporus* gene cluster has been sequenced, cloned and heterogeneously expressed, but utilizing this technique still requires the use of the host organism[52,79]. Therefore, although some changes can be made to the amino acid structure, no dramatic changes can be done. For example, Cubist Inc.© was able to delete the methyltransferase module responsible for converting glutamate to 3-methylglutamate, but they were unable to change this residue for anything other than glutamate[67]. This highlights that combinatorial biosynthesis is ultimately reliant on the specificity of the host organism for certain modules, with no guarantee that added modules will be accepted by this bacterium. This issue is also apparent in the inability to alter the stereochemistry of certain amino acids at positions 2, 8 and 11. Overall, combinatorial biosynthesis is a helpful tool in discovering more lipopeptide antibiotics; unfortunately, this method is restricted to the limitations of what each bacterial NRPS can handle.

1.5.2 The Chemo-enzymatic Approach to Dap and A5 Analogs

The chemo-enzymatic approach to Dap analog synthesis involves the use of solid phase peptide synthesis (SPPS) to prepare a linear Dap analog which, after removal from the solid support, is then cyclized using a thioesterase/cyclase[10,40,73,78]. This approach is appealing as a larger variety of amino acids can be used, compared to the biosynthetic approach, as the NRPS machinery is mostly avoided. Grunewald, *et al*. synthesized nine Dap analogs with this approach utilizing a CDA cyclase enzyme[73]. The analogs tested are shown in Table 1.4.

Entry	Compound	MIC (μg/mL) at 73.6 mg/L Ca^{2+}
1	Dap-L-N2E12	20
2	*Authentic Dap*	3
3	Dap-L-N2E12 linear	>960
4	Dap- L-N2N3E12	80
5	Dap- L-N2N7E12	>960
6	Dap- L-N2N9E12	>960
7	Dap- L-N2Q12	30
8	Dap- L-N2D11E12	>320
9	Dap- L- N2AlocE12	80
10	Dap- L-N2E12W13	100
11	Dap- L-N2K6E12W13	100

Table 1.4 MIC's of the analogs created by the chemo-enzymatic approach using a CDA cyclase[73]. The analogs were tested against *B. subtilis* PY79 at 73.6 mg/L calcium.

At the time of this work, the stereochemistry of asparagine2 in Dap was believed to be of the L form and so an L-asparagine was used. It was later determined that Dap contains a D-asparagine at this position[57]. Moreover, in all of their analogs, 3-methylglutamate was replaced with glutamate, since 3-methylglutamate is very challenging to synthesize[68]. Consequently, most of their Dap analogs were triple mutants containing glutamate in place of 3-methylglutamte12, the unintended L-asparagine2 substitution, and the additional substitution of interest at a third position within the peptide. Nevertheless, this study still provided some useful information regarding the importance of certain amino acids to Dap activity.

Aspartate at positions 7 and 9, have been suggested to be important for calcium binding, as they are part of the DXDG sequence found in the EF hand motif of many calcium binding proteins[73,78]. This appears accurate, as the replacement of these amino acids with asparagine (entries 5 and 6, in Table 1.4), abolished activity. Another interesting finding was the relatively minor decrease

in activity found when aspartate3 and 3-methylglutamate12 were replaced with asparagine and glutamine, respectively (entries 4 and 7, in Table 1.4). This suggests that these particular residues are not directly involved in calcium binding.

Two years after this work was published, Kopp, *et al.* reported an improved chemo-enzymatic approach to Dap and A5 analogs[78], by replacing the CDA cyclase with one native to Dap and A5's own NRPSs, which resulted in higher peptide yields[78]. In this work, the Dap analogs contained D-asparagine at position 2 and glutamate instead of 3-methylglutamte at position 12. They synthesized nine new analogs of Dap and A5 (Table 1.5).

Entry	Compound	MIC (μg/mL) at 73.6 mg/L Ca^{2+}
1	*Authentic Dap*	3
2	Dap-E12	11
3	A54145(Val)	200
4	A54145(Ile)	25
5	Dap($A54_{1-3}$)	20
6	Dap($A54_{1-6}$)	20
7	A54145(Dap)	25
8	A54145(NXDG)	>900
9	A54145(DXNG)	>900
10	A54145(NXNG)	>900

Table 1.5 MIC's of the analogs created by the chemo-enzymatic approach using a Dap or A5 cyclase. The analogs were tested against *B. subtilis PY79* at 73.6 mg/L calcium. Dap-E12 varied from authentic Dap, by glutamate in position 12, instead of 3-methylglutamate. All other analogs were based off Dap-E12. Kopp, *et al.*'s A54145 varied from native A54145 by asparagine instead of hydroxyl-asparagine in position 3, aspartate instead of methoxy-aspartate in position 9 and glutamate instead of 3-methylglutamate in psotion12. A54145(Val) and A54145(Ile) had these amino acids in position 13. Dap(A541-3) and Dap(A541-6) had Dap-E12's structure with the amino acids native to A54145 replaced for either the first three or six residues. A54145(Dap) had a diaminopropionic acid residue instead of threonine4, thus creating an amide linkage. A54145-(NXDG), -(DXNG), and –(NXNG) had asparagine's in replace of aspartate residues, in positions 7 and 9 alone and together.

The glutamate13 analog of Dap (entry 2, in Table 1.5) only saw a ~5 fold decrease in activity. They determined that position 13 of A5 is largely sensitive to changes in amino acids (entries 3 and 4 in Table 1.5), compared to what has been observed previously with Dap. They also made two A5 and Dap hybrids. The first analog had residues 1-3 of Dap (tryptophan, D-asparagine and aspartate) replaced with tryptophan, D-glutamate and asparagine, native to A5 (entry 5 of Table 1.5). The second hybrid had the initial 6 amino acids changed, having tryptophan-D-asparagine-aspartate-threonine-glycine-ornithine replaced with tryptophan-D-glutamate-asparagine-threonine-sarcosine-alanine (entry 6 of Table 1.5). These both exhibited significantly reduced activity.

Overall, the chemo-enzymatic approach shows another unique way to synthesize Dap analogs. There are, unfortunately, several downsides to this approach. Although this allows for a more diverse number of amino acids to be incorporated, there are still limits due to the specificity of each cyclase. The overall yields for this reaction were also quite low[73,78], which makes this method non-ideal for the creation of a library of analogs. The peptides have to be purified by HPLC both before and after cyclization, which does not make it very amenable to high throughput analog synthesis. Nevertheless, the analogs synthesized by this method highlighted the importance of several amino acids in Dap.

1.5.3 Chemical Synthesis of Dap Analogs

Dap analogs have been prepared via semi- or total synthesis[68,93,94]. Although many analogs can and have been made by other methods, the synthetic approach allows for any and all Dap analogs to be made, without having to rely on the limitations of *Streptomyces roseosporus* selective enzymes, mainly the NRPS domains and cyclases.

Semi-synthesis involves making structural alterations to native Dap. This can include removing the acyl tail[60] and replacing the exocyclic amino acids[69] or altering the structure of certain amino acids within the macrolactone ring[95,96]. Another option is altering the fatty acyl tail moiety attached to the *N*-terminal tryptophan residue of Dap.

Eli Lily© researchers first investigated this semi-synthesis, following the initial discovery of Dap[10,60]. Debono, *et al.* studied the effects of different fatty acyl tails on the activity of A21978C[60]. They utilized an *Actinoplanes utahensis* strain of bacteria for de-acylation, and then re-acylated the terminal tryptophan through addition of varying acyl tail lengths coupled with activated esters. They

determined that the fatty acyl tail composition is highly important to the antibiotics activity, with an optimal balance of activity and toxicity for the decanoyl moiety, which they termed Daptomycin. Dap was promising as it was also found to have the highest therapeutic index in mice. When the tail length was increased above a decanoyl residue the MIC became slightly lower, but the LD_{50} decreased drastically. When the tail length was lowered below a decanoyl group the activity was dramatically reduced.

Knight-Connoni, *et al.* utilized semi-synthesis to create several Dap analogs in which the decanoyl tail was replaced with cyclic or aromatic hydrocarbons[97]. From their studies, a novel antibiotic was discovered. This antibiotic, surotomycin, contains an (E)-3-(4-pentylphenyl)but-2-enoyl tail instead of Dap's intrinsic decanoyl group. Surotomycin was determined to have high activity against *Clostridium difficile*, with a high therapeutic index. It entered Phase III clinical trials in 2014 but these studies were discontinued in February of 2016 as it failed to exhibit non-inferiority to current therapies.

Cubist Inc.© has made many Dap analogs by attaching a wide variety of chemical entities to the ornithine residue via an array of different chemical procedures[95,96]. Many of these analogs retained activity though none made it to human clinical trials. These results suggested that the ornithine residue is not overly important for antibacterial activity. The role of this amino acid for Dap's mode of action is still unclear.

He, *et al.* replaced the tryptophan residue in Dap with a wide range of unnatural aromatic amino acids[69]. In this procedure, Dap was first protected on the ornithine with an allyl group. The decanoyl tail was then removed enzymatically, and tryptophan1 by Edman degradation. A surprisingly large number of these analogs exhibited activity close to that of Dap. Some of these analogs also had increased activity in the presence of lung surfactant compared to Dap. This work highlights that the tryptophan residue is not essential for activity and it can be changed to further improve Dap's antibacterial properties.

Only recently was the total synthesis of Dap completed. In 2013, Lam, *et al.* reported the first total synthesis of Dap[94]. Unfortunately, they were unable to form the ester bond between threonine and kynurenine either in solution or on a solid support. They had to resort to a 12-step solution phase synthesis of a tetrapeptide, which contained the crucial ester linkage between kynurenine13 and threonine4. They then used this tetrapeptide as a building block in their solid phase synthesis. The cyclization was achieved via a solution phase serine ligation reaction; unfortunately, the antibacterial

activity was never determined. This combination of solid and solution phase chemistry made for a very laborious synthesis and is therefore not well suited to the preparation of large numbers of analogs.

In 2014, Martin, *et al.* also reported the total chemical synthesis of several Dap analogs[93]. They synthesized a branched, acyclic version of their Dap analogs in the solid phase, which, after cleavage from the solid support, was cyclized in solution to give the Dap analogs. They did not have the same issues as Lam, *et al.* with regard to depsi bond formation because they utilized a diaminopropionic acid (DAPA) derivative instead of threonine at position 4, which resulted in the Dap analogs having an amide linkage between residue 4 and 13 instead of an ester linkage. Four analogs were prepared (Table 1.6). One analog contained DAPA at position 4 and glutamate in place of 3-methylglutamate at position 12 (entry 2, Table 1.6). Another contained DAPA at position 4, glutamate in place of 3-methylglutamate at position 12 and tryptophan at position 13 (entry 3, Table 1.6). The other two analogs were the enantiomers of these analogs (entries 4 and 5, Table 1.6). The analogs containing the correct stereochemistry were 100-200 times less active than Dap, indicating that the ester bond and/or the methyl group of the threonine side chain is crucial for activity. The enantiomers of these analogs were inactive, which suggests that the overall stereochemistry of Dap is vital to activity.

Entry	Compound	MIC (μM) at 50 mg/L Ca^{2+}
1	Daptomycin	3
2	Dap-DAPA4E12	201
3	Dap-DAPA4E12W13	101
4	Dap-DAPA4E12 (ent)	Not active
5	Dap-DAPA4E12W13 (ent)	Not active

Table 1.6 MIC's of the analogs created by the combinatorial synthetic approach by Martin, *et al*. The analogs were tested against *S. aureus* ATCC 29123 at 50 mg/L calcium. Dap-DAPA4E12 varied from authentic Dap by having a diaminopropionic acid instead of threonine at position 4, thus creating an amide linkage for cyclization. This analog also had a glutamate instead of 3-methylglutamte in position 12. Dap-DAPA4E12W13 was based of the previous analog but with kynurenine replaced with tryptophan at position 13. The last two analogs in the table are the enantiomers of the previously described derivatives.

In 2015, Lohani, *et al.* published the total synthesis of Dap performed entirely on the solid phase[68] using a combination of Fmoc amino acids and azido acids. Several Dap analogs were initially synthesized using this approach (Table 1.7).

Entry	Compound	MIC (μg/mL)	
		B. subtilis ATCC 1046	*B. subtilis PY79*
1	Daptomycin	0.75[a], 0.5[b,c]	0.75[a]
2	Dap-(2S,3S)-MeGlu	40[a], 5.0[b], 5.0[c]	>40[a]
3	Dap-E12W13	1.5[a]	3.0[a]
4	Dap-E12Y13	35[a], 3.0[b], 1.3[c]	ND

Table 1.7 MIC's of the analogs created by total synthesis by Lohani, *et al*. The analogs were tested against two *B. subtilis* strains at 5 mM[a], 25 mM[b] and 100 mM[c] $CaCl_2$. Dap-(2S,3S)-MeGlu replaced the 3-methylglutamate in position 13 with the opposite stereochemistry. Dap-E12W13 had glutamate instead of 3-methylglutamate in position 12 and tryptophan instead of kynurenine in position 13. Dap-E12Y13 had glutamate instead of 3-methylglutamate in position12 and tyrosine instead of kynurenine in position 13.

When the stereochemistry of the side chain of 3-methylglutamate was reversed (entry 2, Table 1.7), the activity was greatly reduced. It has been observed previously that the substitution of 3-methylglutamate with glutamate, and kynurenine with tryptophan, separately, decrease activity[67,78,98]. Unexpectedly, when both were simultaneously replaced (entry 3, Table 1.7), the activity was comparative to Dap at 5 mM calcium.

Another analog of Dap was synthesized that had 3-methylglutamate replaced with glutamate and kynurenine replaced with tyrosine (entry 4, Table 1.7)[68]. This analog was found to be approximately 50-fold less active than Dap at 5 mM calcium, but only 6- and 3-fold less active at 25 and 100 mM calcium, respectively. This trend was also observed with the Dap-(2S,3S)-MeGlu analog. This suggests that these substitutions reduce Dap activity, at least in part, by reducing calcium affinity.

The approach developed by Lohani, *et al.* was recently improved upon,[99] and the new method used to create several new Dap analogs based upon Dap-E12W13 (Table 1.8). When a glutamine is

replaced with 3-methylglutamate (entry 2, Table 1.8), the resulting analog is 10-fold less active than Dap at 5 mM calcium but as active as Dap at 100 mM calcium. This suggests that the glutamate residue is involved in calcium binding, though probably not directly. When aspartate7 was replaced with alanine (entry 4, Table 1.8), activity was completely lost, even at high calcium concentrations. This indicates that this amino acid is likely directly involved in binding calcium, which is plausible as it is contained within the DXDG motif.

Entry	Compound	MIC (μg/mL)		
	$CaCl_2$ (mM)	*1.8*	*5.0*	*100.0*
1	Daptomycin	1.0	0.75	0.5
2	Dap-Q12W13	ND	7	0.75
3	Dap-E12W13	5.0	1.5	1.5
4	Dap-A7E12W13	>100	>100	>100
5	Dap-S4E12W13	>100	65	3
6	Dap-E3E12W13[a]	N/A	40	1.5
7	Dap-K6E12W13[a]	1.0	1.0	0.5

Table 1.8 MIC's of other analogs utilizing Lohani, *et al.*'s methodology. The analogs were tested against *B. subtilis* ATCC 1046 at 1.8 mM, 5.0 mM and 100 mM $CaCl_2$. Dap-Q12W13 had glutamine instead of 3-methylglutamate in position 12 and tryptophan instead of kynurenine in position 13. Dap-E12W13 had glutamate instead of 3-methylglutamate in position 12 and tryptophan instead of kynurenine in position 13. All other analogs listed were based of Dap-E12W13, with the corresponding amino acid changes shown. [a]Dap-E3E12W13 and Dap-K6E12W13 are unpublished data, synthesized by Dr. Chuda Lohani and characterized by Robert Taylor.

Surprisingly, when aspartate3 was replaced with glutamate (entry 6, Table 1.8), the activity was greatly reduced. Similarly, when threonine4 was replaced with serine (entry 5, Table 1.8), the activity was also significantly reduced. In both of these analogs the only difference is a methylene or methyl group. These two analogs highlight that even the smallest of changes to the structure of Dap can have large implications on global activity.

One very interesting analog that was synthesized is the triple mutant Dap-K6E12W13. This analog has three of the non-proteinogenic amino acids (ornithine, 3-methylglutamate and kynurenine)

native to Dap, replaced with structurally similar proteinogenic ones (lysine, glutamate and tryptophan). The activity of this analog was almost identical to native Dap against *Bacillus subtilis* strains at physiological (1.25 mM) or greater than physiological concentrations of calcium (5 and 100 mM). This analog was therefore investigated further against several *Staphylococcus aureus* strains (Table 1.9).

	MSSA		MRSA	
	ATCC 6538	ATCC 25293	Isolate 1-3	Isolates 4, 5
(1.25 mM Ca^{2+})				
Dap	0.75	1.0	1.0	1.5
Dap-K6E12W13	3.0	3.0	3.0	>3.0
(5.0 mM Ca^{2+})				
Dap	0.75	0.5	0.5	0.5
Dap-K6E12W13	0.3	0.5	0.5	0.5

Table 1.9 MIC's of Dap and Dap-K6E12W13 on various strains of either methicillin-susceptible (MSSA), or methicillin-resistant (MRSA), *Staphylococcus aureus*. Two calcium concentrations were used, either 1.25 mM or 5.0 mM $CaCl_2$. The MRSA strains were distinct clinical isolates, not contained in type culture collections. Data shown in table is unpublished work by Robert Taylor.

Dap-K6E12W13 is an important discovery in the synthesis of new Dap analogs. This analog proves that it is possible to obtain an analog that has activity that is at least equal to that of Dap. Moreover, it also shows that several of the non-proteinogenic amino acids, which can be time-consuming and challenging to prepare, are not required for high activity. This analog is currently being used in Dr. Taylor's laboratory as a lead for the synthesis of new and improved Dap analogs and for studying Dap's mechanism of action. Overall, from this section, it is clear that SPPS is a powerful approach to the synthesis and preparation of a large scale of new Dap analogs.

1.6 Methodologies Utilized to Study Daptomycin's Action Mechanism

Although structure-activity relationship studies have determined the importance of a few of Dap's residues, it is not possible to predict which amino acids should be varied in order to obtain analogs with improved activity. It would be easier to determine which amino acids should be varied with certainty and in greater molecular detail, if the mechanism of action of Dap was known. Many action mechanisms have been proposed for Dap and a variety of methodologies/techniques have been employed to investigate Dap's action mechanism. A few of these methodologies/techniques are outline in this section, with a focus on the ones that were used throughout this thesis. In Section 1.7, the various mechanisms that have been proposed for Dap are outlined.

1.6.1 Membrane Systems

Ideally, when studying Dap viable pathogenic bacterial strains, which are treated clinically with Dap, should be used. Dap action has indeed been investigated on several pathogenic bacteria, including *S. aureus, E. faecalis, E. faecilium* and *S. pneumoniae*. Unfortunately, pathogenic bacteria can be somewhat dangerous to use and require a level II biosafety facility. Therefore, non-pathogenic bacteria, mainly *Bacillus subtilis*, have been used frequently to study Dap. The limitations of the use of *B. subtilis* as a stand-in for pathogens, such as *S. aureus* are discussed in more detail within Chapter 4.

A convenient approach for studying how Dap interacts with bacterial membranes is to use simplistic model membranes. There are different types of model membranes including monolayers, planar lipid membranes and unilamellar liposomes, which are small (SUV), large (LUV) or giant (GUV). Since bacterial membranes consist of a bilayer in aqueous solvent, unilamellar liposomes are the best-suited model membranes to investigate Dap. Liposomes are prepared by mixing varying phospholipids, followed by hydration/agitation of these lipids with aqueous solvent. The liposomes will vary in size and bilayer thickness initially, and are considered multiple lamellar vesicles (MLVs). MLVs are further subjected to varying methods, including sonication (for preparing SUVs) or extrusion (for preparing LUVs). LUVs (≥100 nm) have less curvature strain than SUVs (10-50 nm) and are used primarily in this thesis.

It is desirable when studying Dap that the model membrane used mimics the lipid composition of a clinically susceptible pathogen, such as *S. aureus*. Several studies have shown that

the lipid composition of the *S. aureus* contains a large percentage of PG (~80%), with lower percentages of lysyl-PG and cardiolipin (CL), at ~15% and 10%[100,101–103,104]. It should be noted that the lipid composition of bacteria varies strain to strain (See Chapter 4 for more detail). The model membrane most commonly used to study Dap in the literature, consists of a one-to-one mixture of phosphatidylcholine (PC) and phosphatidylglycerol (PG). Although this composition varies compared to a *S. aureus* cytoplasmic membrane, Muraih, *et al.* showed that Dap requires the same concentration of calcium to observe membrane interaction on either these model membranes or bacterial membranes. This was accomplished by utilizing fluorescence with a perylene labeled Dap analog[105]. *S. aureus* contains >50% PG, but higher percentages of PG have been shown to cause LUVs (used primarily in this thesis) to be less stable. Although PC is not found in Gram-positive bacteria[106], it is a neutral phospholipid and Dap has only been found to interact with this lipid at very high calcium concentrations[105]. Therefore, PC can be regarded as an inert "filler lipid" that allows investigations of the interaction of Dap with the other, "specific" lipids such as PG. The Leonenko group has also shown recently that model membranes (both monolayers and LUVs) can be made that more closely mimic the membrane composition of *S. pneumoniae*[66]. These lipid mixtures have been utilized to investigate the sequestering of Dap by lung surfactant. The role of the lipid head group when comparing varying bacteria and the effect of the acyl tail composition of these membranes, are discussed in more detail within Chapter 4.

1.6.2 Characterizing the Interaction of Daptomycin with Membranes

The interaction of Dap with model and bacterial membranes has been examined using an extensive array of techniques, such as: circular dichroism (CD)[82,107], nuclear magnetic resonance (NMR)[82,85,108,109], isothermal titration calorimetry (ITC)[110,111], fluorescence spectroscopy[45,84,112–120] and atomic force microscopy (AFM)[55]. Each of these techniques has their own unique advantages and disadvantages. ITC and fluorescence spectroscopy are discussed below, as these were the two dominant techniques that were utilized in this thesis to study the interaction of Dap with model membranes.

ITC has been used in the literature to study the interaction of Dap with PG containing membranes[110,111]. ITC provides information on the binding energies (enthalpy, Gibbs free energy, entropy) of Dap within membranes and its interaction/stoichiometry with calcium.

ITC is a sensitive calorimetric technique used to determine the full thermodynamic profile of a system, by directly measuring the release (exothermic) or absorption (endothermic) of the heat in a reaction[121–124]. ITC works by dispensing one reactant into a reaction cell, and then injecting the other reactant in small increments. The heat released or consumed with each injection is observed by measuring the electric energy required to restore the reaction cell to the preset temperature, which is maintained in a reference cell (an example of this type of isotherm is shown in Figure 1.12). This creates an isotherm of peaks that eventually reach a saturation point (Figure 1.12B). The calorimeter then converts this raw data into an integrated curve shown in Figure 1.12C, with the molar ratio representing the x-axis and the enthalpy representing the y-axis. From this isotherm, the thermodynamic parameters can be calculated and the data can be modeled through external software (namely Origin software). To model this data, one must assume one or multiple equilibria; varying the stoichiometry and equilibrium constants until the best fit to the data, with the smallest number of variable parameters, is determined.

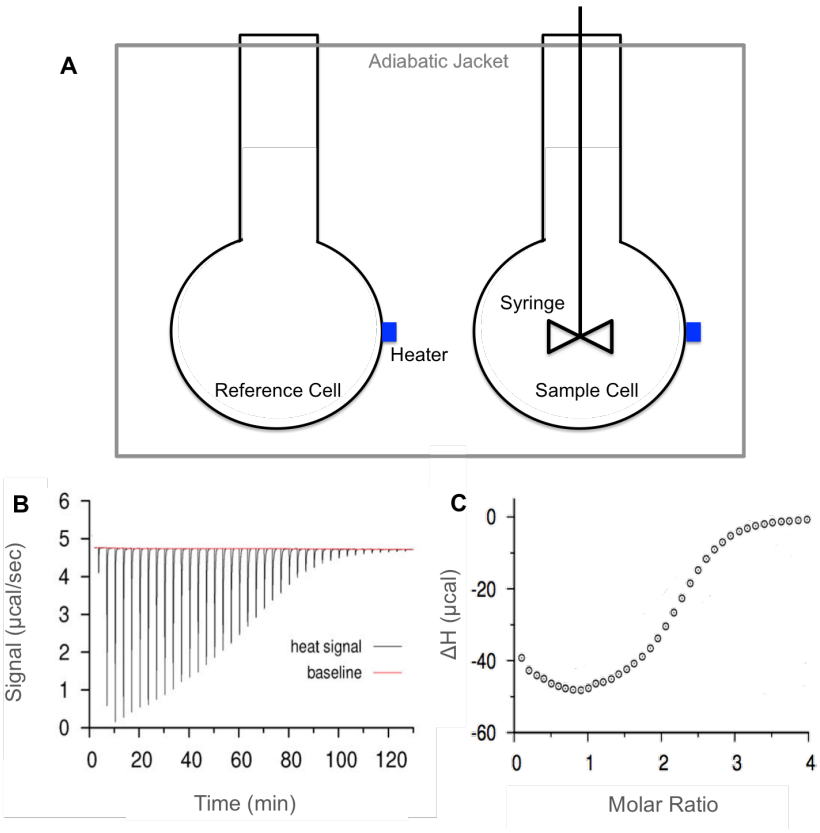

Figure 1.12 Isothermal titration calorimetry (ITC). A: The calorimeter is composed of two cells, a reference cell and a sample cell. The reference cell is maintained at a constant temperature. The

syringe both injects reactant into the sample cell and stirs the mixture. B: The isotherm that is generated from the changes in electric energy after, in this case, an exothermic reaction has occurred within the sample cell. The peaks will lose intensity over time due to a saturation effect. C: The integrated isotherm shows the molar ratio of ligand to reactant, versus the enthalpy. Each point represents the area under one peak of the curve in B.

Fluorescence spectroscopy has proven to be a powerful technique for probing how specific parts of Dap interact with membranes. When Dap interacts with membranes in the presence of calcium, it goes from the polar environment of the aqueous solvent to the apolar environment of the membrane. If any intrinsic or extrinsic fluorophores attached to Dap experience this change in environment, a blue shift and/or a significant increase in the intensity of the fluorescence spectrum occurs. Depending on the fluorophore used, a blue shift will be more prominent (tryptophan) versus an intensity increase (pyrene, perylene, NBD, etc.).

Dap, as discussed briefly in Section 1.3 contains the fluorophores, kynurenine and tryptophan. Since kynurenine's quantum yield is higher than tryptophan[76], and its excitation spectrum ($\lambda_{ex,max}$ = 360 nm) overlaps with the emission spectrum of tryptophan ($\lambda_{em,max}$ = 340 nm) a photon originating from the excitation of tryptophan will transfer to the kynurenine and so only kynurenine fluorescence is observed. This phenomenon is known as fluorescence resonance energy transfer (FRET).

Semi-synthesis has been used in the literature to incorporate external fluorophores, usually ones that has a much higher quantum yield than a standard amino acid, into Dap[105,116,125–127]. This has been done with a variety of fluorophores including pyrene[45,125], perylene[105], nitrobenzoxadiazole[126] and acrylodan[116,127].

Another indirect method of studying Dap is through using a fluorescent dye in solution or in the membrane, including 3,3'-Dipropylthiadicarbocyanine iodide ($DiSC_3$)[49,128], 4,4′-[1,4,10,13-tetraoxa-7,16 diazacyclooctadecane-7,16-diylbis(5-methoxy-6,2-benzofurandiyl)]bis-1,3 benzenedicarboxylic acid (PBFI)[112,118], calcein[82,114] and laurdan[119], that can be detected when Dap is in proximity to a membrane or eliciting an effect. The use of dyes to study Dap is explored in Section 1.7, when the mechanism of action of Dap is discussed. Overall, fluorescence is a very versatile and important technique in studying Dap, mainly due to its high sensitivity.

1.7 Proposed Mechanisms of Action for Daptomycin

Dap has been studied for over 30 years and yet its mechanism of action has not been determined with certainty. Many research groups have investigated the action mechanism of Dap on bacterial cells. Determining the mechanism of action should allow for a more rational approach to the creation of new analogs of Dap that will, hopefully, combat growing multi-drug resistance bacteria. This section outlines the many different proposed mechanisms of Dap action, including confirmed and suspected targets for Dap activity.

1.7.1 Target of Daptomycin Action

Daptomycin, as discussed in Section 1.3, is a calcium-dependent antibiotic. Eliopoulos, *et al*. first reported this dependence on calcium, when they observed that it was required in the growth medium when analyzing the antibacterial activity of Dap[129]. When calcium was replaced with other divalent ions (Mg^{2+}, Zn^{2+}, or Ba^{2+}) activity was not observed[129]. Barry, *et al.* observed maximal Dap activity when the concentration of calcium in the medium was 50 mg/L (1.25 mM)[130], corresponding to the concentration found within human blood plasma. Calcium-dependent antibiotics, including Dap, contain a highly conserved sequence of amino acids, related to their affinity for calcium. This sequence motif (DXDG) has been found in many proteins that bind calcium selectively, including calmodulin[11,40,72,73].

In Section 1.5, it was observed that when either aspartate (D) residue within this motif was replaced with asparagine or alanine, activity was completely lost even at high calcium ion concentrations[99]. This suggests that this conserved sequence is likely selectively binding to calcium. The 'X' position contains a D-amino acid in both Dap and A5, suggesting the stereochemistry of this amino acid is important to calcium affinity. Very recently, Barnawi, *et al.* synthesized an alanine scan of a Dap analog that has 3-methylglutamate12 replaced with glutamate and kynurenine13 replaced with tryptophan. This Dap-E12W13 analog showed only a 3-4-fold decrease in activity comparative to Dap at physiological calcium concentrations (1.25 mM). Barnawi, *et al.* showed that the further replacement of D-alanine8 with L-alanine8 had a ~80 fold increase in MIC. This suggests that the stereochemistry of this position is important but not vital to activity.

Canepari, *et al.* have demonstrated, using radiolabelled Dap, that Dap interacts with the cell wall and membrane but not to the cytosolic components[131]. Initial studies on Dap utilized model

membranes consisting of both phosphatidylcholine (PC) and PC-cholesterol[76,132]. Although Dap was shown to insert within[76] and permeabilize these membranes, detected using planar bilayer conductivity[132], they are, unfortunately, not a good model to mimic bacterial cells as they contain no PG[87,106].

PG is a required lipid for Dap activity[9,11,12,40,48,52,104]. CD spectroscopy has shown that Dap when bound to calcium and membranes that contain PC and PG, undergoes a significant conformational change[82]. It was also observed that the inclusion of PG into model membranes significantly increased the fluorescent quantum yield of the kynurenine residue in comparison to liposomes that did not contain PG[76,82]. This suggests that kynurenine is inserting more deeply into PG than the PC.

Several research groups have determined the stoichiometry of Dap to PG in model membranes. Muraih, *et al.* showed, using a Dap analog that had perylene attached to the terminal tryptophan residue, that the stoichiometry was 1:1[115]. However, work by Zhang, *et al.* suggested, utilizing isothermal titration calorimetry (ITC), that Dap actually has a 1:2 stoichiometry with PG[110]. The model membranes each group utilized could explain the reason for these discrepancies. The work with perylene-Dap used a bicelle, whereas ITC analysis used a liposome. Bicelles would allow for Dap to insert into both the inner and outer leaflets, whereas liposomes might only detect insertion on the outer leaflet. Another reason for these different stoichiometries could be the nature of the experimental technique, whereby fluorescence detects only one binding interaction with PG wherase ITC detects two. In either case, these data support the findings mentioned above that Dap inserts into PG within the membrane, selectively and directly.

Streptomyces roseosporus is the organism that naturally produces Dap[10]. Since it is also a Gram-positive bacterium, one would expect Dap to kill its host. Ingeniously, *S. roseosporus* contains very little if any PG within its membrane[9,11,12,57]. It has also been shown that lower percentages of PG within *S. aureus* strains diminish the bactericidal activity of Dap[133]. Dap has also been shown to interact with PG rich regions (cell division septa) within the model organism *B. subtilis*[134,135]. PG is also absent from mammalian cells, which may explain Dap's low toxicity in humans [38]. All of these findings further support that PG is absolutely required for Dap activity, but not strictly for membrane interaction.

1.7.2 Membrane Depolarization, Membrane Integrity and Oligomer Formation

In 1987, Allen, *et al.* using a potassium selective electrode, reported that Dap, promoted the loss of intracellular potassium ions from *S. aureus*[136]. In 1991, they reported that Dap, in a Ca^{2+}-dependent manner, promoted the release of the membrane permeant anion teteraphenylphosphonium bromide (TPP)[137]. On the basis of these results, the authors suggested that dissipation of membrane potential might be the primary mechanism of action of Dap. Previous studies demonstrating Dap's inhibition of protein, RNA, DNA, peptidoglycan, lipid and LTA biosynthesis with equal facility was proposed to be a downstream effect of the loss of membrane potential[74].

To further elucidate the role of membrane potential loss in the mechanism of action of Dap, Silverman, *et al.* examined the effect of Dap on the membrane potential under conditions typically used for determining the time-kill kinetics of Dap[46]. Using both fluorometric and flow cytometric assays they found that at 8 times the MIC, a concentration required due to the high cell density, that the cell viability of *S. aureus* decreased in parallel with changes in membrane potential, in a dose-dependent manner. No loss of membrane potential or loss of cell viability occurred at a concentration of Dap equal to the MIC, over 60 minutes. They observed that bactericidal activity and membrane depolarization occurred on the same time scale, suggesting that depolarization is the primary mechanism of action of Dap. Employing a K^+-sensitive fluorescent probe, they demonstrated that Dap triggered K^+ release from *S. aureus* in a Ca^{2+}-dependent manner and that K^+ release was correlated with bactericidal activity[46]. The much slower loss of membrane potential that was promoted by Dap compared to the pore-forming peptide nisin and the proton ionophore CCCP (which disrupted membrane potential within 5 min) suggested to them that Dap's action mechanism was different from these and other antibacterials that are capable of rapid depolarization of bacterial membranes. The trans-membrane pH gradient of cell membranes remained intact, suggesting that Dap is forming a membrane lesion that is selective for only small cations to pass across the bilayer. Free protons might also diffuse across the membrane, but this proton concentration will be quite low and undetected. The authors proposed a model for the mechanism of action of Dap (Figure 1.13) where Dap inserts into the bacterial cytoplasmic membrane in a Ca^{2+}-dependent fashion presumably by interaction with PG. This is followed by oligomerization to give either ion channels, larger non-specific pores or irregular aggregate structures. Formation of any of these structures would disrupt the functional integrity of the membrane and trigger release of K^+ ions and cell death[46].

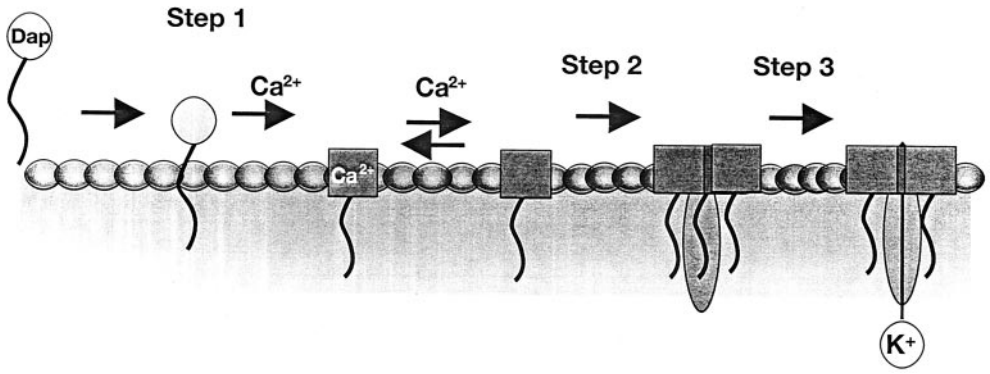

Figure 1.13 The mechanism of action of Dap proposed by Silverman, *et al.*[46] The authors proposed that Dap inserts into bacterial membranes (that contain PG) in a calcium dependent manner. Once bound to the membrane Dap oligomerizes, forming ion channels or non-specific pores that allow for the relapse of potassium ions from the cell, resulting in cell death. The figure was used with permission.

Rubinchik, *et al.* using the same fluorometric assay employed by Silverman, *et al*. also reported that Dap, at 8 times its MIC, induced depolarization of *S. epidermidus* within 15 minutes and cell viability decreased in parallel with the reduction in membrane potential[138].

Several groups have reported that, in contrast to Silverman, *et al.*[46] and Rubinchik, *et al.*[138], loss of membrane potential is not temporal with cell death[82,128]. Jung, *et al.* examined Dap-induced membrane depolarization of *S. aureus* using a fluorometric assay similar to that employed by Silverman, *et al.*[82] In contrast to Silverman, *et al.* results, where membrane potential was reduced by >90% within 30 min of adding Dap; Jung, *et al.* reported that at 10-fold above the MIC, 99% of bacterial killing also occurred but only 36% membrane depolarization was reported, after 90 minutes. Jung, *et al.* proposed that depolarization might be a consequence rather than the cause of cell death[82].

Using a fluorometric assay similar to that employed by Silverman, *et al.,* Hobbs, *et al.* also reported that loss of viability preceded membrane depolarization of *S. aureus* upon exposure to 4 times the MIC of Dap[128]. The capacity of the cells to synthesize macromolecules was used as an indicator of the viability of the bacteria. These workers suggested that membrane depolarization may not be solely responsible for loss of viability and may also involve more general damage to the membrane.

A report that clinical isolates of *S. aureus* that have developed reduced susceptibility to Dap did not display membrane depolarization at a dose 2 fold higher than MIC also suggests that

membrane depolarization may not be the only cause of cell death by Dap[139]. Although interesting, this study must be taken with caution, as the assay was dependent on the release of calcein from *S. aureus* cells. As will be discussed below, Dap does not allow for the transport of calcein, therefore the argument that this indicates a lack of permeabilization is erroneous.

Scanning electron microscopy (SEM) studies have shown that Dap does not cause lysis of *S. aureus* and *E. faecalis*, at concentrations of Dap that far surpass the MIC (8 mg/mL)[140]. Transmission electron microscopy (TEM) experiments have also shown that Dap does not cause lysis of *S. aureus*, at Dap concentrations only slightly above its MIC (4 μg/mL)[114]. Cotroneo, *et al.* showed that Dap, at concentrations above its MIC (4 μg/mL), caused a thousand-fold decrease in cell viability but that the optical density remained the same[114]. This indicates that the cells were dying but that lysis was not occurring. As noted above, Silverman, *et al.* has proposed that depolarization is the controlling factor for bactericidal action[46]. In direct contrast, Müller, *et al.* stated, through optical density measurements, that lysis of *B. subtilis* at a concentration of Dap above its MIC (4 μg/mL) does occur[119]. The reason for this discrepancy is not clear, but the type of bacteria studied might have influenced the results.

The effect of Dap on membrane integrity has been examined by monitoring the loss or uptake of fluorescent organic molecules into or out of model liposomes and bacteria upon exposure to Dap. One of these dyes is calcein (Figure 1.14). Cotroneo, *et al.* reported that treatment of calcein-loaded *S. aureus* cells with 2 μg/mL of Dap produced rapid bactericidal activity without significant calcein release[114]. In contrast, both the pore-forming antibiotic nisin and lysostaphin, which is bactericidal through the destruction of the *S. aureus* cell wall, exhibited 100% calcein release after just 20 minutes[114]. This suggests that Dap transports ions smaller than calcein across the membrane.

Another fluorescent dye, To-Pro3, which interacts with and strains DNA, was unable to enter cells when treated with Dap[114]. Several researchers have also attempted to utilize the live-dead dye, propidium iodide[46,119,141]. This dye has been used widely to determine if cells are alive or not. Rubinchik, *et al.* stated that this dye was able to cross bacterial membranes in the presence of Dap, as witnessed by a change in this dye's fluorescence[138]. Unfortunately, propidium iodide is very similar in structure to ethidium bromide, which is used to study the efficiency of bacterial efflux systems[142]. Ion gradients or ATP, both of which disappear upon Dap activity, drive many efflux systems. Therefore, propidium iodide, when observed to be entering cells, is measuring more than one process. This makes the results obtained from studying propidium iodide harder to interpret.

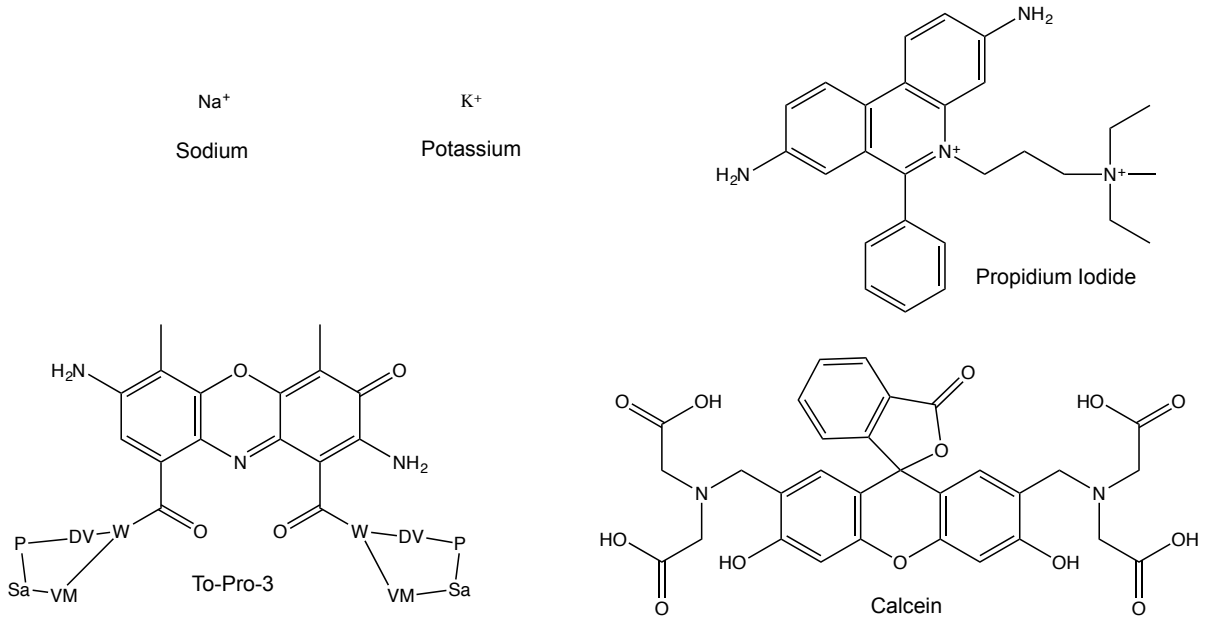

Figure 1.14 The relative size comparison of several dyes used in the study of Dap's pore. Dap has been shown to transport small cations, mainly sodium and potassium. In the To-Pro-3 structure, several amino acids are shown. These include: tryptophan (W), D-valine (DV), Proline (P), Sarcosine (Sa) and methyl-valine (VM).

The effect of Dap on the integrity of model membranes using calcein has provided similar results to the work on bacterial cells mentioned above. The Hancock group loaded model membranes with calcein.[138] Calcein was retained inside membranes after exposure to Dap indicating that it was being prevented from leaving the liposome.

Using a coupled fluorescence assay, Zhang, *et al.* found that Dap forms ion selective pores in model membranes[45]. This assay (Figure 1.15), similar to one developed by Clement, *et al.*[143] utilized a pH sensitive fluorophore, pyranine. Pyranine was encapsulated within the model membranes, and a pH gradient was created across the membrane. The use of two buffers containing either low salt (inside liposome) or high salt (outside liposome) concentrations produced a dual salt/pH gradient across a model membrane, stabilizing the charged ion ratio across the bilayer. When a proton ionophore, cyanide m-chlorophenyl hydrazone (CCCP, 5 nM) was added alone to these membranes minimal pyranine fluorescence is observed. The high concentration of salt ions outside the liposome will prevent the flow of protons against the liposomes diffusional potential. Dap (1-2 μM) when added alone (with calcium) also produced minimal fluorescence. It is not until both compounds are added collectively that proper efflux of protons concomitantly with influx of salt ions can occur. This

release of protons increases the pH of the internal buffer, deprotonating the pyranine reside found within, increasing its fluorescent signal[143].

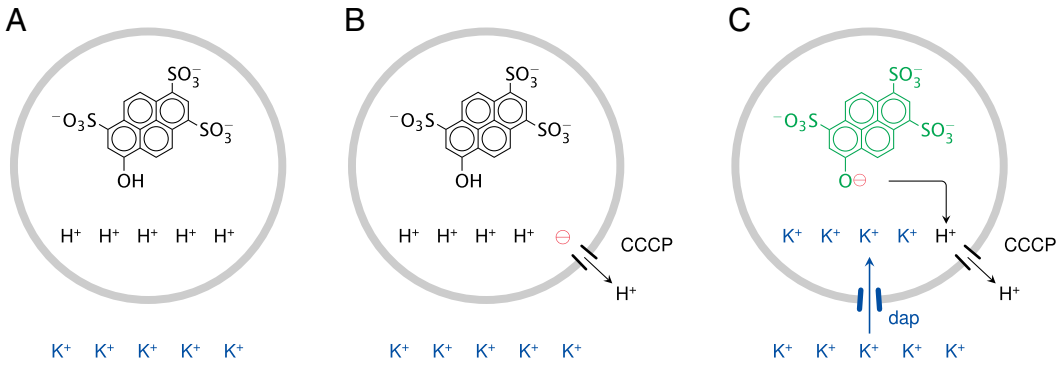

Figure 1.15 Schematic for the permeabilization assay explored by Zhang, *et al*.[45] A: Liposomes are encapsulated with the pH sensitive fluorophore, pyranine, in a low salt concentration and low pH buffer. The external buffer contains a high concentration of salt (in this case K^+) and a more alkaline pH. This creates a salt-pH gradient across the membrane, equalizing the charge ratio across the liposome. B: When a proton ionophore, cyanide m-chlorophenyl hydrazone (CCCP) is added alone, no proton efflux is observed as the charge ratio of the ions present is not kept constant. C: When both Dap and CCCP are added in unison an influx of K^+ (Dap) occurs concomitantly with an efflux of proton (CCCP). This removal of protons from the liposome creates a more alkaline buffer inside the liposome, deprotonating the hydroxyl group of the pyranine, increasing its fluorescent signal. This figure was used with permission.

The authors demonstrated that Dap form pores in DMPC/DMPG liposomes[45]. The pores are selective for cations, with permeabilities being highest for Na^+, K^+, and other alkali metal ions. The permeability was approximately two-times less for Mg^{++}, and even lower for the organic cations choline and hexamethonium. Anions were excluded. Dap-promoted leakage of K^+ was slow compared with that of valinomycin, a K^+-specific ionophore, at comparable concentrations.

As stated above, Silverman, *et al.* first theorized that Dap forms oligomeric structures within the membrane that lead to pore formation[46]. This is plausible, as many pore forming compounds form oligomers in cell membranes[144,145]. Studies on model liposomes support this hypothesis.

Using a polarity-sensitive fluorophore nitrobenzodiaxole (NBD), attached to the ornithine6 residue of Dap, Muraih, *et al.* were able to detect Ca^{2+}-dependent FRET between the kynurenine residue of unlabelled Dap and the NBD group of NBD-Dap on liposomes[126]. These liposomes contained DMPC, combined with or without DMPG, as well as membrane vesicles prepared from *B. subtilis* cells. The presence of PG was necessary for FRET to occur as no FRET was observed with

liposomes containing just DMPC. Self-quenching of NBD fluorescence was observed using just NBD-Dap at concentrations similar to those required for biological activity, on both DMPC/DMPG liposomes and *B. subtilis* cell membranes but not on DMPC liposomes. Self-quenching could be reversed upon the addition of an excess of unlabeled Dap[126]. These results strongly indicate that Dap oligomerizes on model and bacterial membranes. The proposed oligomers were found to be stable for several hours. The number of subunits contained in one Dap oligomer was determined to be approximately 7 in DMPC/DMPG liposomes.

Zhang, *et al.* have provided evidence that oligomerization is necessary but not sufficient for activity[110]. In a mixture of CB-182,462 (a semi-synthetic derivative of A5, Figure 1.16) and Dap on DMPC/DMPG liposomes (5 mM Ca^{2+}), the fluorescence of the tryptophan residue in CB-182,462 was largely suppressed by FRET to the kynurenine residue of Dap, indicating the formation of hybrid oligomers[110].

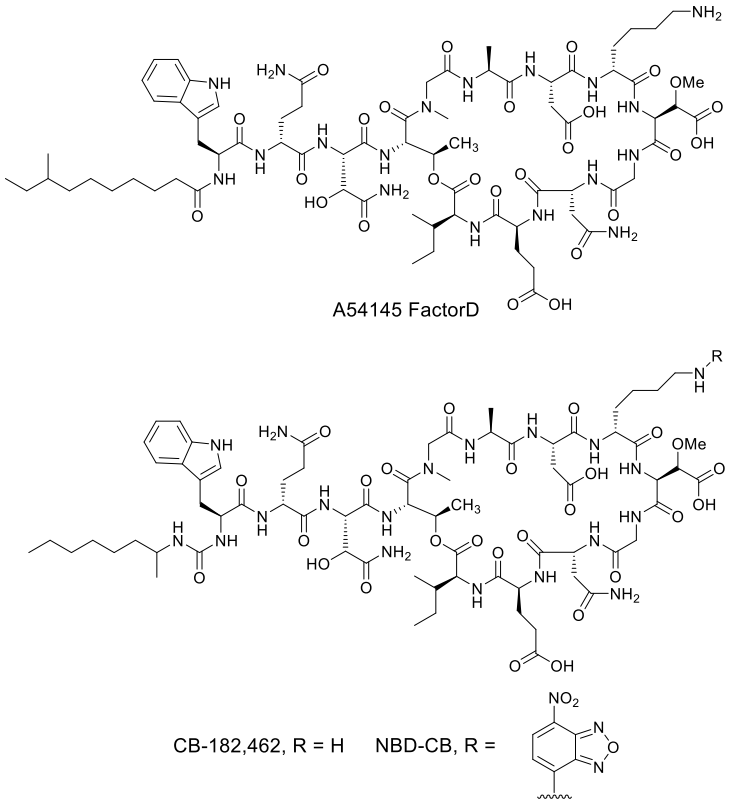

Figure 1.16 Structures of A5, CB-182,462 and NBD-labeled CB-182,462 (NBD-CB).

The authors also concluded that self-quenching of NBD fluorescence in NBD-labeled CB-182,462 (NBD-CB, Figure 1.16) on *B. subtilis* cell membranes was inhibited by unlabelled Dap, indicating that hybrid oligomers can also form on bacteria cell membranes. ITC studies using DOPC/DOPG liposomes indicated that the thermodynamic stability of the hybrid, pure Dap, and pure CB oligomers is approximately the same[110]. However, Dap and CB displayed less than additive antibacterial activity suggesting that the hybrid oligomers were functionally impaired and that oligomerization alone is not sufficient for antibacterial activity. This result also provides evidence that oligomerization contributes to the bactericidal effect of Dap (or CB-182,462) on bacterial membranes; if each individual monomer contributed independently and proportionally to the antibacterial action, combinations of the two antibiotics should have displayed strictly additive activity.

Muraih, *et al.* have used excimer fluorescence to look at Dap oligomerization on membranes[105]. As excimer fluorescence requires very close interaction between two fluorophores, the detection of excimer fluorescence imposes a more stringent constraint on the distance of the interaction than that implied by the observation of FRET in their previous studies. The *N*-terminal decanoyl group of Dap was replaced with perylene butanoic acid (perylene-Dap, Figure 1.17).

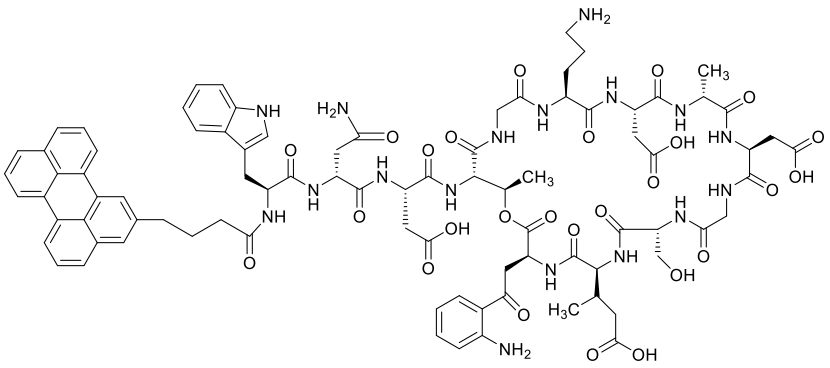

perylene-Dap

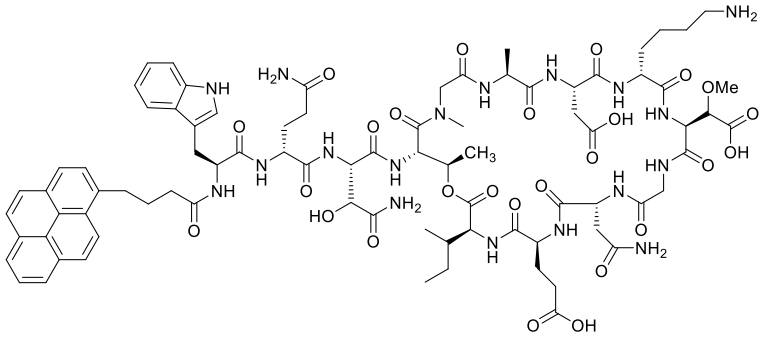

Py-A54145

Figure 1.17 Structures of perylene-labeled Dap (perylene-Dap) and pyrene-labeled A54145 Factor D (Py-A54145).

While perylene-Dap exhibited little or no excimer formation in solution or in the presence of DMPC liposomes and Ca^{2+}, strong Ca^{2+}-dependent excimer fluorescence was observed upon incubation of perylene-Dap with DMPC/DMPG liposomes and with bacterial cells[105]. The formation of perylene excimers on model membranes was inhibited by unlabeled Dap. The formation of perylene excimers in the presence of *B. subtilis* cells was inhibited by NBD-CB providing further support that hybrid oligomers can form on bacterial membranes. The extent of oligomerization of perylene-Dap was determined to be greater than 90% on DMPC/DMPG liposomes and slightly lower on bacterial membranes.

Zhang, *et al.* have studied the oligomerization of A5 using pyrene-labeled A5 (Py-A54145), Figure 1.17)[125]. In their study, different states of membrane-bound A5 could be distinguished, and their molar fractions determined as a function of calcium concentrations. Their results indicate that

A5 undergoes two Ca^{2+}-dependent transitions upon insertion within the membrane and oligomerization[125]. A mutual interaction of the Py-A54145 molecules was observed as the Ca^{2+} concentration was increased to up to 1 mM. Although membrane insertion was 90% complete at 1 mM Ca^{2+}, the excimer fluorescence increased further as the concentration of Ca^{2+} was increased above 1 mM indicating that the interaction between the pyrene moieties became tighter and/or involved a larger number of subunits. It should be noted that this work was carried out simultaneously with the work presented in Chapter 2, therefore this knowledge was not known beforehand.

Zhang, *et al.* also showed that Dap can translocate between the inner and outer leaflets of a model membrane[111]. They determined this using a dithionite quenching experiment and NBD-Dap. This experiment is described in Figure 1.18. If the NBD group is accessible to dithionite, the dithionite will quench NBD fluorescence. However, if the NBD group is buried within a membrane, it is not accessible to dithionite and so its fluorescence cannot be quenched. It was found that dithionite could quench only 50% of the fluorescence of NBD-Dap bound to DMPC/DMPG liposomes, suggesting that one half of the NBD-Dap was in the outer leaflet and the other half was in the inner leaflet of the membrane[111]. The presence of cardiolipin (whose presence in bacterial membranes may impart resistance to Dap, see Section 1.8) prevented translocation from the outer to the inner leaflet[111].

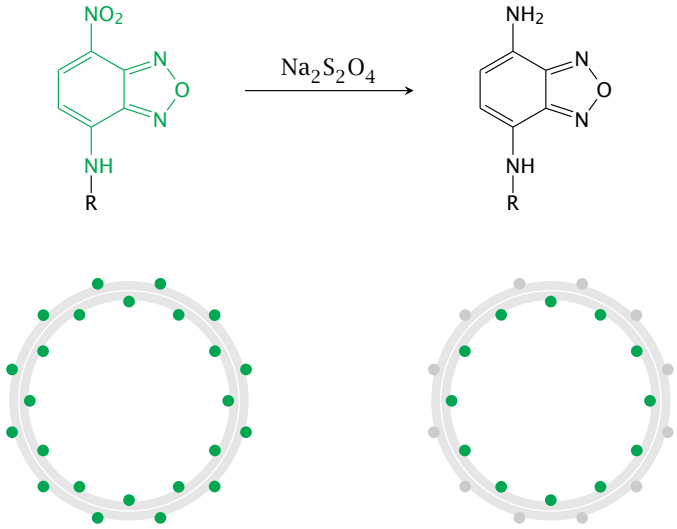

Figure 1.18 Schematic for a dithionite quenching experiment, utilizing nitrobenzoxadiazole (NBD). The NBD is attached to the ornithine residue of Dap. When bound to a membrane, Dap will partition across both membrane leaflets. Dithionite is known to quench NBD's fluorescence, and its addition will initially quench the NBD found only on the outer leaflet. Therefore, the percentage of Dap's translocation into the inner membrane leaflet can be determined.

On the basis of the above-mentioned oligomerization and translocation studies, Zhang, *et al.* suggested that Dap initially forms a tetramer in the outer membrane leaflet. This tetramer translocates to the inner leaflet and then combines with a second tetramer in the outer leaflet, which gives an octameric pore (Figure 1.19). Cardiolipin prevents the translocation to the inner leaflet (Figure 1.19C).

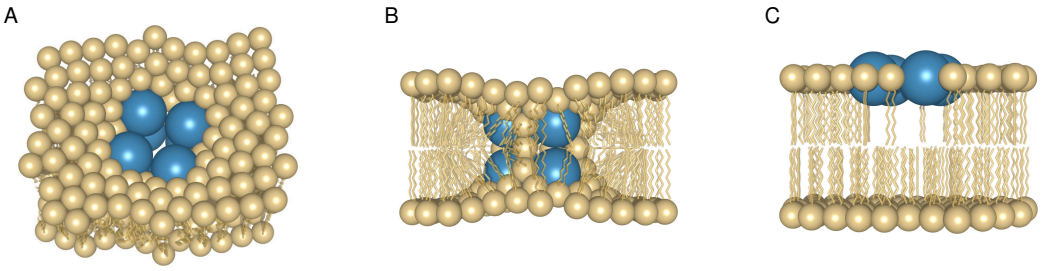

Figure 1.19 A hypothetical model of the membrane inserted oligomer of Dap. A and B: Top and side views of the octamer that spans both leaflets, leading to pore formation. C: When cardiolipin is included within the membrane, Dap is prevented from translocating to the inner leaflet, forming a tetramer that is retained in the outer leaflet. This model was constructed based on the fluorescence data described above, by Dr. Michael Palmer[40]. The Figure was used with permission.

Recently, Müller, *et al.* provided evidence that Dap does not form discrete pores in *B. subtilis*[119]. They utilized inductively coupled plasma – optical emission spectroscopy (ICP-EOS) on *B. subtilis* cells that were treated with either valinomycin or Dap. When valinomycin was added, they observed a dramatic decrease in the concentration of potassium in the cell, indicating that valinomycin was causing a selective efflux of this cation. When these cells were treated with Dap at concentrations that caused cell death but did not induce cell lysis (3.5 μg/mL), they did not see loss of potassium or any other common mono or divalent cations. However, the authors were not clear in their experimental if calcium was present during the experiment (after the cells were initially washed with ethylenediaminetetraacetic acid (EDTA)). Since this detail was omitted, it is difficult to conclude if the experiment was conducted properly. If calcium was not added, it is logical that Dap would not form a pore.

1.7.3 Disruption of Cell Wall Synthesis Enzymes and Macromolecules

Daptomycin has been compared directly to another cyclic peptide, nisin. Nisin has also been observed to form a pore within bacterial membranes, and to function by inhibiting peptidoglycan synthesis[146]. As discussed in the previous section, when permeabilization occurs, a loss of ions leads to the depolarization of the membrane. This loss of membrane potential will immediately reduce the production of ATP[128]. ATP is necessary in the function of many enzymes involved in cell wall synthesis[147,148]. Therefore, to truly understand if Dap selectively inhibits this synthesis, researchers must report more detailed analyses more than just whole cell death.

It has been suggested that the biosynthesis of lipoteichoic acid (LTA), is one of the primary targets of Dap[136]. Although the exact role of LTA in Gram-positive bacteria is still uncertain, it is crucial to the viability of Gram-positive bacteria as mutants display significant growth and physiological defects.

In *E. faecium* and *S. aureus*, Canepari, *et al.* showed that Dap, at its MIC concentration, inhibited the incorporation of glycerol into lipoteichoic acid (LTA) by greater than 90% and the incorporation of phosphate into teichoic acid by greater than 50%, in 20 min[131]. Partial blockage of RNA, DNA, protein and PepG biosynthesis was also found to occur in *E. faecium*. Dap was shown to interact with the cell wall and cell membrane irreversibly and not enter the cytoplasm. Later, they demonstrated, using *E. faecium* protoplasts, that Dap caused 82% inhibition of LTA biosynthesis,

40% inhibition of lipid biosynthesis as well as 14-23% inhibition of RNA, DNA and protein biosynthesis[149].

Laganas, *et al.* have provided evidence that suggests that inhibition of LTA biosynthesis is not the target of Dap[150]. They demonstrated that Dap, at two times its MIC and in the presence of Ca^{2+}, inhibited all macromolecular synthesis in *S. aureus*, *E. faecalis* and *E. hirae* without kinetic or dose specificity for LTA. The possibility that the bactericidal activity of Dap might require ongoing LTA biosynthesis, even if it was not the primary target, was also investigated. As it was known that treatment of *S. aureus* and *E. faecalis* for 1 hour with rifampin results in a complete cessation of macromolecular synthesis, including that of LTA, with no significant loss in bacterial viability, they reasoned that if active or concurrent LTA biosynthesis is required for the action of Dap, then pre-treatment with rifampin should protect bacteria from the activity of Dap[150]. Exposure to Dap at eight times the MIC for 1 hour effectively killed both exponentially growing and rifampin-growth-arrested *S. aureus*. In contrast, the growth-arrested *S. aureus* was protected against the bactericidal activity of ciprofloxacin, an antibiotic that requires active cell division, as well as RNA and protein synthesis[150]. This suggests that LTA biosynthesis is not required for Dap activity. It is unlikely that LTA itself is a target for Dap as it was shown that addition of purified LTA, at concentrations up to 500 μg/mL, did not inhibit the activity of Dap against *S. aureus* and *E. faecalis*[150].

Hachmann, *et al*. has observed, through use of BOPIDY-labeled Dap, that when *Bacillus subtilis*[134] is exposed to Dap it locates to the cell division septum, probably because of the higher percentage of PG found there. Dap was also found to locate to regions where vancomycin and penicillin are usually located. This led some researchers to initially believe that Dap had a similar mode of action to these cell wall synthesis inhibitors. Pogliano, *et al.* suggested that membrane curvature was crucial to Dap's activity[135]. They stated that Dap prefers negative curvature, but failed to determine whether Dap was distributed between membrane leaflets. This theory also does not account for the curvature difference between the outer and inner leaflets, as Dap is likely to interact with both. In a recent study, Müller, *et al.* further disproved this curvature theory by analyzing the effects of Dap addition to a membrane bound ATPase complex[119]. This complex has been used as a reporter for abnormal membrane shapes[151]. From this work they determined that Dap had no effect on this reporter, suggesting that Dap is not selectively choosing a membrane of negative curvature, as previously thought. Nevertheless, when Dap localizes to the cell division septa of *B. subtilis*, likely due to the higher percentage of PG found here, elongated cells are observed[134]. This would suggest

that cell division is affected, especially since DiviVA, a protein that controls cell division, is localized here also. When cells of *S. aureus* were examined for similar morphological changes, elongated cells were not seen, however; cells displayed aberrant division septa[114]. The lack of elongation of the clinically susceptible *S. aureus* cells suggests that Dap could be deregulating cell division, but not actually inhibiting it.

Müller, *et al.* recently proposed a new mechanism of action for Dap[119]. Proteomic studies suggested that Dap inhibits cell wall synthesis in *B. subtilis*. They provide evidence that interaction of Dap to *B. subtilis* membranes leads with a rearrangement of fluid lipid domains, affecting overall membrane fluidity. This resulted in the rapid detachment of the membrane-associated lipid II synthase MurG and the phospholipid synthase PlsX from the interior of the cell membrane. Both proteins preferentially co-localize with fluid membrane microdomains. Although their data, obtained using a range of fluorescence and proteomic techniques, support their claim, they did not acknowledge some of the previous research into this area. This includes the work by Laganas, *et al.* that suggested that Dap is not involved in cell wall synthesis inhibition since it was effective on bacteriostatic cells[150]. Bacteriostatic cells would not require active MurG. Similarly, Wolf, *et al.* showed that Dap is still active against bacterial L-forms which do not contain a cell wall[152]. This supports the notion that the dislodgment of MurG is not required for Dap activity. That being said, PlsX is likely to be active even in bacteriostatic cells. It is therefore possible that Dap works through a dual mechanism of action, dislodging this enzyme and also forming a pore.

1.7.4 Lipid Flip-Flop, Membrane Fusion and Lipid Extraction

Several researchers have shown, through studies on model membranes, that the interactions of Dap with the membrane can induce more dramatic disruptions of the membrane itself[82,109,120]. The studies described below were done utilizing model membranes only, and therefore must be taken tentatively since these mechanisms have not been shown to occur with Dap-susceptible bacteria.

The Hancock group showed several unique interactions of Dap within model membranes. Jung, *et al.* observed, using differential scanning calorimetry (DSC) and NMR spectroscopy, that Dap (at concentrations above its MIC, 8 μg/mL), when added to PC/PG containing membranes, caused membrane fusion[109]. They stated that this likely occurred due to Dap reducing the charge of the acidic lipids on the outer membrane, making two or more vesicles more likely to interact. The authors

pointed out that it is unlikely that this mechanism would occur *in vivo*. This is due to the presence of the cell wall surrounding Gram-positive bacteria. This cell wall is thick (~80 nm[38]) and therefore it is highly unlikely that two or more cells would fuse together based on Dap interacting with their cytoplasmic membranes. Jung, *et al.* also observed a rapid flip flop in their model membranes with addition of Dap, when they incorporated a fluorophore (NBD) labeled synthetic lipid[82]. The increased polarity imparted by NBD on the acyl chain may have affected the vertical mobility of this lipid in the fluid bilayer.

Recently, Chen, *et al.* suggested a novel mechanism of action for Dap[120]. They stated that Dap was selectively causing an extraction of lipids from their model membranes. They concluded this by visualizing the treatment of giant unilamellar vesicles with Dap, while keeping the vesicles under slightly negative pressure, with a pipette. When Dap was added they saw the vesicles retract from the pipette, which they stated was due to an increase in surface tension, solely through specific lipid molecule extraction. However, the author's did not comment on the fact that Dap could be increasing the surface tension in other ways, including adding a strain to the membrane curvature.

Overall, from this section it is clear that there are numerous proposed mechanisms of action for Dap. Among these are pore formation, inhibition of cell wall synthesis, lipid extraction, and cell division disruption. The most experimentally supported mechanism, substantiated on both model membranes and bacterial cells involves Dap oligomerization in the membrane resulting in the formation of a cation-selective pore which leads to membrane depolarization and cell death[40,45,46,48,59,110,126,153–156].

1.8 Proposed Mechanisms of Resistance for Daptomycin

Although Dap has been used clinically for almost 15 years,[12] clinical isolates of Dap-resistant bacteria are still relatively rare.[9,10,12] Nevertheless, resistance to Dap is a growing concern as clinical isolates of Dap-resistant bacteria are appearing with increasing frequency[59]. Determining how bacteria become resistant to Dap may allow for the rational development of Dap analogs that are active against Dap-resistant bacteria and can provide vital clues to elucidating Dap's mechanism of action.

1.8.1 Reduction in PG Levels

Most Gram-positive bacteria contain three main phospholipids, phosphatidylglycerol (PG), lysyl-PG and cardiolipin (CL) (Figure 1.18)[38]. PG, as discussed previously, is necessary for Dap activity. Therefore a decrease in the percentage of PG within the bacterial membrane would, logically, decrease Dap's antibacterial effect. This likely explains the resistance of *Streptomyces roseosporus,* the natural producer of Dap, as this bacterium contains very little PG in its cell membrane[9,10]. This inherent feature also explains the lowered toxicity of Dap in humans, since mammalian cells contain less PG than most Gram-positive bacteria. Bacteria have recognized Dap's dependence on PG, and therefore the main mechanism of Dap resistance is through cell membrane alternation, including PG depletion[48].

The *pgsA* gene encodes a phosphatidyltransferase, that is directly involved in the production of PG[134,157,158]. Mutations in this gene that reduce this enzymes activity have been found to lower the precentage of PG in the cell membrane. Such mutations have been shown to occur in Dap-resistant *B. subtillis* and *S. aureus*.

1.8.2 Mutations of *mprF* and Role of Lysyl-PG

Lysyl-PG is a common phospholipid found in Gram-positive bacteria[87]. The biosynthesis of lysyl-PG occurs through a transesterification reaction that utilizes a PG lipid and lysyl-tRNA[159,160]. MprF, a multiple peptide resistance factor enzyme, mediates this process. MprF has a dual function (Figure 1.20) whereby it converts a PG lipid to lysyl-PG and then flips the lysyl-PG to the outer leaflet[161,162].

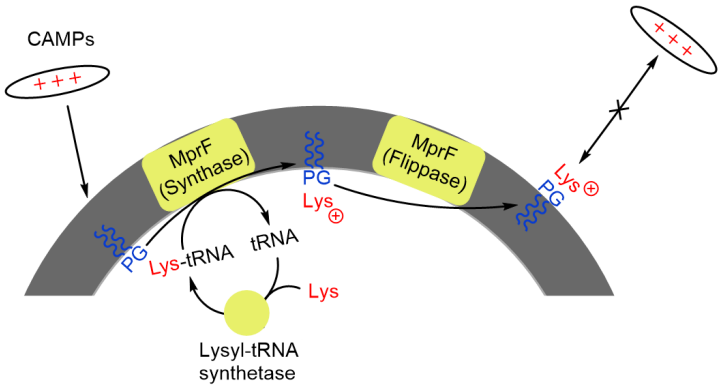

Figure 1.20 The function of MprF. The MprF protein first converts PG into lysyl-PG through a transesterification process. The second step involves the flipping of lysyl-PG from the inner to outer membrane leaflet. The increase in positive charge on the outer leaflet prevents cationic antimicrobial peptides (CAMPs) from undergoing membrane insertion. Image is adapted from Ernst, *et al*[161].

Unlike PG, which bears a negative charge, lysyl-PG bears a positive charge. Lysylation of PG results in an increase in the positive charge on the surface of the cell membrane. It has been proposed that this affects the ability of Dap to interact with the membrane, by preventing or interfering with a proposed Ca^{2+}-bridged interaction between the phosphate group of PG and an aspartate residue on Dap.

Isolates of *S. aureus* that are resistant to Dap show an increase in the percentages of lysyl-PG within the membrane, through an up-regulation of MprF[48,104]. Expectedly, depletion of MprF causes a hypersensitivity to Dap. Kilelee, *et al.* suggested that lysyl-PG's resistance only occurs after Dap has become membrane bound[163]. This is supported with work by Mishra, *et al.* who found that not all mutations in MprF alter the membrane charge ratio[164]. Therefore it is possible that up regulation of *MprF* simply results in a reduction of the percentage of PG in the membrane. In summary, the increase in the amount of lysyl-PG in the membrane could affect Dap's ability to function by three different mechanisms: by reducing the percentage of PG within the membrane, by repelling Dap and, when Dap is finally bound, by exerting another, currently unknown, effect.

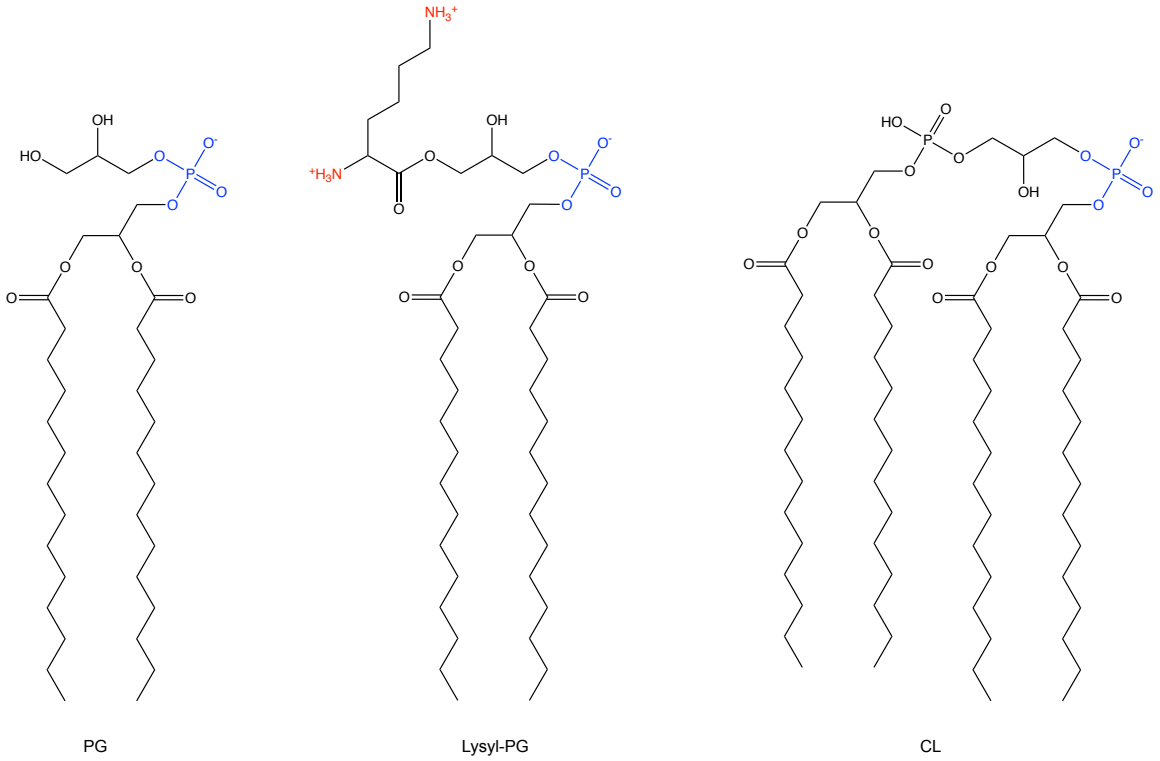

Figure 1.21 Chemical structures of the three major phospholipids found in Gram-positive bacteria. Phosphatidylglycerol (PG), lysyl-PG and cardiolipin (CL) all have myristoyl acyl tails for representation. The anionic groups are shown in blue, the cationic groups in red. The net charge of CL has been controversial in recent years. Kates, *et al.* showed, through a potentiometric approach that the phosphate pKa's are 2.8 and ~7.5-9.5[165]. Recent evidence by Sathappa, *et al.* suggests that each phosphate could instead act as independent strong acids, resulting in a net charge of -2[166]. The true net charge of CL, therefore, still remains unclear.

1.8.3 YycFG (WalKR) Mutations

The *yycFG* operon is a group of genes involved in Dap-resistant phenotypes. Among the proteins that the *yycFG* operon encodes are YycG and YycF[11]. These two proteins are part of a two-component regulatory system required for viability in Gram-positive bacteria. The *yycFG* system functions as a master regulatory system for cell wall metabolism and biofilm formation[167]. In *B. subtilis*, YycG is the histidine kinase of the *yycFG* system, and is localized to the cell division septum where it regulates cell division and cell wall restructuring[168].

Several mutations in different locations of the *yycFG* operon in Dap resistant *S. aureus* were reported by Howden, *et al.*, but the exact contribution of these mutations is unclear[169]. Nevertheless, a

single amino acid change in YycG was sufficient to increase Dap's MIC from 0.5 to 2 μg/L, a value that is sufficient for clinical Dap resistance. In *E. faecium*, mutations in yycFG operon have been found in Dap-resistant strains[155].

Baltz has pointed out that, in addition to the genetic studies mentioned above, other lines of evidence suggest a relationship between yycG and Dap's MOA[11]. Both Dap and YycG are found near the cell division septum of bacteria. Dap has also been shown to induce minor morphological changes on both *S. aureus* and *B. subtilis*, leading to unnatural division septa. When YycG is depleted, these septa are also changed. The depletion of YycG has been shown to cause cell death without lysis, similar to Dap. YycFG also positively regulates biofilm formation while Dap treats *S. aureus* biofilms effectively. Baltz therefore suggested a dual mechanism of action for Dap: interruption of YycG and membrane depolarization[11].

1.8.4 LiaRS Activation

Dap has also been found to activate a membrane associated transcriptional regulator, LiaRS[134,170]. This two-component regulator is thought to be involved in the cell membrane adaptive responsive to antibacterials. Both Hachmann, *et al.* and Wecke, *et al.* have observed that when *B. subtilis* was treated with Dap, the expression of LiaRS increased >400 fold[134,170]. Friulimicin, another calcium-dependent antibiotic that is similar to Dap, was found not to up-regulate the production of LiaRS[170]. This suggests that Dap's activation of this protein regulator is specific. Arias, *et al.* characterized several LiaRS mutations found in clinical isolates of both *E. faecalis* and *E. faecium* that induce resistance to Dap[171]. When LiaRS was activated, the expression of both LiaI and LiaH were greatly increased[172]. These proteins are known to segregate to separate domains of the plasma membrane but their role in Dap resistance is, to date, unknown.

1.8.5 Cardiolipin

Cardiolipin (CL) is a phospholipid found in most Gram-positive bacterial membranes. Hachmann, *et al.* observed that the lipid composition of strains of *S. aureus*, which were Dap-resistant, had a decrease in the PG percentages within the membrane[157]. The lysyl-PG percentages were increased, but the CL percentages remained relatively unchanged. This suggests that Dap

resistant strains are not overproducing CL synthase. The role of CL in Dap's resistance is, therefore, still not well understood.

Recently, Zhang, *et al.* explored the role of CL in Dap resistance utilizing model membranes that contained varying percentages of CL[111]. Through use of both ITC and fluorescence studies (explained in Section 1.7) the authors showed that Dap inserted into liposomes containing CL. Although Dap was able to interact with these membranes, the translocation of the oligomer to the inner leaflet was prevented. This therefore prevented a pore from forming, suggesting that CL is directly inhibiting oligomer interaction within the membrane. However, the fact that the production of CL is not increased in Dap-resistant strains suggests that CL may not be overly important for Dap resistance *in vivo*.

1.8.6 Other Possible Mechanisms of Resistance

Tran, *et al.* outlined that some non-pathogenic bacteria have developed enzymes that hydrolyze the ester bond in Dap, thus destroying the antibiotic[48]. This has not yet been observed to occur in clinical isolates.

Enhanced expression of the *dlt* operon has been found to occur in Dap-resistant *S. aureus* strains[49,89,164,173]. Genes of the dlt operon are involved in the introduction of D-alanine to cell wall teichoic acids of the Gram-positive bacteria. The modification of LTA with a positively charged residue (the terminal amino group of alanine) could repel Dap from the membrane, reducing Dap's activity.

1.9 Research Goals and Objectives and Thesis Overview

From Section 1.7, it is clear that although the mechanism of action for Dap is still not known with certainty, the mechanism that is best supported by the experimental evidence involves Dap oligomerization in the cell membrane which leads to the formation of cation-selective pores, which results in membrane depolarization and, finally, cell death. The goal of this thesis is to further investigate this proposed mechanism of action.

In Chapter 2, the objective was to determine the stoichiometry of calcium to Dap in the presence of liposomes and how calcium concentration affects Dap oligomerization and membrane

insertion. These results of these studies suggest that the binding of the first calcium ion to Dap causes oligomer formation of Dap in the membrane. The binding of a second calcium ion to Dap causes a deeper insertion of this oligomer.

In Chapter 3, the objective was to determine how pre-oligomerization of Dap affects antibacterial activity. This was investigated though the synthesis and characterization of a Dap dimer. These studies revealed that the bacterial cell wall plays an important role in Dap resistance.

In Chapters 4 and 5, the objective was to determine the effect of liposome acyl chain composition on Dap's ability to interact with, oligomerize, and form pores in liposomes. Overall, these results demonstrated that the lipid acyl chain composition has drastic effects on the activity of Dap, which may explain the difference in Dap susceptibility among Gram-positive bacteria.

Chapter 2

Two successive calcium-dependent transitions mediate membrane interaction and oligomerization of Daptomycin and the related antibiotic A54145[1]

2.1 Introduction

The mechanism of action for Daptomycin (Dap) is subject to continued debate among researchers. It has been shown in the literature that a required step in Dap's mechanism involves its insertion within the cytoplasmic membrane of Gram-positive bacteria, specifically to phosphatidylglycerol (PG)[40,45,111,126]. Dap is also known to require calcium for activity and many have theorized that Dap inserts into the membrane in multiple calcium binding events[40,45,111,125,126]. Previous studies have suggested that Dap forms distinct oligomeric structures within the membrane, with 6-8 subunits per oligomer[115].

In the literature, model membrane systems have been used widely to study the mode of action of Dap[45,109,118,120], mainly due to the ability to freely adjust the membrane composition. A one-to-one mixture of phosphatidylcholine (PC) and PG has been used previously to study Dap[109,118,125,126]. While this model doesn't closely mimic the membranes of Gram-positive bacteria, it nevertheless has been shown to be sufficient to determine that Dap's interaction with the membrane is calcium-

[1] The results displayed in this chapter have been published: "Two successive calcium-dependent transitions mediate membrane interaction and oligomerization of daptomycin and the related antibiotic A54145," by Robert Taylor, Khalida Butt, Bradley Scott, TianHua Zhang, Jawad K. Muraih, Evan Mintzer, Scott Taylor and Michael Palmer, **2016**, *Biochim. Biophys. Acta., 1858,* 1999-2005[116].

Authors contributions: Dr. Scott Taylor synthesized and purified acrylodan-Dap. Robert Taylor and Khalida Butt ran the ITC experiments. Robert Taylor completed all other results. Manuscript was written and devised by Dr. Michael Palmer.

dependent[76,82]. Although PC is not found in Gram-positive bacteria[106], its incorporation allows for a more direct determination on the role of Dap to PG interaction. This is due to the fact that PC is a neutral lipid, and therefore would not be involved in Dap-Ca^{2+}-PG interactions. Dap has also been found to only interact with PC only membranes at un-physiologically high calcium concentrations and that oligomerization was not observed[126]. With this model, Dap was shown to form oligomers of definitive size, spanning both membrane leaflets[126], forming an ion selective pore[45]. The exact details remain to be elucidated, with particular interest on calcium stoichiometry. Circular dichroism (CD) experiments suggest that Dap has two structural transitions when calcium is present, both in solution and with membranes[82]. Recently Lee, *et al.* have suggested, through CD experiments, that calcium interacts with Dap, in the membrane, in a 3:2 Ca^{2+}:Dap ratio[174].

Isothermal titration calorimetry (ITC) experiments determined that Dap likely has two calcium-binding interactions within model membranes, but which amino acids were involved was unclear. Fluorescence was explored to answer this question, utilizing a fluorophore sensitive to polarity changes (acrylodan). Acrylodan is advantageous due to its prominent blue shift and fluorescence increase when surrounded by a hydrophobic medium[175]. This property was utilized to study the oligomer formation of Dap when bound to calcium. A similar antibiotic to Dap, in terms of structure, was also investigated. A54145-Factor D (A5) contains a tryptophan in the first position, with an acrylodan on the lysine8 residue. This allowed for a further study of four different amino acid positions, 1, 6, 8 and 13 (Figure 2.3). A5 has not been studied in as much detail as Dap but (as discussed in Chapter 1) their mechanism of action should be similar, as both require calcium and PG for proper activity and have very similar antibacterial activities[72]. Zhang, *et al.* also showed that mixtures of Dap with a semi-synthetic analog of A5, CB-182,462, form partially functional hybrid oligomers, thus suggesting that A5 likely has a very similar mode of action to Dap[110].

The experiments shown here outline that Dap (and likely A5) interact with the membrane in two successive calcium-binding events. With the first binding of calcium, Dap inserts into the membrane and forms oligomeric structures that are retained in the outer leaflet. The second calcium ion causes deeper insertion and, potentially, translocation of the oligomers into the inner leaflet. The oligomers on each leaflet are then united, thus forming a trans-membrane ion selective pore[45].

2.2 Materials and Methods

2.2.1 Synthesis of Acrylodan-Labeled Daptomycin

Briefly, acrylodan (Setareh Biotech, Eugene, OR, USA) was attached to the unique free side chain amino group of ornithine6 of Dap (generously provided by Jared Silverman, Cubist Inc.©) in potassium phosphate buffer at pH 8.0 for 24 hours. The product was then purified by HPLC and purity was confirmed by HPLC and mass spectrometry. For details and procedures on the synthesis and purification of the acrylodan-Dap, see Appendix A.

2.2.2 Synthesis of Acrylodan-Labeled A54145-Factor D

Briefly, acrylodan (Setareh Biotech, Eugene, OR, USA) was attached to the unique free side chain amino group of lysine8 of A54145-Factor D (generously provided by Jared Silverman, Cubist Inc.©) in sodium phosphate buffer for 5 days. The product was then purified by HPLC and purity was confirmed by HPLC and mass spectrometry. For details and procedures on the synthesis and purification of the acrylodan-A5, see Appendix A.

2.2.3 Antibacterial Activity

Antimicrobial susceptibility tests were performed according to Wiegand, *et al.*[176] with minor revisions. Serial dilutions of Dap, A5, acrylodan-Dap and acrylodan-A5 were prepared using 96-well microtitre plates in Luria-Bertani (LB) broth (for *Bacillus subtilis* ATCC 1046) that was supplemented with 5 mM calcium chloride. Inoculation was performed by first diluting overnight cultures to a turbidity of a 0.5 McFarland standard. This diluted culture was then added to the plate in a 1:1 mixture, with the appropriate antibiotic volume.

Growth was assessed visually after incubation at 30^{o}C (for *Bacillus subtilis* ATCC 1046) overnight. The transition from translucency (inhibition) to high turbidity (growth) occurred abruptly. Intermediate turbidity occurred only rarely, but when this was observed this concentration was not considered inhibitory. Control experiments included testing a positive (growth) and a negative (sterility) control. Each antibiotic concentration was tested three times and in triplicate.

2.2.4 Preparation of Liposomes

Lipids used included 1,2-dimyristoyl-sn-glycero-3-phosphocholine (DMPC), 1,2-dimyristoyl-sn-glycero-3-phospho-(1'-rac-glycerol) (sodium salt; DMPG), 1,2-dioleoyl-sn-glycero-3-phosphocholine (DOPC), and 1,2-dioleoyl-sn-glycero-3-phospho-(1'-rac-glycerol) (sodium salt; DOPG). All lipids were obtained from Avanti Polar Lipids, Alabaster, AL, USA.

Equal proportions of phosphatidylcholine (PC) and phosphatidylglycerol (PG) were added to a round bottom flask and dissolved in a 3:1 mixture of chloroform:methanol. The dissolved lipids were dried under purified nitrogen and kept under high vacuum overnight. The dried lipid film was then suspended in HEPES-buffered saline (20 mM HEPES, 150 mM NaCl, pH 7.4) and vortexted until all lipids were detached from flask and suspended in buffer. These multilamellar vesicles were extruded under pressurized nitrogen through polycarbonate membranes (0.1 nm in diameter), fifteen times, to produce LUVs[177]. During the preparation of the LUVs the temperature of flasks/extruder that contained lipids was kept at 30^{o}C, above the transition temperature of the lipid species. In fluorescence experiments, dimyristoyl lipids (DMPC/DMPG) were used, whereas dioleoyl lipids (DOPC/DOPG) were used for ITC experiments.

2.2.5 Fluorescence Spectroscopy

Steady state experiments were acquired by using a PTI QuantaMaster 4 instrument, with a Xenon lamp (Ushio Inc.) as the source. The samples contained HEPES-buffered saline with native and acrylodan-labeled Dap and A5, alone or in combination at final total concentrations of 3 μM. Calcium was added or titrated in as described throughout Section 2.3. Excitation wavelengths were 280 nm for tryptophan in the case of A5, 365 nm for native Dap, acrylodan-Dap and acrylodan-A5. All fluorescence measurements were run in triplicates and were carried out at 37°C.

2.2.6 Isothermal Titration Calorimetry (ITC)

ITC titrations were carried out on a MicroCal ITC 200 instrument (GE Healthcare), with similar conditions to previous work by Dr. Evan Mintzer[111]. DOPC/DOPG (1/1 molar ratio) were loaded into the ITC cell at final concentrations of 3.55 to 4.55 mM total lipid. This was premixed

with Dap at final concentrations ranging from 150 to 510 μM. The Dap stock concentrations were determined by spectrophotometry, measuring the kynurenine13 residue[178]. Calcium chloride was loaded into the injection syringe (Malvern Instruments Ltd.) at 5 or 10 mM and injected in increments of 1 or 2 μL. External software (created by Dr. Michael Palmer) was used to integrate and baseline-correct the heat peaks observed. The integrated heats were fitted using models that assumed a single type of binding sites, or the sequential binding to two types of sites, with either fixed or variable calcium/Dap stoichiometry. All ITC measurements were carried out at 25^{o}C, as this temperature was previously shown to be adequate for measuring Ca^{2+}-Dap interactions in model membranes[111].

2.3 Results

2.3.1 Calcium Stoichiometry

As discussed in Chapter 1, calcium was determined early on in Dap studies to be required for proper activity and membrane interaction. In 2014, Zhang, *et al.* supported these observations, through the use of ITC (performed by Dr. Evan Mintzer)[111]. Unfortunately, little emphasis was given to the stoichiometry of calcium to Dap. Determining this stoichiometry should provide additional detail on the mode of action. To accomplish this, calcium (5 or 10 mM) was titrated into a sample that contained 150 to 510 μM Dap with an excess of liposomes (3.55 to 4.55 mM). An excess of liposomes was used to more directly study the stoichiometric interaction of calcium to Dap. The membranes used were a 1/1 molar ratio of dioleoylphosphatidylcholine (DOPC)/ dioleoylphosphatidylglycerol (DOPG). The most reproducible isotherm with the largest heats observed was found with the following conditions: 510 μM of Dap, 3.55 mM DOPC/DOPG and 10 mM calcium titrated into the 200 μL cell, at 1 μL increments. The raw ITC trace for one such experiment is shown in Figure 2.1A. Controls were run with calcium titrated into Dap and LUV separately. Calcium alone caused very minimal signal in either case, as shown by the titration of calcium into LUV alone (Figure 2.1A, blue line). The peaks, integrated relative to the baseline shown in red, resulted in an isotherm shown in Figure 2.1B. There is an initial downward slope in the isotherm but the raw trace shows similar heats generated for these data points. As the titration proceeds, the remaining free Dap decreases after each injection of calcium. This decrease in free Dap leads to peaks that appear shorter but are only wider, indicating a slower rate of reaction.

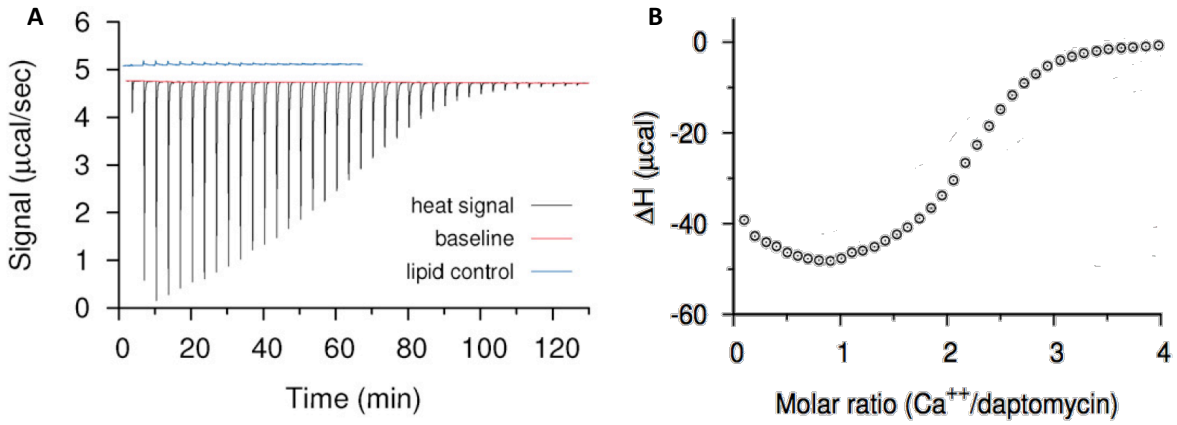

Figure 2.1 Isothermal titration calorimetry (ITC) for calcium titrated into a mixture of Dap and LUV. A: A raw trace for a representative isotherm showing calcium binding to Dap. In this case, calcium (10 mM) was titrated into a 200 µL cell, at 1 µL increments, that contained Dap (510 µM) and LUV (3.55 mM). The adjusted baseline is shown in red. When calcium was titrated into LUV alone, minimal signal was observed (blue line). B: The integrated peaks (ΔH) from the raw trace are plotted against the molar ratio of calcium.

The data was then modeled using software developed by Dr. Michael Palmer, as shown in Figure 2.2. Using a model that dictates that a single class of calcium binding sites exists, all with the same affinity to Dap, a stoichiometry of 2 fits the data better than assuming a stoichiometry of 1 or 3 (Figure 2.2A). When the stoichiometry was not confined to a defined integer and allowed to vary freely, a stoichiometry of 2.40 calcium ions to Dap was calculated. Although this model is a better fit to the isotherm, it is still relatively inaccurate (Figure 2.2B, blue line). When a model that allows for multiple binding sites was used a better fit was observed. The model that proved to be most successful, giving a more plausible stoichiometry of 2.06, assumed two sequential binding sites for calcium, of distinct affinity (Figure 2.2B, red line).

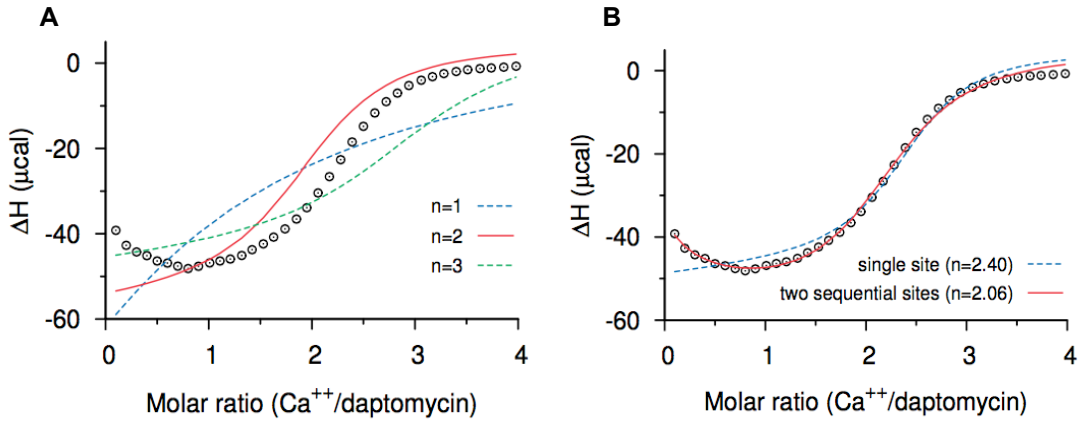

Figure 2.2 Modeled isotherms for the determination of calcium stoichiometry to Dap. A: External software was used to model the data assuming binding was occurring. The stoichiometry was varied freely. B: When the stoichiometry from the previous model was not restricted to an integer, a calcium stoichiometry of 2.40 was calculated (blue line). This model was more accurate than Figure 2.2A but still did not fit line perfectly. When the model assumed distinct, sequential binding of calcium, the model fit more accurately (red line). This modeled isotherm gave a calcium to Dap stoichiometry of 2.06.

From six independent experiments, the averaged stoichiometry was found to be 1.81±0.29. If it is assumed that calcium binds solely Dap and PG within the membrane, the results suggest that a stoichiometry of 2 calcium ions to Dap (not 1.81). A stoichiometry of 2:1 suggests that two distinct calcium-binding events occur with Dap. The potential for an uneven number, including a 3:2 Ca^{2+}:Dap ratio, recently reported by Lee, *et al.*[174], is possible, and remains to be explored in more detail. The important finding with the results presented here is that greater than one calcium ion is necessary for oligomer formation of Dap and therefore it is expected that separate calcium-binding events could be observed with fluorescence. The reaction heats and dissociation constants were calculated, shown in Table 2.1. Both the dissociation constant and enthalpy was found to be lower with the second addition of calcium, suggesting a more favourable interaction with the oligomers. This favourable interaction could be what drives the oligomer to translocate into the inner leaflet.

Parameter		*Average*	*Standard Deviation*
Stoichiometry (Ca^{2+}/Dap)		1.81	0.29
First Step	ΔH	-4.36 kJ/mol	0.48 kJ/mol
	K	5.65 x 10^4 M^{-1}	3.65 x 10^4 M^{-1}
Second Step	ΔH	-6.57 kJ/mol	1.14 kJ/mol
	K	2.98 x 10^4 M^{-1}	1.61 x 10^4 M^{-1}

Table 2.1 Parameters for the binding of calcium to Dap within 1/1 DOPC/DOPG membranes. Stoichiometries, reaction heats (ΔH), and dissociation constants (K) are shown, with their standard deviations. Only the parameters for the model that assumes two sequential binding sites with distinct affinities are shown. Averages and standard deviations were calculated form six different experiments.

2.3.2 Calcium-Dependent Changes in Fluorescence Emission Scans

Fluorescence has been used extensively to study the interaction of Dap to model membranes. Dap requires the presence of calcium and phosphatidylglycerol for membrane insertion. Muraih, *et al.* proposed that multiple calcium ions are involved in an oligomeric pore formation[115,126]. In this work, Dap was labeled with a nitrobenzoxadiazole (NBD) moiety on the ornithine6 residue. NBD is a fluorophore that shows an increase in signal when bound to a hydrophobic membrane. Based on their results, Muraih, *et al.* suggested that multiple calcium ions are required for Dap membrane interaction. This finding was supported by the ITC results presented previously, arguing that two calcium ions are involved in Dap to membrane interaction. To distinguish the suspected two-calcium binding events, a more sensitive fluorophore was used. The NBD group was replaced with acrylodan, still at the ornithine6 residue (Figure 2.3). Acrylodan is a fluorophore that is highly sensitive to its environment[127,175]. Therefore replacing NBD with acrylodan gives a more sensitive measurement of the binding properties of ornithine. Acrylodan also has a higher quantum yield than NBD, allowing for a better fluorescent signal.

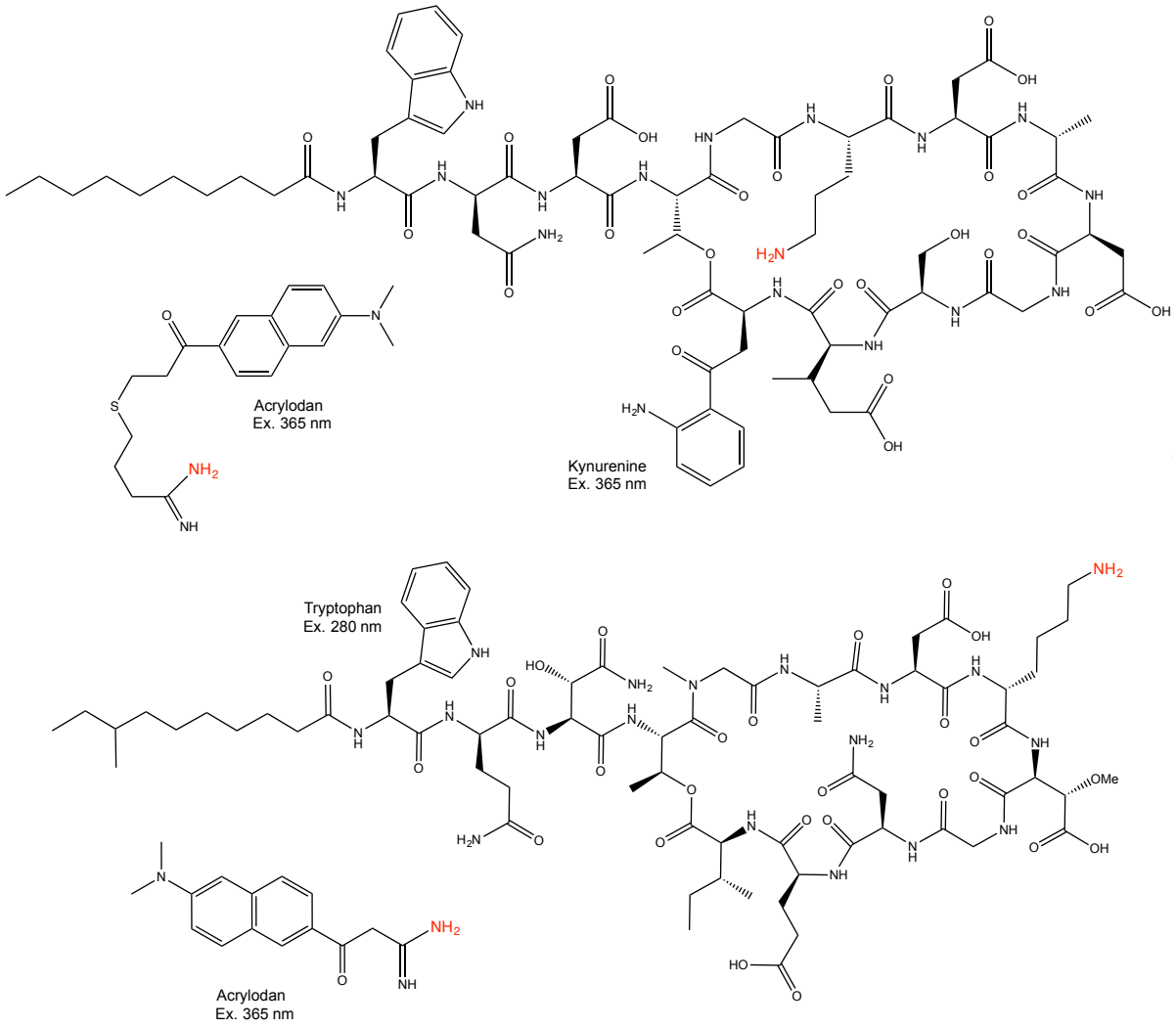

Figure 2.3 Structures of acrylodan, Dap and A5. Top: The structure of Dap. The terminal amino group of ornithine6 is highlighted in red. Thiol-linked acrylodan is shown and highlighted in red to display where the acrylodan is found on Dap. Bottom: The structure of A5. The terminal amino group of lysine8 is highlighted in red. Acrylodan is shown and highlighted in red to show where the acrylodan is found on A5. The excitation wavelengths of each fluorophore are also stated.

When in a hydrophobic environment, acrylodan experiences a distinct blue shift and fluorescence increase[175,179]. This can be seen when acrylodan-Dap is added to LUV (1/1 DMPC/DMPG) and calcium is titrated in, Figure 2.4.

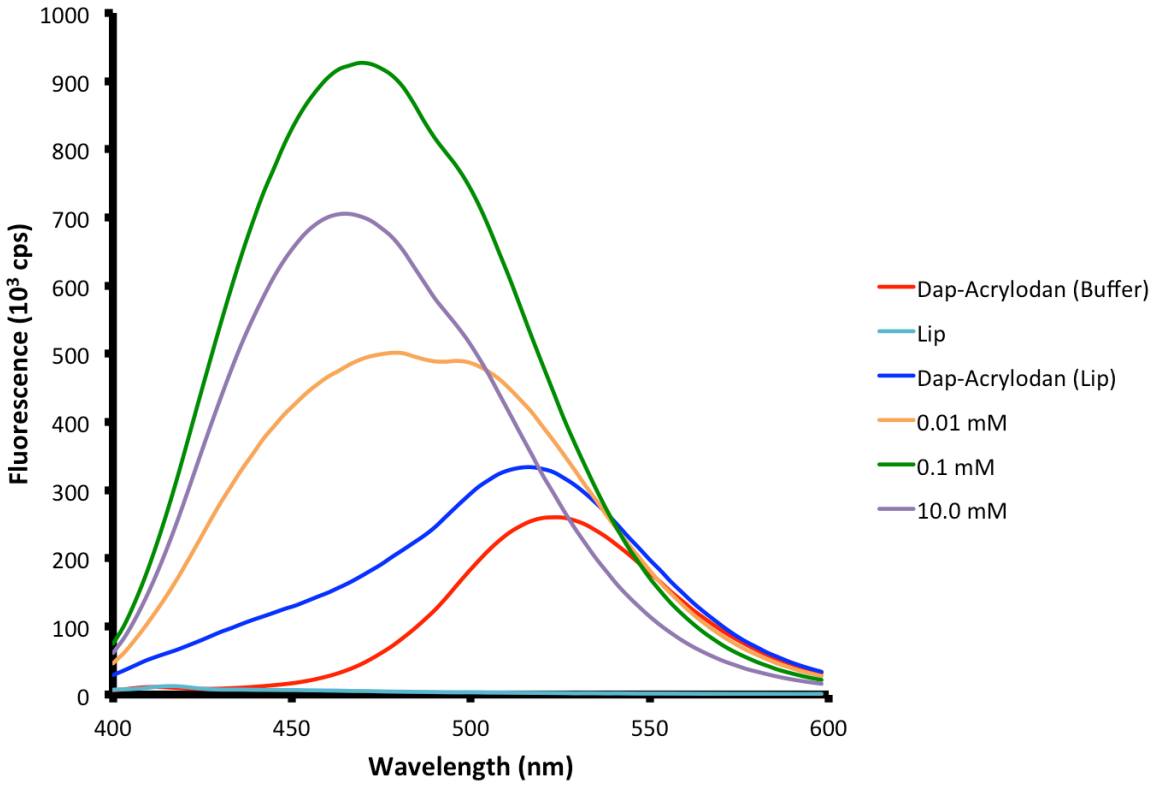

Figure 2.4 Acrylodan's sensitivity to a non-polar environment. Acrylodan-Dap (3 μM) was added to LUV (250 μM) and calcium was titrated in from 10 μM to 10 mM. Acrylodan's signal is greatly dependent on the environment. When 0.1 mM Ca^{2+} is added, acrylodan has a prominent blue shift and fluorescence increase. Upon addition of higher concentrations of calcium, the acrylodan signal decreases and experiences no red shift. There is a very slight blue shift, indicating kynurenine is more deeply inserted into a hydrophobic medium.

Acrylodan-Dap was used to study the interaction of ornithine6, to the membrane, in order to observe oligomer formation. The addition of calcium causes the acrylodan signal to increase (Figure 2.4). This signal intensity shows two distinct stages, suggesting the presence of separate calcium binding effects on acrylodan. The calcium binding phases observed through fluorescence can then be correlated to the ITC results. It is important to note that native Dap contains a kynurenine (an intrinsically fluorescent amino acid), which overlaps with acrylodan in its emission spectrum. However, acrylodan has a much higher quantum yield than kynurenine and approximately four times the absorbance[76]. Therefore at all calcium concentrations the acrylodan signal dominates the spectrum.

Both native Dap and acrylodan-Dap were incubated with 1/1 DMPC/DMPG LUV for 3

minutes, in HEPES-buffered saline. Calcium was then added to the sample stepwise from 10 μM to 100 mM to observe the calcium concentrations required for membrane insertion. As seen in Figure 2.5, the kynurenine within native Dap shows minimal signal increase until 0.1 mM calcium with a maximal signal at >0.1 mM calcium. In contrast, acrylodan Dap has a distinct blue shift and fluorescence increase with the addition of just 10 μM calcium, with maximal signal occurring at ~ 0.1 mM calcium. The addition of any more calcium causes a decrease in fluorescence intensity (Figure 2.5). At these calcium concentrations, acrylodan experiences a slight blue shift (green to purple line of Figure 2.4) which could be attributed to either acrylodan inserting more deeply within the membrane or the kynurenine residue of Dap starting to insert. The decrease in acrylodan signal suggests that mutual acrylodan interactions might be occurring within the membrane. From Figure 2.5, it is clear that there are two calcium transitions occurring, one at ~ 0.1 mM calcium, the second at higher concentrations, >0.1 mM.

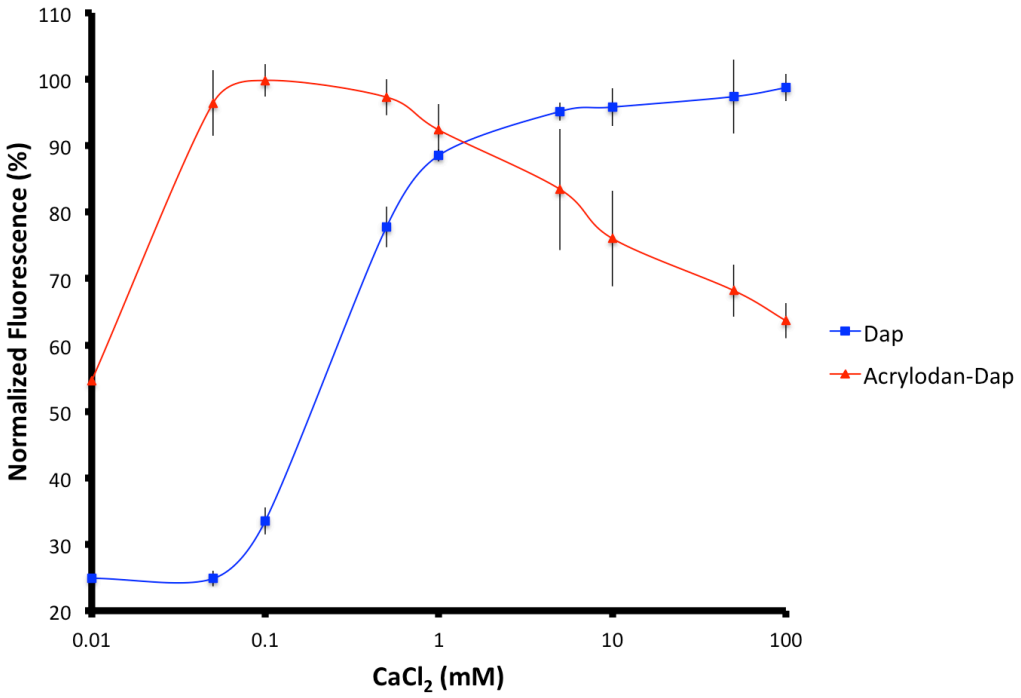

Figure 2.5 Comparison of kynurenine fluorescence between Dap and acrylodan-Dap. Dap or acrylodan-Dap (3 μM) was added to LUV (250 μM) and titrated with calcium. In the case of Dap, there is minimal signal until >0.1 mM calcium, where the signal intensity of kynurenine greatly increases. Acrylodan-Dap's signal increases sharply from 10 μM to 0.1 mM calcium. The addition of higher concentrations of calcium causes a fluorescence decrease. This data suggests two calcium-binding interactions are occurring. Both samples were excited at 365 nm and emitted from 400-600 nm. Error bars represent the standard deviation of three different experiments, ran at 37°C.

The experiments were repeated, where Dap and acrylodan-Dap were replaced with A5 and acrylodan-A5. Acrylodan was attached to the lysine8 residue of A5, shown in Figure 2.3. In regards to calcium saturation, Acrylodan-A5 showed similar trends in fluorescence compared to acrylodan-Dap, shown in Figure 2.6. Acrylodan-A5 had maximal signal at 0.1 mM calcium; the addition of higher concentrations (>0.1 mM) caused a decrease in signal intensity, identical to that seen for acrylodan-Dap. Once acrylodan-A5 reaches its maximal signal at 0.1 mM Ca^{2+}, higher calcium concentrations do not induce any blue or red shift. This suggests that the slight blue shift seen in Figure 2.4 (green to purple line of acrylodan-Dap's emission spectrum) is due to the intrinsic kynurenine of Dap starting to insert into the membrane. A5 does not contain kynurenine, and therefore measuring the tryptophan found natively in A5 was feasible. This inherent structural difference also allowed the study of another residue, position 1, on its interaction with calcium and

the membrane. Tryptophan experiences a distinct blue shift upon entering a hydrophobic environment, but the signal intensity is relatively unchanged. The interaction of native A5 with the liposome was therefore observed by measuring the mean tryptophan wavelength at each calcium concentration. When comparing the interaction of kynurenine and tryptophan of Dap and A5, respectively, in regards to calcium saturation, they behave identically, in that, higher calcium concentrations are required to cause membrane insertion. The difference in calcium concentrations necessary for membrane interaction, between both labeled to un-labeled analogs, suggests two separate calcium-binding events.

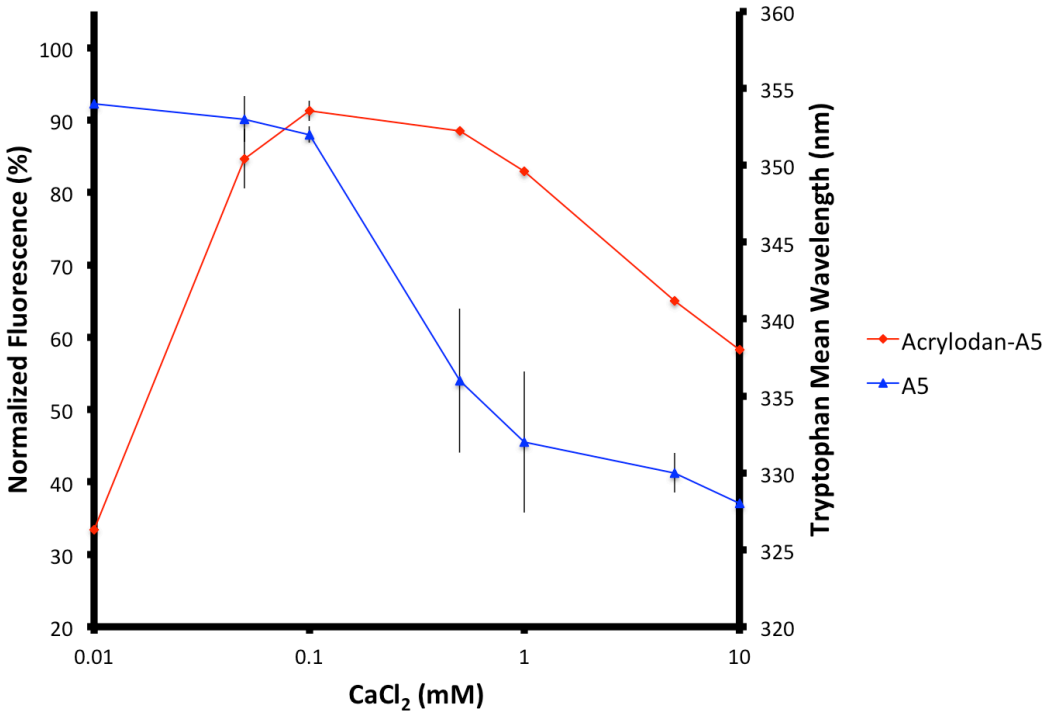

Figure 2.6 Comparison of fluorescence between A5 and acrylodan-A5. A5 or acrylodan-A5 (3 μM) was added to LUV (250 μM) and titrated with calcium. In the case of A5, the tryptophan experiences a blue shift at >0.1 mM calcium. A5 was excited at 280 nm and emitted from 300-400 nm. Acrylodan-A5's signal increases sharply from 10 μM to 0.1 mM calcium. The addition of higher concentrations of calcium causes a fluorescence decrease. This data suggests two calcium-binding interactions are occurring. Acrylodan-A5 was excited at 365 nm and emitted from 400-600 nm. Error bars represent the standard deviation of three different experiments, ran at 37^{o}C.

2.3.3 Concentration-Dependent Self-Quenching of Acrylodan

From Figure 2.5, it is clear that acrylodan-Dap inserts into the membrane at low calcium concentrations. At higher concentrations of calcium the kynurenine of native Dap inserts, and the acrylodan-Dap signal decreases. Since this decrease is not accompanied by a red shift, the effect most likely occurs in the membrane. It was speculated that this decrease is due to concentration-dependent self-quenching of acrylodan. This result is also seen when NBD-Dap is used[126]. When bound to the membrane at lower calcium concentrations, the acrylodan moieties are far enough apart to prevent self-quenching. When more calcium is added the acrylodan residues become closely aligned causing a quenching effect. To study this further, acrylodan-Dap was mixed in a fivefold excess of native Dap. If the quenching is due to the acrylodan interacting closely, separating them by native Dap should form hybrid oligomers that prevent a signal decrease (Figure 2.7).

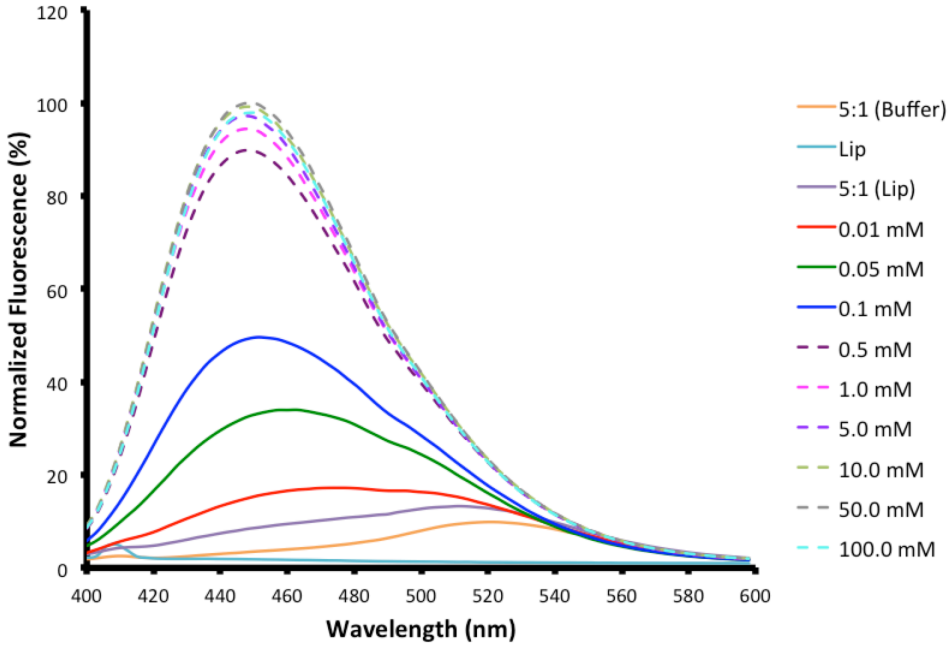

Figure 2.7 Kynurenine overtaking the acrylodan-Dap spectrum. A 5:1 Dap:acrylodan-Dap ratio (3 μM total) was added to LUV (250 μM) and titrated with calcium. When kynurenine is in excess over acrylodan, the spectrum mimics that of native Dap. This ratio does not give any information of the self-quenching of acrylodan, since acrylodan's signal is minor.

Although this does reduce self-quenching (Figure 2.7), the signal from kynurenine appears to over-shadow this spectrum. Due to the kynurenine being in a five-fold excess over acrylodan, the self-quenching experiment mirrored a standard emission spectrum of native Dap (Figure 2.5). To remove this error a Dap analog was used that has the kynurenine replaced with a tryptophan, but

retains antibacterial activity. This analog, Dap-E12W13[68] is a double mutant, replacing the kynurenine residue for tryptophan and the 3-methylglutamate residue for glutamate. The activity of Dap and Dap-E12W13 has been determined previously on *Bacillus subtilis*, with values of 0.75 and 1.5 µg/mL (at 5 mM Ca^{2+}), respectively[68]. The emission spectrum (Figure 2.8, blue line) suggests that tryptophan inserts into the membrane at the same concentration of calcium, compared to kynurenine. When a 5:1 Dap-E12W13:acrylodan-Dap ratio was tested, the self-quenching was greatly diminished (Figure 2.8, green line). As mentioned above, acrylodan-Dap experiences a slight blue shifting when the second calcium ion is bound (green to purple line of Figure 2.4). In contrast, when the second calcium-binding event occurs, acrylodan-A5 does not experience a second blue shift, suggesting that the kynurenine residue intrinsic to Dap is inserting into the membrane. This highlights that the acrylodan-Dap emission spectrum is observing, to a lesser extent, both calcium binding phases.

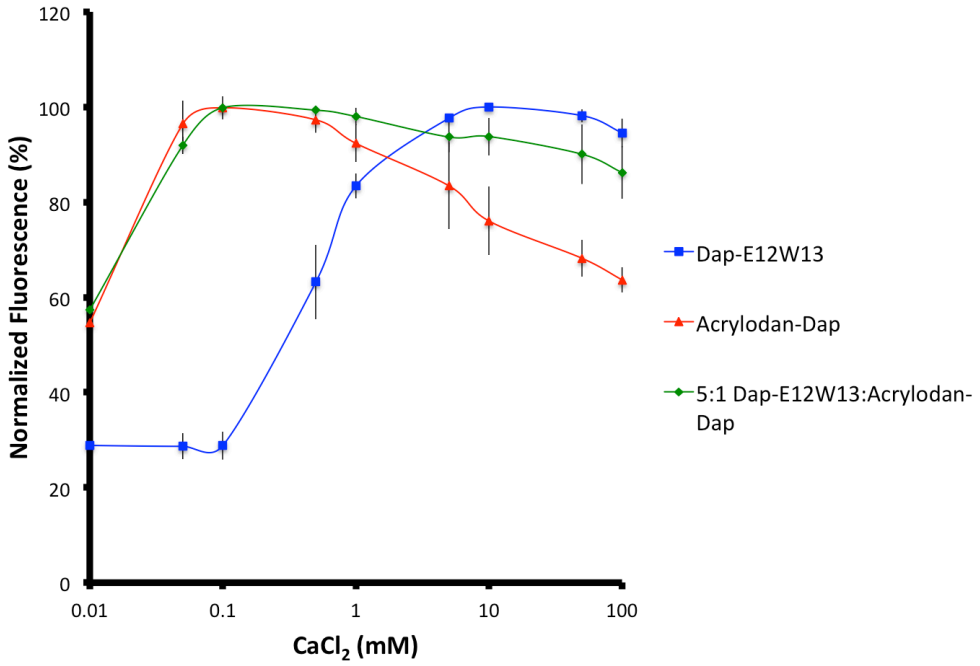

Figure 2.8 Concentration-dependent self-quenching of acrylodan-Dap. Dap-E12W13, acrylodan-Dap and a 5:1 Dap-E12W13:acrylodan-Dap ratio (3 µM) was added to LUV (250 µM) and titrated with calcium. When DapE12W13 is utilized, instead of Dap, the self-quenching of acrylodan-Dap is mostly prevented at higher calcium concentrations. Although Dap-E12W13 does not contain a kynurenine the tryptophan experienced similar fluorescent increases compared to kynurenine, and therefore was plotted through maximum fluorescent signal not mean tryptophan wavelength (shown before for A5). Error bars represent the standard deviation of three different experiments, ran at 37°C.

The same experiments were also carried out with A5 and acrylodan-A5. These results, shown in Figure 2.9, had identical trends to those seen for Dap. A5 does not contain kynurenine, and therefore a separate analog was not necessary. The 5:1 A5:acrylodan-A5 ratio shows that the quenching seen for acrylodan-A5 is suppressed in the hybrid oligomers. Although the 5:1 ratio experiments were run in triplicates, the error bars were relatively large. This may explain the slightly lowered fluorescence seen for the 5:1 ratio at 0.1 mM Ca^{2+}.

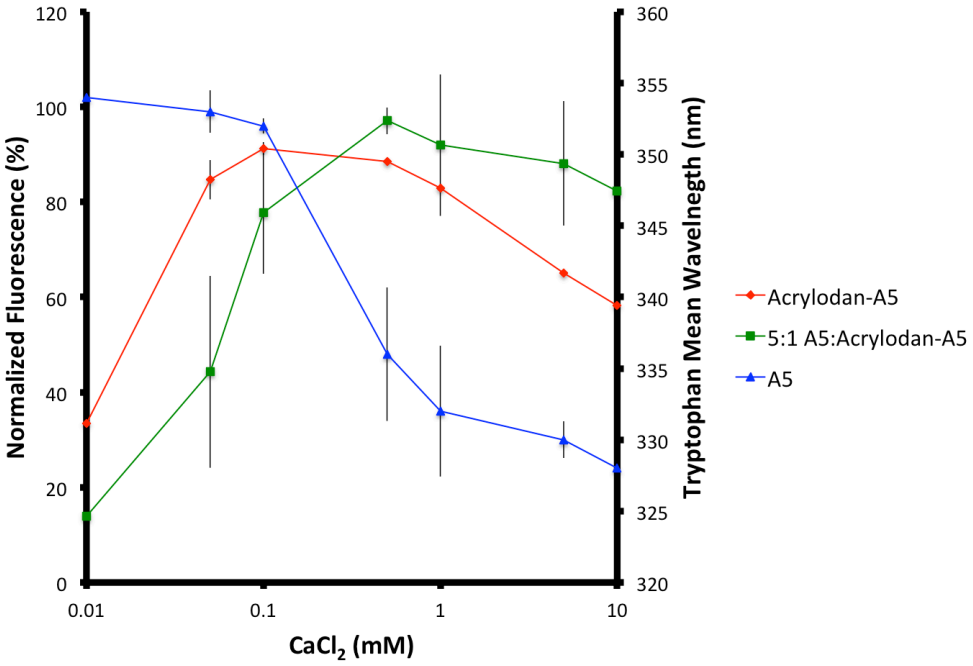

Figure 2.9 Concentration-dependent self-quenching of acrylodan-A5. A5, acrylodan-A5 and a 5:1 A5:acrylodan-A5 ratio (3 μM) was added to LUV (250 μM) and titrated with calcium. The self-quenching of acrylodan-A5 is greatly diminished when the acrylodan moieties are separated by native A5. Error bars represent the standard deviation of three different experiments, ran at 37°C.

When comparing these results to the ITC experiments, the data suggests that the first calcium ion, shown at 0.1 mM calcium, facilitates membrane insertion of ornithine6 of Dap or lysine8 of A5. The second calcium binding event, >0.1 mM, causes kynurenine of Dap or tryptophan of A5 to insert more deeply and the acrylodan residues to interact closely, both within and across leaflets, decreasing the signal.

2.3.4 Calcium-Dependent Changes in Fluorescence Anisotropy

Fluorescence anisotropy was utilized to further study the observed two calcium-binding events. Both Dap and A5 were incubated with 1/1 DMPC/DMPG liposomes for 3 minutes, in HEPES-buffered saline. Calcium was then titrated stepwise from 10 µM to 100 mM, with 3 min incubations, to observe the effect of membrane interaction with anisotropy. Anisotropy reflects a fluorophore's diffusional rotation when excited with polarized light[180]. A sample containing a specific fluorophore is excited with vertically polarized light, exciting a sub-population of these fluorophores that are orientated parallel to the plane of polarization of this light beam. These molecules then freely rotate within the limited lifetimes of their excited states. The molecule's final orientation is compared to the initial vertically polarized light[180]. Dap and A5 are relatively small molecules and therefore the whole molecule is able to freely rotate. When in buffer they will rotate more quickly, having a lower anisotropy value. The individual side chains will experience different degrees of rotation depending on their bound state. If certain amino acids of Dap or A5 insert into a rigid membrane, their rotation should diminish, increasing the anisotropy (close to one). For each sample shown in Figure 2.11, a blank consisting of liposomes and buffer was used.

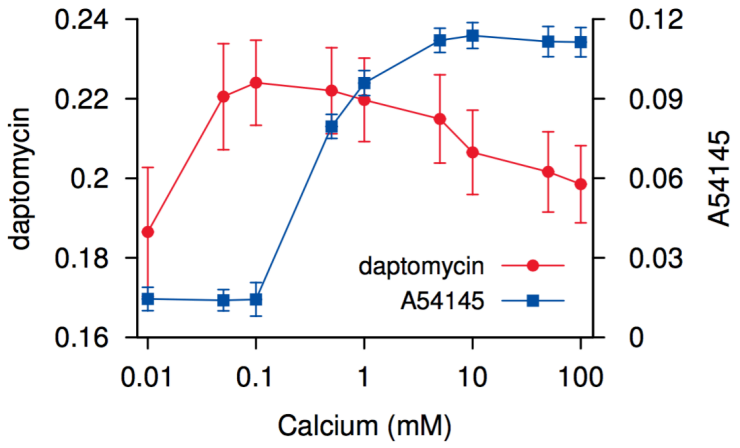

Figure 2.10 Anisotropy results for Dap and A5. Dap or A5 (3 µM) were added to 1/1 DMPC/DMPG (250 µM) and titrated with calcium. The data for both Dap (red line) and A5 (blue line) are overlaid in the plot. Error bars represent the standard deviations of three separate experiments, ran at 37°C.

As seen in Figure 2.10, the anisotropy of A5 mirrors the tryptophan emission blue shift (Figure 2.6). At higher concentrations of calcium (>0.1 mM), the anisotropy of A5 increases. This suggests the tryptophan is not membrane associated until the second calcium-binding event. In the

case of Dap, the anisotropy increases rapidly, with a maximal signal at 0.1 mM calcium. From Figure 2.5, it is clear that the ornithine6 residue likely inserts into the membrane first. This anisotropy data is directly measuring the kynurenine residue of Dap. The fact that it's anisotropy increases at 0.1 mM, divergent from the emission scans shown previously (Figure 2.5), suggests that when Dap is initially bound by ornithine6, kynurenine is being restricted to rotate comparative to the Dap backbone. This could be due to its position on the macrolactone ring, resulting in a configuration that restricts its movement without proper insertion. At higher calcium concentrations, kynurenine sees a decrease in anisotropy. This suggests that kynurenine becomes less rotationally restricted, when the Dap oligomer is more deeply membrane inserted. The decrease in anisotropy could therefore be attributed to an increase in homo-FRET of kynurenine. The kynurenine residues will be in closer proximity when in an oligomeric state within the membrane, therefore able to exhibit FRET between two identical fluorophores[181]. Homo-FRET would likely increase kynurenine's angular distribution, therefore decreasing the anisotropy seen in Figure 2.10, as the residue's ability to rotate will be increased slightly.

Overall, ITC shows calcium is binding to Dap in a 2:1 ratio, within the membrane. The fluorescence results for the native and acrylodan-labeled Dap and A5 show a similar sequential binding of calcium. Acrylodan-Dap/A5 interacts with the membrane first, at low calcium concentrations. This suggests that residues six and eight are inserting into the membrane initially, but restricting the movement of the other amino acids, mainly in the thirteenth position. The whole peptide therefore likely binds the first calcium ion, causing the peptide to force into a specific configuration. The second calcium ion causes a self-quenching of the acrylodan residues, suggesting a slightly altered configuration that brings the acrylodan residues into close proximity. This added calcium then causes a deeper insertion of this oligomer, which is seen through the fluorescence increase of kynurenine and tryptophan.

2.4 Discussion

The results from ITC and fluorescence agree that two distinct calcium-binding events occur. A schematic model was made to better visualize the two calcium binding events, shown in Figure 2.11.

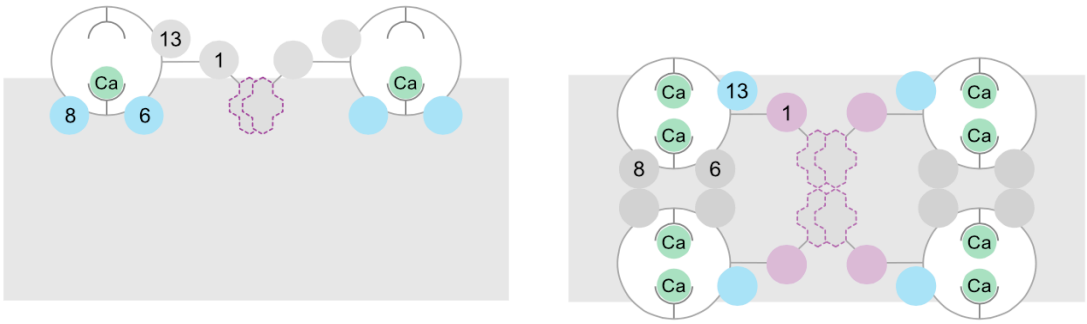

Figure 2.11 Overall schematic for the ITC and fluorescence experiments. Left: The initial oligomeric structure is shown bound to the membrane. The first calcium (green) binding event is evident by the insertion of acrylodan, from labeled Dap at ornithine6 (blue 6) and A5 at lysine8 (blue 8). The purple dotted polygon represents the semi-synthetically labeled A5 analog. The pyrene is in replacement of the fatty acyl tail of A5. The kynurenine13 (grey 13) of Dap and tryptophan1 (grey1) of A5 do not sense the hydrophobic membrane at this concentration of calcium. Right: The oligomer inserts more deeply and translocates with the second calcium-binding event. At this concentration the acrylodan moieties exhibit concentration-dependent self-quenching. The kynurenine13 (blue 13) and tryptophan1 (purple 1) of Dap and A5 insert into the membrane. This image depicts that only four monomers of Dap form a pore, but the more plausible subunit stoichiometry is 6-8 monomers[115].

As shown in this figure, the first binding of calcium occurs at ~0.1 mM. At this concentration the acrylodan groups on ornithine6 (Dap) and lysine8 (A5) insert into the hydrophobic membrane. This was seen with a pronounced blue shift and fluorescence increase when measuring acrylodan-labeled Dap/A5. At this concentration the kynurenine13 of Dap and tryptophan1 of A5 are not bound to the membrane. Once the calcium concentration is increased to >0.1 mM, the oligomeric structure inserts more deeply. At this concentration the acrylodan moieties experience concentration-dependent self-quenching. Although it is unclear within Figure 2.11, this self-quenching will likely occur both across the membrane and within each leaflet. This suggests that when a second calcium ion is bound, the oligomers within leach leaflet interact more closely, bringing the acrylodan residues closer together. The kynurenine13 and tryptophan1 of Dap and A5 also insert into the membrane with the second calcium. This suggests that the first calcium-binding event causes the macrolactone ring to interact with the membrane. The second calcium causes the rest of the Dap/A5 structure, particularly close to the fatty acid tail to insert.

In a 2016 article[125], a similar calcium effect on Dap interaction was theorized. In this work a pyrene moiety was semi-synthetically added to A5, replacing the fatty acyl tail. This work also found that Dap bound to calcium in two steps, shown through pyrene excimer fluorescence[125]. Interestingly, at 0.1 mM calcium, the Py-A54145 exhibited mutual association, shown through excimer formation.

This indicated that the pyrene moieties were in a very close orientation. At higher calcium concentrations, >0.1 mM, the Py-A54145 showed an increase in the monomeric pyrene concentration that formed excimers. This suggests many pyrene monomers are forming in close proximity, possibly due to an association of tetramers across membrane leaflets. Zhang, *et al.* showed, through a dithionite-quenching assay (Section 1.7.2), that Dap oligomers translocate evenly between the leaflets of myristoyl chained lipid membranes[111]. The subunit stoichiometry of these oligomers was found to be 6-8, suggesting that tetramers are interacting across leaflets. The authors noted that the inclusion of cardiolipin (a suspected resistance mechanism of Dap) was found to prevent this translocation, showing a reduced oligomer subunit stoichiometry, suggesting that Dap tetramers link together across leaflets to form a functional pore. This work, along with the results presented above, suggests that the first calcium-binding event to Dap causes membrane insertion of an oligomeric structure. This oligomer is bound only enough to allow the acrylodan to insert but does cause the thirteenth residue to be strained, which is suggested by the increase in kynurenine's anisotropy. The second calcium-binding event then causes a deeper insertion of this oligomer and, likely, a translocation of the oligomer to the inner leaflet.

The experiments from ITC and fluorescence, and also pyrene excimer fluorescence correlate well together. The most successful model for the ITC isotherm gave a value of two distinct binding sites with different affinity. In a later chapter (Chapter 4-5), the effect of the lipid acyl chain is investigated. Preliminary work shows that ITC produces a stoichiometry of two calcium ions to Dap on DOPC/DOPG membranes and a slightly lower value on DMPC/DMPG membranes. The reason for this discrepancy is still unknown. Recently, Lee, *et al.* proposed that the stoichiometry of calcium to Dap, within DOPC/DOPG LUVs, is instead 1.5:1[174], not 2:1 in this case. This discrepancy may be due to the techniques used, ITC in this work versus circular dichroism. The model used for the data shown in Figure 2.2, also assumed that calcium bound strictly to Dap and PG within the membrane, supported by the fluorescence data discussed above, whereas Lee, *et al.*'s binding did not use a model. Further, Lee, *et al.* utilized a calcium concentration from 0-1 mM, which may not have caused calcium saturation with Dap. Future ITC work is needed to better elucidate these diverging findings.

The work presented in this chapter highlights that, within the membrane, Dap is interacting with two separate calcium ions, but which amino acids are involved is still unclear. Dap and A5 contain several conserved anionic residues, particularly aspartate7 and aspartate9[73,99]. These amino acids are also conserved across other calcium binding antibiotics, including the

amphomycin/friulimicin family[53,182]. The four amino acids surrounding these aspartate residues also make up the EF-motif consisting of residues DXDG, found in calmodulin binding proteins[40,73,77,82]. When these aspartates are replaced with asparagine, a cationic amino acid, the activity of Dap is reduced[68,73]. This indicates that these amino acids are most likely binding to calcium, as their anionic properties are required. This still leaves another, unknown, calcium binding region. Interestingly, Lohani, *et al.* synthesized an analog of Dap that replaces the 3-methylglutamate12 with glutamate and the kynurenine13 with tyrosine, Dap-E12Y13[68]. This antibiotic's antibacterial activity was found to be highly dependent on the concentration of calcium present. This suggests that the twelfth and/or thirteenth amino acids could be involved in a calcium-binding event. Recently, Barnawi, *et al.* showed that when the kynurenine at position 13 is replaced with alanine the activity is greatly diminished, compared to the replacement of 3-methylglutamate12 for alanine[98]. This suggests that position 13 may have a larger role in calcium interaction than expected. Replacing aspartate3 for asparagine, in Dap, diminished the activity ~80 fold[73,99]. Although the data presented here suggests that is residue is bound internally in the membrane when the Dap oligomers translocate, the reduced activity seen when the anionic properties are lost suggests it could have some role in calcium interaction. Future experiments are still required in order to fully elucidate which residues, apart from those found in the DXDG motif, are absolutely necessary for calcium binding.

A possible issue in this work could be the diminished antibacterial activity of the acrylodan-labeled Dap and A5. The acrylodan-labeled A5 retained 50% activity compared to A5. The acrylodan-labeled Dap retained only 25% compared to Dap. One could argue that this decrease in activity could mean their interaction with calcium and the membrane is diminished, comparative to the native antibiotics. While this possibility cannot be excluded, it was found that the labeled analogs detected the first calcium-binding event, where the native compounds detected the second. If the labeled compounds had reduced calcium affinity, they would not have bound to the membrane before the native compounds. It is also worth noting that two successive transitions were also evident in a related study that used only a single labeled analog[125]. The anisotropy results, which did not use a label on Dap or A5, also outline that two calcium-dependent transitions are occurring.

Collectively, the ITC and fluorescence studies, utilizing acrylodan-labeled Dap and A5, show that two calcium-dependent binding events are occurring. The lipopeptide binds to the first calcium ion causing insertion of the ornithine6 residue of Dap or lysine8 residue of A5. The inserted monomers then form an oligomer within the outer leaflet, observed through excimer formation with a

pyrene labeled A5 analog. The anisotropy studies suggest that the macrolactone ring of Dap is in close proximity to the membrane, restricting movement of the thirteenth amino acid. The second calcium-binding event causes a deeper insertion and translocation of this oligomer into the inner leaflet, supported by results from Zhang, *et al*[111]. This is observed through an increase in kynurenine and tryptophan's emission. The acrylodan residues are quenched at this concentration suggesting that the Dap subunits within each leaflet and across the membrane are in a very close proximity. Py-A54145 experiments also show an increase in the excimer signal intensity, due to a higher number of pyrene monomers forming excimers, at this concentration, suggesting an interaction between tetramers across leaflets. This interaction of tetramers likely forms a pore, leading to permeabilization of the cell membrane[40,45,126]. This mechanism is reminiscent of many structurally diverse oligomer-forming, membrane-permeabilizing protein toxins that also form oligomeric "pre-pores" prior to the functional, membrane-inserted pores[183–185]

Chapter 3

An Acyl-Linked Dimer of Daptomycin is Strongly Inhibited by the Bacterial Cell Wall[2]

3.1 Introduction

Resistance to Daptomycin (Dap) is a growing concern, with some clinical trials already showing lower Dap activity[49,89,186]. To overcome this issue, many analogs of Dap have been synthesized, through various methods (Section 1.5), to better understand the mode of action of this antibiotic, and to potentially increase activity.

In this work, a dimer of Dap (Figure 3.1) was synthesized in an attempt to improve oligomer formation, therefore improving antimicrobial activity. An octadecanedioate linker, replacing the fatty acyl tails, connected two Dap monomers. Oligomer formation would likely have a high entropic cost, due to the creation of an ordered system (of monomeric Dap) within the membrane. This dimer Dap could slightly decrease the oligomer formation's entropic cost, which would shift the equilibrium of oligomerization to lower monomer concentrations, thus improving activity. The fatty acyl chains are in close proximity within the oligomer[105,125] and therefore joining them together should not impose any unfavourable constraints.

Previous studies have shown Dap's ability to oligomerize[115] and permeabilize[45] equimolar PC/PG model membranes. In this work, it was found that the dimer was also able to interact,

[2] The results displayed in this chapter have been published: "An Acyl Linked Dimer of Daptomycin is Strongly Inhibited by the Bacterial Cell Wall," by Robert Taylor, Bradley Scott, Scott Taylor and Michael Palmer, **2017**, *ACS – Infect. Dis., 3,* 462-466[117].

Authors contributions: Dr. Scott Taylor synthesized and purified the Dap dimer. L-form's were cultured from *B. subtilis* PDC 134 by Bradley Scott. Robert Taylor did all other experiments. Manuscript was written and devised by Dr. Michael Palmer. Level II MIC results were completed in Dr. Gary Dmitrenko's laboratory, with training of the flow hood from Valerie Goodfellow and Carol Tanner.

oligomerize and permeabilize model membranes. However, this dimeric Dap was found to be inactive against Gram-positive bacteria. It was speculated that since the dimer is much larger than native Dap, it might be too large to pass the peptidoglycan layer of the cell. To investigate this theory, L-form bacteria (cells lacking a cell wall but remain viable[187]) were utilized. The dimer proved to be highly active on these cells.

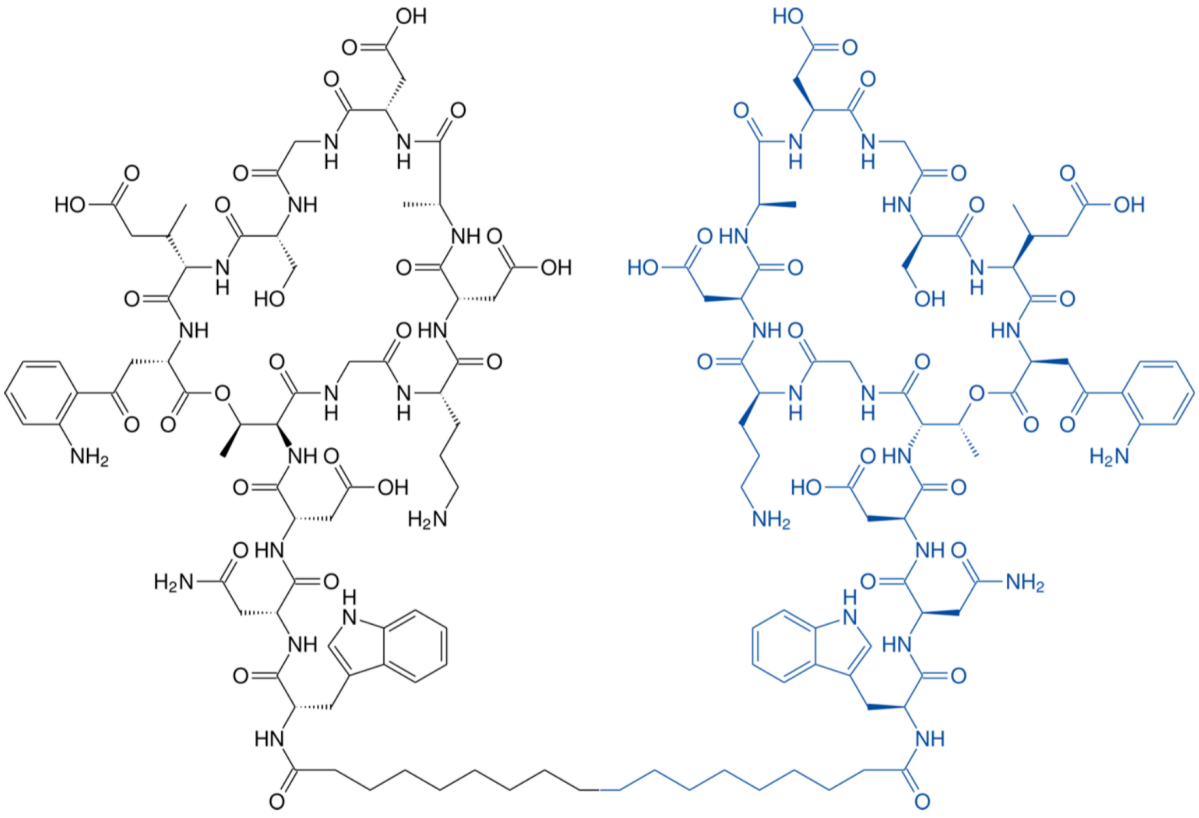

Figure 3.1 Structure of the dimeric Dap analog. The monomers of Dap are connected, at the *N*-terminal regions, by a bivalent octadecanedioate linker.

The work herein suggests that the dimer of Dap is unable to pass the outer cell wall of Gram-positive bacteria. Once the cell wall is removed (L-forms and liposomes) the dimer is able to interact with the membrane having an activity comparable to native Dap. The dimer also proved to transport sodium ions more rapidly than native Dap on model membranes, potentially suggesting improved oligomer formation. Overall, this data suggests that Dap must be in a monomeric state to traverse the peptidoglycan layer and insert into the membrane.

3.2 Methods and Materials

3.2.1 Synthesis of Dimeric Daptomycin

Briefly, the side-chain amino group of Dap's ornithine residue was protected with a *tert*-butyloxycarbonyl (BOC) protecting group. The decanoyl residue of Dap was enzymatically removed. Two Dap monomers (with their decanoyl groups removed) were then linked through acylation with an activated octadecanedioate. For details and procedures on the synthesis and purification of the dimeric Dap, see Appendix A.

3.2.2 Antibacterial Activity

Antimicrobial susceptibility tests were performed as outlined in Section 2.2.3, with minor additions. Serial dilutions of monomeric and dimeric Dap were prepared in Luria-Bertani (LB) broth (for *Bacillus subtilis*) or Mueller-Hinton broth (for *Staphylococcus aureus*) that was supplemented with the concentrations of calcium indicated in Table 3.1-3.3 (Section 3.3). Growth was assessed visually after incubation at 30^{o}C (for *Bacillus subtilis*) or 37^{o}C (for *Staphylococcus aureus*) overnight.

3.2.3 Preparation of Liposomes

LUVs consisting of DMPC/DMPG were prepared as described in Section 2.2.4.

3.2.4 Fluorescence Spectroscopy

Steady state experiments were performed as described in Section 2.2.5 for monomeric and dimeric Dap.

3.2.5 Permeabilization Assay Utilizing Pyranine

The permeabilization assay was followed similar to Zhang, 2014[45], with some revisions. DMPC/DMPG lipids, at an equimolar concentration, were prepared as described in Section 2.2.4. Pyranine (Sigma Aldrich, 1 mM) was entrapped within the liposomes through vortexing with a low

pH buffer (5 mM MES, 5 mM Tricine, 5 mM NaCl, 250 mM sucrose, pH 6.0) until all lipids were suspended. LUVs were prepared through extrusion, through 100 nm polycarbonate filters, with pressurized nitrogen. The resulting pyranine entrapped LUVs were passed through a size exclusion column (Bio-Rad P-6DG, Bio-Rad, Richmond, CA, USA), to remove the excess non-entrapped pyranine.

Dap (2 μM) and the proton ionophore carbonyl cyanide m-chlorophenyl hydrazone (CCCP, 5 nM), were added alone or in combination, as indicated. The buffer used during measurements was a higher pH than what was used for pyranine encapsulation (5 mM MES, 5 mM Tricine, 100 mM NaCl, 250 mM sucrose, pH 8.0). Calcium chloride, at the reported concentrations, was pre-mixed with buffer before addition of LUVs. At time 0, LUVs and/or analogs were added to the cuvette. Fluorescence (excitation wavelength, 460 nm; emission wavelength, 510 nm) was monitored for 300 seconds. Triton X-100 (0.1%) was then added to solubilize the LUVs. The fluorescence intensity after Triton X-100 was added was used to normalize the entire curve. All permeabilization assays were run at 30^{o}C. A schematic for the permeabilization assay is shown in Figure 3.2.

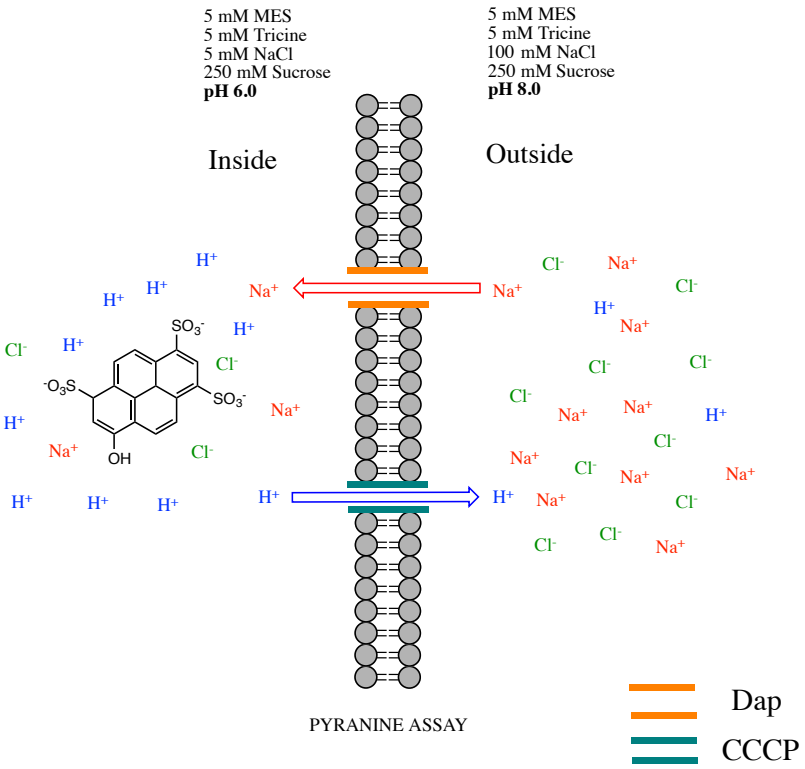

Figure 3.2 A schematic for the permeabilization assay, utilizing LUVs entrapped with pyranine. The internal LUV buffer had a low pH and salt concentration. Outside the LUV the buffer pH was more alkaline, with an excess of salt (NaCl). This created an opposing ion concentration gradient across the membrane. When Dap or CCCP are added separately, proper in/efflux is unable to occur. It is not until both are present in unison that allows for the pH inside the LUVs to increase, deprotonating the pyranine, resulting in a fluorescence intensity increase. CCCP is necessary to allow efflux of protons, balancing the charge gradient across the leaflets.

3.2.6 Generation and Antibacterial Testing of L-form Bacteria

The *Bacillus subtilis* strain PDC 134 has been engineered to make expression of several enzymes in peptidoglycan synthesis dependent on xylose[187]. This allows L-forms to be obtained simply by withdrawing xylose. Xylose-free LB medium, supplemented with MSM (20 mM magnesium chloride, 500 mM sucrose and 20 mM maleic acid) at pH 7.0 was inoculated with a liquid culture of PDC 134 grown beforehand in the presence of xylose (0.5% w/v) and chloramphenicol (20 mg/mL). The culture was incubated at 30°C overnight. To suppress growth of residual vegetative forms, ampicillin was added to this culture at 75 µg/mL. Conversion of the rod-shaped vegetative cells to spherical L-forms was confirmed by microscopy (Figure 3.3). Ampicillin was not present in the Dap MIC tests. Antimicrobial activity tests were described as in Section 3.2.2, except that LB-

MSM medium was used and incubation at 30°C was performed until the growth controls were unequivocally positive, which took 3-4 days.

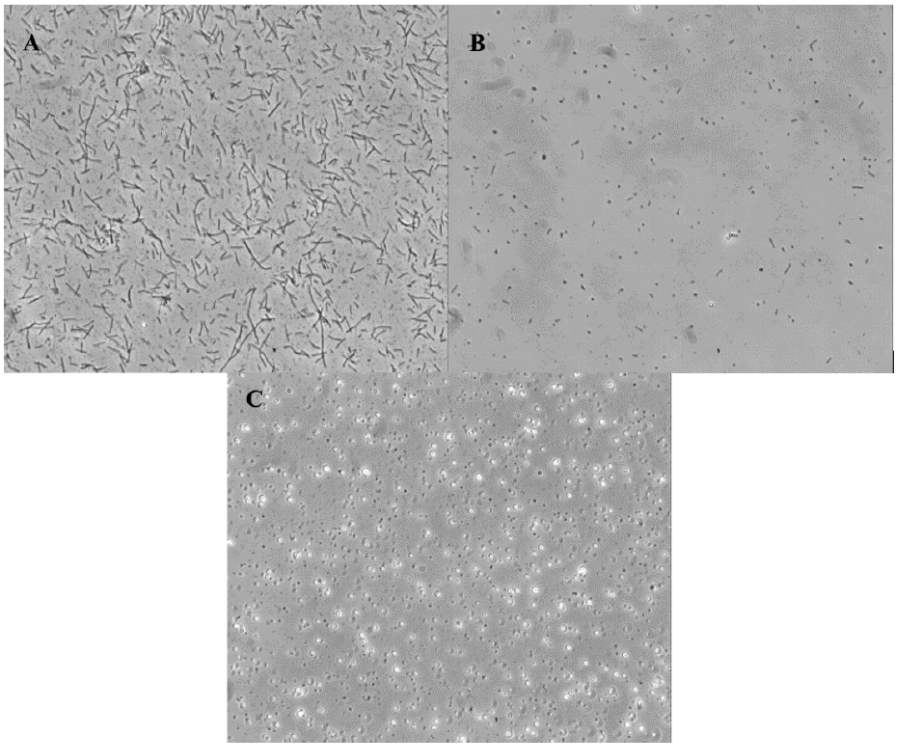

Figure 3.3 The microscopy results for the *B. subtilis* PDC 134 strain. A: One colony of PDC 134 N-forms (vegetative cells) grown in LB broth, supplemented with 0.5% xylose and 20 µg/mL chloramphenicol. B: PDC 134 N-forms subcultured in MSM LB broth. C: PDC 134 N- and L-forms subcultured into MSM LB broth, supplemented with 75 µg/mL ampicillin, giving a pure L-form culture. Figure was taken from Bradley Scott's M.Sc. Thesis[188] with permission.

3.3 Results

3.3.1 Antibacterial Assays for the Dimeric Daptomycin

The most supported model for Dap action is through oligomer formation on the membrane. These oligomers then translocate and form a functional pore, causing the permeabilization of small cations. It was speculated that oligomer formation would have an entropic cost, as a more ordered system of monomeric Dap was created within the membrane. Since the dimeric Dap has the lipid tails connected, it could slightly lower this entropic cost. In theory, this dimeric Dap would allow for oligomer formation and permeabilization to occur at a lower antibiotic concentration and potentially

require lower calcium concentrations. To test whether this analog was similar in activity to Dap, both the monomer and dimer were tested for antibacterial activity on *Bacillus subtilis* ATCC 1046 (Table 3.1).

	Bacillus subtilis ATCC 1046		
$CaCl_2$ (mM)	1.8	5.0	100
Dap	1.0	0.75	0.5
Dap Dimer	>100	>100	7.5

Table 3.1 Minimum Inhibitory Concentrations (MICs, μg/mL) of Dap and dimeric Dap on *B. subtilis* ATCC 1046. The MICs were done on *Bacillus subtilis* ATCC 1046 at varying calcium concentrations, in LB broth. Assays were preformed five times, with each assay run in triplicate.

As can be seen in Table 3.1, the dimer had extremely low activity on *B. subtilis*, having an MIC value greater than 100 μg/mL. Interestingly, the dimers activity increased greatly when the calcium concentration was increased to un-physiologically high levels. An explanation is proposed in Section 3.4. The dimer was also tested against several strains of *Staphylococcus aureus*, both susceptible and resistant to methicillin. These findings are shown in Table 3.2.

	MSSA		MRSA	
	ATCC 6538	ATCC 25293	Isolate 1-3	Isolates 4, 5
Dap	0.25	0.5	0.5	0.5
Dap Dimer	5	75	30	75

Table 3.2 MICs (μg/mL) of Dap and dimeric Dap on strains of *S. aureus*. The MICs were done on various strains of *S. aureus*, either susceptible (MSSA) or resistant (MRSA) to methicillin. Calcium (1.25 mM) was used for all assays, in Mueller Hinton broth. The MRSA strains were distinct clinical isolates, not contained in type culture collections. Assays were preformed three times, with each assay run in triplicate.

The dimeric Dap again showed low activity against both MSSA and MRSA strains of *S. aureus*. As seen in Table 3.2, the MIC values of monomeric and dimeric Dap were much lower than

expected with the MSSA ATCC 6538 strain. This strain appears to be more susceptible than any other strain tested but the trend between the monomer and dimer is the same.

3.3.2 Membrane Insertion of the Dimer to LUVs

One possible explanation for why there is such a marked reduction in the dimeric Dap's activity shown in Tables 3.1-3.2 could be a lack of membrane pore formation. To better understand the dimer's ability to interact with the membrane, fluorescence spectroscopy was utilized. Kynurenine is an intrinsic fluorophore of Dap and can be used to determine if Dap is inserting into the membrane or not (Section 1.6.2)[76,116]. The insertion of the monomeric and dimeric Dap was tested using an equimolar ratio of PC/PG (Figure 3.4).

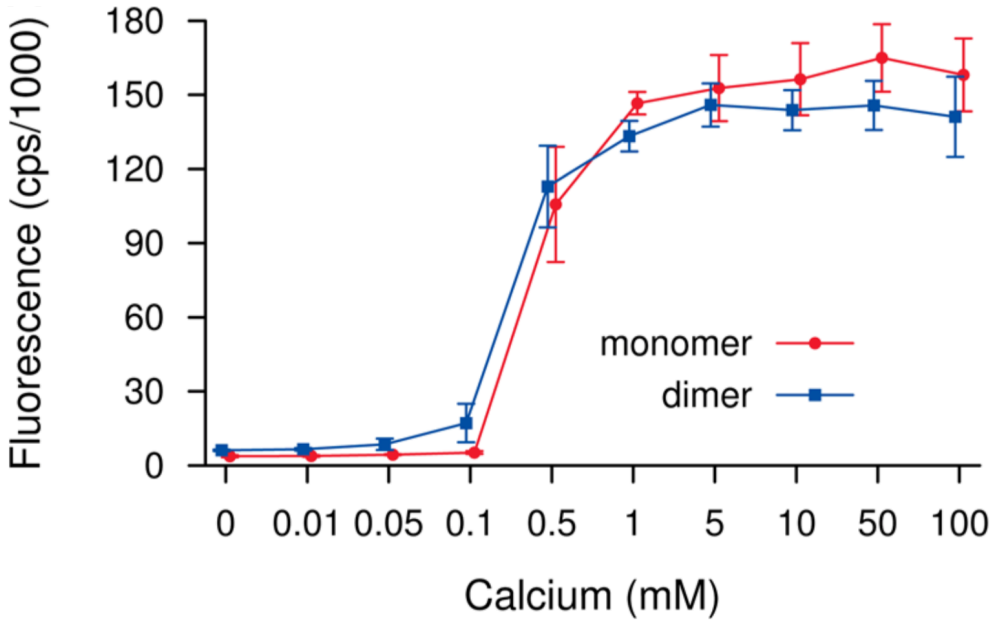

Figure 3.4 Dap (3 μM) and dimeric Dap (1.5 μM) membrane interaction with DMPC/DMPG LUVs (250 μM, total lipid). The kynurenine residue experiences a fluorescence increase as a function of calcium concentration. The monomer and dimer of Dap show identical trends, showing that >0.1 mM calcium is necessary for insertion. Error bars represent standard deviations from two experiments, ran at 37°C.

The dimer interacts with the PC/PG membrane, comparable to the monomer, at half the molar concentration. Although a lower concentration of the dimer is necessary to observe membrane

interactions, the same concentrations of calcium are necessary, compared to the monomer. This could suggest that pre-oligomerization is not decreasing the entropic cost of oligomer formation by a measurable amount. Both antibiotics require >0.1 mM calcium to cause signal intensity increase in kynurenine. This signal increase indicates a membrane insertion event.

3.3.3 Permeabilization of Daptomycin and Dimeric Daptomycin

Previously, Zhang, *et al.* has shown the permeabilization ability of Dap, in a coupled fluorescence assay[45]. This assay was further developed and used in this work to determine if dimeric Dap causes ion transport on DMPC/DMPG liposomes. Unexpectedly, the dimer permeabilized the membranes more rapidly than Dap (Figure 3.5), without the need for the proton ionophore CCCP. The reason for the unexpected decrease seen when the dimer and CCCP are added in unison is not clear but could suggest that the dimer is forming pores large enough to allow sodium ions and buffer bound protons to pass across the membrane freely. Additionally, the dimers signal plateaus at ~ 100 s, suggesting that immediate lysis of the membrane is not occurring, compared to the addition of the membrane solubilizing detergent, Triton X-100. The reason for this plateau in signal is currently unknown, but might suggest that a larger pore formed by the dimer rapidly creates an equilibrium of charged ions across the bilayer.

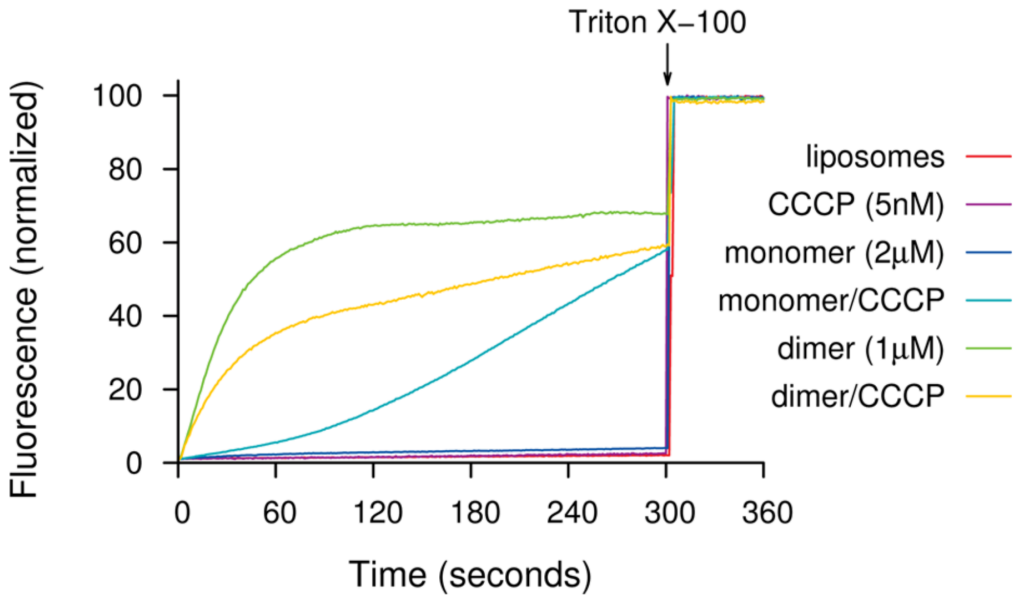

Figure 3.5 Permeabilization assay on PC/PG membranes, utilizing pyranine. The fluorescence of pyranine entrapped in the liposomes rises with the internal pH as protons are exchanged across the membrane for sodium ions that permeate across pores formed by Dap. The experimental is described in Section 3.2.5. Only when Dap and CCCP are present in unison does the pyranine signal increase. The dimeric Dap does not require CCCP to form a pore. Experiments were run in triplicate at 30°C.

The fluorescence work described previously highlights that the dimeric Dap is interacting with model membranes (Figure 3.4) and forming a functional pore (Figure 3.5) on liposomes. Still, the activity of the dimer is greatly diminished. This suggests that another factor is preventing the antibacterial activity of the dimer against both *B. subtilis* and *S. aureus*. Although the dimeric Dap might decrease the entropic cost of oligomer formation the overall size is greatly increased, compared to native Dap. It was speculated that this increase in size could be preventing dimeric Dap from passing across the cell wall of Gram-positive bacteria.

3.3.4 Antibacterial Assays on L-form Bacteria

To test this hypothesis, L-form bacteria were utilized. L-forms are Gram-positive cells that lack an outer cell wall but are still viable. These L-forms have been used in the literature to study the activity of several antibiotics[187]. Wolf, *et al.* originally constructed several L-form strains, one in particular, PDC 134, is described in their 2012 paper[187]. The PDC 134 L-form strain of *B. subtilis* was

used in this thesis, because it has several enzymes in the murein synthesis, mainly the *murE* operon expression system, under the control of xylose. If xylose is present, vegetative rod cells form. In the absence of xylose, the rod cells are converted to cell wall lacking L-forms[189]. These L-forms are highly sensitive to osmotic lysis and therefore require osmolarity protection, in this case, with sucrose. This PDC 134 strain was used to produce both vegetative and L-form bacteria. The L-forms were confirmed by microscopy (Figure 3.3) and a lysis check in water. The activities of the dimeric and monomeric Dap antibiotics were tested against these cells (Table 3.3).

	Bacillus subtilis strain				
	1046			*PDC 134*	
$CaCl_2$ (mM)	*1.8*	*5.0*	*100*	*5*	*5*
L-forms (Y/N)	N	N	N	N	Y
Dap	1.0	0.75	0.5	0.5	0.075
Dap Dimer	>100	>100	7.5	25	0.2

Table 3.3 MICs (μg/mL) of Dap and dimeric Dap on *B. subtilis* PDC 134. The MICs done on *B. subtilis* ATCC 1046 were completed at varying calcium concentrations, in LB broth. The *B. subtilis* PDC 134 strain produced vegetative (N-forms) or L-form bacteria and was tested at 5 mM calcium chloride. Assays were preformed five times, with each assay run in triplicate.

As is shown in Table 3.3, the dimer's activity is drastically improved with the L-form bacteria. The monomer also shows a 10-fold increase in activity. These data suggest that the dimer, and even the monomer to a certain extent, is prevented from reaching the bacterial membrane by the murein layer. Once they are membrane inserted, pore formation occurs, as observed previously on model membranes.

3.4 Discussion

In the literature, the most supported mode of action of Dap involves oligomer formation on membranes containing PG. This oligomer formation is likely to have an entropic cost, due to the increase in order when comparing an oligomer to individual monomeric molecules. In this work, it was thought that by reducing the entropic cost of oligomer formation, activity would be increased. To

investigate this, a dimeric Dap analog was synthesized that connected the *N*-terminal tryptophan residues of two monomers, by an octadecanedioate linker. Unexpectedly, the activity of the dimer against vegetative *B. subtilis* (Table 3.1) and *S. aureus* (Table 3.2) strains was much lower, in comparison to the monomer. Initially it was suspected that the dimer might be forming unfavourable steric constraints within the membrane, preventing permeabilization to occur. From the experiments with liposomes, it is clear that not only does the dimer insert into the membrane (Figure 3.4) at the same calcium concentration compared to Dap but permeabilization of sodium ions occurs more rapidly (Figure 3.5). The presence of carbonyl cyanide m-chlorophenyl hydrazone (CCCP) is required for Dap permeabilization, to allow for a proton efflux with simultaneous influx of sodium. In the case of the dimer, CCCP is not required, and actually decreases the fluorescence. This suggests the dimer is forming a larger pore than native Dap, allowing for a more rapid influx of sodium ions, and also a transport of buffer bound protons. Future work involving the determination of the subunit stoichiometry of the oligomers formed by dimeric Dap, in a similar study shown by Muraih, *et al.*[115] would allow for a better determination of the dimer's pore size, within model membranes.

Although the dimer was interacting with model membranes and forming a functional pore on liposomes, the question still remained as to why the activity was so low on vegetative cells. One possibility for this reduced activity is the fact that the dimer is much larger than native Dap. Due to this increased size, the dimer might be unable to cross the cell wall of Gram-positive bacteria. The cell wall is known for its antibiotic selectivity, acting as a barrier to the cell membrane. Increases in cell wall thickness[186] and the extent of D-alanine modification on cell wall lipotechoic acids[49,89] have previously been associated with Dap resistance, in clinical isolates. To determine if the cell wall was involved in this dimer resistance, a strain of *B. subtilis* was cultured (constructed by Wolf, *et al.*[187]) that had control of the murein synthesis (with the presence or absence of xylose). In the absence of xylose, *B. subtilis* PDC 134 cells lack a cell wall but still remain viable, when the osmolarity is retained. The monomer and dimer of Dap were tested against these cell wall lacking bacteria (L-forms). As shown in Table 3.3, the dimer's activity was dramatically increased on these L-forms, from 25 to 0.2 μg/mL (for PDC 134). The monomer of Dap surprisingly also saw an increase in activity. The vegetative form of this PDC 134 strain showed similar results to the other *B. subtilis* and *S. aureus* strains tested. This highlights that the mutations in the PDC 134 strain[189] are not having an effect on the susceptibility of these vegetative cells. The results presented in Table 3.3 suggest that the dimer, and to a certain extent the monomer, are unable to pass the outer cell wall of the bacteria tested.

In a recent study, it has been speculated that the mechanism of action for Dap is through inhibition of cell wall synthesis enzymes[119]. In this proposed mechanism, Dap inserts into the membrane and oligomerizes and then, by redistributing the lipids within the outer membrane, flips Dap oligomers to the inner leaflet. This dislodges cell wall synthesis enzymes, mainly PlsX and MurG, from the cell membrane, resulting in cell death. However, the observation made here and earlier[187] that Dap kills L-forms, reaffirms that Dap's mechanism of action does not hinge on disruption of cell wall synthesis. This is at least true with *B. subtilis*. Permeabilization of the bacterial cell membrane has been observed repeatedly before for Dap, suggesting that pore formation is the primary mode of action[46,137,190]. Dap has also been shown to readily kill bacterial cells, which are prevented from dividing by a bacteriostatic antibiotic, rifampicin[191]. If they are prevented from dividing, they are likely to be protected from death by inhibition of cell wall synthesis alone. Even though the data suggests that permeabilization through pore formation is the mechanism of action for Dap, more empirical evidence is required, therefore, the possibility still remains that Dap both permeabilizes membranes and inhibits cell wall biosynthesis, similar to the lantibiotic nisin[42].

In Table 3.1, it was shown that when the calcium concentration was increased to un-physiologically high concentrations (100 mM), that the MIC of the dimer was greatly increased (>100 to 7.5 μg/mL). This suggests that the added calcium could be 'shielding' the dimer while passing through the murein layer. If the inability of the dimer to pass through the cell wall is due to not only size but also charge, the added calcium could be making the dimer more electrostatically neutral. This would then allow a more efficient passage across the cell wall, leading to permeabilization. Although it was expected that the activity of the dimer should be identical to Dap (0.075 μg/mL) on L-forms, the dimer was shown to have lower activity (0.2 μg/mL). This is unexpected since the dimer caused such a rapid transport of sodium ions seen in the coupled pyranine assay (Figure 3.5). This could be explained by a dual mechanism of action, where Dap is both permeabilizing the membrane and inhibiting a part of some biosynthetic pathway[119,135,138,190,192], whereby the dimer is unable to promote this later mechanism. However, the antibacterial activity of Dap varies with the length of the fatty acyl residue[60], and accordingly the replacement of Dap's native decanoyl residue by octadecanedioate to effect dimerization might also account for the observed difference in activity. To better distinguish these two mechanisms of action for Dap, studies involving the permeabilization assays with pyranine on L-form bacteria would be useful. Since L-form bacteria lack a cell wall, Dap should not cause ion transport temporally with model membranes, if cell synthesis inhibition was a primary mechanism of action.

Overall, this work shows that the cell wall is an important obstacle in the action of Dap, and future work that looks into developing Dap analogs needs to take into account the size constraints for Dap activity. In a study of Dap aggregation utilizing NMR[55], it was suggested that Dap, at relatively high concentrations, might form oligomeric aggregates of 14 subunits that approach the membrane. Since a dimer of Dap is unable to pass the cell wall it seems unlikely that a 14 subunit non-covalent aggregate is possible. The work shown in this chapter suggests that Dap must approach and interact with the membrane as a monomer.

Chapter 4

Daptomycin Pore Formation is Restricted by Lipid Acyl Chain Composition[3]

4.1 Introduction

Dap has been found to depolarize *Staphylococcus aureus* cells through membrane permeabilization[46,191]. In contrast, a recent paper stated that Dap, at bactericidal concentrations, does not induce potassium leakage from *Bacillus subtilis* cells, suggesting instead that Dap is inserting into the membrane and causing the dislodgment of cell wall synthesis enzymes[119]. Dap's mechanism of action on model membranes is debated amongst researchers even more. Two studies, from the Hancock group, that used Dap concentrations far higher than bactericidal concentrations suggested that the membranes undergo rapid lipid flip-flop when Dap is bound[82]. Their work also stated that Dap, at high concentrations, permeabilized membranes allowing the probe calcein to leave[82]. In their more recent studies they argued that the membranes undergo fusion when Dap is bound, suggesting a non-selective Dap interaction with the membrane and a permeabilization event that is non-specific[109]. Another study noticed that Dap shrank the surface of giant unilameller vesicles, stating that this effect was due to Dap removing specific lipids from the membrane, causing a membrane lesion[120]. In this work, they utilized a large dye called Texas Red within the liposomes, which did not leak out. From this the authors suggested the membrane lesion was unable to allow ions to pass, and only extract

[3] The results displayed in this chapter have been published: "Daptomycin Pore Formation is Restricted by Lipid Acyl Chain Composition," by Robert Taylor, David Beriashvili, Scott Taylor and Michael Palmer, **2017**, *ACS Infect. Dis., 3,* 11, 797-801[209].

Authors contributions: David Beriashvili ran the translocation and oligomer formation assays with NBD-Dap. Dr. Scott Taylor synthesized the PBFI probe. The ratiometric analysis was done by Dr. Michael Palmer, with experiments ran by David Beriashvili and Robert Taylor. Robert Taylor ran all other synthesis and experiments. Manuscript was written and devised by Dr. Michael Palmer.

specific lipids. In a separate study, a coupled fluorescence assay utilizing a fluorescent probe pyranine found that Dap permeabilized large unilamellar vesicles[45]. The pores that formed in these vesicles were selective for small cations, mainly sodium and potassium.

Due to the varying results with bacteria and model membranes, especially in regards to different experimental conditions, the true mechanism of action for Dap still remains unclear. That being said, all scientists agree that Dap first requires insertion into the cell membrane, which may give insight into why Dap's mechanism of action is continually elusive. The lipid composition of the cell membrane varies between bacterial strains. In the literature, model membranes that have been used to study Dap's mechanism of action have also between greatly varied in terms of lipid composition. This inherent property of membranes could be the reason for Dap's varying mechanistic models.

Dap is dependent on the membrane for activity but most scientific research into Dap's mechanism have ignored the importance of the complexity of membrane lipid composition. While most model studies used mixtures of phosphatidylcholine (PC) and PG, these phospholipids differed widely in their acyl chain composition. The Hancock group speculated that Dap non-selectively permeabilizes membranes, leading to lipid flip-flop[82] and membrane fusion[109]. This work utilized palmitoyl-oleoyl lipids. Membrane shrinkage leading to lipid extraction, reported by Chen, *et al*.[120] used dioleoyl lipids. Cation-selective pore formation of Dap by Zhang, *et al*.[45] was demonstrated using dimyristoyl lipids.

The work herein was done to better understand these model membrane systems and their effect on Dap activity. The researchers above paid attention to the lipid head groups but neglected the importance of the acyl chain. In this study, the permeabilization of Dap was compared on each lipid type mentioned, with Dap concentrations that are similar to those required for antibacterial activity. Under these conditions it was observed that only dimyristoyl lipids permitted transport of ions. The lack of permeabilization in the other models corresponded to a reduced membrane translocation of Dap within the membrane and an overall decrease in oligomer subunit stoichiometry. The results presented demonstrate that the acyl chain moieties of lipids are vital to Dap's permeabilization and activity. This may shed light onto why permeabilization of Dap was observed in *Staphylococcus aureus* but not *Bacillus subtilis*, as these bacteria vary in their lipid composition.

4.2 Methods and Materials

4.2.1 Synthesis of NBD-Daptomycin

Briefly, the side-chain amino group of Dap's ornithine residue mixed with 7-chloro-4-nitrobenzoxadiazole (NBD-Cl) for 1 hour at 55^{o}C, under reflux. Sodium bicarbonate was added to buffer the reaction. After 1 hour was reached, concentrated hydrochloric acid was added to quench the reaction. For details and procedures on the synthesis and purification of NBD-Dap, see Appendix A.

4.2.2 Antibacterial Activity

Antimicrobial susceptibility tests were performed as outlined in Section 2.2.3, with minor additions. Serial dilutions of Dap and NBD-Dap were prepared in Luria-Bertani (LB) broth (for *Bacillus subtilis* ATCC 1046) that was supplemented with 5 mM calcium chloride.

4.2.3 Preparation of Liposomes

Lipids used included those described in Section 2.2.4, with the addition of 1-palmitoyl-2-oleoyl-sn-glycero-3-phosphocholine (POPC) and 1-palmitoyl-2-oleoyl-sn-glycero-3-phospho-(1'-rac-glycerol) (sodium salt; POPG). All lipids were obtained from Avanti Polar Lipids, Alabaster, AL, USA.

The methodology for liposome preparation of equimolar mixtures of LUV's has been described in a preceding chapter (Section 2.2.4).

4.2.4 Fluorescence Spectroscopy

Steady state experiments were performed as described in Section 2.2.5.

4.2.5 Permeabilization Assays Utilizing Pyranine

The methodology for the permeabilization assay with pyranine has been described in a preceding chapter (Section 3.2.5).

4.2.6 Ion-Leakage Assays with PBFI

Ion-Leakage assays were preformed exactly like Zhang, *et al.*[118] with several added controls. POPC/POPG liposomes were prepared as described above at an equimolar concentration (8.2 mM total lipid). 4,4′-[1,4,10,13-Tetraoxa-7,16-diazacyclooctadecane-7,16-diylbis(5-methoxy-6,2-benzofurandiyl)]bis-1,3-benzenedicarboxylic acid (PBFI) was dissolved in HEPES-buffer (20 mM HEPES, pH 7.4). PBFI (0.85 mM, 1 mL) was added to the POPC/POPG lipids and sonicated for 45 minutes in a bath sonicator. After sonication the liposomes were filtered through a 0.22 μm filter. The liposomes were then run on a size-exclusion column (Sephadex G-50) to remove non-encapsulated PBFI, using a potassium buffer (20 mM HEPES, 200 mM KCl, pH 7.4) as the eluent.

Fluorescence (excitation wavelength, 338 nm; emission wavelength, 507 nm) was acquired on a PTI Quanta Master 4 instrument. At time 0, PBFI entrapped liposomes (0.55 mM total lipid) were added to potassium buffer. Dap (4.8 μM), valinomycin (0.5 μM) or Dap-E12W13 (4.8 μM) was added, separately, each with calcium chloride (0.6 mM) after 60 s. At 300 s, the assay was terminated using Triton X-100 (0.1%) to solubilize the liposomes. The fluorescence intensity after Triton X-100 was added was used to normalize the entire curve. All assays were run at room temperature.

4.2.7 Oligomer Subunit Stoichiometry Experiments

Oligomer subunit stoichiometry of Dap was performed identical to Muraih, *et al.*[115] LUV's were prepared as described above, in HEPES-buffered saline (20 mM HEPES, 150 mM NaCl, pH 7.4). Pre-mixed ratios (4:1, 6:1, 8:1 and 10:1) of Dap and NBD-Dap, respectively, at a final concentration of 10 μM, were added to each LUV suspension in HEPES-buffered saline with calcium (5 mM). Fluorescence resonance energy transfer (FRET) (excitation wavelength, 365 nm; emission wavelengths, 400-600 nm) was acquired on a PTI Quanta Master 4 instrument after a 3-minute incubation. Unlabeled Dap (4 μM) was then added, with a 3-minute incubation time, to correct for

FRET between (as opposed to within) oligomers. The relative kynurenine fluorescence was calculated with the following equation (equations and assumptions made were followed by Muraih, *et al.*[115]):

$$F_r = \frac{D_2}{D_1}\left(\frac{I_1 - I_0}{I_2\frac{V_2}{V_1} - I_1}\right)$$

F_r – Relative kynurenine fluorescence

D_1/D_2 – Molar amounts of native Dap added at first and second step

I_0, I_1, I_2 – Emission intensities at 445 nm of a liposome blank and the reaction mixture before and after Dap is added

V_1/V_2 – Volumes before and after Dap addition, respectively. Used to account for the 4% dilution due to adding Dap.

In this experiment, kynurenine of Dap is the donor and NBD of NBD-Dap is the acceptor. In order to calculate the subunit stoichiometry, several assumptions were made:

1. All Dap oligomers have the same number of subunits
2. Conversion of monomeric Dap to oligomers is quantitative on the time scale of the experiment
3. When native Dap and NBD-Dap are mixed before application to membranes, they will form oligomers randomly, without any positive or negative mutual discrimination
4. In hybrid oligomers, the kynurenine fluorescence of all unlabeled Dap molecules is completely quenched by FRET. Therefore, any remaining kynurenine fluorescence originates from oligomers that consist of unlabeled Dap only
5. Oligomers are stable on the time scale of the experiment

According to assumption 3, Dap and NBD-Dap will form oligomers randomly. To account for all native Dap monomers that formed donor only oligomers, from the pre-mixture, the following equation was used.

$$D = \frac{d^n}{d} = d^{n-1}$$

D – fraction of all Dap, from pre-mixture, before oligomerization, that formed Dap only oligomers

d – The fraction of Dap, after oligomerization has occurred, that was incorporated into oligomers of both Dap and NBD-Dap

d_n – The fraction of Dap, after oligomerization has occurred, that formed Dap only oligomers

Assumption 4 states that any native Dap that forms mixed oligomers will be quenched by FRET. In other words, when excited, these Dap subunits will transfer the photons from kynurenine to NBD, thus eliminating kynurenine signal. Therefore, in the pre-mixture, only oligomers that formed with Dap only (represented by fraction D, above) will have signal from kynurenine. The fraction D then simplifies to equal the relative kynurenine fluorescence seen in pre-mixed oligomers, i.e. F_r (from the first equation). Substituting F_r for D in the second equation yields:

$$n = 1 + log_d(F_r) = 1 + \frac{\ln(F_r)}{\ln(d)}$$

The subunit stoichiometry (n) of the oligomer can be determined by comparing the kynurenine fluorescence of the mixed oligomers to that of pure Dap oligomers.

4.2.8 Membrane Translocation Assays with Dithionite

Membrane translocation assays were conducted similar to Zhang, *et al.*[111] but with some deviations. The buffer used for all samples was HEPES-buffered saline, supplemented with 25 mM calcium chloride. The assay was affected by the concentration of calcium present. At 25 mM the experimental variation was minimal compared to lower concentrations. A mixture of Dap:nitrobenzodiaxole (NBD)-Dap, at a molar ratio of 2:1, respectively, was added to the varying liposomes at a final concentration of 1 μM. A mixture of native Dap was necessary to prevent NBD-Dap self-quenching. The sample was allowed to incubate for 5 minutes before collecting the spectrum. Fluorescence (excitation wavelength, 465 nm; emission wavelength, 530 nm) was acquired on a PTI Quanta Master 4 instrument. Dithionite (1 mM) was added at 60 seconds to quench the NBD-Dap. A lower dithionite concentration was used, compared to Zhang, *et al*. to improve batch-to-batch reproducibility. When the dithionite concentration was increased to greater than 3-4 mM, there was extensive NBD quenching. It is suspected that this may be related to the introduction of sulfuric acid that forms through spontaneous chemical decay[193], but this has not systematically been examined

yet. At 300 seconds, Triton X-100 (0.1%, total) was added to solubilize the membranes, exposing all NBD groups.

4.3 Results

4.3.1 Membrane Insertion of Daptomycin into Dimyristoyl, Dioleoyl and Palmitoyl-oleoyl Liposomes

The interaction of Dap has been shown previously to occur on dimyristoylphosphatidylcholine (DMPC) and dimyristoylphosphatidylglycerol (DMPG) membranes[45,115,116]. The kynurenine residue intrinsic to Dap has a prominent blue shift and fluorescence increase as the residue becomes inserted into the hydrophobic membrane[76]. Equimolar mixtures of PC to PG containing liposomes, with three different acyl chain compositions, were measured for kynurenine's ability to insert (Figure 4.1). The lipid mixtures used were a one-to-one molar ratio of: DMPC/DMPG, dioleoylphosphatidylcholine (DOPC)/dioleoylphosphatidylglycerol (DOPG) and palmitoleoylphosphatidylcholine (POPC)/palmitoleoylphosphatidylcholine (POPG).

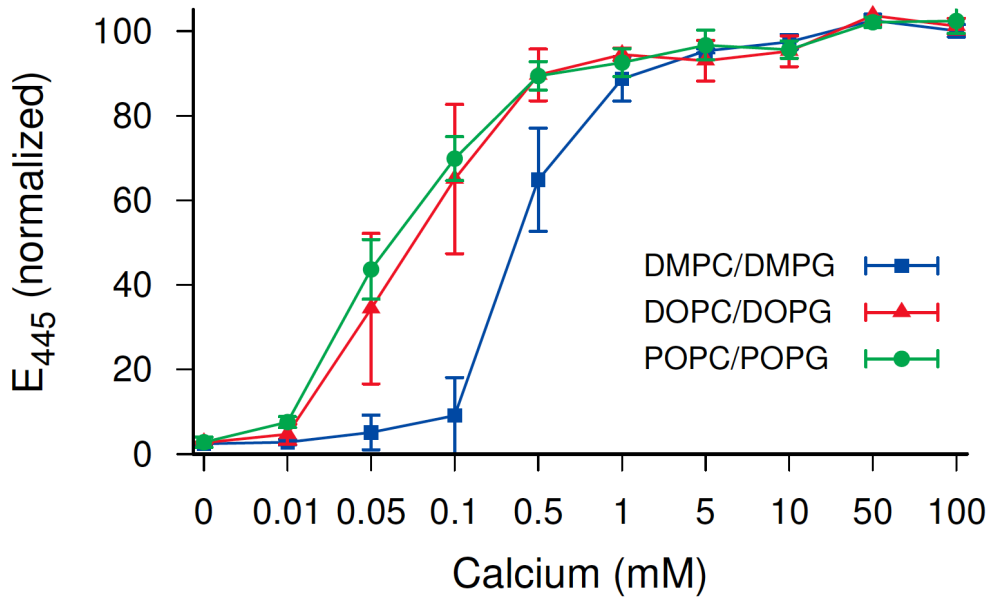

Figure 4.1 Daptomycin membrane interaction on three different types of large unilamellar vesicles (LUVs). LUVs consisting of DMPC/DMPG, DOPC/DOPG and POPC/POPG (molar ratio of 1/1 for PC to PG, 250 μM) were incubated with Dap (3 μM) at varying calcium concentrations, for 3 minutes. An increase in the intrinsic kynurenine residue (excitation, 365 nm; emission, 445 nm) indicates membrane insertion. Error bars represent the standard deviation of three different experiments, ran at 37°C

The interaction of Dap to these membranes is calcium-dependent. The increase in kynurenine's fluorescence, indicative of membrane insertion, occurs as the concentration of calcium is increased. Dap inserts into both DOPC/DOPG and POPC/POPG more avidly than the DMPC/DMPG but all show that the saturation point for kynurenine's signal occurs at a calcium concentration of >0.1 mM.

4.3.2 Biologically Relevant Concentrations of Daptomycin Permeabilize Dimyristoyl but not Dioleoyl or Palmitoyl-oleoyl Membranes

Previously, Zhang, *et al.*[45] reported that Dap causes the permeabilization for small cations in LUVs. This was done utilizing a coupled fluorescence assay, with pyranine, as discussed in Section 1.7.2[143]. Briefly, pyranine is loaded into liposomes and a pH/salt gradient is created across the bilayer. When ions are able to transport across the membrane, protons leave the liposome increasing the pH, causing an increase in pyranine's fluorescence intensity. Equimolar mixtures of PC to PG containing

membranes, consisting of DMPC/DMPG, DOPC/DOPG and POPC/POPG were tested, as shown in Figure 4.2.

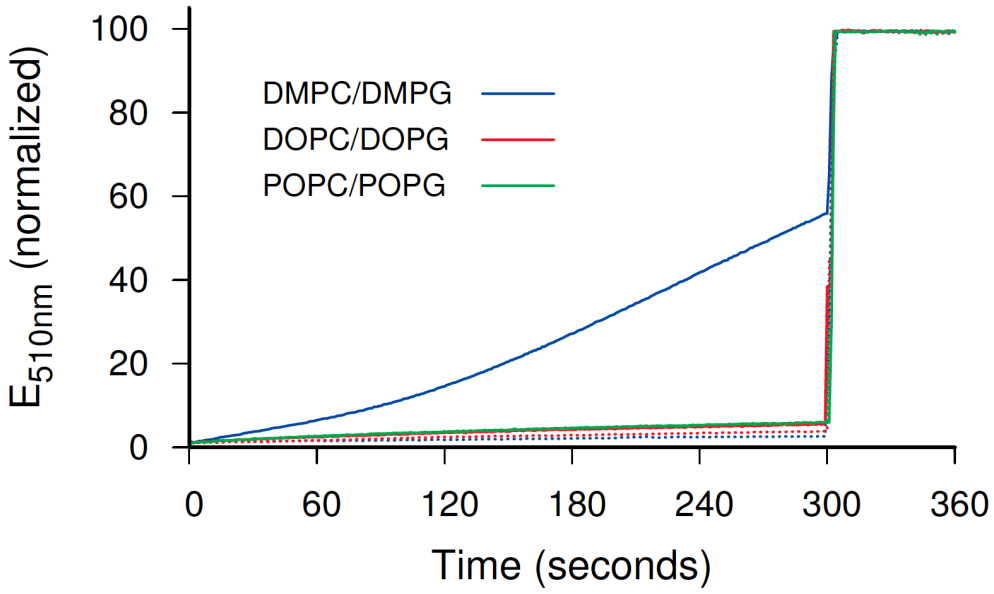

Figure 4.2 Permeabilization of Dap on three different LUVs. DMPC/DMPG, DOPC/DOPG, POPC/POPG (molar ratio of 1/1 for PC to PG, 250 μM) were entrapped with pyranine (1 mM) with a low pH and low sodium buffer. Time-based fluorescence was measured (excitation, 470 nm; emission, 510 nm) for 360 seconds. The loaded LUVs were incubated with a calcium (5 mM) pre-mixed buffer, which contained a high pH and increased sodium ions, thus creating a proton/sodium gradient across the bilayer. A proton ionophore carbonyl cyanide m-chlorophenyl hydrazone (CCCP, 5 nM) and Dap (2 μM) were added both separately or not at all (dotted lines) and together (solid lines) and measured from 0-300 seconds. At 300 seconds, Triton X-100 was added (0.1%) to solubilize the membranes. The experiments were run in triplicates at 30°C.

Controls were run with each separate lipid type with liposomes either alone or adding: CCCP (5 nM), Dap (2 μM) and Dap/CCCP. Other controls with valinomycin (0.5 μM) and gramicidin (10 nM) were also preformed, exactly as described by Zhang, *et al.*[111] In the case of valinomycin, a potassium selective carrier, no increase in signal was seen for DMPC/DMPG or POPC/POPG liposomes, due to the absence of potassium. For DOPC/DOPG valinomycin did cause a fluorescence increase. The reason for this is unknown. In the case of gramicidin, a rapid increase in fluorescence was observed. Gramicidin is a cation-selective channel[194]; having a very rapid rate of ion transport (10^6 ions per second[194]). Zhang, *et al.* observed that Dap's rate of transport was only ~0.12 ions per second[45], indicating that although both of these antibiotics form pores on model membranes, they

cannot be directly compared, in the context of ion transport rates. In Figure 4.2, it was observed that both DOPC/DOPG and POPC/POPG prevented Dap cation permeabilization. The DMPC/DMPG liposomes allowed for proper permeabilization at bactericidal concentrations of Dap. All three of these lipid types contain the same head group moieties, but differ in their acyl chain composition. Therefore, the difference in Dap permeabilization must be attributed to their fatty acyl tail groups.

A relatively recent study also utilized pyranine to examine membrane permeabilization of Dap (Figure 4.3). Zhang, *et al.*[118] were unable to mimic an equimolar PC to PG ratio, using a 3 to 1 ratio instead, but stated that the DMPC/DMPG membranes are susceptible to CCCP alone, at 10 nM. This could be due to the low calcium concentrations used, as it was found by Taylor, *et al.*[117] that calcium concentrations of > 1 mM was necessary for liposome stability. The inclusion of sucrose was found to also greatly improve stability. Zhang, *et al.*'s results, although interesting, suggest that their liposomes, without any analog added, are quite unstable and therefore the results are inconclusive. The experimental conditions and results used throughout this thesis and by Zhang, *et al.* are compared in Figure 4.3 below.

Condition	Zhang, *et al.*
Lip/Ca^{2+}/Dap/CCCP (μM)	274/270/2.2/0.01
DMPC:DMPG ratio	3:1
Internal Buffer	15 mM Na_2HPO_4, 4 mM Pyranine, pH 6.2
External Buffer	15 mM Na_2HPO_4, 200 mM KCl, pH 7.2
Temperature	35°C

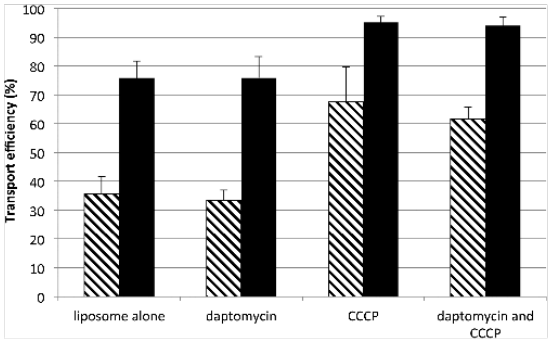

Condition	Taylor, *et al.*
Lip/Ca^{2+}/Dap/CCCP (μM)	250/5000/2.0/0.005
DMPC:DMPG ratio	1:1
Internal Buffer	5 mM MES/Tricine, 5 mM NaCl, 250 mM sucrose, 1.0 mM Pyranine, pH 6.0
External Buffer	5 mM MES/Tricine, 100 mM NaCl, 250 mM sucrose, pH 8.0
Temperature	30°C

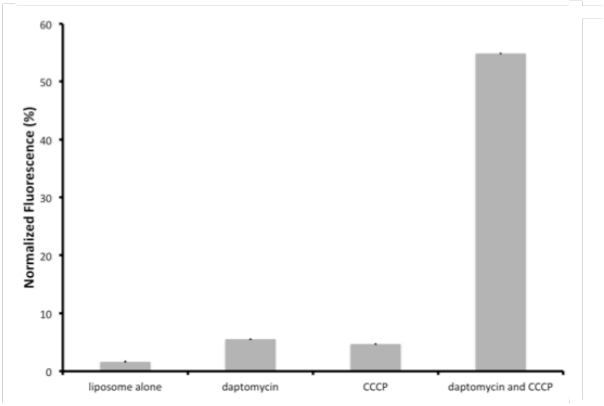

Figure 4.3 Compared results of Zhang, *et al.*[118] and Taylor, *et al.*[117] in the permeabilization assay with pyranine. Top: The conditions and results for Zhang, *et al.* are shown. The slashed bars represent 5 min incubation and the black bars represent 30 min incubation, with the compounds shown. The bar graph was reprinted with permission from Zhang, J.; Scoten, K.; Straus, S. K. *Am. Chem. Soc. – Infect. Dis.* 2016, *2,* 682-687. Copyright 2016, American Chemical Society. Bottom: The conditions and results for Taylor, *et al.* are shown. The bars represent 5 min incubations. As seen, the conditions used were widely different which may explain Zhang, *et al.* observing highly unstable liposomes

Zhang, *et al*. also used POPC/POPG, at an equimolar ratio, with this pyranine coupled assay and showed no Dap permeabilization[118]. However, using another assay that employed potassium and sodium probes, PBFI and SBFI (Figure 4.4), the same authors concluded that POPC/POPG membranes were in fact permeabilized by Dap, for both ions.

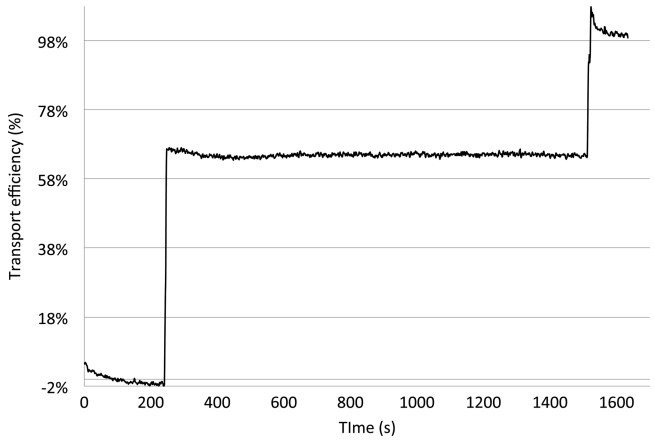

Figure 4.4 Permeabilization assay using the conditions by Zhang, *et al.* utilizing PBFI[118]. 1/1 POPC/POPG (0.55 mM) LUV's were encapsulated with PBFI (as described in Section 4.2.6). $CaCl_2$ (0.6 mM) was added to LUV's and ran for ~200 seconds. Dap (4.8 μM) was then added. Zhang, *et al.* attributed this instantaneous increase in fluorescence to Dap forming an ion selective pore for potassium (or sodium, utilizing SBFI). Triton X-100 was added at ~1500 seconds to solubilize the membranes. The figure was used with permission.

Since Zhang, *et al*. used the same concentrations for Dap in both assays the results appear quite contradictory. To resolve this question, the PBFI-based assay as described by Zhang, *et al.*[118] was repeated, but with some added controls that were absent from the original publication.

One large flaw with this PBFI assay is the strong spectral overlap that PBFI and Dap share, in both their absorption and fluorescence. The kynurenine residue of Dap has a maximal excitation at 365 nm, and emits at 445 nm. PBFI was excited at 338 nm and emitted at 507 nm[118]. It was speculated that the difference in these excitation/emission wavelengths was too small and that overlap would be present. To determine if this was the case, Dap's membrane interaction (similar to Figure 4.1) was tested on POPC/POPG (one-to-one molar ratio of PC to PG) at the concentrations used for Zhang, *et al*.'s PBFI work. Dap (4.8 μM) was added to POPC/POPG (0.55 mM) LUVs and mixed with calcium (0.6 mM). The excitation and emission spectra were determined, shown in Figure 4.5.

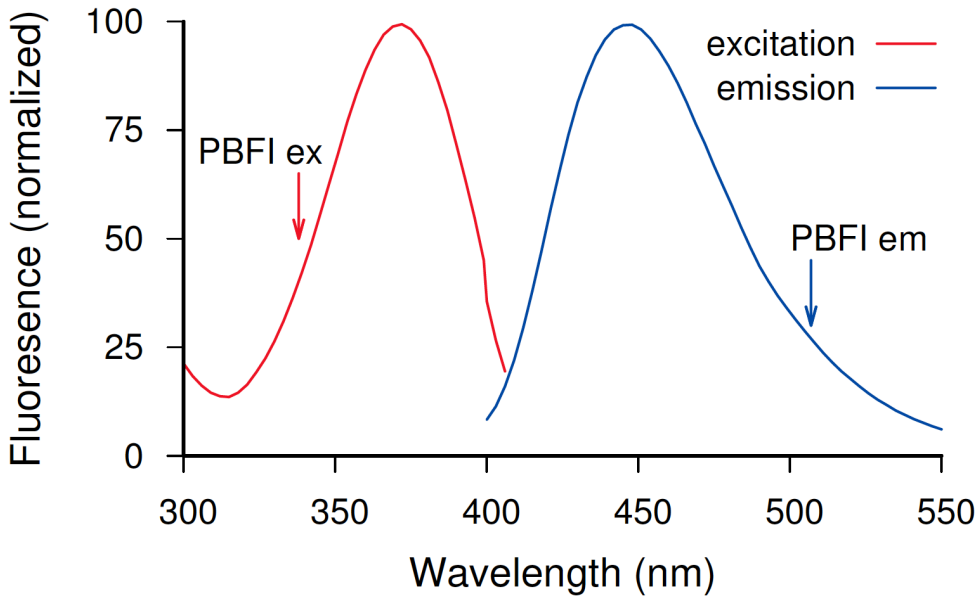

Figure 4.5 Excitation and emission spectra of Dap added to POPC/POPG (1/1 molar ratio, 550 μM). Dap (4.8 μM) was added to LUVs in HEPES-buffered saline with 0.6 mM calcium and incubated for 3 minutes. The excitation and emission wavelengths for PBFI are shown, overlapping with the excitation (red) and emission (blue) of Dap on these membranes.

The red and blue arrows (Figure 4.5) show the excitation and emission wavelengths used for PBFI, respectively. These results show that when PBFI is excited, Dap will also get excited. The emission of Dap when excited at 338 nm is ~half the signal intensity than when excited at 365 nm, but a strong signal is still observed. Zhang, *et al.*'s work was repeated, where PBFI was entrapped within POPC/POPG liposomes through sonication. The excess PBFI was removed by gel filtration with a high salt buffer (20 mM HEPES, 200 mM KCl, pH 7.4) as the elutant. Loaded liposomes were then measured through fluorescence (excitation, 338 nm; emission, 507 nm) with Dap added with or without calcium (Figure 4.6).

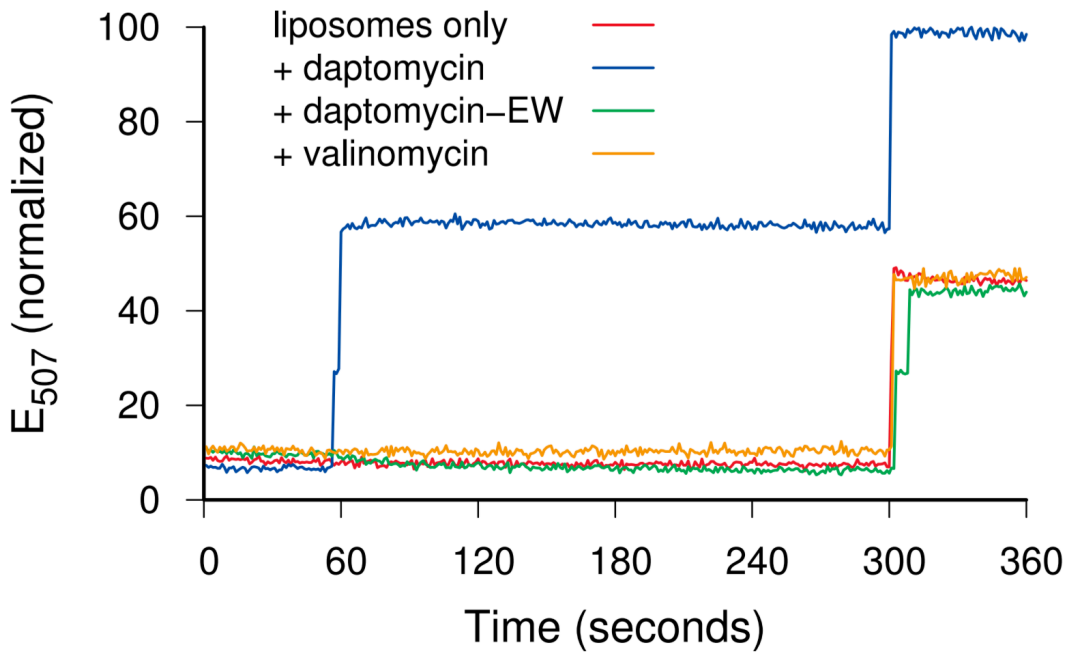

Figure 4.6 Time-based fluorescence scan of PBFI loaded POPC/POPG LUVs (1/1 molar ratio, PC to PG, 550 μM). A potassium ion sensitive probe, PBFI (0.85 mM) was loaded into POPC/POPG LUVs in buffer (20 mM HEPES, pH 7.4). Fluorescence was measured (excitation, 338 nm; emission, 507 nm) for 360 seconds. At 0 seconds, buffer (20 mM HEPES, 200 mM KCl, pH 7.4) was mixed with PBFI loaded LUVs. At 60 seconds, either valinomycin (0.5 μM) or Dap (4.8 μM)/Dap-E12W13 (4.8 μM) were added with 0.6 mM calcium. At 300 seconds, Triton X-100 (0.1%) was added to solubilize the membranes. Of all tested compounds, only Dap produced a step change in fluorescence emission. The potassium ionophore valinomycin as well as Dap-E12W13, which contains tryptophan instead of kynurenine in position 13[68], are indistinguishable from control and only exhibit increased fluorescence when the entrapped PBFI is released into the buffer by Triton X-100. The experiments were run in triplicates at room temperature.

If a pore formed, one would expect a gradual increase in Dap's signal, over time, similar to the pyranine results seen in Figure 4.2. Interestingly, when Dap and calcium were added to PBFI loaded liposomes the fluorescence instantaneously increased and then remained constant until Triton X-100 was added. The Triton X-100 causes the membranes to solubilize, causing any PBFI within the membranes to be exposed to the high potassium buffer and fluoresce. When taking into account that there is an extensive overlap between Dap and PBFI's excitation and emission spectra, this result can be explained. The instantaneous increase in signal when Dap and calcium are added must be attributed to the kynurenine insertion into the POPC/POPG membranes. In Figure 4.1, it was shown that at >0.1 mM calcium, maximal signal occurred for Dap. The calcium concentrations used in this work was 0.6 mM, suggesting that the intensity increase was solely due to kynurenine.

To prove that this was the cause of this rapid increase in signal a separate analog of Dap was used. This analog, Dap-E12W13[68], has the 3-methylglutamate of position twelve changed to glutamate and the kynurenine residue of position thirteen changed to tryptophan. Lohani, *et al.* synthesized this analog through solid phase peptide synthesis[68]. The antibacterial activity (MIC) of this analog was compared to Dap. Dap-E12W13 was found to have an MIC of 1.5 µg/mL; Dap's MIC was found to be 0.75 µg/mL (on *B. subtilis* ATCC 1046 at 5 mM calcium). The interaction of this analog was tested against DMPC/DMPG LUVs and found to insert (Figure 4.7A) and permeabilize (Figure 4.7B) the model membranes at the same concentrations necessary for Dap.

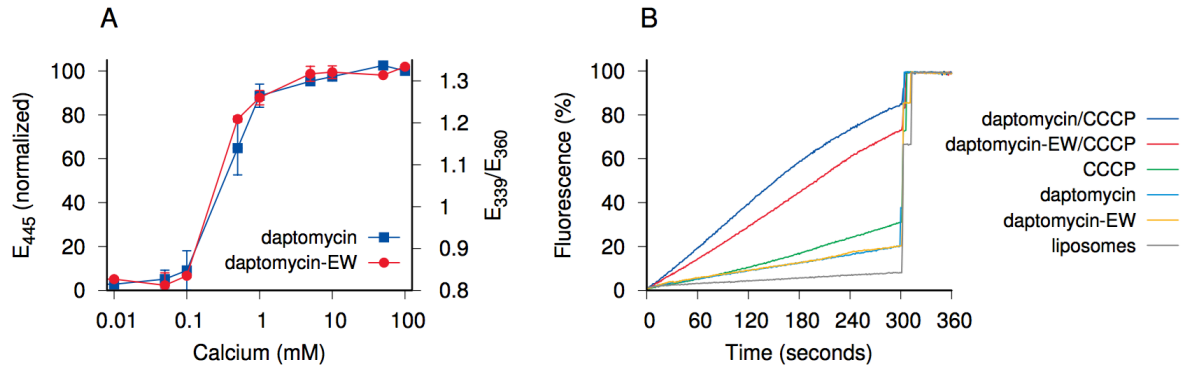

Figure 4.7 The interaction and permeabilization of the Dap analog Dap-E12W13 on model membranes. A: DMPC/DMPG LUVs (1/1 molar ratio, 250 µM) were incubated with Dap (3 µM) and Dap-E12W13 (3 µM) at varying calcium concentrations, for 3 minutes. Insertion of Dap was monitored using kynurenine (E_{445}), whereas insertion of Dap-E12W13 was monitored by the blue shift of tryptophan (E_{339}/E_{365}). Error bars represent the standard deviation of triplicate experiments, ran at 37°C. B: Permeabilization of Dap and Dap-E12W13 were monitored on DMPC/DMPG membranes, utilizing pyranine (1 mM). DMPC/DMPG LUVs (1/1 molar ratio, 250 µM) were entrapped with pyranine (1 mM) with a low pH and sodium buffer. Time-based fluorescence was measured (excitation, 470 nm; emission, 510 nm) for 360 seconds. The loaded LUVs were incubated with a calcium (5 mM) pre-mixed buffer, which contained a high pH and increased sodium ions, thus creating a proton/sodium gradient across the bilayer. A proton ionophore carbonyl cyanide m-chlorophenyl hydrazone (CCCP, 5 nM), Dap (2 µM) and Dap-E12W13 (2 µM) were added both separately or not at all (dotted lines) and together (solid lines) and measured from 0-300 seconds. At 300 seconds, Triton X-100 was added (0.1%) to solubilize the membranes. The experiments were run in triplicates at 30°C.

This data suggests that the Dap-E12W13 analog interacts with the membrane by the same mechanism as Dap, and therefore is useful in validating the PBFI assay. When this analog was used, in Figure 4.6 (green line), the instantaneous increase in fluorescence was not observed, due to the lack

of kynurenine present. This indicates that the signal seen for Dap and calcium permeabilization, with the PBFI assay, is entirely due to kynurenine.

A "mock" PBFI assay was also performed, where the same experiment shown in Figure 4.6 was repeated, expected with a lack of PBFI present (Figure 4.8). These POPC/POPG membranes were tested with Dap and Dap-E12W13 at the same concentrations presented above. This plot shows that Dap will be excited even in the absence of PBFI, further demonstrating that the signal seen by Zhang, *et al.*[118], was erroneous.

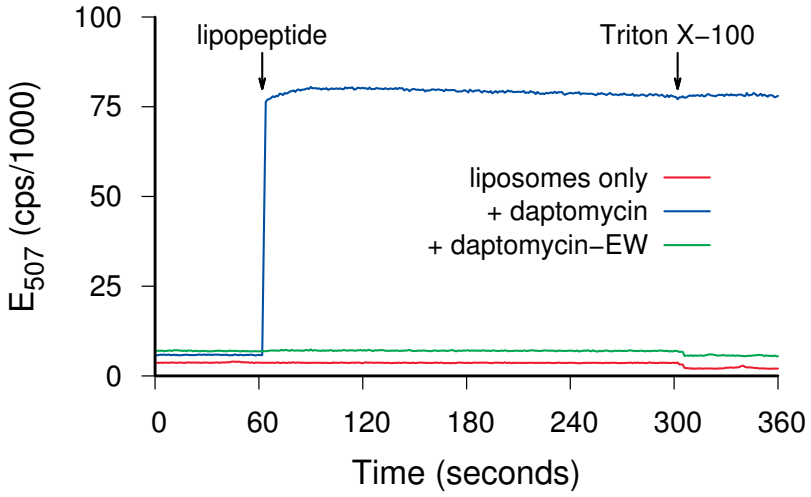

Figure 4.8 Mock PBFI assay to demonstrate Dap's signal overlap. The time-based fluorescence spectrum of POPC/POPG LUVs (1/1 molar ratio, PC to PG, 550 μM) without PBFI added. Fluorescence was measured (excitation, 338 nm; emission, 507 nm) for 360 seconds. At 0 seconds, buffer (20 mM HEPES, 200 mM KCl, pH 7.4) was mixed with LUVs. At 60 seconds, either Dap (4.8 μM) or Dap-E12W13 (4.8 μM) was added with 0.6 mM calcium. At 300 seconds, Triton X-100 (0.1%) was added to solubilize the membranes. Since no dye was present, Triton X-100 had minimal signal. Dap produced a step change in fluorescence emission. Dap-E12W13, which contains tryptophan instead of kynurenine in position 13[68], are indistinguishable from control. The experiments were run in duplicate at room temperature.

Zhang, *et al.*'s PBFI work[118] also utilized a sodium probe, SBFI. The analogous experiments with the sodium indicator SBFI were not carried out in this study, since the fluorophore in SBFI is the same as PBFI. The excitation wavelength used for SBFI is 333 nm, and therefore it would be suspected that the results shown here would be the same for this probe. The data obtained and shown by Zhang, *et al.*[118] with PBFI and SBFI do not support the conclusion that POPC/POPG membranes are permeabilized toward potassium or sodium by Dap.

4.3.3 Translocation and Oligomer Formation of Daptomycin on Dioleoyl Membranes

In Chapter 2, it was suggested that the mechanism of action of Dap occurs through two calcium-binding events. The first calcium ion causes Dap to oligomerize in the outer cytoplasmic membrane. The second calcium ion causes a deeper insertion and translocation of this oligomer. DOPC/DOPG and POPC/POPG, as seen previously, prevent permeabilization of Dap but which phase of calcium-binding they inhibit was unclear. To attempt to solve this question, the ability of Dap to translocate across leaflets and even further, the oligomer stoichiometry of Dap within the membrane, was investigated. To determine if translocation was occurring, a dithionite quenching experiment was done utilizing NBD-Dap (Figure 4.9).

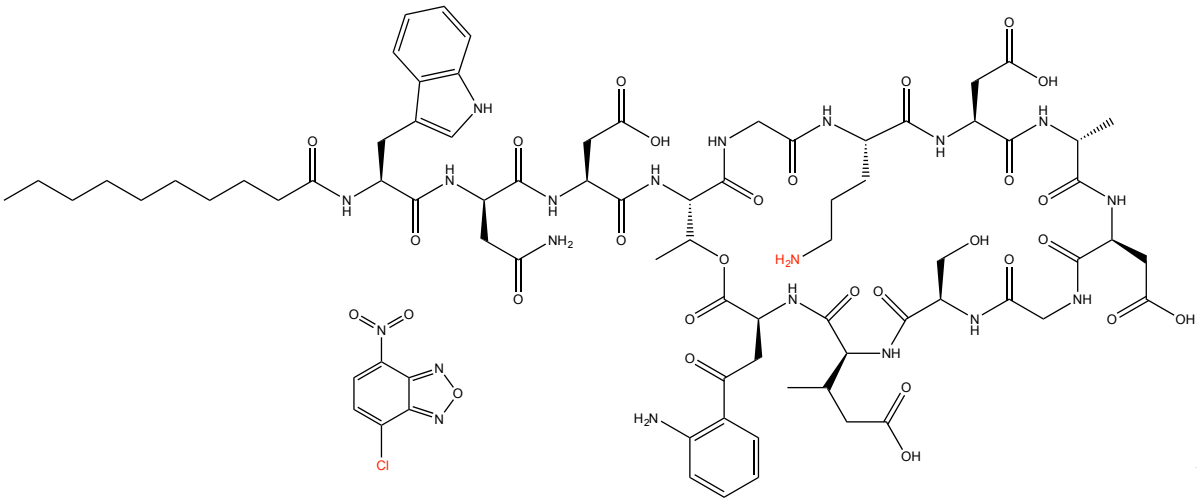

Figure 4.9 Structures of Dap and the NBD moiety. The NBD moiety is attached to the ornithine6 residue of native Dap.

In this assay (Figure 4.10), NBD-Dap was pre-mixed with native Dap (to prevent NBD self-quenching) and allowed to insert into the membranes. After a baseline was reached, dithionite was added to quench the NBD-Dap[195] that would be found on the outer leaflet. The NBD-Dap that had translocated before addition of dithionite would be found on the inner leaflet of the membrane and therefore be protected, initially, from dithionite. Over time the NBD groups gradually become reduced by dithionite in the external buffer, since NBD-Dap is able to transiently move back and forth

across the membrane leaflets[45]. The addition of Triton X-100 was used to solubilize the membranes, allowing for any remaining NBD groups to be quenched, showing minimal signal.

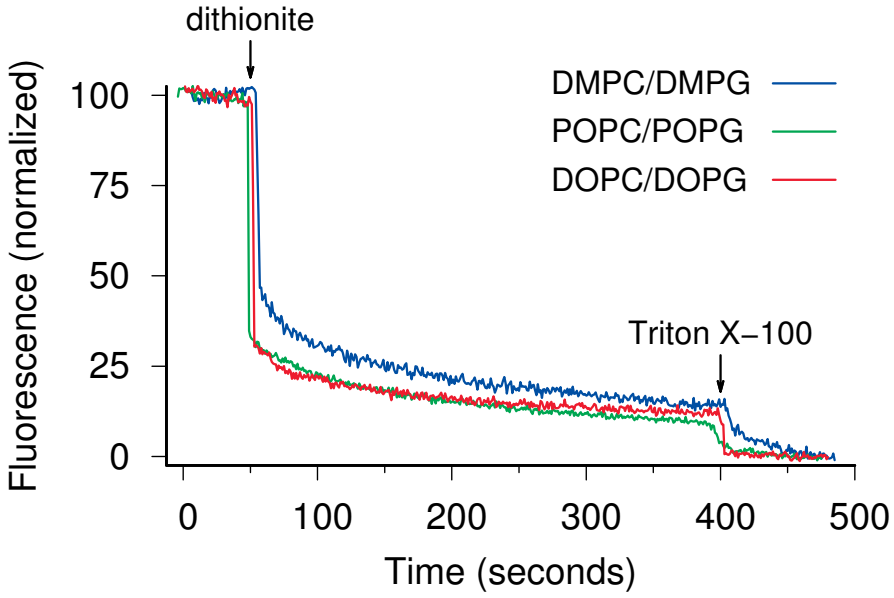

Figure 4.10 Translocation of NBD-Dap across DMPC/DMPG and DOPC/DOPG LUVs. The LUVs were each incubated with a 2:1 mixture of Dap to NBD-Dap (1 μM total), respectively, at 25 mM calcium. At 60 seconds, dithionite (1 mM) was added to quench the NBD-Dap exposed to the external buffer. At 400 seconds, Triton X-100 (0.1%) was added to solubilize the membrane, exposing any NBD-Dap contained in inner leaflet that has not yet been quenched. NBD fluorescence was measured over time (excitation wavelength, 478 nm; emission wavelength, 520 nm; each curve is the average of three separate experiments). Curves are offset by 5 seconds to avoid overlap, to better visualize the difference in translocation.

Zhang, *et al.*[111] reported that close to 50% of the NBD-Dap inserted into DMPC/DMPG membranes are immediately quenched and therefore approximately 50% of NBD-Dap is on the outer leaflet. This correlates with the results displayed in Figure 4.10, which show 48%±6% quenching of NBD immediately. In a control experiment to confirm that Dap does not lead to the transport of dithionite, Zhang, *et al.* added NBD labeled phosphatidylethanolamine (PE) into these DMPC/DMPG membranes. They observed 50% quenching of NBD with and without Dap added, confirming that Dap does not cause the transport of dithionite across the membrane. On DOPC/DOPG or POPC/POPG membranes, ~70% are immediately reduced, with remaining NBD signals of 31%±3%

and 35%±1%, respectively (Figure 4.10). This suggests that the translocation of NBD-Dap across these membranes is partially prevented. When the incubation time before adding dithionite to these membranes was increased, the difference in NBD quenching was minimal, suggesting there is a shift in the distribution of NBD-Dap across DOPC/DOPG and POPC/POPG membranes.

Although DOPC/DOPG and POPC/POPG membranes prevent some translocation of oligomers into the inner leaflet, ~30% is still translocated. This suggests another factor is, in part, preventing permeabilization. A potential reason for the lack of ion transport could be an inability for Dap oligomers in opposing leaflets to be proper aligned. To investigate this, the number of monomers of Dap per oligomer in the membrane was determined. This subunit stoichiometry result utilized a FRET based assay that determined the ratio of florescence within and between Dap/NBD-Dap oligomers[115]. From this ratio, the average number of subunits was calculated (Section 4.2.7 details the methodology). Zhang, *et al.*[45] reported that DMPC/DMPG membranes had a Dap subunit stoichiometry of >6, whereas values of 4.7±0.7 subunits and 3.6±0.9 subunits were observed on DOPC/DOPG and POPC/POPG membranes, respectively. The data between DOPC/DOPG and POPC/POPG membranes are compatible, with a subunit stoichiometry of ~4. This suggests that tetramers found in each leaflet of the membrane are unable to align across the bilayer, preventing FRET to occur, and ultimately accounting for the absence of pore formation.

4.4 Discussion

Many proposed mechanisms of action for Dap are found in the literature, with many groups utilizing model membranes. The effect of the lipid head group in these membranes has been examined in detail, proving that Dap requires PG for activity[40], and also suggesting the presence of lysyl-PG[134] and cardiolipin (CL)[107] to be resistance mechanisms. Although extensive work has been done into the varying head groups of lipids, little emphasis has been given to the composition of the acyl tails.

The important finding to this chapter is the extreme difference between DMPC/DMPG membranes and DOPC/DOPG or POPC/POPG containing membranes. Dap permeabilizes DMPC/DMPG membranes rapidly, while the other lipids are permeabilization resistant (Figure 4.2). Interestingly, Dap not only inserts to but also oligomerizes on these permeabilization resistant liposomes. This highlights that the study of Dap, using model membranes, must be done carefully.

The chain composition of these membranes must be taken into consideration when examining the activity and mechanism of Dap, and cannot be chosen strictly based on technical simplicity.

Zhang, *et al*.[118] utilized a potassium-sensitive fluorophore, PBFI, to detect Dap permeabilization. They suggested from their work that permeabilization is ion selective. Unfortunately, Dap's intrinsic kynurenine residue overlaps strongly with the excitation of this PBFI (Figure 4.5). This gave rise to an instantaneous increase in fluorescence after Dap was added, that was previously attributed to indicate ion leakage. Several experiments were performed to show that the kynurenine residue of Dap was the main cause for this increase. To further confirm this fluorescent jump, dual wavelength ratio metric experiments were preformed (Figure 4.11). Dap was added to POPC/POPG liposomes containing PBFI as outlined in Section 4.2.6. Again, an instantaneous increase was observed when Dap and calcium were added. The increase seen was significantly larger when the sample was emitted at 445 nm (the maximal emission of kynurenine). This further highlights that the increase seen is due to kynurenine insertion, as the intensity is comparable to the emission scan of Dap itself. The addition of Triton X-100 to the PBFI loaded POPC/POPG showed similar intensity increases with either wavelength, which is also comparable to the PBFI emission spectrum. From the data here and in Section 4.3.2, it is clear that the observed increase in fluorescence seen by Zhang, *et al*. is entirely due to a fluorescence artifact. The POPC/POPG membranes do not allow for Dap permeabilization, as shown in Figure 4.2.

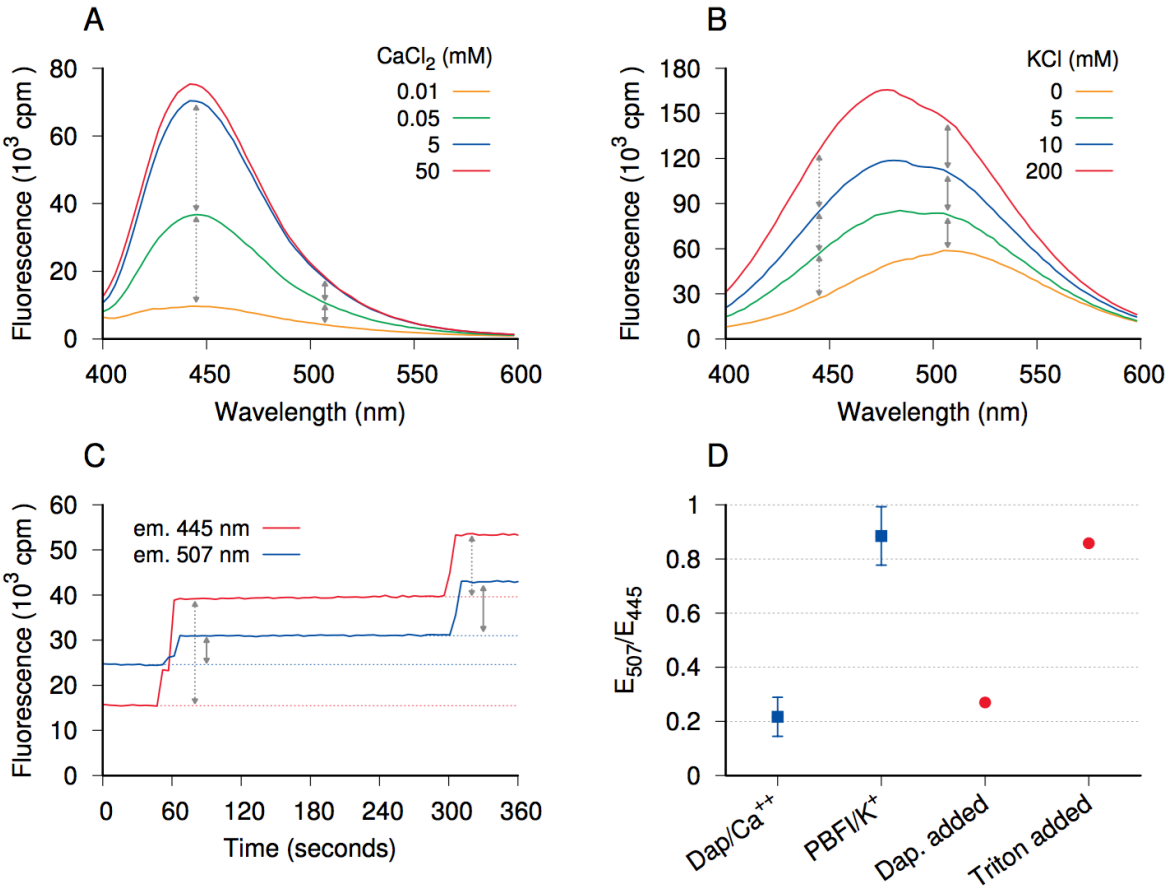

Figure 4.11 Dual wavelength monitoring of the PBFI assay of permeabilization using Dap. A: Emission spectrum of Dap on POPC/POPG LUVs (1/1 molar ratio, 0.55 mM) at varying calcium concentrations. Solid and dashed arrows indicate changes in emission at 507 and 445 nm, respectively. These differences were used to calculate the characteristic emission ratio shown in D. B: Emission spectrum of PBFI, in the presence of 0.1% Triton X-100. There was a blue shift upon Triton X-100 addition with the addition of potassium. Triton X-100 was added to mimic the conditions used in C. Solid and dashed arrows indicate changes in emission at 507 and 445 nm, respectively. C: Dual wavelength time-based emission scan of Dap added to PBFI loaded POPC/POPG LUVs. Solid and dashed arrows indicate changes in emission after adding Dap (60 seconds) and Triton X-100 (300 seconds) at 507 and 445 nm. These ratios were also used in the calculations for part D. D: Ratios of emission changes at 507 and 445 nm calculated A-C. Adding Dap to PBFI loaded liposomes causes a change that resembles an increased kynurenine emission, whereas adding Triton X-100 causes a change resembling an increase in PBFI emission.

In order to compare our experimental observations with bacterial membranes a look into the lipid composition of these bacteria is required. The numbers given below are complied from different references, which used different quantitative methods and growth conditions that may have affected

experimental results. The experimental growth conditions, primarily pH and temperature, have shown to have large implications on the final lipid composition of bacterial strains[100,86,101,106].

Among all *B. subtilis* species, the most common bacterial lipids consist of terminally methylated, either *iso* or *anteiso*, branched acyl chains[196,100]. These chains range from 14-17 carbons in length[196,100]. The percentage of mono-unsaturated tails is minor and poly-unsaturation is virtually non-existent[196]. In the case of *S. aureus,* the acyl composition is similar to *B. subtilis*[100,197], but fifteen carbon branched chains are the most prevalent[197], with minor percentages of unsaturation[100]. Dap is also used clinically against *Enterococcus faecalis*[198]. This bacterium has a fairly different acyl chain composition from those previously discussed. This bacterium is composed of mainly 16 and 18 carbon lengths, with 10-15% longer mono-unsaturated chains[48,104]. These varying percentages are shown in Figure 4.12, below.

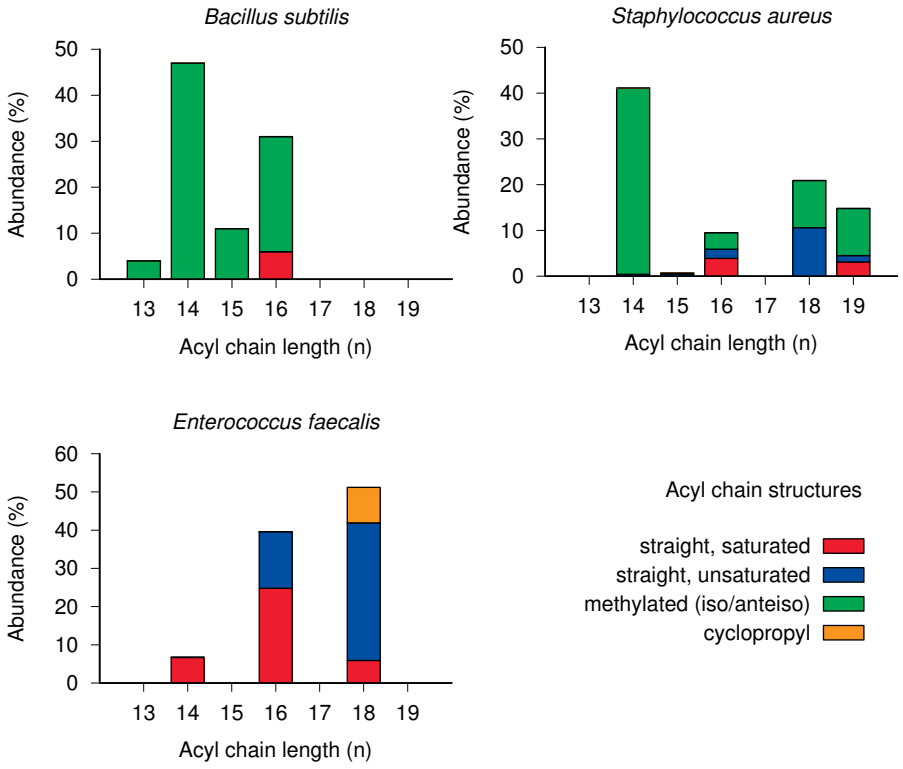

Figure 4.12 Lipid acyl chain composition of varying bacteria mentioned above. The acyl chain structures are colour coded according to their acyl chain moieties. The *iso* and *anteiso* chains were group together as "methylated." From this figure it is clear that *E. faecalis* contains, on average,

longer acyl chains than the other strains discussed. Several references were used for this figure, outlined in the paragraph above.

The bacterial species also vary greatly in lipid head group composition, and this will certainly affect susceptibility or resistance to Dap. Several studies have shown the membranes of *B. subtilis* to contain PG, CL, phosphatidylethanolamine (PE) and lysyl-PG percentages of approximately 35, 13, 35 and 18, respectively[106,199]. In the case of *S. aureus*, the lipid composition has been observed to contain a large percentage of PG (~80%), with lower percentages of lysyl-PG and CL, at ~15% and 10%[100,101–103,104]. *E. faecalis* contains PG, CL and lysyl-PG at percentages of approximately 13%, 30% and 10%[48,104].

All the bacteria mentioned above are highly susceptible to Dap, yet they all have variable phospholipid content. This lipid variation, in conjunction with our data, suggests that consideration of only lipid head moieties is erroneous and that acyl tails are an important, overlooked, factor impacting Dap's bactericidal activity.

Recently, Müller*, et al.* proposed that Dap does not permeabilize *B. subtilis* 168 through pore formation[119]. Interestingly, Bishop, *et al*. showed that *B. subtilis* 168 has a dramatically increased CL percentage, and a low PG content, only 13%[200], compared to other *Bacillus spp*., may also explain the decreased Dap permeabilization observed by Müller, *et al.*[119] This may also account for the slightly diminished activity of Dap against *E. faecalis* strains observed by Barry, *et al.*[130] since this bacterium contains only ~13% PG. Although it is likely that the diminished percentages of the PG lipid are the major reason for decreased activity, the possible effects of acyl tails should not be overlooked. *E. faecalis* contains longer acyl tails than *S. aureus* or *B. subtilis*. The results from this chapter suggest that the decreased activity of Dap within *E. faecalis* could be due to both head group and acyl chain differences. This hypothesis is investigated further in Chapter 5 with the synthesis of a longer tailed Dap analog. Recently, Hines, *et al.* characterized the lipid composition of Dap resistant *S. aureus* strains and observed an increase in the acyl chain length of the bilayer[201], which correlates with the date observed in this chapter. Overall, the findings in this work and in the literature show that bacteria choice must be taken into consideration when studying Dap. The lipid composition of bacteria varies, and therefore to better understand Dap's mechanism, clinically susceptible strains of bacteria, mainly *S. aureus* and *E. faecalis,* should be used. If other strains are used, researchers must take care to note differences in membrane composition.

In previous work, it has been suggested that Dap forms oligomers within the membrane that then translocate across leaflets. This leads to tetrameric oligomers that come together to form a functional octameric pore[111]. Through dithionite quenching experiments it has been shown that Dap is found 50% in the outer and inner leaflets of DMPC/DMPG membranes. POPC/POPG and DOPC/DOPG membranes were shown to interact with Dap more avidly (Figure 4.1) and allow for at least partial translocation (Figure 4.9, ~70% immediate dithionite quenching). Although partial translocation occurs, the Dap oligomers are still restricted to four subunits. One reasoning for this could be a spatial gap, where the Dap tetramers are translocating but the lipid acyl chain composition is preventing the oligomers from interacting. This theory is investigated more deeply in Chapter 5, with synthesis of a longer acyl chain on Dap. Nevertheless, this data highlights that the oligomer formation and translocation of Dap into the inner leaflet is necessary but not sufficient for proper pore formation.

Chapter 5

Investigating the Role of Lipid Chains in Preventing Daptomycin Pore Formation[4]

5.1 Introduction

In the previous chapter, it was shown that the pore formation of Dap was highly dependent on the acyl chain composition of the membrane, and that the lipid composition varies greatly between several bacterial species.[102,103,106,200] Researchers utilize these bacteria to study Dap, as well as varying model membrane systems, with little emphasis on retaining similar acyl tail compositions. Lipid flip flop and membrane fusion was shown with palmitoyl-oleoyl chained lipids[82,109], lipid extraction from bilayers consisting of dioleoyl chained lipids[120] and cation-selective pore formation with myristoyl chained lipids[45]. The use of POPC/POPG and DOPC/DOPG lipids was shown, in the previous Chapter, to prevent permeabilization by Dap. These membranes still allowed for Dap interaction and oligomerization, but the oligomer subunit stoichiometry and translocation into the inner leaflet were found to be lower, compared to DMPC/DMPG. This highlighted that translocation of the oligomer was necessary but not sufficient for pore formation. This divergence between lipid acyl chains may be relevant to the observation of different antibacterial action models of Dap on different bacterial species.

The work herein was done to better understand the reason for this diminished permeabilization. In the previous Chapter, it was suggested that the tetramers that form in each leaflet are being prevented from interacting across leaflets, preventing permeabilization (Figure 5.1).

[4] The results shown in this chapter are unpublished work. Authors contributions: The preliminary dithionite-quenching assay on TMCL membranes (shown in Appendix A) was run by David Beriashvili. Robert Taylor completed all other synthesis and results. David Beriashvili ran replicate trials for Figures 5.4 and 5.10.

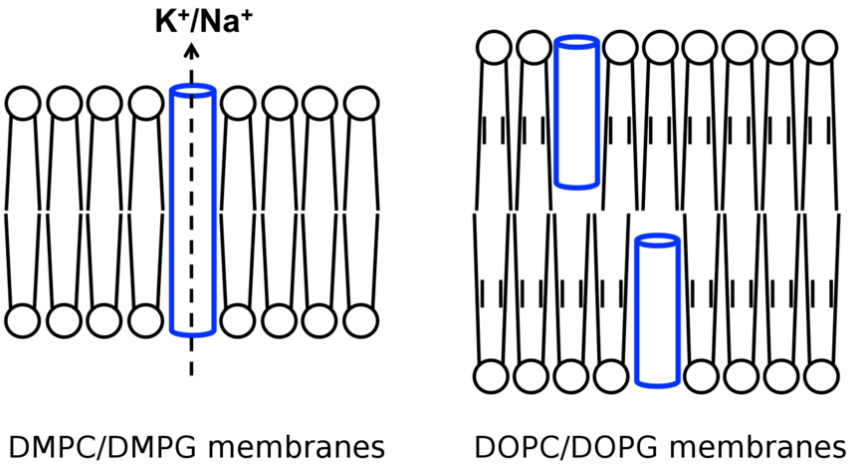

Figure 5.1 Hypothetical model for reduced pore formation seen with membranes containing longer acyl tails. Experimental findings in Chapter 4 show reduced pore formation and translocation of Dap within longer acyl tailed membranes. This suggests that there is a spatial gap occurring. The oleoyl lipids interact with Dap more avidly, than myristoyl containing lipids, but prevent the tetramers in each leaflet to link together, thus preventing permeabilization.

Recently, Zhang, *et al.*[111] observed that cardiolipin (CL) also prevented translocation and pore formation of Dap. Unfortunately, Zhang, *et al.* used a tetraoleoyl-CL (TOCL) and therefore it is unclear whether the effect observed by Zhang, *et al.* was due to the oleoyl chain or the CL head group. The role of CL in the membrane was therefore revisited, with use of a myristoyl chained-CL (TMCL). TMCL and TOCL both prevented Dap permeabilization, suggesting that Zhang, *et al.* conclusions were accurate.

In the previous chapter the use of homogenous acyl tail compositions prevented Dap permeabilization, but it was unclear if this effect was due to the acyl chain itself or the head group. It was speculated that since the only variation between the three lipid species analyzed was the acyl chain, therefore this was the reason for diminished permeabilization. This theory was investigated further, by using hybrid mixtures of both myristoyl and oleoyl chained PC/PG membranes. It was observed that the head group was not involved in the inhibition of this pore. Since these hybrid mixtures contained only 50% DOPC or DOPG, the question then arose as to how much of a DOPC lipid was required to disrupt pore formation. To study this, membranes were utilized that were composed of decreasing percentages of DOPC, with DMPG kept constant at 50%, and DMPC used to balance the final percentage. Unexpectedly, only 1-5% incorporation of DOPC was necessary to

reduce Dap permeabilization. When Dap was added in a molar excess of DOPC, permeabilization resumed. This suggests that the added DOPC is, in some way, acting near-stoichiometrically with Dap, preventing pore formation.

Chapter 4 speculated that DOPC/DOPG was creating a spatial gap across the membrane, preventing tetramers in opposing leaflets to properly align (Figure 5.1). To elucidate the inhibitory effects of these lipids, two different approaches were undertaken. Firstly, it was determined that the unsaturation point of oleoyl chained lipids was not involved in this inhibitory effect, by utilizing a PC lipid with an unsaturated fourteen-carbon acyl chain. This added acyl chain did not alter the ion transport of Dap. To probe the theory of a spatial gap between leaflets, an analog of Dap was synthesized that replaced the decanoyl tail with a longer, fourteen carbon, acyl chain (14C-Dap). This analog is similar to the natural fermentation of Dap derivatives from *S. roseosporus*, which Debono, *et al.* has shown contain fatty acyl tails ≥12 carbons[74]. It was suspected that increasing the acyl chain length of Dap might improve its ability to permeabilize these DOPC/DOPG membranes, by allowing the oligomers in opposing leaflets to properly link together. However, DOPC/DOPG membranes also inhibited the permeabilization of 14C-Dap. This finding further supports the previously mentioned conclusion; that acyl chain composition of membranes has drastic effects on the ability of Dap to form a pore.

5.2 Methods and Materials

5.2.1 Synthesis of 14Carbon-Daptomycin (14C-Dap)

Firstly, a myristic acid succiminidyl ester was synthesized. The steps for this synthesis were done using the method by Gantner, *et al.*[202] Briefly, Myristic acid and N, N'-dicyclohexylcarbodimide were added to a round bottom flask in THF and stirred at room temperature for 10 minutes. N-hydroxysuccinimide was added and the reaction was stirred for 22.5 hours at room temperature. The solvent was removed under reduced pressure, and dry-loaded onto a silica gel column. The column was eluted with 50:1 chloroform:methanol. The product was separated with an $R_f = 0.76$. The product was concentrated under reduced pressure and lyophilized to produce a white powder. For further details regarding the synthesis and purification of the myristic acid succiminidyl ester, see Appendix A.

For the semi-synthesis of 14C-Dap, a solution of Boc-deacyldaptomycin in dry DMF was added to myristic acid succiminidyl ester. Triethylamine was added and the mixture stirred for three days, at room temperature. After this, TFA/0.2% thioanisole was added and stirred at 0^{o}C for 20 minutes, under argon. The sample was then purified by HPLC. For details regarding the synthesis and purification of 14C-Dap, see Appendix A.

5.2.2 Antibacterial Activity

Antimicrobial susceptibility tests were performed as outlined in Section 2.2.3, with minor additions. Serial dilutions of Dap and 14C-Dap were prepared in Luria-Bertani (LB) broth (for *Bacillus subtilis* ATCC 1046) that was supplemented with 5 mM calcium chloride. Growth was assessed visually after incubation at 30^{o}C (for *Bacillus subtilis*).

5.2.3 Preparation of Liposomes

Lipids used included those described in Section 2.2.4, with the addition of 1,2-dimyristoleoyl-*sn*-glycero-3-phosphocholine (14:1 PC), 1',3'-bis[1,2-dioleoyl-*sn*-glycero-3-phospho]-*sn*-glycerol (sodium salt; TOCL) and 1',3'-bis[1,2-dimyristoyl-*sn*-glycero-3-phospho]-*sn*-glycerol (sodium salt; TMCL). All lipids were obtained from Avanti Polar Lipids, Alabaster, AL, USA.

The methodology for liposome preparation of mixtures of LUV's has been described in a preceding chapter (Section 2.2.4).

5.2.4 Fluorescence Spectroscopy

Steady state experiments were performed as described in Section 2.2.5.

5.2.5 Permeabilization Assays Utilizing Pyranine

The methodology for the permeabilization assay with pyranine was described in Section 3.2.5.

5.3 Results

5.3.1 DOPC and POPC Inhibit Membrane Permeabilization by Dap

In Chapter 4 it was speculated that the lack of permeabilization observed with oleoyl chain containing membranes was due to the acyl chain composition, since the only variance between the three lipids tested (DMPC/DMPG, DOPC/DOPG and POPC/POPG) was the fatty acyl chains. Since Dap requires PG to insert into the membrane it was unclear whether PG was a required constituent to cause this inhibition in Dap permeabilization. To elucidate this, permeabilization experiments were run with Dap on hybrid mixtures of oleoyl and myristoyl chained lipids (Figure 5.2). Oleoyl chained PC was mixed with myristoyl chained PG and vice versa, both at equimolar mixtures of PC to PG.

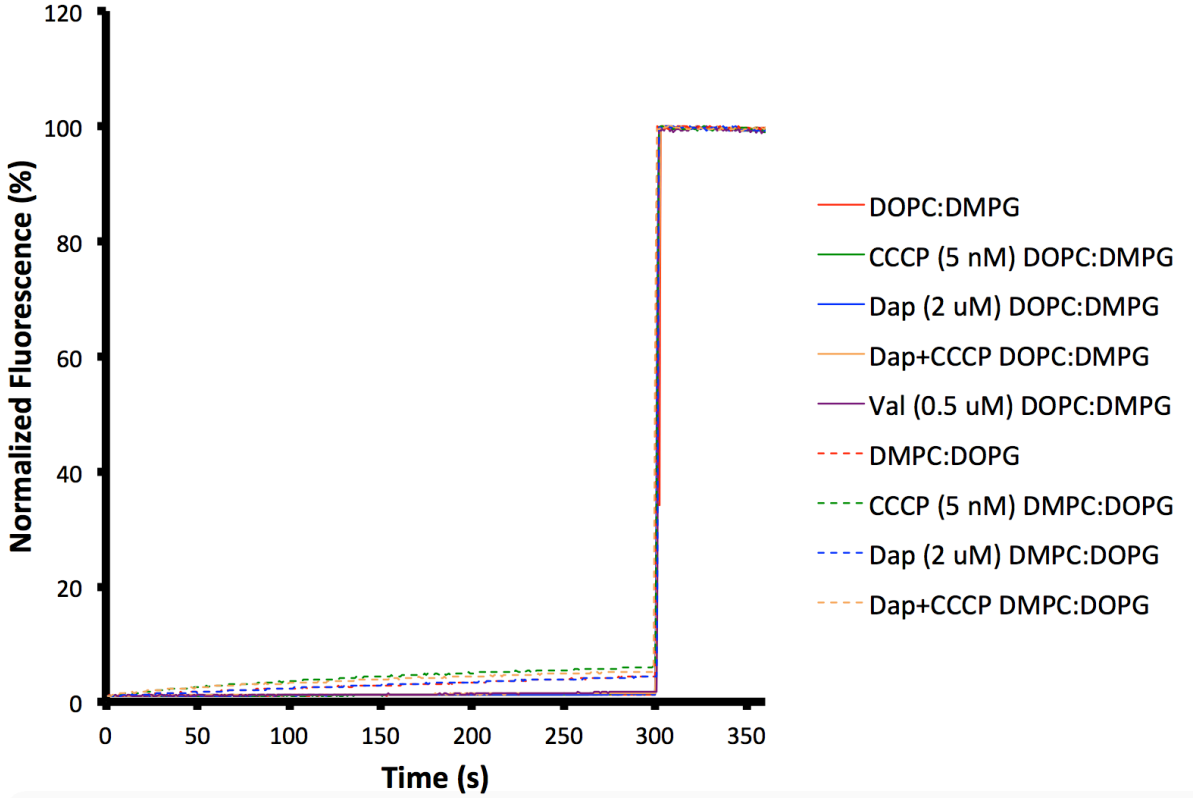

Figure 5.2 Permeabilization assay of Dap on hybrid mixtures of DOPC/DMPG (solid lines) and DMPC/DOPG (dashed lines) with molar ratios of 1/1, PC to PG, 250 μM. LUVs were entrapped with pyranine (1 mM) with a low pH and sodium buffer. Time-based fluorescence was measured (excitation, 470 nm; emission, 510 nm) for 360 seconds. The loaded LUVs were added to calcium (5 mM) buffer, which contained a high pH and increased sodium ions, thus creating a proton/sodium gradient across the bilayer. A proton ionophore carbonyl cyanide m-chlorophenyl hydrazone (CCCP, 5 nM) and Dap (2 μM) were added separately or together. At 300 seconds, Triton X-100 was added (0.1%) to solubilize the membranes. Assays were run in duplicates, at 30^{o}C.

Both hybrid mixtures showed no permeabilization by Dap at typical antibacterial concentrations. This indicates that the presence of only 50% of an oleoyl chained lipid is required to prevent permeabilization, and that this acyl chain can be connected to either PG or a neutral, non-involved head group, PC. This result confirms that the acyl chains inhibit pore formation, even though the PG is likely required to oligomerize the Dap monomers within the membrane.

The analogous experiments with hybrids of palmitoyl-oleoyl chained lipids and myristoyl chained lipids were not performed. This is due to the structural similarities between both oleoyl-containing lipids, shown in Figure 5.3.

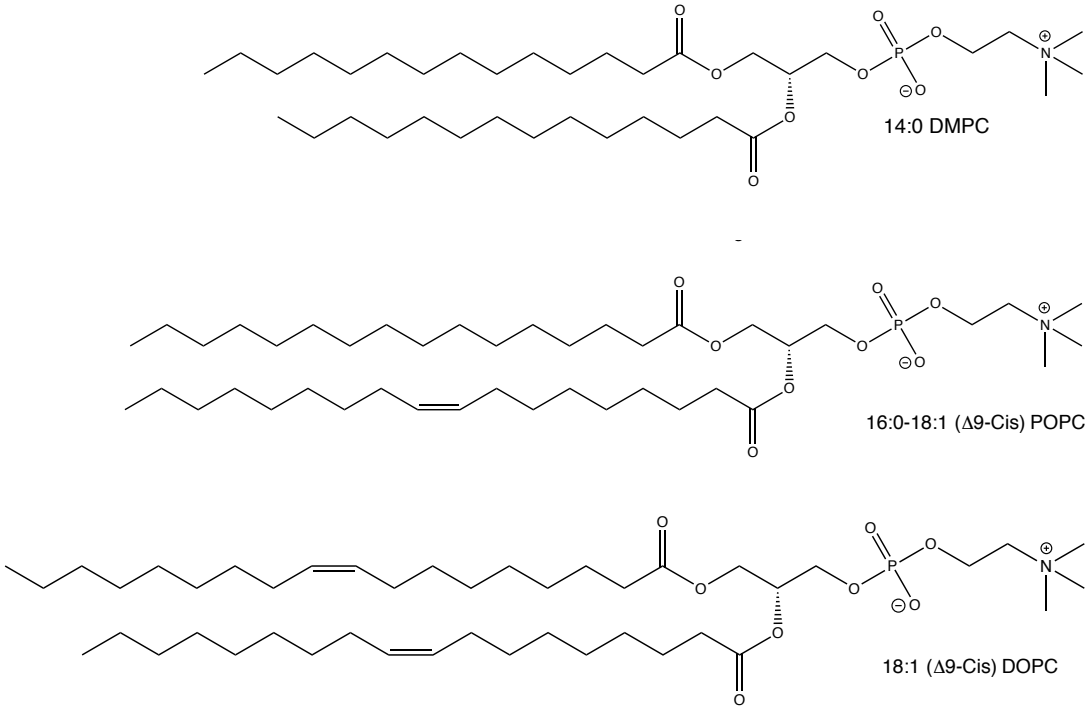

Figure 5.3 Structures of all three lipid types examined. Top: Lipid structure of a myrisotyl PC lipid (DMPC), with a saturated 14-carbon chain. Middle: Lipid structure of a palmitoyl-oleoyl PC lipid (POPC), with one chain being a 16 carbon saturated chain and the other being a oleoyl 18 carbon chain with one unsaturation point. Bottom: Lipid structure of a dioleoyl PC lipid (DOPC), with both chains being 18 carbon chains, with unsaturation points at the ninth carbon of each fatty acid chain.

Since DOPC and POPC both contain an oleoyl chain within their lipid tails, and it was shown in Figure 5.2 that only 50% of an oleoyl chain is necessary to prevent permeabilization, it was speculated that the palmitoyl-oleoyl chained lipids would show similar trends to that of DOPC. This

assumption requires further analysis since POPC, although containing an oleoyl chain also contains a palmitoyl (16:0) chain, which might induce effects not seen with DOPC.

5.3.2 Revisiting the Inhibitory Effect of Cardiolipin

In a recent study, Zhang, *et al*.[111] investigated the effects of cardiolipin (CL) on Dap. CL, also known as di-phosphatidylglycerol, consists of two PG lipids connected through a glycerol head group. The literature suggests that increased conversion of PG to CL can mediate bacterial resistance to Dap. Zhang, *et al.* elucidated that CL caused Dap to be restricted to the outer leaflet, therefore preventing oligomer translocation. The oligomer subunit stoichiometry was also diminished, compared to homogenous DMPC/DMPG, which was ascribed to the inability of oligomers to link together across leaflets.

At the time of those experiments, the role of the lipid acyl chain on Dap activity was not known or considered, and TOCL was used. Since the previous section outlined that oleoyl chained lipids prevent Dap permeabilization, even when they are not part of a required PG lipid, the question arose as to whether the previously described inhibitory effect was in fact due to the CL head group or to the acyl chain. To answer this question, the effect of Dap on liposomes composed of DMPC, DMPG and TMCL was utilized. Zhang, *et al.* stated that the incorporation of only 10% CL was enough to prevent permeabilization, therefore tests were run with 10% TOCL (to confirm these results) and with 10% TMCL. Firstly, the kynurenine fluorescence of Dap was tested against these varying lipid ratios, shown in Figure 5.4.

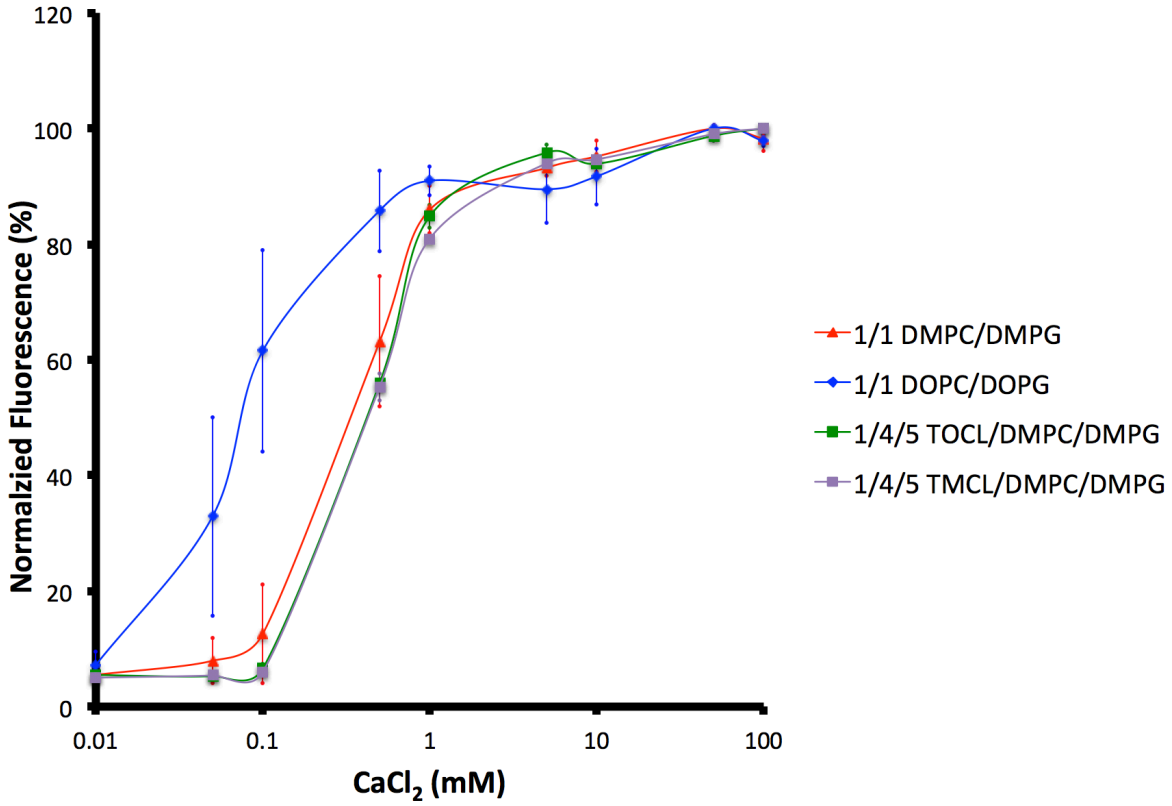

Figure 5.4 Kynurenine fluorescence of Dap was compared against different LUVs, containing cardiolipin. Dap (3 μM) was added to LUVs (250 μM) consisting of: DMPC/DMPG, DOPC/DOPG, TOCL/DMPC/DMPG and TMCL/DMPC/DMPG. Calcium was then titrated into the reaction mixture stepwise, with 3 minute incubations. An increase in kynurenine's signal indicates membrane insertion. Error bars represent the standard deviation of assays were run in triplicates for DMPC/DMPG and DOPC/DOPG and in duplicates for the TOCL and TMCL containing membranes, at 37°C.

The interaction of Dap to the TOCL and TMCL containing membranes resembles that of DMPC/DMPG. This suggests that oligomerization and at least partial translocation is occurring on each of these membranes, further suggested from preliminary work by David Beriashvili demonstrating that TMCL also prevents most (but not all) translocation of Dap oligomers (Appendix A, Figure A17). The permeabilization of Dap on membranes containing TOCL was examined, to confirm the results reported by Zhang, et al.[111] (Figure 5.5).

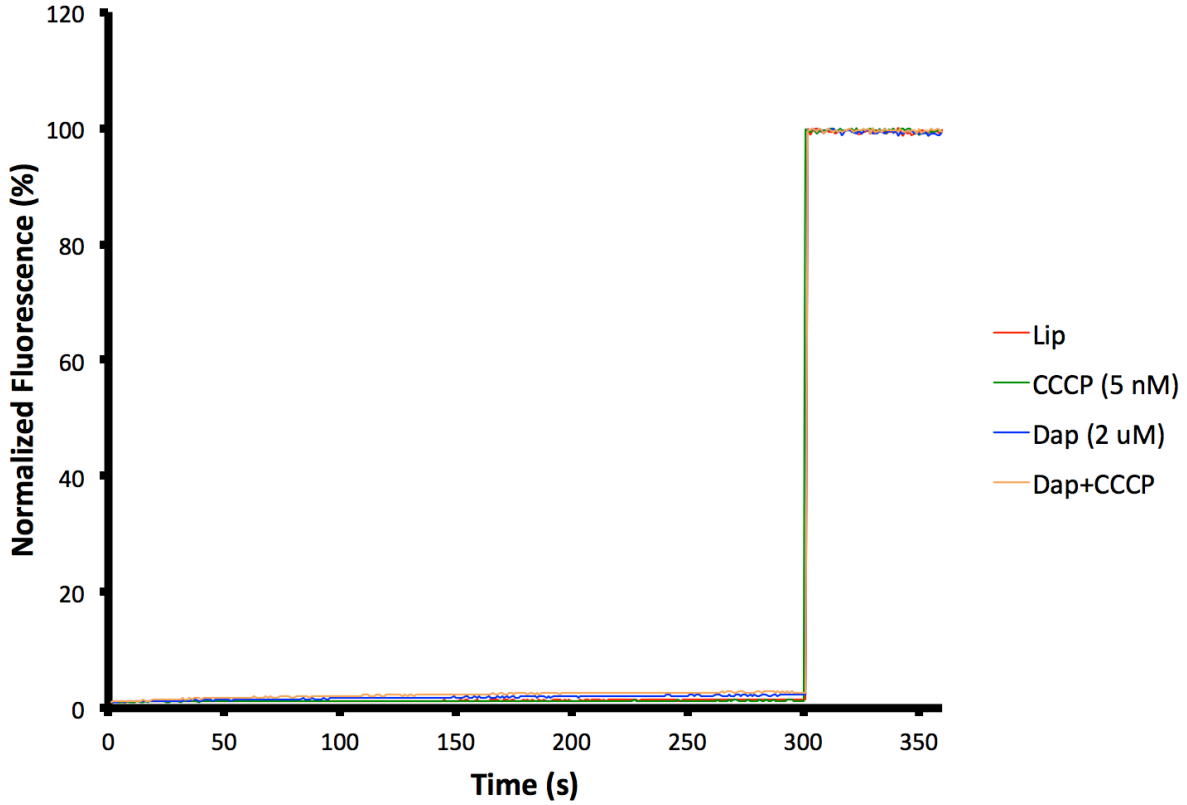

Figure 5.5 Permeabilization assay of Dap on TOCL/DMPC/DMPG (molar ratio 1/4/5, 250 μM). The assay was performed as described in Figure 5.2. Assays were run in duplicates, at 30°C.

The presence of 10% TOCL in a membrane consisting of TOCL, DMPC and DMPG was shown to prevent pore formation of Dap. This supports and confirms the results obtained by Zhang, *et al.* that TOCL is preventing permeabilization. The analogous experiments were then performed with TMCL containing membranes (Figure 5.6).

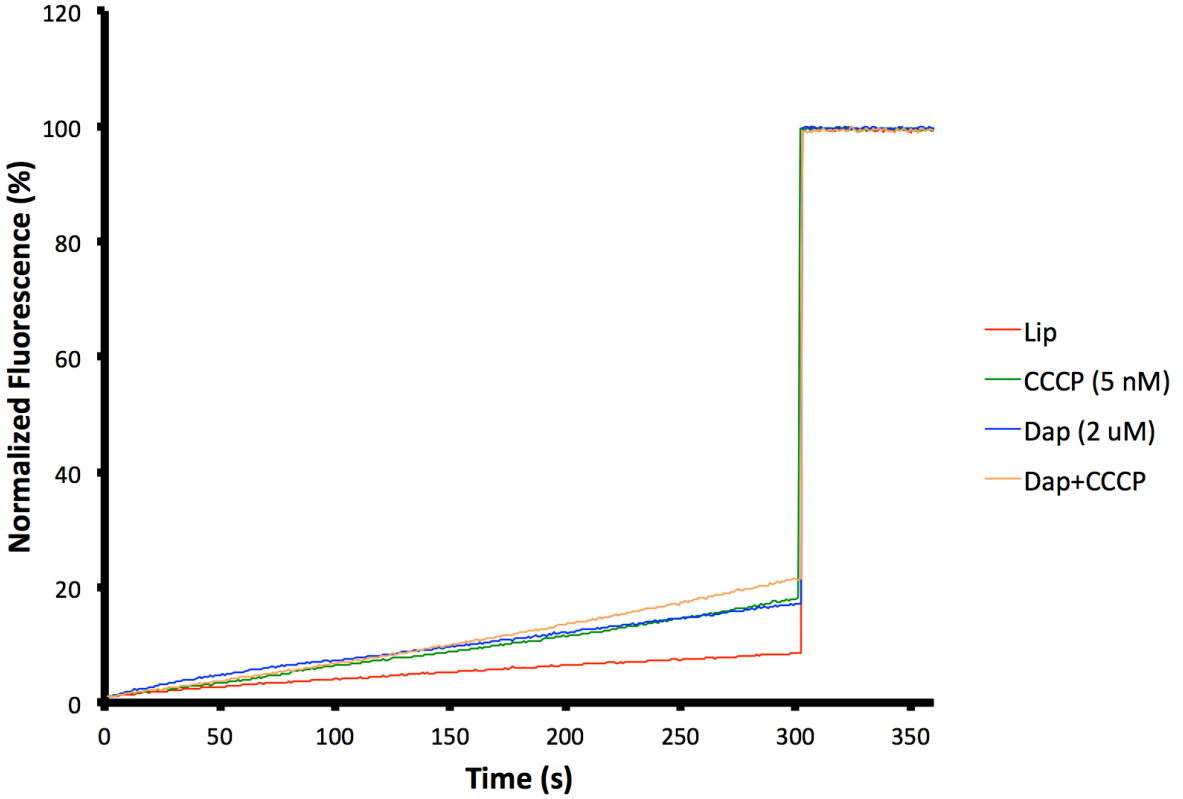

Figure 5.6 Permeabilization assay of Dap on TMCL/DMPC/DMPG (molar ratio 1/4/5, 250 μM). The assay was performed as described in Figure 5.2. Assays were run in duplicates, at 30°C.

As seen in Figure 5.6, pore formation by Dap was significantly reduced with the addition of 10% TMCL. This indicates that CL alone is preventing the pore formation of Dap on liposomes, confirming the results by Zhang, *et al.* TMCL does appear to inhibit permeabilization to a lesser extent that TOCL or DOPC, suggesting that the effect of the acyl tails is more pronounced than the head group.

5.3.3 Percentage of Oleoyl Lipid Required to Prevent Daptomycin Pore Formation

The incorporation of an oleoyl chained lipid (at 50% total lipid) was shown to abolish the ability of Dap to form a pore (Figure 5.2). In the last section it was shown that only 10% CL was necessary to prevent this pore formation (Figure 5.5-5.6). These results prompted the question, how much of a DOPC lipid is necessary to decrease the pore formation of Dap. To answer this, liposomes

were prepared with decreasing percentages of DOPC, while DMPG was kept constant at 50%, and DMPC made up the balance. The use of 50% PG was also done to keep the equimolar ratio of PC to PG constant. The permeabilization assay with pyranine was utilized, with the percentages of DOPC shown in Figure 5.7. The percentage of normalized pyranine fluorescence, relative to the Triton X-100 control, was reported.

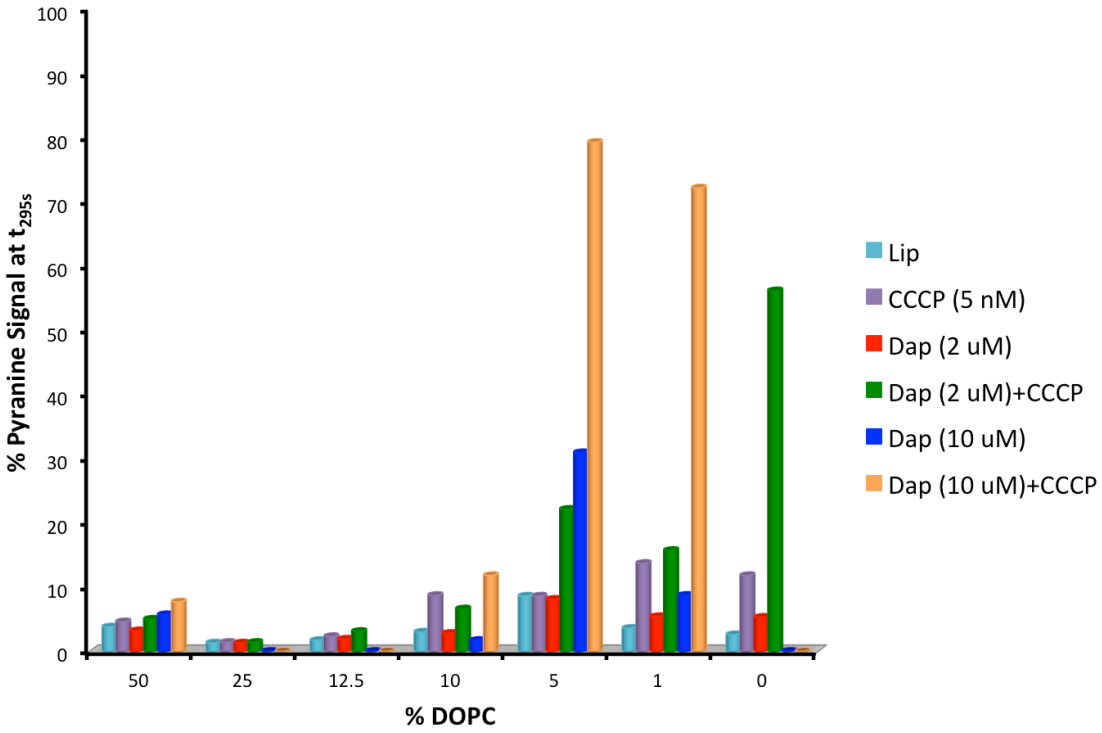

Figure 5.7 The percentage of pore formation for mixtures of LUVs containing: DOPC, DOPG, DMPC and DMPG. The assay was performed as described in Figure 5.2. The percentages were taken from the value at 295 seconds (before Triton X-100 addition). All lipid ratios were done in duplicate trials, except for DMPC/DMPG and DOPC/DOPG, which were in triplicates, standard deviations were within 5-7% for all trials. This table outlines that Dap's pore formation is halted by very low percentages of DOPC (1-5%). The raw spectra for these mixtures are shown in Appendix A. All assays were run at 30°C, as described in Section 5.2.5. The addition of 10 μM Dap was only performed for percentages, 50%, 10%, 5% and 1%.

As observed in Figure 5.7, the controls remained stable and reproducible across all mixtures, all having final percentages < 15%. In the case of homogenous DMPC/DMPG (0%, Figure 5.7), ~60% pore formation is observed, which is similar to what has been seen in previous chapters. In the

case of DOPC/DOPG (50%, Figure 5.7) pore formation is greatly diminished (<10% signal with Dap and CCCP).

Interestingly, Figure 5.7 shows that only 1-5% of DOPC is necessary to reduce Dap pore formation. This pore formation is then improved, upon the addition of higher concentrations of Dap (10 μM). When 1-5% DOPC is added, there will be ~0.5-2.5% in each leaflet, corresponding to ~1.25-6.25 μM DOPC. Since Dap is added at 2 or 10 μM, this data suggests that DOPC is acting stoichiometrically with Dap, which is non-logical, as Dap is known not to interact with PC at physiological calcium concentrations[126]. Another possible theory could potentially be a formation of separate lipid micro-domains that contain DOPC. Dap selectively interacts with DOPC/DOPG (Figure 4.1). This more avid insertion into these oleoyl chained lipids could be causing Dap to interact initially with PG, but then localize to a small patch of DOPC lipids within the membrane. Since it has been suggested that DOPC/DOPG membranes prevent the alignment of Dap oligomers across membrane leaflets, the decrease in permeabilization seen with 1-5% DOPC could be due to a spatial gap. The addition of higher concentrations of Dap would force insertion and pore formation of the lipopeptide into regions of the membrane containing only DMPC/DMPG. Future work is necessary to better elucidate this potential DOPC to Dap dose-response interaction.

5.3.4 Understanding the Reason for the Oleoyl Lipid's Ability to Prevent Daptomycin Permeabilization

As described previously, the inhibitory effects observed on DOPC/DOPG membranes are thought to be due to a reduced translocation of oligomers into the inner leaflet of the membrane, concomitantly with an inability of oligomers to align across leaflets. This theory was examined further by analyzing the structural differences between DOPC/DOPG and DMPC/DMPG, since DMPC/DMPG membranes have been observed to allow for Dap permeabilization. As seen in Figure 5.3, DOPC and DMPC have two main structural differences. The first is the presence of an unsaturation point at the ninth carbon. To determine if this was the reason for decreased pore formation, a 14:1 PC lipid was utilized. This lipid chain contains a 14-carbon chain, like DMPC/DMPG, but with an unsaturation point at the ninth carbon. The permeabilization experiment with this lipid is shown in Figure 5.8.

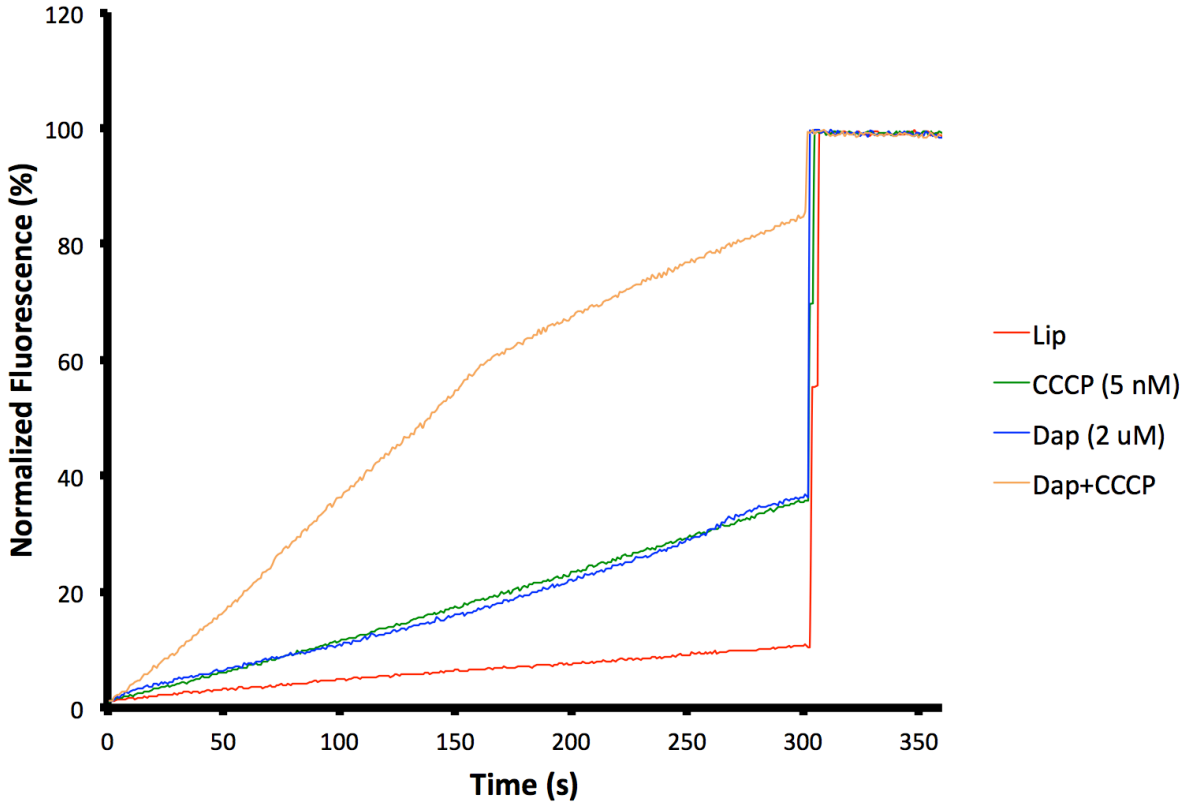

Figure 5.8 Permeabilization of Dap on 14:1PC/DMPC/DMPG (molar ratio 1/4/5, 250 μM). The assay was performed as described in Figure 5.2. Assays were run in duplicates, at 30°C.

This lipid mixture contained 10% of the 14:1 PC lipid, within DMPC/DMPG LUVs. This percentage was used since it was observed in the previous section that 10% DOPC was the lowest percentage necessary to prevent any measurable pore formation (Figure 5.7). This 14:1 PC lipid does not inhibit the pore formation of Dap, suggesting that the presence of the unsaturation alone is not important to permeabilization. As can be seen in Figure 5.8, the controls for this experiment were much larger than with a homogenous membrane consisting of DMPC/DMPG. This indicates that the 14:1 PC lipid is affecting liposome stability, although the controls are still considerably lower than the sample that has both added in unison.

It was speculated that if a Dap analog was synthesized that could bridge the spatial gap between leaflets of DOPC/DOPG membranes, permeabilization might occur. In Chapter 2, it was suggested that the acyl tails of Dap oligomers interacted across leaflets. Therefore, if a longer tailed Dap analog was used, the oligomers of Dap might be able to interact across leaflets properly, forming

a pore. It was thought that since DOPC is four carbons longer than DMPC, that the incorporation of a 14-carbon acyl tail to Dap (14C-Dap), instead of its standard decanoyl tail, might induce permeabilization. Additionally, Debono, *et al.* showed that when the fermentation of *S. roseosporus* is not altered, i.e. external addition of fatty acyl tails is not performed, that naturally produced Dap contains fatty acyls tails ≥12 carbons. It was thought that an increase to 14 carbons would be sufficient to bridge this gap. This 14C-Dap was produced semi-synthetically (Figure 5.9).

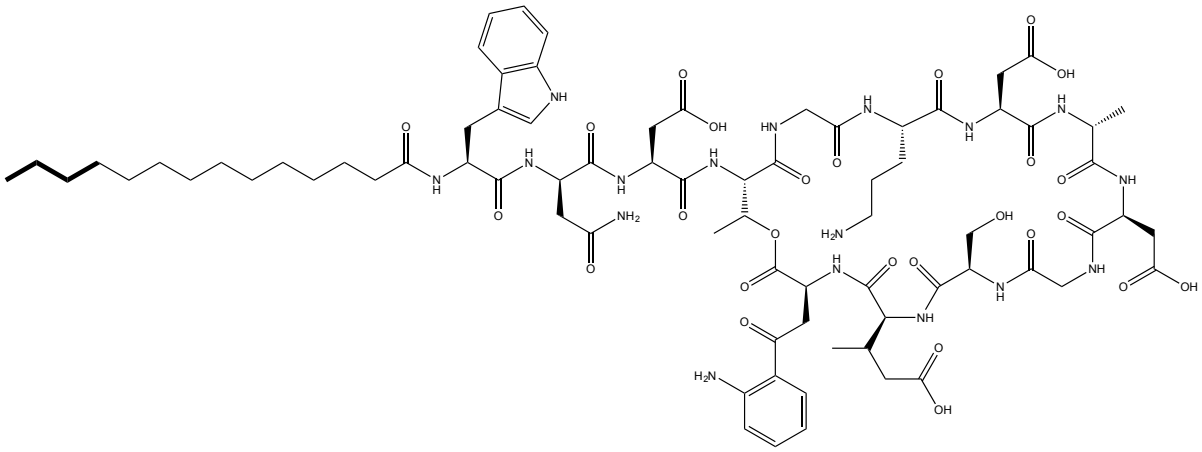

Figure 5.9 Structure of 14C-Dap. The myristoyl moiety was attached to the terminal tryptophan residue, increasing native Dap's fatty acid tail by four carbons (bolded). The minimum inhibitory concentration (MIC) of 14C-Dap was found to be lower than native Dap with a value of 0.5 μg/mL, over 0.75 μg/mL for Dap (tested on *Bacillus subtilis* ATCC 1046, 5 mM calcium).

This 14C-Dap was found to have comparable activity to native Dap on *Bacillus subtilis* (Figure 5.9), suggesting that the increased carbon tail should not impose any constraints on oligomer and pore formation. To confirm this, the kynurenine fluorescence was measured with both DMPC/DMPG and DOPC/DOPG containing membranes, shown in Figure 5.10.

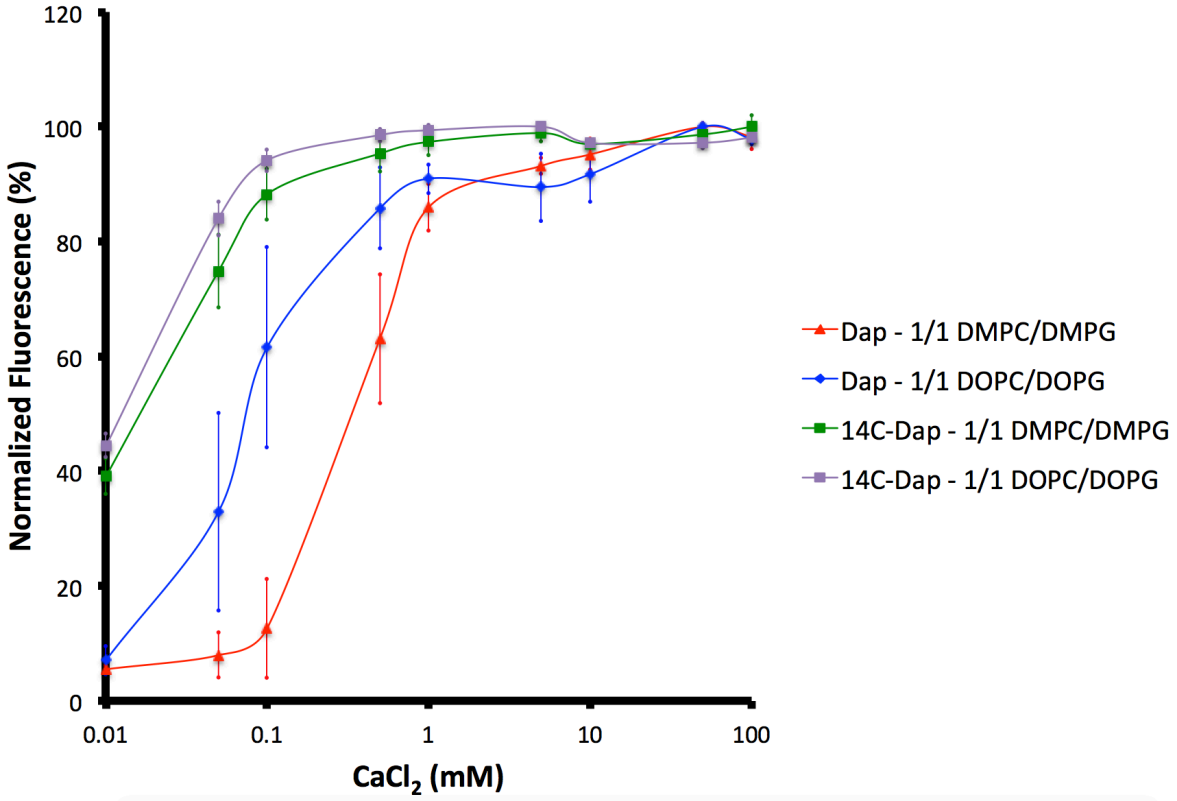

Figure 5.10 Kynurenine fluorescence of Dap and 14C-Dap were compared against different LUVs. The assay was performed as described in Figure 5.4. Error bars represent the standard deviations of each assay, run in triplicates, at 37°C.

The 14C-Dap analog was found to interact more avidly than Dap on both membrane compositions. In both cases, 14C-Dap and Dap have similar calcium concentrations required for saturation (>0.1 mM). This highlights that the 14C-Dap is interacting with both membranes equally. The ability of permeabilization for 14C-Dap was then tested on DMPC/DMPG membranes that contained pyranine, shown in Figure 5.11.

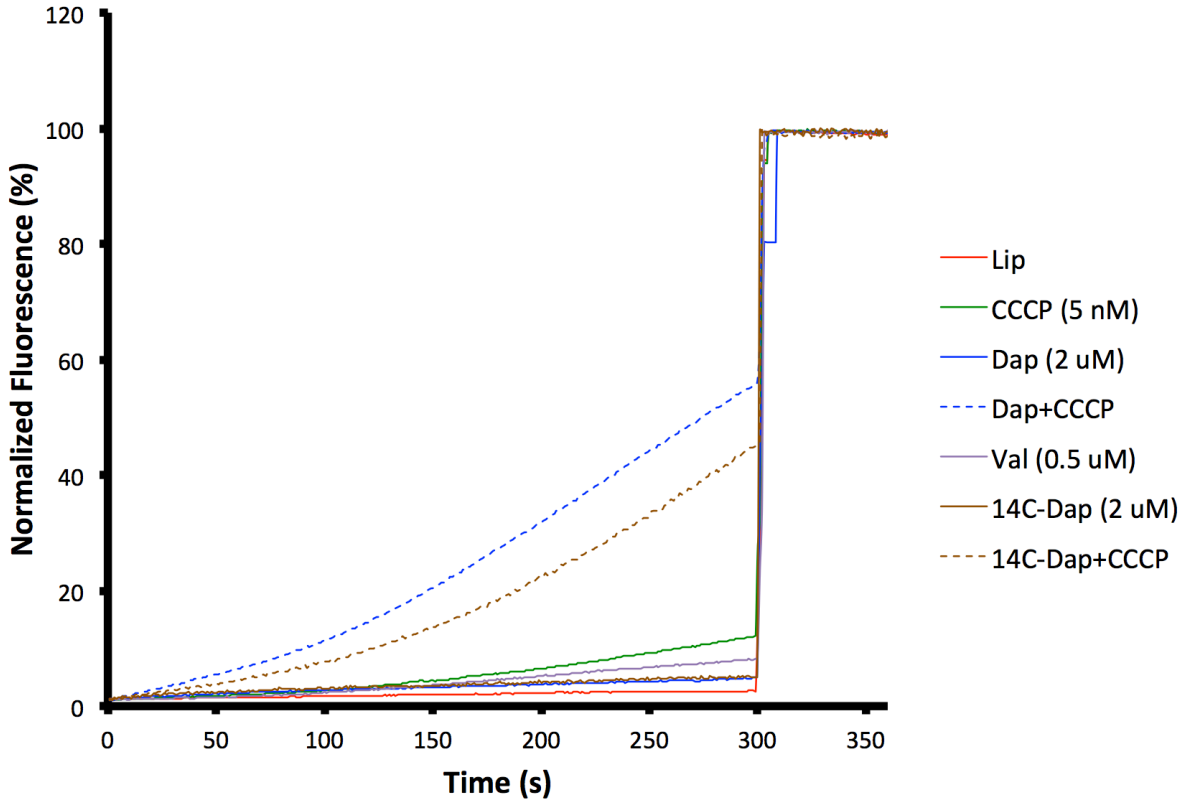

Figure 5.11 Permeabilization of Dap and 14C-Dap on DMPC/DMPG (molar ratio 1/1, PC to PG, 250 μM). The assay was performed as described in Figure 5.2. Assays were run in triplicates, at 30°C.

As expected, 14C-Dap permeabilizes DMPC/DMPG. This indicates that the 14C-Dap is also able to form oligomers that translocated across the membrane leaflets, forming a functional pore. The 14C-Dap was then tested against oleoyl lipids, DOPC/DOPG, shown in Figure 5.12.

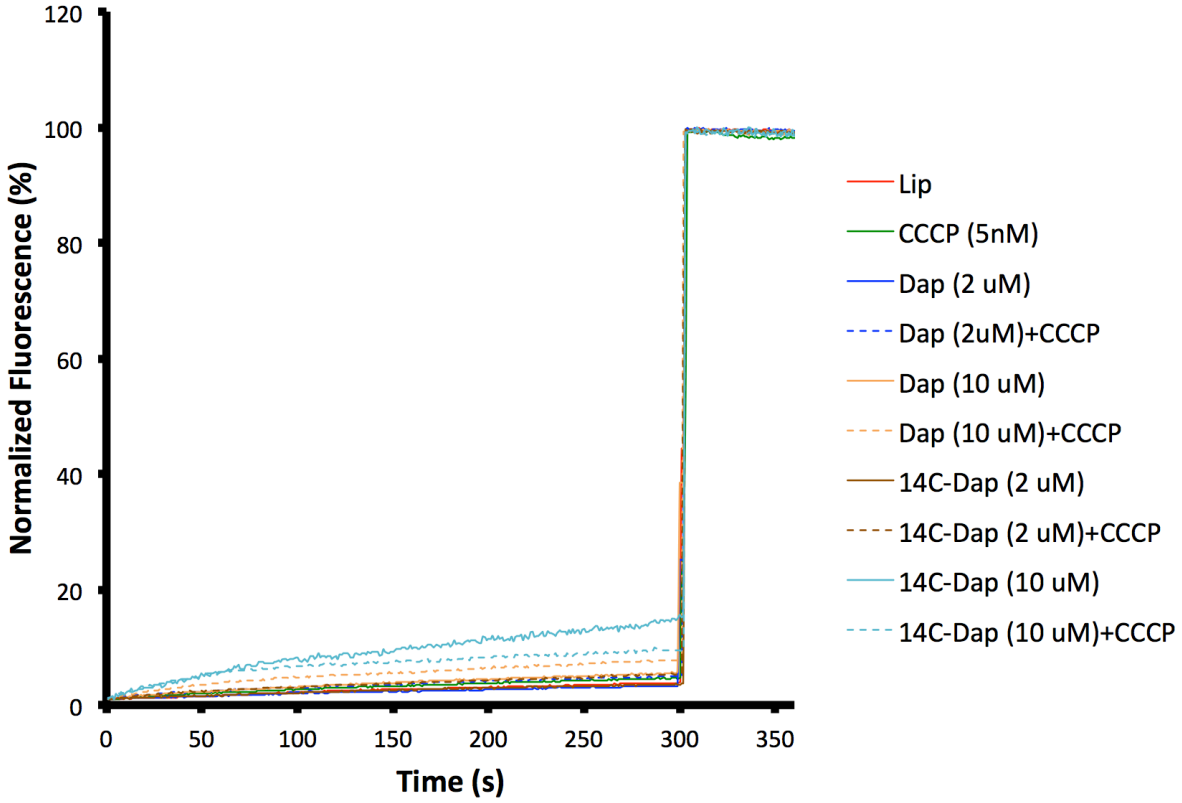

Figure 5.12 Permeabilization of Dap and 14C-Dap on DOPC/DOPG (molar ratio 1/1, PC to PG, 250 μM). The assay was performed as described in Figure 5.2. Assays were run in triplicates, at 30°C.

Unexpectedly, pore formation of 14C-Dap was prevented on DOPC/DOPG at low and high concentrations. However, there is a slight increase in signal observed at higher concentrations of 14C-Dap, when no CCCP is added. This mirrors data observed in Chapter 3 that suggested that a Dap dimer created larger pores within the membrane, negating the requirement of CCCP. Testing the permeabilization of 14C-Dap at even higher concentrations on these liposomes may show a similar non-dependence of CCCP.

5.4 Discussion

In Chapter 4 it was shown that the presence on longer, unsaturated lipid acyl chains detrimentally affected the permeabilization of Dap. Three lipid compositions, DOPC/DOPG, POPC/POPG and DMPC/DMPG were utilized, with Dap permeabilization only observed on the latter (Figure 4.2). Since the variation of these membranes is their acyl chain moieties, it was speculated

that this was the sole reason for decreased permeabilization. Since Dap requires PG to insert into the membrane[9,11,40] it was unclear whether PG was a required constituent to cause this inhibition in Dap permeabilization. To elucidate this, permeabilization experiments were run with Dap on hybrid mixtures of oleoyl and myristoyl chained lipids (Figure 5.2). Oddly, the presence of PG is not required to prevent permeabilization, confirming the results in Chapter 4, that the acyl chain is the sole reason for a lack of pore formation, regardless of head group.

In 2014, Zhang, *et al.* showed that the presence of cardiolipin (CL) into model membranes prevented the translocation of Dap oligomers and an inability for any oligomer to link together across leaflets[111]. At the time of this article, the role of lipid acyl chain composition was unknown and therefore a TOCL lipid was utilized. Since oleoyl chained lipids attached to a neutral PC head group were found to prevent permeabilization, it was unclear if the results obtained by Zhang, *et al.* were measuring the interaction of CL in the membrane or the oleoyl chain. This was therefore revisited, and a myristoyl chained CL (TMCL) was utilized. It was observed that both TOCL and TMCL, at 10% total lipid, prevented Dap permeabilization in DMPC/DMPG membranes. This suggests that the conclusions drawn by Zhang, *et al.* were accurate, and that the inhibition of permeabilization with acyl chains could be through a similar mechanism of resistance.

Since only 10% TMCL was necessary to induce inhibition of Dap permeabilization the question arose as to how much of a longer chained DOPC lipid was necessary to prevent this permeabilization. From Figure 5.7, it was shown that only 1-5% DOPC incorporation is required to prevent Dap permeabilization. This is a strikingly low concentration, corresponding to ~0.5-2.5% DOPC in each membrane leaflet. When taking into account that the total liposome concentration used is 250 μM, the molar concentration of DOPC found within the membrane is ~1.25-6.5 μM. Dap, at 2 μM is prevented from forming a pore, but when Dap is increased to 10 μM, pore formation resumes. This suggests a dose response activity of Dap within these membranes. One theory is that the added DOPC lipid could be forming micro-domains within the membrane, supported by the literature that with eukaryotic cells, bacterial membrane lipids have been shown to create separate domains[203], and Dap appears to interact preferentially to some of them[134,135,157]. Although Dap has been found to bind more avidly with DOPC/DOPG containing membrane, it is unlikely that Dap is binding directly to DOPC. Dap is likely binding to DMPG, but then potentially localizing to areas of the membrane that contain higher percentages of DOPC. These patches might then inhibit Dap pore formation similar to that seen with a homogenous DOPC/DOPG membrane, by preventing both translocation and

alignment of oligomers across leaflets. Another theory, based on the extremely low concentration of DOPC necessary to prevent Dap permeabilization could be that DOPC is acting somewhat stoichiometrtically to Dap. This is counterintuitive, as Dap does not bind DOPC only containing membranes.[126] The acyl chains of lipids might have a more direct interaction with Dap oligomers, interrupting the interaction of Dap fatty acyl tails across leaflets. Future work is necessary to better elucidate the role of DOPC in preventing Dap pore formation, specifically focusing on the interaction of stoichiometric concentrations of DOPC on the membrane insertion of Dap.

DOPC/DOPG membranes are clearly affecting the ability of Dap to form a pore, but the exact reason for this remains unclear. Oleoyl chained lipids differ from the Dap permeabilizing myristoyl chain lipids in regards to unsaturation and an increase carbon length (Figure 5.3). The role of unsaturation was studied using a 14:1 PC lipid, incorporated into DMPC/DMPG membranes. It was observed that this lipid does not affect Dap pore formation, suggesting that unsaturation alone is not involved in the inhibition. In Chapter 2 it was speculated that Dap oligomers interact across leaflets, potentially through their acyl chains. This is supported by Zhang, *et al.*'s findings that Dap oligomers translocate evenly across DMPC/DMPG membranes[111], concomitantly with the finding that a pyrene labeled A5 analog showed two stages of excimer formation, with one stage potentially occurring across leaflets[125] (See Chapter 2 for details). It was theorized that a longer chained Dap analog, similar to the structure of naturally produced Dap[60], could potentially bridge the spatial gap that was speculated to occur between leaflets of DOPC/DOPG membranes. Since these membranes are four carbons longer than DMPC/DMPG, the addition of a fourteen carbon tail was added to Dap (14C-Dap). It was speculated that this increased length, would allow for oligomers to link together across leaflets. This 14C-Dap was shown to interact identically with both DMPC/DMPG and DOPC/DOPG, suggesting that oligomer formation was occurring on each lipid type. Unexpectedly, DOPC/DOPG membranes also inhibited 14C-Dap. This suggests that the inhibition observed by DOPC/DOPG membranes is not limited to their increased carbon length. This could indicate that a more complex mechanism of inhibition due to DOPC/DOPG membranes might be occurring. The increase in Dap's acyl tail could be causing constraint or improper associations within the membrane, leading to a lack of permeabilization observed. This could explain the slightly reduced pore formation observed on DMPC/DMPG membranes, compared to Dap (Figure 5.11). Future work involves the use of lipids that contain longer acyl chains (16:0 or 18:0), performing a similar study as that shown in Figure 5.8. An addition of a 16:0 or 18:0 acyl chained PC into DMPC/DMPG membranes might better explain the lack of a pore formation observed with both Dap and 14C-Dap on DOPC/DOPG membranes. In

summary, although questions remain to be answered about the interaction of Dap oligomers with oleoyl chained lipids, the data in this chapter supports the previous contention that the lipid composition has drastic effects of the ability of Dap to form a pore.

Chapter 6

Summary and Future Work

6.1 Summary

As discussed throughout this thesis the mechanism of action for the important lipopeptide antibiotic, Daptomycin (Dap), still remains under debate. This thesis attempted to further elucidate the most experimentally supported mode of action, which is the permeabilization of small cations through formation of a pore.

Fluorescence and ITC were utilized to study the interaction of calcium, Dap and a model membrane. Through use of native and acrylodan-labeled Dap and A5 (a similar antibiotic in both structure and activity), four separate amino acids were probed, corresponding to residues 1, 6, 8 and 13 of the lipopeptides. From this work it was determined that calcium interacts with Dap in two sequential steps. The first calcium ion causes the macrolactone ring of Dap, particularly residues 6 and 8 to insert into the membrane. At this concentration, Zhang, *et al.* observed excimer formation through use of a pyrene labeled A5 analog. Taken together, the results suggest that the first calcium ion causes oligomer formation in the outer membrane leaflet, with the tails interacting within the membrane. The second calcium ion forces this oligomer to be inserted more deeply into the membrane. This was observed through the emission increase of residues 1 and 13 of Dap and A5. At this concentration the acrylodan residues also experience concentration dependent self-quenching, suggesting a more tightly bound oligomer. The local concentration of pyrene monomers that could form excimers, observed by Zhang, *et al.* was also increased, suggesting that the second calcium was not only causing a deeper oligomer insertion but also a translocation of oligomers in the inner leaflet (or proper alignment of already translocated oligomers across leaflets). Zhang, *et al.* supported this using an NBD-Dap analog, showing that Dap oligomers translocate evenly between the leaflets of myristoyl chained lipid membranes, upon addition of higher calcium concentrations.

Oligomer formation is necessary for Dap activity. This oligomer formation would likely have an entropic cost. To lower this cost a dimer of Dap was synthesized that connected the *N*-terminal tryptophan's of two monomers by an octadecanedioate linker. It was thought that this dimer might improve oligomer formation, thus improving overall activity. Unexpectedly, the dimer was relatively inactive on both *Bacillus subtilis* and *Staphylococcus aureus* strains. Interestingly, the dimer inserted into model membranes and formed a functional pore. It was speculated that the dimer might be too large to pass the peptidoglycan layer of Gram-positive bacteria. Call wall lacking bacteria, L-forms, were cultured, and the dimer was shown to be active on these cells. Additionally, the activity of the dimer was greatly improved when the concentration of calcium was increased to un-physiologically high concentrations, when tested against vegetative cells. This suggests an inability of the dimer to pass the cell wall, which could be due, primarily, to electrostatics. Overall, this work highlights that Dap must traverse the cell wall and then insert into the cytoplasmic membrane as a monomer.

The effect of membrane lipid composition on Dap activity was then investigated. In the literature, many studies on the mode of action, and on the role of specific lipids, have been performed. Unfortunately, these studies did not take into account the possible effects of lipid acyl chain composition. This work highlighted that Dap, even though it interacts similarly to varying model membranes, composed of oleoyl, palmitoyl-oleoyl or myristoyl chained lipids, only permeabilizes the latter. The palmitoyl-oleoyl and oleoyl chained lipids also showed reduced membrane translocation and smaller subunit stoichiometry. This suggests that translocation of the Dap oligomer is necessary but not sufficient for Dap pore formation.

The reason for the diminished permeabilization observed with oleoyl chain containing membranes was then explored. Only 1-5% of an oleoyl lipid was required to reduce Dap's pore formation on model membranes. Permeabilization was restored when the molar percentage of Dap surpassed the molar percentage of the DOPC lipid within the DMPC/DMPG membrane. This suggests a specific dose response interaction is occurring with DOPC and Dap, within the membrane.

DOPC/DOPG membranes differ from DMPC/DMPG membranes by a unsaturation point at the ninth carbon and longer acyl tail. Studies with an unsaturated myristoyl chained PC lipid showed that unsaturation has minimal effects on pore formation. The effect of the oleoyl chained lipids increased carbon length was investigated through the synthesis of a longer tailed Dap analog, as it was expected that this increase in length would bridge the spatial gap between DOPC/DOPG membrane leaflets. This longer tailed Dap analog exhibited antibacterial activity equal to that of Dap.

This analog was able to form pores in DMPC/DMPG liposomes but not DOPC/DOPG liposomes, suggesting that the inhibition of pore formation observed by oleoyl chained lipids is more complicated than originally thought. Overall, these results demonstrate that the lipid acyl chain composition has drastic effects on the activity of Dap, which may explain the difference in Dap susceptibility among different bacteria.

6.2 Future Work

6.2.1 Studying Permeabilization of Bacteria Susceptible to Daptomycin

As discussed in this thesis, the lipid composition of the membrane has drastic effects on the permeabilization of Dap. Many scientists have used varying lipids to study Dap, which could explain why there are varying proposed modes of action of this antibiotic. Interestingly, in the literature *Staphylococcus aureus* has been shown to be permeabilized by Dap[46,114,191], whereas *Bacillus subtilis* has not[119]. The lipid composition could be the main reason for these differences in permeabilization. The use of membranes composed of phosphatidylcholine (PC) and phosphatidylglycerol (PG) is a simplistic model to study the interaction of Dap to PG, but these membranes do not capture the complexity of a pathogenic bacterial cell membrane. To better understand the *in vivo* mechanism of Dap action, the use of natural bacterial membranes is crucial. These bacterial systems, mainly *Staphylococcus aureus*, which Dap is used against, can be stripped of all components except the lipids, usually done through a cholorform/methanol extraction. The methodology used in this thesis could then be utilized, but with a membrane system that is much more similar to a bacterial membrane. Investigating the permeabilization of Dap with techniques explored by Silverman, *et al.*[46] on these model liposomes would also allow for a better understand of Dap's membrane interaction.

Although this approach would allow for a more accurate lipid composition, there are still shortcomings. The localization of lipid head groups within the membranes and the potential interaction of Dap with transmembrane proteins would require the use of live bacterial systems.

The importance of PG for Dap's activity has been shown countless times both *in vitro* and *in vivo*. Nevertheless, *Bacillus polymyxa*, which only contains ~3% PG in its membrane[204], would allow for a viable cell system to study this inherent resistance. *B. polymyxa* also contains a higher PE

content, compared to other *Bacillus spp.* which would allow for an *in vivo* system to study the potential role of this lipid in Dap activity and its mode of action.

The inhibition of cell wall synthesis enzymes is a prominent proposed mode of action for Dap in the literature[119,136,149]. To better determine if Dap interacts with this process, to use of mycoplasma is useful, since mycoplasma bacteria lack a cell wall/cell wall synthesis enzymes[205] and are therefore similar to L-forms[152] (discussed in Chapter 3[117]). The use of these bacteria could potentially give a model membrane system, which is viable. It has been speculated that part of Dap's mechanism of action is through inhibition of cell wall synthesis enzymes[119]. Since mycoplasma lack these enzymes, this work could determine if pore formation or cell wall enzyme inhibition, is the true mode of action. Also, the cell membrane of these bacteria can be varied depending on the lipid content within the growth medium[205]. This could allow for a viable cell system to that better mimics the cell membrane of pathogenic bacteria, susceptible to Dap.

6.2.2 Developing Analogs to Study and Improve Daptomycin's Activity

The synthesis of new analogs of Dap is a focus point of many researchers, to better understand Dap's mechanism of action and to develop analogs that improve activity. There are several different approaches to analog synthesis (discussed in Chapter 1), but the most recent advancement is that of total synthesis. This has been shown by Lohani, *et al.* to be a promising route to the development of new Dap analogs due to the ability to alter each amino acid in the structure of Dap specifically[99]. Unfortunately, with 20 standard amino acids to choose from, the creation of every type of analog possible for Dap is impossible. Therefore, a more rational approach is necessary, focusing on the role of each amino acid in Dap's activity. This could help identify crucial interactions within oligomers of Dap and the lipid membrane. To determine the residues vital to Dap activity an alanine scan can be used. Alanine is a chemically inert amino acid that has been used for years to study the effect of specific amino acids in a proteins structure. Very recently, Barnawi, *et al*. investigated an alanine scan of Dap, showing that the replacement of some amino acid positions (D-asparagine2, glycine5, ornithine6 and D-serine11) for alanine had lower reduced activity than all other amino acids tested[98]. The replacement of these positions with other standard amino acids might produce an analog with greater activity than native Dap. The incorporation of cysteine into these positions could also allow for the attachment of varying fluorophores at different positions in Dap,

which could be used to further elucidate these residues interactions with calcium and the bacterial membrane.

Fluorine ^{19}F-NMR is another approach to further elucidate the mechanism of action of Dap. The fluorine atom is sensitive to its environment and exhibits a peak-broadening effect in hydrophobic environments[206]. Targeting specific amino acids in the structure of Dap with a fluorinated compound, could allow for a better understanding of Dap's oligomerization within membranes. Overall, Dap is a complex peptide, but through peptide synthesis, the creation of new and improved antibiotics to combat the ever-growing concern of antibiotic-resistant bacteria, is right around the corner.

Letter of Copyright Permission

Permission for Figure 1.1:

10/20/2017 Rightslink® by Copyright Clearance Center

Copyright Clearance Center RightsLink®

Home | Create Account | Help

AMERICAN SOCIETY FOR MICROBIOLOGY

Title: Challenges of Antibacterial Discovery
Author: Lynn L. Silver
Publication: Clinical Microbiology Reviews
Publisher: American Society for Microbiology
Date: Jan 1, 2011
Copyright © 2011, American Society for Microbiology

LOGIN
If you're a copyright.com user, you can login to RightsLink using your copyright.com credentials. Already a RightsLink user or want to learn more?

Permissions Request

ASM authorizes an advanced degree candidate to republish the requested material in his/her doctoral thesis or dissertation. If your thesis, or dissertation, is to be published commercially, then you must reapply for permission.

BACK | CLOSE WINDOW

Copyright © 2017 Copyright Clearance Center, Inc. All Rights Reserved. Privacy statement. Terms and Conditions.
Comments? We would like to hear from you. E-mail us at customercare@copyright.com

The author of the book "Biochemical Pharmacology," Dr. Michael Palmer, gave permission for Figure 1.2 and Figure 1.3 to be used in this thesis. (Palmer, M.; Chan, A.; Dieckmann, T.; Honek, J. *Biochemical Pharmacology*; John Wiley & Sons, Inc.: Hoboken, New Jersey, 2012.)

Permission for Figure 1.9:

11200 Rockville Pike
Suite 302
Rockville, Maryland 20852

August 19, 2011

American Society for Biochemistry and Molecular Biology

To whom it may concern,

It is the policy of the American Society for Biochemistry and Molecular Biology to allow reuse of any material published in its journals (the Journal of Biological Chemistry, Molecular & Cellular Proteomics and the Journal of Lipid Research) in a thesis or dissertation at no cost and with no explicit permission needed. Please see our copyright permissions page on the journal site for more information.

Best wishes,

Sarah Crespi

American Society for Biochemistry and Molecular Biology
11200 Rockville Pike, Rockville, MD
Suite 302
240-283-6616
JBC | MCP | JLR

The authors of the journal article "The action mechanism of Daptomycin," Dr. Scott Taylor and Dr. Michael Palmer, gave permission for Figure 1.10 and Figure 1.18 to be used in this thesis. (Taylor, S. D.; Palmer, M. *Bioorganic Med. Chem.* **2016**, *24*, 6253–6268.)

Permission for Table 1.3:

Permission for Figure 1.12:

Title: Correlation of Daptomycin Bactericidal Activity and Membrane Depolarization in Staphylococcus aureus

Author: Jared A. Silverman, Nancy G. Perlmutter, Howard M. Shapiro et al.

Publication: Antimicrobial Agents and Chemotherapy

Publisher: American Society for Microbiology

Date: Aug 1, 2003

Copyright © 2003, American Society for Microbiology

LOGIN

If you're a copyright.com user, you can login to RightsLink using your copyright.com credentials. Already **a RightsLink user** or want to learn more?

Permissions Request

ASM authorizes an advanced degree candidate to republish the requested material in his/her doctoral thesis or dissertation. If your thesis, or dissertation, is to be published commercially, then you must reapply for permission.

BACK CLOSE WINDOW

Permission for Figure 1.14:

11200 Rockville Pike
Suite 302
Rockville, Maryland 20852

August 19, 2011

American Society for Biochemistry and Molecular Biology

To whom it may concern,

It is the policy of the American Society for Biochemistry and Molecular Biology to allow reuse of any material published in its journals (the Journal of Biological Chemistry, Molecular & Cellular Proteomics and the Journal of Lipid Research) in a thesis or dissertation at no cost and with no explicit permission needed. Please see our copyright permissions page on the journal site for more information.

Best wishes,

Sarah Crespi

American Society for Biochemistry and Molecular Biology
11200 Rockville Pike, Rockville, MD
Suite 302
240-283-6616
JBC | MCP | JLR

The author of the thesis "Daptomycin : studies on its action mode and on bacterial resistance with model membranes," Bradley Scott, gave permission for Figure 3.3 to be used in this thesis. (Scott, B. I. Daptomycin : studies on its action mode and on bacterial resistance with model membranes by, University of Waterloo, 2016.)

Permission for Figure 4.3 (Top Right bar graph) and Figure 4.4:

Bibliography

1. Wainwright, M. *Mycologist* **1989**, *3*, 21–23.
2. Hare, R.; Florey, W.; Gardner, A. D.; Heatley, N. G.; Jennings, M. A.; Orr-Ewing, J.; Sanders, A. G.; Abraham, E. P.; Chain, E.; Fletcher, C. M.; Florey, H. W. *Med. Hist.* **1982**, *26*, 1–24.
3. Grad, F. P. *Bull. World Health Organ.* **2002**, *80*, 983–984.
4. Laing, R. *Lancet* **2003**, *361*, 1723–1729.
5. Wright, G. D. *Adv. Drug Deliv. Rev.* **2005**, *57*, 1451–1470.
6. Demerec, M. *J. Bacteriol.* **1948**, *56*, 63–74.
7. Foster, T. J. *J. Clin. Invest.* **2004**, *114*, 1693–1696.
8. Collignon, P.; Powers, J. H.; Chiller, T. M.; Aidara-Kane, A.; Aarestrup, F. M. *Clin. Infect. Dis.* **2009**, *49*, 132–141.
9. Bionda, N.; Pitteloud, J.-P.; Cudic, P. *Future Med. Chem.* **2013**, *5*, 1311–1330.
10. Baltz, R. H.; Miao, V.; Wrigley, S. K. *Nat. Prod. Rep.* **2005**, *22*, 717–741.
11. Baltz, R. H. *Curr. Opin. Chem. Biol.* **2009**, *13*, 144–151.
12. Eisenstein, B. I.; Oleson, Jr., F. B.; Baltz, R. H. *Clin. Infect. Dis.* **2010**, *50*, S10-15.
13. Hsu, L.-Y.; Leong, M.; Balm, M.; Chan, D. S.; Huggan, P.; Tan, T.-Y.; Koh, T.-H.; Hon, P.-Y.; Ng, M. M.; Li-Yang Hsu, C. *J. Med. Microbiol.* **2010**, *59*, 1509–1513.
14. Strebhardt, K.; Ullrich, A. *Nat. Rev.* **2008**, *8*, 473–480.
15. Zaffiri, L.; Gardner, J.; Toledo-Pereyra, L. H. *J. Investig. Surg.* **2012**, *25*, 67–77.
16. Palmer, M.; Chan, A.; Dieckmann, T.; Honek, J. *Biochemical Pharmacology*; John Wiley & Sons, Inc.: Hoboken, New Jersey, 2012.
17. Silver, L. L. *Clin. Microbiol. Rev.* **2011**, *24*, 71–109.
18. DiMasi, J. A.; Hansen, R. W.; Grabowski, H. G. *J. Health Econ.* **2003**, *22*, 151–185.
19. Demain, A. L.; Sanchez, S. In *Antibiotics: Current Inovations and Future Trends*; Demain, A. L., Sanchez, S., Eds.; Caister Academic Press: Norfolk, UK, 2015; pp 65–66.
20. Emerson De Lima Procópio, R.; Reis Da Silva, I.; Martins, M. K.; Lúcio De Azevedo, J.;

Magali De Araújo, J. *Brazilian J. Infect. Dis.* **2012**, *16*, 466–471.

21. Abrudan, M. I.; Smakman, F.; Grimbergen, A. J.; Westhoff, S.; Miller, E. L.; van Wezel, G. P.; Rozen, D. E. *Proc. Natl. Acad. Sci.* **2015**, *112*, 11054–11059.

22. Trevor, A. J.; Katzung, B. G.; Kruidering-Hall, M. *Katzung & Trevor's Pharmacology Examination & Board Review Chapter 43 : Beta-Lactam Antibiotics & Other Cell Wall Synthesis Inhibitors*, 11th ed.; Weitz, M., Lebowitz, H., Eds.; McGraw-Hill Education: New York City, New York, 2015.

23. Waxman, D. J.; Strominger, J. L. *Annu. Rev. Microbiol.* **1983**, *52*, 825–869.

24. Williams, D. H.; Barna, J. C. J. *Annu. Rev. Microbiol.* **1984**, *38*, 339–357.

25. Prosser, G. A.; Pedro de Carvalho, L. S. *Biochemistry* **2013**, *52*, 7145–7149.

26. Marquardt, J. L.; Brown, E. D.; Lane, W. S.; Haley, T. M.; Ichikawa, Y.; Wong, C.-H.; Walsh, C. T. *Biochemistry* **1064**, *33*, 10646–10651.

27. Pollock, T. J.; Thorne, L.; Yamazaki, M.; Mikolajczak, M. J.; Armentrout, R. W. *J. Bacteriol.* **1994**, *176*, 6229–6237.

28. Stone, K. J.; Stromingert, J. L. *PNAS* **1971**, *68*, 3223–3227.

29. Kleijn, L. H. J.; Oppedijk, S. F.; Hart, P. 't; Van Harten, R. M.; Martin-Visscher, L. A.; Kemmink, J.; Breukink, E.; Martin, N. I. *J. Med. Chem.* **2016**, *59*, 3569–3574.

30. Schuwirth, B. S.; Borovinskaya, M. A.; Hau, C. W.; Zhang, W.; Vila-Sanjurjo, A.; Holton, J. M.; Doudna Cate, J. H. *Science* **2005**, *310*, 827–834.

31. Cocito, C.; Giambattista, M. D.; Nyssen, E.; Vannuffel, P. *J. Antimicrob. Chemother.* **1997**, *39*, 7–13.

32. Grollmant, A. P. *Biochemistry* **1966**, *56*, 1867–1874.

33. Kloss, P.; Xiong, L.; Shinabarger, D. L.; Mankin, A. S. *J. Mol. Biol.* **1999**, *294*, 93–101.

34. Weinmann, R.; Roeder, R. G. *PNAS* **1974**, *71*, 1790–1794.

35. Shen, L. L.; Pernet, A. G. *PNAS* **1985**, *82*, 307–311.

36. Maxwell, A. *Trends Microbiol.* **1997**, *5*, 102–108.

37. Wehrli, W.; Knusel, F.; Schmid, K.; Staehelin, M. *Biochemistry* **1968**, *61*, 667–673.

38. Luckey, M. *Membrane Structural Biology*, 2nd ed.; Cambridge University Press: Cambridge, United Kingdom, 2014.

39. Bahar, A. A.; Ren, D. *Pharmaceuticals* **2013**, *6*, 1543–1575.

40. Taylor, S. D.; Palmer, M. *Bioorganic Med. Chem.* **2016**, *24*, 6253–6268.

41. Newton, B. A. *Bacteriol. Rev.* **1956**, *20*, 14–27.

42. Hasper, H. E.; Kramer, N. E.; Smith, J. L.; Hillman, J. D.; Zachariah, C.; Kuipers, O. P.; Kruijff, B.; Breukink, E. *Science* **2006**, *313*, 1636–1637.

43. Yeaman, M. R.; Yount, N. Y. *Pharmacol. Rev.* **2003**, *55*, 27–55.

44. Hasper, H. E.; Kramer, N. E.; Smith, J. L.; Hillman, J. D.; Zachariah, C.; Kuipers, O. P.; Krujiff, B. de; Breukink, E. *Science* **2006**, *313*, 1636–1637.

45. Zhang, T.; Muraih, J. K.; Maccormick, B.; Silverman, J.; Palmer, M. *Biochim. Biophys. Acta* **2014**, *1838*, 2425–2430.

46. Silverman, J. A.; Perlmutter, N. G.; Shapiro, H. M. *Antimicrob. Agents Chemother.* **2003**, *47*, 2538–2544.

47. Saar-Dover, R.; Bitler, A.; Nezer, R.; Shmuel-Galia, L.; Firon, A.; Shimoni, E.; Trieu-Cuot, P.; Shai, Y. *PLoS Pathog.* **2012**, *8*, 1–13.

48. Tran, T. T.; Munita, J. M.; Arias, C. A. *Ann. N. Y. Acad. Sci.* **2015**, *1354*, 32–53.

49. Bertsche, U.; Weidenmaier, C.; Kuehner, D.; Yang, S.-J.; Baur, S.; Wanner, S.; Francois, P.; Schrenzel, J.; Yeaman, M. R.; Bayer, A. S. *Antimicrob. Agents Chemother.* **2011**, *55*, 3922–3928.

50. Eisenstein, B. I. *Clin. Microbiol. Infect.* **2008**, *14*, 10–16.

51. Nadrah, K.; Strle, F. *Chemother. Res. Pract.* **2011**, *10*, 1–10.

52. Robbel, L.; Marahiel, M. A. *J. Biol. Chem.* **2010**, *285*, 27501–27508.

53. Strieker, M.; Marahiel, M. A. *ChemBioChem* **2009**, *10*, 607–616.

54. Sauermann, R.; Rothenburger, M.; Graninger, W.; Joukhadar, C. *Pharmacology* **2008**, *81*, 79–91.

55. Straus, S. K.; Hancock, R. E. W. *Biochim. Biophys. Acta* **2006**, *1758*, 1215–1223.

56. Steenbergen, J. N.; Alder, J.; Thorne, G. M.; Tally, F. P. *J. Antimicrob. Chemother.* **2005**, *55*, 283–288.

57. Miao, V.; Oise, M.-F.; Ffet-Legal, C.; Brian, P.; Brost, R.; Penn, J.; Whiting, A.; Martin, S.; Ford, R.; Parr, I.; Bouchard, M.; Silva, C. J.; Wrigley, S. K.; Baltz, R. H. *Microbiology* **2005**, *151*, 1507–1523.

58. Tally, F. P.; Debruin, M. F. *J. Antimicrob. Chemother.* **2000**, *46*, 523–526.

59. Rubio, A.; Moore, J.; Varoglu, M.; Conrad, M.; Chu, M.; Shaw, W.; Silverman, J. A. *Mol. Membr. Biol.* **2012**, *29*, 1–8.

60. Debono, M.; Abbott, B. J.; Molloy, R. M.; Fukuda, D. S.; Hunt, A. H.; Daupert, V. M.; Counter, F. T.; Ott, J. L.; Carrell, C. B.; Howard, L. C.; Boeck, L. D.; Hamill, R. L. *J. Antibiot.* **1988**, *XLI*, 1093–1105.

61. Oleson, F. B.; Berman, C. L.; Kirkpatrick, J. B.; Regan, K. S.; Lai, J.-J.; Tally, F. P. *Antimicrob. Agents Chemother.* **2000**, *44*, 2948–2953.

62. Rose, W. E.; Rybak, M. J.; Kaatz, G. W. *J. Antimicrob. Chemother.* **2007**, *60*, 334–340.

63. Carpenter, C. F.; Chambers, H. F. *Clin. Infect. Dis.* **2004**, *38*, 994–1000.

64. Dvorchik, B. H.; Brazier, D.; Debruin, M. F.; Arbeit, R. D. *Antimicrob. Agents Chemother.* **2003**, *47*, 1318–1323.

65. Silverman, J. A.; Mortin, L. I.; Vanpraagh, A. D. G.; Li, T.; Alder, J. *Surfactant Inhib. Daptomycin* **2005**, *191*, 2149–2152.

66. Lee, B. Y. Antimicrobial Peptide Daptomycin and its Inhibition by Pulmonary Surfactant : Biophysical Studies using Model Membrane Systems by, University of Waterloo, 2017.

67. Baltz, R. H. *Am. Chem. Soc. - Synth. Biol.* **2014**, *3*, 748–758.

68. Raj Lohani, C.; Taylor, R.; Palmer, M.; Taylor, S. D. *Org. Lett.* **2015**, *17*, 748–751.

69. He, Y.; Li, J.; Yin, N.; Herradura, P. S.; Martel, L.; Zhang, Y.; Pearson, A. L.; Kulkarni, V.; Mascio, C.; Howland, K.; Silverman, J. A.; Keith, D. D.; Metcalf, C. A. *Bioorg. Med. Chem. Lett.* **2012**, *22*, 6248–6251.

70. Boeck, L. D.; Wetzel, R. W. *J. Antibiot.* **1990**, *XLIII*, 607–615.

71. Miao, V.; Brost, R.; Chapple, J.; She, K.; Coefet, M.-F.; Gal, -Le; Baltz, R. H. *J. Microbiol. Biotechnol.* **2006**, *33*, 129–140.

72. Nguyen, K. T.; He, X.; Alexander, D. C.; Li, C.; Gu, J.-Q.; Mascio, C.; Praagh, A. Van; Mortin, L.; Chu, M.; Silverman, J. A.; Brian, P.; Baltz, R. H. *Antimicrob. Agents Chemother.* **2010**, *54*, 1404–1413.

73. Grünewald, J.; Sieber, S. A.; Mahlert, C.; Linne, U.; Marahiel, M. A. *J. Am. Chem. Soc.* **2004**, *126*, 17025–17031.

74. Debono, M.; Barnhart, M.; Carrell, C. B.; Hoffmann, J. A.; Occolowitz, J. L.; Abbott, B. J.; Fukuda, D. S.; Hamill, R. L.; Biemann, K.; Herlihy, W. C. *J. Antibiot.* **1987**, *XL*, 761–777.

75. Qiu, J.; Kirsch, L. E. *J. Pharm. Sci.* **2014**, *103*, 853–861.

76. Lakey, J. H.; Ptak, M. *Biochemistry* **1988**, *27*, 4639–4645.

77. Robbel, L.; Marahiel, M. A. *J. Biol. Chem.* **2010**, *285*, 27501–27508.

78. Kopp, F.; Grünewald, J.; Mahlert, C.; Marahiel, M. A. *Biochemistry* **2006**, *45*, 10474–10481.

79. Miao, V.; Coë, M.-F.; Gal, F.-L.; Nguyen, K.; Brian, P.; Penn, J.; Whiting, A.; Steele, J.; Kau, D.; Martin, S.; Ford, R.; Gibson, T.; Bouchard, M.; Wrigley, S. K.; Baltz, R. H. *Chem. Biol.* **2006**, *13*, 269–276.

80. Ball, L.-J.; Goult, C. M.; Donarski, J. A.; Micklefield, J.; Ramesh, V. *Org. Biomol. Chem.* **2004**, *2*, 1872–1878.

81. Rotondi, K. S.; Gierasch, L. M. *Biopolym. - Pept. Sci. Sect.* **2005**, *80*, 374–385.

82. Jung, D.; Rozek, A.; Okon, M.; Hancock, R. E. W. *Chem. Biol.* **2004**, *11*, 949–957.

83. Gibbs, A. C.; Bjorndahl, T. C.; Hodges, R. S.; Wishart, D. S. *J. Am. Chem. Soc.* **2002**, *124*, 1203–1213.

84. Ho, S. W.; Jung, D.; Calhoun, J. R.; Lear, J. D.; Okon, M.; Scott, W. R. P.; Hancock, R. E. W.; Straus, S. K. *Eur. Biophys. J.* **2008**, *37*, 421–433.

85. Scott, W. R. P.; Baek, S.-B.; Jung, D.; Hancock, R. E. W.; Straus, S. K. *Biochim. Biophys. Acta* **2007**, *1768*, 3116–3126.

86. Houtsmuller, U. M. T.; Van Deenen, L. L. M. *Biochim. Biophys. Acta* **1965**, *106*, 564–576.

87. van Deenen, L. L. M. *Naturwissenschaften* **1972**, *59*, 485–491.

88. Bunkó, G.; Vértesy, L.; Sheldrick, G. M. *Acta Crystallogr. Sect. D* **2005**, *61*, 1160–1164.

89. Bertsche, U.; Yang, S.-J.; Kuehner, D.; Wanner, S.; Mishra, N. N.; Roth, T.; Nega, M.; Schneider, A.; Mayer, C.; Grau, T.; Bayer, A. S.; Weidenmaier, C. *Public Libr. Sci. - One* **2013**, *8*, 1–11.

90. Nguyen, K. T.; Ritz, D.; Gu, J.-Q.; Alexander, D.; Chu, M.; Miao, V.; Brian, P.; Baltz, R. H. *PNAS* **2006**, *103*, 17462–17467.

91. Baltz, R. H. In *Antimicrobials: New and Old Molecules in the Fight Against Multi-Resistant Bacteria*; Flavia, M., Olga, G., Eds.; Springer-Verlag Berlin Heidelberg: New York City, New York, 2014; pp 109–139.

92. Floss, H. G. *J. Biotechnol.* **2006**, *124*, 242–257.

93. Hart, P. 't; J Kleijn, L. H.; Bruin, G. de; Oppedijk, S. F.; Kemmink, J.; Martin, N. I. *Org. Biomol. Chem.* **2014**, *12*, 913–919.

94. Yung Lam, H.; Zhang, Y.; Liu, H.; Xu, J.; T Wong, C. T.; Xu, C.; Li, X. *J. Am. Chem. Soc.* **2013**, *135*, 6272–6279.

95. Siedlecki, J.; Hill, J.; Parr, I.; Yu, X.; Morytko, M.; Zhang, Y.; Silverman, J.; Controneo, N.; Laganas, V.; Li, T.; Li, J.; Keith, D.; Shimer, G.; Finn, J. *Bioorg. Med. Chem. Lett.* **2003**, *12*, 4245–4249.

96. Hill, J.; Siedlecki, J.; Parr, I.; Morytko, M.; Yu, X.; Zhang, Y.; Silverman, J.; Controneo, N.; Laganas, V.; Li, T.; Lai, J.-J.; Keith, D.; Shimer, G.; Finn, J. *Bioorg. Med. Chem. Lett.* **2003**, *13*, 4187–4191.

97. Knight-Connoni, V.; Mascio, C.; Chesnel, L.; Silverman, J. *J. Ind. Microbiol. Biotechnol.* **2016**, *43*, 195–204.

98. Barnawi, G.; Noden, M.; Taylor, R.; Lohani, C.; Beriashvili, D.; Palmer, M.; Taylor, S. D. *Biopolym. - Pept. Sci.* **2018**, 1–9.

99. Raj Lohani, C.; Taylor, R.; Palmer, M.; Taylor, S. D. *Bioorg. Med. Chem. Lett.* **2015**, *25*, 5490–5494.

100. Kates, M. *Advances in Lipid Research, Vol. 2 - Bacterial Lipids*, 1st ed.; Paoletti, R.,

Kritchevsky, D., Eds.; Academic Press: New York City, New York, 1964.

101. Houtsmuller, U. M. T.; van Deenen, L. L. *Biochim. Biophys. Acta* **1964**, *84*, 96–98.

102. Salzberg, L. I.; Helmann, J. D. *J. Bacteriol.* **2008**, *190*, 7797–7807.

103. Joyce, G. H.; Hammond, R. K.; White, D. C. *J. Bacteriol.* **1970**, *104*, 323–330.

104. Mishra, N. N.; Bayer, A. S. *Antimicrob. Agents Chemother.* **2013**, *57*, 1082–1085.

105. Muraih, J. K.; Harris, J.; Taylor, S. D.; Palmer, M. *Biochim. Biophys. Acta - Biomembr.* **2012**, *1818*, 673–678.

106. den Kamp, J. A.; Redai, I.; van Deenen, L. L. *J Bacteriol* **1969**, *99*, 298–303.

107. Davlieva, M.; Zhang, W.; Arias, C. A.; Shamoo, Y. *Antimicrob. Agents Chemother.* **2013**, *57*, 289–296.

108. Ball, L.-J.; Goult, C. M.; Donarski, J. A.; Micklefield, J.; Ramesh, V. *Org. Biomol. Chem.* **2004**, *2*, 1872–1878.

109. Jung, D.; Powers, J. P.; Straus, S. K.; Hancock, R. E. W. *Chem. Phys. Lipids* **2008**, *154*, 120–128.

110. Zhang, T.; Muraih, J. K.; Mintzer, E.; Tishbi, N.; Desert, C.; Silverman, J.; Taylor, S.; Palmer, M. *Biochim. Biophys. Acta - Biomembr.* **2013**, *1828*, 302–308.

111. Zhang, T. H.; Muraih, J. K.; Tishbi, N.; Herskowitz, J.; Victor, R. L.; Silverman, J.; Uwumarenogie, S.; Taylor, S. D.; Palmer, M.; Mintzer, E. *J. Biol. Chem.* **2014**, *289*, 11584–11591.

112. Silverman, J. A.; Perlmutter, N. G.; Shapiro, H. M. *Antimicrob. Agents Chemother.* **2003**, *47*, 2538–2544.

113. Mascio, C. T. M.; Alder, J. D.; Silverman, J. A. *Antimicrob. Agents Chemother.* **2007**, *51*, 4255–4260.

114. Cotroneo, N.; Harris, R.; Perlmutter, N.; Beveridge, T.; Silverman, J. A. *Antimicrob. Agents Chemother.* **2008**, *52*, 2223–2225.

115. Muraih, J. K.; Palmer, M. *Biochim. Biophys. Acta* **2012**, *1818*, 1642–1647.

116. Taylor, R.; Butt, K.; Scott, B.; Zhang, T.; Muraih, J. K.; Mintzer, E.; Taylor, S.; Palmer, M.

Biochim. Biophys. Acta - Biomembr. **2016**, *1858*, 1999–2005.

117. Taylor, R. M.; Scott, B.; Taylor, S.; Palmer, M. *Am. Chem. Soc. - Infect. Dis.* **2017**, *3*, 462–466.

118. Zhang, J.; Scoten, K.; Straus, S. K. *Am. Chem. Soc. - Infect. Dis.* **2016**, *2*, 682–687.

119. Müller, A.; Wenzel, M.; Strahl, H.; Grein, F.; Saaki, T. N. V; Kohl, B.; Siersma, T.; Bandow, J. E.; Sahl, H.-G.; Schneider, T.; Hamoen, L. W. *PNAS* **2016**, *113*, 7077–7086.

120. Chen, Y.-F.; Sun, T.-L.; Sun, Y.; Huang, H. W. *Biochemistry* **2014**, *53*, 5384–5392.

121. Tellinghuisen, J. *J. Phys. Chem. B* **2005**, *109*, 20027–20035.

122. Freire, E.; Mayorga, O. L.; Straume, M. *Anal. Chem.* **1990**, *62*, 950A–959A.

123. Yokoyama, H.; Ikeda, K.; Wakabayashi, M.; Ishihama, Y.; Nakano, M. *Langmuir* **2013**, *29*, 857–860.

124. *Biocalorimetry 2: Applications of Calorimetry in the Biological Sciences*; Ladbury, J. E., Doyle, M. L., Eds.; John Wiley & Sons, Inc.: Hoboken, New Jersey, 2004.

125. Zhang, T.; Taylor, S. D.; Palmer, M.; Duhamel, J. *Biophys. J.* **2016**, *111*, 1267–1277.

126. Muraih, J. K.; Pearson, A.; Silverman, J.; Palmer, M. *Biochim. Biophys. Acta* **2011**, *1808*, 1154–1160.

127. Mims, M. P.; Carol, B. S.; Sparrow, J. T.; Morrisett, J. D. *Biochemistry* **1993**, *32*, 9215–9220.

128. Hobbs, J. K.; Miller, K.; O 'neill, A. J.; Chopra, I. *J. Antimicrob. Chemother.* **2008**, *62*, 1003–1008.

129. Eliopoulos, G. M.; Willey, S.; Reiszner, E.; Spitzer, P. G.; Caputo, G.; Moellering, R. C. *Antimicrob. Agents Chemother.* **1986**, *30*, 532–535.

130. Barry, A. L.; Fuchs, P. C.; Brown, S. D. *Antimicrob. Agents Chemother.* **2001**, *45*, 1919–1922.

131. Canepari, P.; Boaretti, M.; Del Mar Lle6, M.; Satta2, G. *Antimicrob. Agents Chemother.* **1990**, *34*, 1220–1226.

132. Lakey, J. H.; Lea, E. J. A. *Biochim. Biophys. Acta* **1986**, *859*, 219–226.

133. Batrakov, S. G.; Bergelson, L. D. *Chem. Phys. Lipids* **1978**, *21*, 1–29.

134. Hachmann, A.-B.; Angert, E. R.; Helmann, J. D. *Antimicrob. Agents Chemother.* **2009**, *53*, 1598–1609.

135. Pogliano, J.; Pogliano, N.; Silverman, J. A. *J. Bacteriol.* **2012**, *194*, 4494–4504.

136. Allen, N. E.; Hobbs, J. N.; Alborn, W. E.; Baker, J.; Boeck, L. D.; Debono, M.; Ensminger, P. W.; Hamill, R. L.; Krupinski, V. M.; Molloy, R. M.; Ott, J. L. *Antimicrob. Agents Chemother.* **1987**, *31*, 1093–1099.

137. Alborn, W. E.; Allen, N. E.; Preston, D. A. *Antimicrob. Agents Chemother.* **1991**, *35*, 2282–2287.

138. Rubinchik, E.; Schneider, T.; Elliott, M.; Scott, W. R. P.; Pan, J.; Anklin, C.; Yang, H.; Dugourd, D.; Müller, A.; Gries, K.; Straus, S. K.; Sahl, H. G.; Hancock, R. E. W. *Antimicrob. Agents Chemother.* **2011**, *55*, 2743–2754.

139. Jones, T.; Yeaman, M. R.; Sakoulas, G.; Yang, S. J.; Proctor, R. A.; Sahl, H. G.; Schrenzel, J.; Xiong, Y. Q.; Bayer, A. S. *Antimicrob. Agents Chemother.* **2008**, *52*, 269–278.

140. Wale, L. J.; Shelton, A. P.; Greenwood, D. *J. Med. Microbiol* **1989**, *30*, 5–4.

141. Rubinchik, E.; Schneider, T.; Elliott, M.; Scott, W. R. P.; Pan, J.; Anklin, C.; Yang, H.; Dugourd, D.; Müller, A.; Gries, K.; Straus, S. K.; Sahl, H. G.; Hancock, R. E. W. *Antimicrob. Agents Chemother.* **2011**, *55*, 2743–2754.

142. Patel, D.; Kosmidis, C.; Seo, S. M.; Kaatz, G. W. *Antimicrob. Agents Chemother.* **2010**, *54*, 5070–5073.

143. Clement, N. R.; Gould, J. M. *Biochemistry* **1981**, *20*, 1534–1538.

144. Bhakdi, S.; Fussle, R.; Tranum-Jensent, J. *Biochemistry* **1981**, *78*, 5475–5479.

145. Milne, J. C.; Furlong, D.; Hanna, P. C.; Wall, J. S.; Collier, R. J. *J. Biol. Chem.* **1994**, *269*, 20607–20612.

146. Wiedemann, I.; Breukink, E.; Van Kraaij, C.; Kuipers, O. P.; Bierbaum, G.; De Kruijff, B.; Sahl, H. G. *J. Biol. Chem.* **2001**, *276*, 1772–1779.

147. Michelet, B.; Boutry, M. *Plant Physiol.* **1995**, *108*, 1–6.

148. Navarre, W. W.; Schneewind, O. *Microbiol. Mol. Biol. Rev.* **1999**, *63*, 174–229.

149. Boaretti, M.; Canepari, P. *Antimicrob. Agents Chemother.* **1995**, *39*, 2068–2072.

150. Laganas, V.; Alder, J.; Silverman, J. A. *Antimicrob. Agents Chemother.* **2003**, *47*, 2682–2684.

151. Strahl, H.; Bürmann, F.; Hamoen, L. W. *Nat. Commun.* **2014**, *5*, 1–11.

152. Wolf, D.; Domínguez-Cuevas, P.; Daniel, R. A.; Mascher, T. *Antimicrob. Agents Chemother.* **2012**, *56*, 5907–5915.

153. Alborn, W. E.; Allen, N. E.; Preston, D. A. *Antimicrob. Agents Chemother.* **1991**, *35*, 2282–2287.

154. Allen, N. E.; Alborn, W. E.; Hobbs, J. N. *Antimicrob. Agents Chemother.* **1991**, *35*, 2639–2642.

155. Tran, T. T.; Panesso, D.; Mishra, N. N.; Mileykovskaya, E.; Guan, Z.; Munita, J. M.; Reyes, J.; Diaz, L.; Weinstock, G. M.; Murray, B. E.; Shamoo, Y.; Dowhan, W.; Bayer, A. S.; Arias, C. A. *MBio* **2013**, *4*, 1–10.

156. Hawkey, P. M. *J. Antimicrob. Chemother.* **2008**, *62*, iii7-iii14.

157. Hachmann, A.-B.; Sevim, E.; Gaballa, A.; Popham, D. L.; Antelmann, H.; Helmann, J. D. *Antimicrob. Agents Chemother.* **2011**, *55*, 4326–4337.

158. Peleg, A. Y.; Miyakis, S.; Ward, D. V; Earl, A. M.; Rubio, A.; Cameron, D. R.; Pillai, S.; Moellering, R. C.; Eliopoulos, G. M. *PLoS One* **2012**, *7*, 1–8.

159. Nesbitt, J. A.; Lennarz, W. J. *J. Biol. Chem.* **1968**, *243*, 3088–3095.

160. Gould, R. M.; Lennarz, W. J. *J. Bacteriol.* **1970**, *104*, 1135–1144.

161. Ernst, C. M.; Staubitz, P.; Mishra, N. N.; Yang, S.-J.; Hornig, G.; Kalbacher, H.; Bayer, A. S.; Kraus, D.; Peschel, A. *PLoS Pathog* **2009**, *5*, 1–9.

162. Staubitz, P.; Neumann, H.; Schneider, T.; Wiedemann, I.; Peschel, A. *FEMS Microbiol. Lett.* **2004**, *231*, 67–71.

163. Kilelee, E.; Pokorny, A.; Yeaman, M. R.; Bayer, A. S. *Antimicrob. Agents Chemother.* **2010**, *54*, 4476–4479.

164. Mishra, N. N.; Bayer, A. S.; Weidenmaier, C.; Grau, T.; Wanner, S.; Stefani, A.; Cafiso, V.; Bertuccio, T.; Yeaman, M. R.; Nast, C. C.; Yang, S. J. *PLoS One* **2014**, *9*, 13–18.

165. Kates, M.; Syz, J.-Y.; Gosser, D.; Haines, T. H. *Lipids* **1993**, *28*, 877–882.

166. Sathappa, M.; Alder, N. N. *Biochim. Biophys. Acta - Biomembr.* **2016**, *1858*, 1362–1372.

167. Dubrac, S.; Boneca, I. G.; Poupel, O.; Msadek, T. *J. Bacteriol.* **2007**, *189*, 8257–8269.

168. Fukushima, T.; Szurmant, H.; Kim, E.; Perego, M.; Hoch, J. A. *Mol. Microbiol.* **2009**, *69*, 621–632.

169. Howden, B. P.; Mcevoy, C. R. E.; Allen, D. L.; Chua, K.; Gao, W.; Harrison, P. F.; Bell, J.; Coombs, G.; Bennett-Wood, V.; Porter, J. L.; Robins-Browne, R.; Davies, J. K.; Seemann, T.; Stinear, T. P. *PLOS Pathog.* **2011**, *7*, 1–15.

170. Wecke, T.; Zühlke, D.; Mäder, U.; Jordan, S.; Voigt, B.; Pelzer, S.; Labischinski, H.; Homuth, G.; Hecker, M.; Mascher, T. *Antimicrob. Agents Chemother.* **2009**, *53*, 1619–1623.

171. Arias, C. A.; Panesso, D.; Mcgrath, D. M.; Qin, X.; Mojica, M. F.; Miller, C.; Diaz, L.; Tran, T. T.; Rincon, S.; Barbu, E. M.; Reyes, J.; Roh, J. H.; Lobos, E.; Sodergren, E.; Pasqualini, R.; Arap, W.; Quinn, J. P.; Shamoo, Y.; Murray, B. E.; Weinstock, G. M. *N. Engl. J. Med.* **2011**, *365*, 892–900.

172. Domínguez-escobar, J.; Wolf, D.; Fritz, G.; Höfler, C.; Wedlich-söldner, R.; Mascher, T.; München, L. *Mol. Microbiol.* **2014**, *92*, 716–732.

173. Fischer, A.; Yang, S. J.; Bayer, A. S.; Vaezzadeh, A. R.; Herzig, S.; Stenz, L.; Girard, M.; Sakoulas, G.; Scherl, A.; Yeaman, M. R.; Proctor, R. A.; Schrenzel, J.; François, P. *J. Antimicrob. Chemother.* **2011**, *66*, 1696–1711.

174. Lee, M.-T.; Hung, W.-C.; Hsieh, M.-H.; Chen, H.; Chang, Y.-Y.; Huang, H. W. *Biophys. J.* **2017**, *113*, 82–90.

175. Prendergast, F. G.; Meyer, M.; Carlson, G. L.; Iida, S.; Potter, J. D. *J. Biol. Chem.* **1983**, *258*, 7541–7544.

176. Wiegand, I.; Hilpert, K.; Hancock, R. E. W. *Nat. Protoc.* **2008**, *3*, 163–175.

177. Mayer, L. D.; Hope, M. J.; Cullis, P. R. *Biochim. Biophys. Acta* **1986**, *858*, 161–168.

178. Tsentalovich, Y. P.; Snytnikova, O. A.; Sherin, P. S.; Forbes, M. D. E. *J. Phys. Chem. A* **2005**, *109*, 3565–3568.

179. Postupalenko, V. Y.; Shvadchak, V. V; Duportail, G.; Pivovarenko, V. G.; Klymchenko, A.

S.; Mély, Y. *Biochim. Biophys. Acta* **2011**, *1808*, 424–432.

180. Lakowicz, J. R. In *Principles of Fluorescence Spectroscopy*; Springer US: New York City, New York, 2006; pp 353–382.

181. Gautier, I.; Tramier, M.; Durieux, C.; Coppey, J.; Pansu, R. B.; Nicolas, J.-C.; Kemnitz, K.; Coppey-Moisan, M. *Biophys. J.* **2001**, *80*, 3000–3008.

182. Schneider, T.; Gries, K.; Josten, M.; Wiedemann, I.; Pelzer, S.; Labischinski, H.; Sahl, H. G. *Antimicrob. Agents Chemother.* **2009**, *53*, 1610–1618.

183. Bravo, A.; Gill, S. S.; Sobero, M. *Toxicon* **2006**, *49*, 423–435.

184. Shepard, L. A.; Shatursky, O.; Johnson, A. E.; Tweten, R. K. *Biochemistry* **2000**, *39*, 10284–10293.

185. Walker, B.; Braha, O.; Cheley, S.; Bayley, H. *Chem. Biol.* **1995**, *2*, 99–105.

186. Cui, L.; Tominaga, E.; Neoh, H.-M.; Hiramatsu, K. *Antimicrob. Agents Chemother.* **2006**, *50*, 1079–1082.

187. Wolf, D.; Domínguez-Cuevas, P.; Daniel, R. A.; Mascher, T. *Antimicrob. Agents Chemother.* **2012**, *56*, 5907–5915.

188. Scott, B. I. Daptomycin : studies on its action mode and on bacterial resistance with model membranes by, University of Waterloo, 2016.

189. Domínguez-Cuevas, P.; Mercier, R.; Leaver, M.; Kawai, Y.; Errington, J. *Mol. Microbiol.* **2012**, *83*, 52–66.

190. Allen, N. E.; Alborn, W. E.; Hobbs, J. N. *Antimicrob. Agents Chemother.* **1991**, *35*.

191. Mascio, C. T. M.; Alder, J. D.; Silverman, J. A. *Antimicrob. Agents Chemother.* **2007**, *51*, 4255–4260.

192. Canepari, P.; Boaretti, M.; Del Mar Lleo, M.; Satta, G. *Antimicrob. Agents Chemother.* **1990**, *34*, 1220–1226.

193. Mckenna, C. E.; Gutheil, W. G.; Song, W. *Biochim. Biophys. Acta* **1991**, *1075*, 109–117.

194. Kelkar, D. A.; Chattopadhyay, A. *Biochim. Biophys. Acta* **2007**, *1768*, 2011–2025.

195. McIntyre, J. C.; Sleight, Richard, G. *Biochemistry* **1991**, *30*, 11819–11827.

196. Kaneda, T. *Bacteriol. Rev.* **1977**, *41*, 391–418.

197. White, D. C.; Frerman, F. E. *J. Bacteriol.* **1968**, *95*, 2198–2209.

198. Rybak, M. J.; Hershberger, E.; Moldovan, T.; Grucz, R. G. *Antimicrob. Agents Chemother.* **2000**, *44*, 1062–1066.

199. Ló Pez, C. S.; Alice, A. F.; Heras, H.; Rivas, E. A.; Sá Nchez-Rivas, C. *Microbiology* **2006**, *152*, 605–616.

200. Bishop, D. G.; Rutberg, L.; Samuelsson, B. *Eur. J. Biochem* **1967**, *2*, 448–453.

201. Hines, K. M.; Waalkes, A.; Penewit, K.; Holmes, E. A.; Salipante, S. J.; Werth, B. J. *Am. Soc. Microbiol. Journals* **2017**, *2*, 1–16.

202. Gantner, M.; Schwarzmann, G.; Sandhoff, K.; Kolter, T. *J. Lipid Res.* **2014**, *55*, 2692–2704.

203. Ló Pez, D.; Kolter, R. *Genes Dev.* **2010**, *24*, 1893–1902.

204. Epand, R. M.; Walker, C.; Epand, R. F.; Magarvey, N. A. *Biochim. Biophys. Acta - Biomembr.* **2016**, *1858*, 980–987.

205. Archer, D. B. *J. Gen. Microbiol.* **1975**, *88*, 329–338.

206. Salgado, J.; Grage, S. L.; Kondejewski, L. H.; Hodges, R. S.; Mcelhaney, R. N.; Ulrich, A. S. *J. Biomol. NMR* **2001**, *21*, 191–208.

207. Traut, R. R.; Bollen, A.; Sun, T.; Hershey, J. W. B.; Sundberg, J.; Pierce, L. R. *Biochemistry* **1973**, *12*, 3266–3273.

208. Thulborn, K. R.; Beddard, G. S. *Biochim. Biophys. Acta* **1982**, *693*, 246–252.

209. Taylor, R.; Beriashvili, D.; Taylor, S.; Palmer, M. *ACS Infect. Dis.* **2017**, *3*, 797–801.

Appendix A

Unless otherwise stated, the thesis author, Robert Taylor, performed all synthesis and experiments shown in this appendix.

Chapter 2

The semi-synthesis and purification of the acrylodan-labeled Daptomycin (completed by Dr. Scott Taylor):

Acrylodan (Setareh Biotech, Eugene, OR, USA) was attached to the unique free side chain amino group of ornithine6 of Dap (generously provided by Jared Silverman, Cubist Inc.©). The amino group of ornithine was first converted to a sulfhydryl group using Traut's reagent[207], to which acrylodan was then attached. To a solution of Dap (20 mg, 0.0123 mmol) in potassium phosphate buffer (50 mM, pH 8.0, 0.5 mL) was added Traut's reagent (3.0 mg, 0.0281 mmol, 1.8 equiv). The mixture was stirred for 1 h. A solution of acrylodan (5.5 mg, 0.0246 mmol, 2 equiv) in DMF (1 mL) was added and the mixture was stirred for 24 h.

The mixture was concentrated under reduced pressure and lyophilized to give a white powder. The product was then purified by HPLC on a reversed-phase column (Higgins Analytical, C-18, 10 μm) utilizing a mobile phase of 0.1% trifluoroacetic acid with milli-q water and an acetonitrile gradient from 50% to 80%. The chromatogram has one major peak corresponding to the product (t_r = 8.4 min). This gave pure acrylodan-Dap as a pale yellow solid after lyophilization. The purity was confirmed by HPLC (Figure A1) and mass spectrometry (Figure A2).

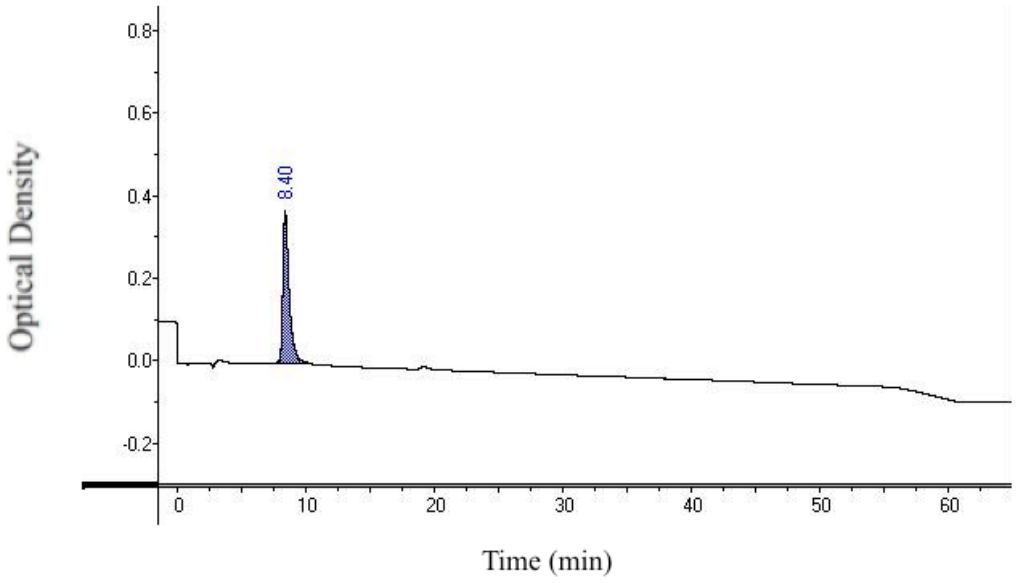

Figure A1. The analytical RP-HPLC chromatogram (at 220 nm) of pure acrylodan-Dap is shown.

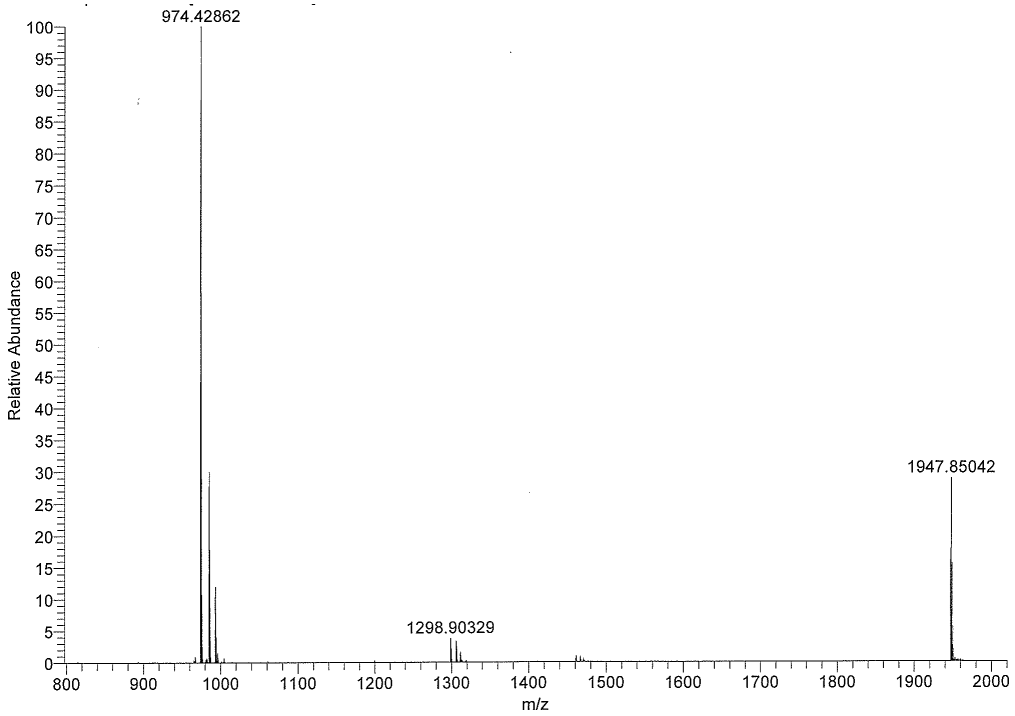

Figure A2. The ESI^+-MS of acrylodan-Dap is shown. The peaks with m/z = 1947, 974 and 1298 correspond to the singly, doubly and triply charged dimer peaks of the product.

Acrylodan (Setareh Biotech, Eugene, OR, USA) was attached to the unique free side chain amino group of lysine8 of A54145-Factor D (generously provided by Jared Silverman, Cubist Inc.©). To a solution of A5 (5 mg) in sodium phosphate buffer (50 mM, pH 8.0, 0.25 mL) was added a solution of acrylodan (1.0 mg) in DMF (0.25 mL) and the mixture stirred for 5 days at room temperature.

The mixture was concentrated under reduced pressure and lyophilized to give a white powder. The product was then purified by RP-HPLC (Higgins Analytical, C-18, 10 μm) utilizing a mobile phase of 0.1% trifluoroacetic acid with milli-q water and an acetonitrile gradient from 40% to 50%. The chromatogram has three peaks corresponding to the product (t_r = 39 min), native Dap (t_r = 23 min), and a disubstituted acrylodan analog (t_r = 43 min). This gave pure acrylodan-A5 as a white solid after lyophilization (2.75 mg, 48.5% yield). The purity was confirmed by RP-HPLC (Figure A3) and mass spectrometry (Figure A4).

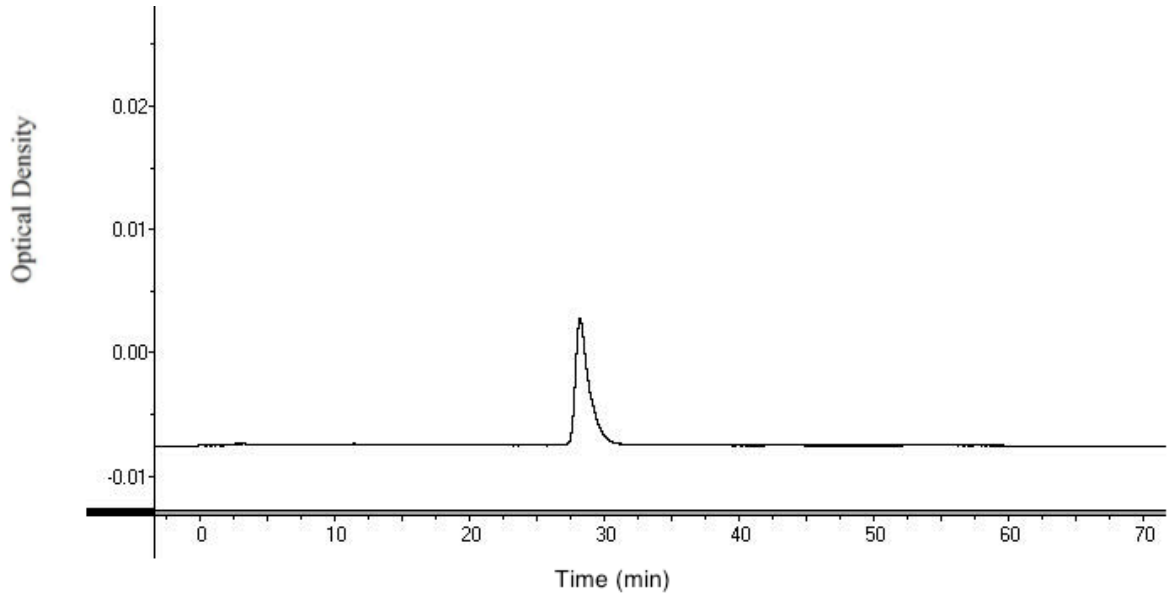

Figure A3. The analytical RP-HPLC chromatogram (at 220 nm) of pure acrylodan-A5 is shown.

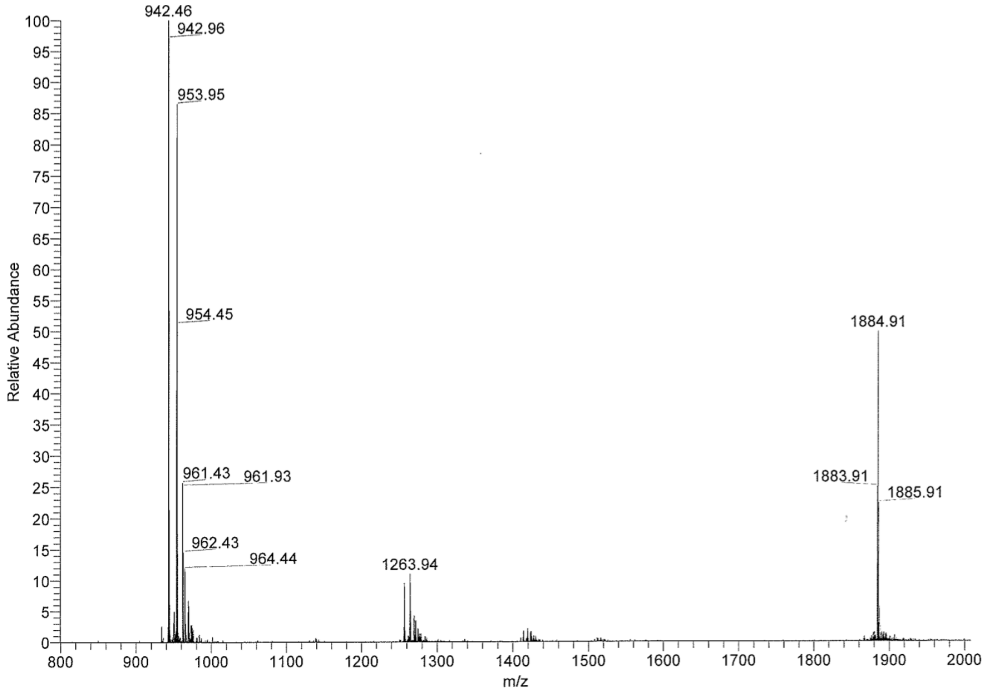

Figure A2. The ESI^+-MS of the acrylodan-A5 is shown. The peaks with m/z = 1884, 942 and 1263 correspond to the singly, doubly and triply charged dimer peaks of the product.

Chapter 3

The synthesis and purification of the activated octadecanedioate (completed by Dr. Scott Taylor):

1,18-octadecanedioic acid (1, 48.1 mg, 0.153 mmol) was treated with a solution of N-hydroxysuccinimide (106 mg, 0.923 mmol) and 1-ethyl-3-(3-dimethylaminopropyl)carbodiimide hydrochloride (EDC, 177 mg, 0.923 mmol) in anhydrous DMF (2 mL) and stirred at room temperature under argon for 6 days. The solvent was removed under reduced pressure, diethyl ether (20 mL) was added, and the suspension was vacuum filtered. The filtrate was washed with milli-q water (1 x 20 mL) and brine (1 x 20 mL), then dried ($MgSO_4$). The sample was then filtered, and the solvent was removed under reduced pressure to obtain Bis(2,5-dioxopyrrolidin-1-yl)octadecanedioate as white solid (60.0 mg, 74%). 1H NMR (300 MHz, CDCl3): δ 2.81 (s, 8H), 2.57 (t, J = 7.5 Hz, 4H), 1.72 (quint, J = 7.4 Hz, 4H), 1.37-1.23 (m, 24H); 13C NMR (75.5 MHz, CDCl3): δ 24.5, 25.5, 28.7, 29.0, 29.3, 29.5, 29.6, 29.6, 30.9, 168.7, 169.2; LRMS (ESI-MS) m/z (%): 509 (M+,100); HRMS (ESI+-MS) calcd. for C26H41N2O8 509.2863; found 509.2877.

The semi-synthesis and purification of the dimeric Dap (completed by Dr. Scott Taylor):

To a solution of Boc-deacyldaptomycin (15.6 mg, 10 μmol) in dry DMF (0.5 ml) was added Bis(2,5-dioxopyrrolidin-1-yl)octadecanedioate (3 mg, 6 μmol, 0.6 eq.). Triethylamine (7 μL, 50 μmol, 5 eq.) was added and the mixture stirred for two days. Analytic RP-HPLC of the mixture showed that all of the Boc-deacyldaptomycin was consumed and a single major peak was present (t_r = 26.3 min, Higgins Clipeus analytical C-8 column, 5 μm) utilizing a mobile phase of 0.1% trifluoroacetic acid with milli-q water and an acetonitrile gradient from 5% to 100% over 45 minutes. The solvent was removed under reduced pressure and the residue dissolved in milli-q water and lyophilized. The resulting white powder was dissolved in ice-cold trifluoroacetic acid containing 2% thioanisole and stirred at 0 ^{o}C (ice bath) for 20 minutes, following concentration under reduced pressure.

The residue was taken up in milli-q water and lyophilized to give a white powder. The powder was dissolved in milli-q water and purified by semi-preparative RP-HPLC (Higgins Clipeus C-18 semi-preparative column, 10 μm) utilizing a mobile phase of 0.1% trifluoroacetic acid with milli-q water and an acetonitrile gradient from 30% to 40% over 70 minutes, then remaining at 40% acetonitrile for 5 minutes. This gave one major peak corresponding to dimeric Dap at t_r = 68.8 min. This product was lyophilized to give pure Dap dimer as a white solid (7 mg). The purity was confirmed by RP-HPLC (Figure A5) and mass spectrometry (Figure A6).

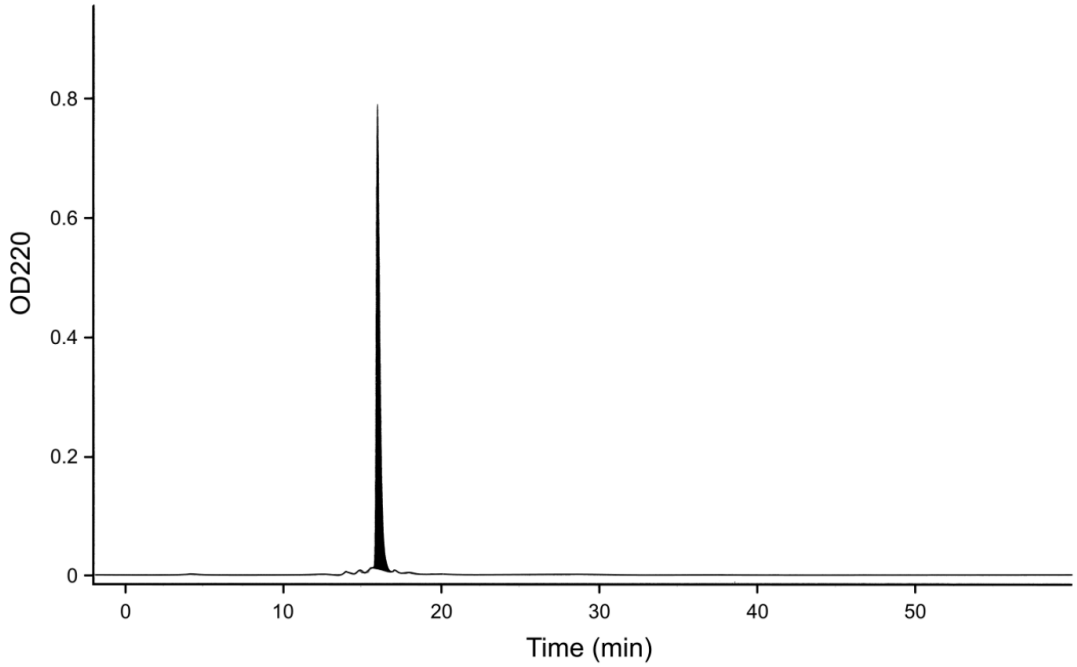

Figure A5. The analytical RP-HPLC chromatogram (at 220 nm) of pure Daptomycin dimer is shown.

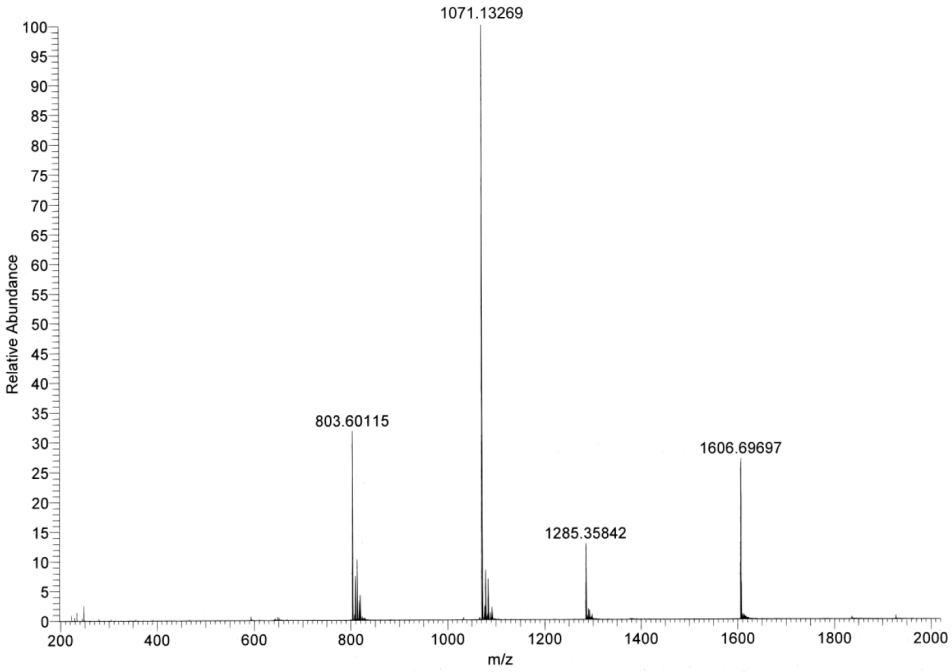

Figure A6. The ESI^+-MS of the daptomycin dimer is shown. The peaks with m/z = 803, 1071 and 1606 correspond to the quadruply, triply and doubly charged dimer respectively. The peak at m/z = 1285 corresponds to a quintuply charged dimer-dimer complex.

Chapter 4

The semi-synthesis and purification of nitrobenzoxadiazole *(NBD)-Dap:*

Dap (79.4 mg, 1.0 equiv.) was dissolved in milli-q water (4 mL) into a dual opening 50 mL round bottom flask, with a stir bar. Sodium bicarbonate ($NaHCO_3$, 12.3 mg) was added and both were stirred and brought to 55^{o}C in an oil bath. 7-chloro-4- nitrobenzoxadiazole (NBD-Cl) (10.75 mg, 1.1 equiv.) was dissolved in methanol (HPLC grade, 4 mL). This NBD-Cl was added drop wise to the solution over 10 min, then allowed to stir at 55^{o}C for 1 hour, under reflux. After the 1 hour was reached, 1 M HCl was added to quench the reaction to ~ 2-3 pH units. The solution was then rotovaped to dryness and lyophilized.

Analytic RP-HPLC (Higgins Clipeus, C-18, 10 μm) of the mixture, utilizing a mobile phase of 0.1% trifluoroacetic acid with milli-q water and an acetonitrile gradient from 35% to 45% over 50 minutes, showed two major products. The first peak corresponded to native Dap (t_r = 26 min) and the second, NBD-Dap (t_r = 40 min). These were separated on a semi-preparative column (Higgins Clipeus, C-18, 10 μm) with a linear gradient of 35% to 45% acetonitrile over 50 minutes. The peaks were collected and concentrated; giving pure NBD-Dap, yellow powder, after lyophilization (8.81 mg, 10.1% yield).

The analytical RP-HPLC chromatogram (Higgins Clipeus analytical C-18 column, 5 μm) utilizing a mobile phase of 0.1% trifluoroacetic acid with milli-q water and an acetonitrile gradient from 35% to 45% over 50 minutes, gave pure NBD-Dap showing one peak with a t_r = 41 min (See Figure A7). The high-resolution mass spectrometry showed one singly charged peak at 1784.7 $(M + H^+)^+$ (See Figure A8).

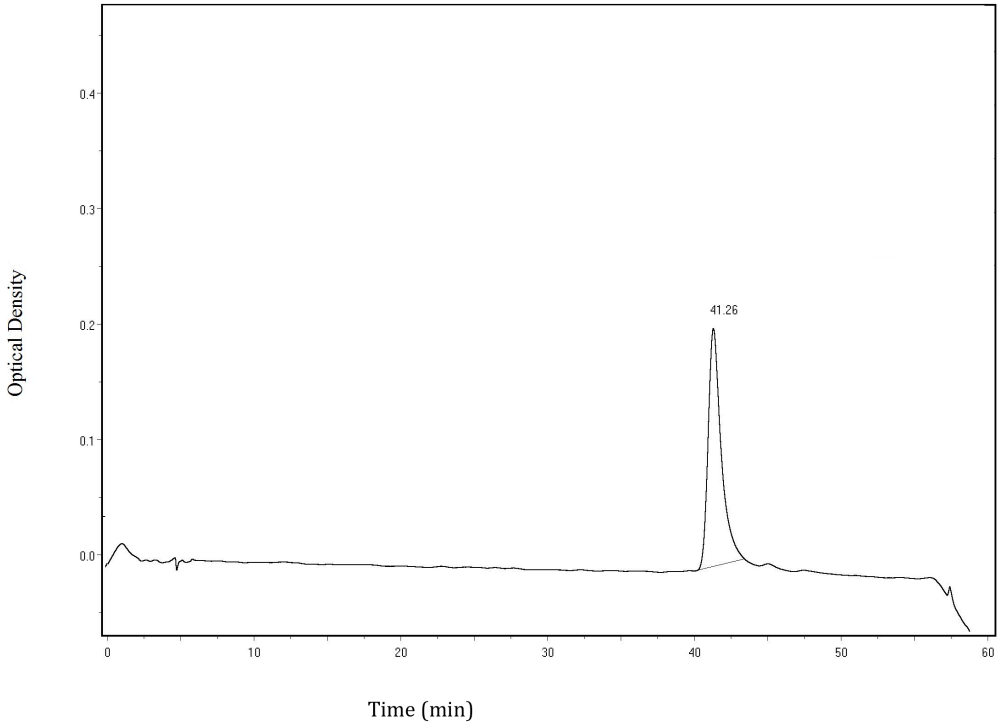

Figure A7. The analytical RP-HPLC chromatogram (at 220 nm) of the pure NBD-Dap is shown.

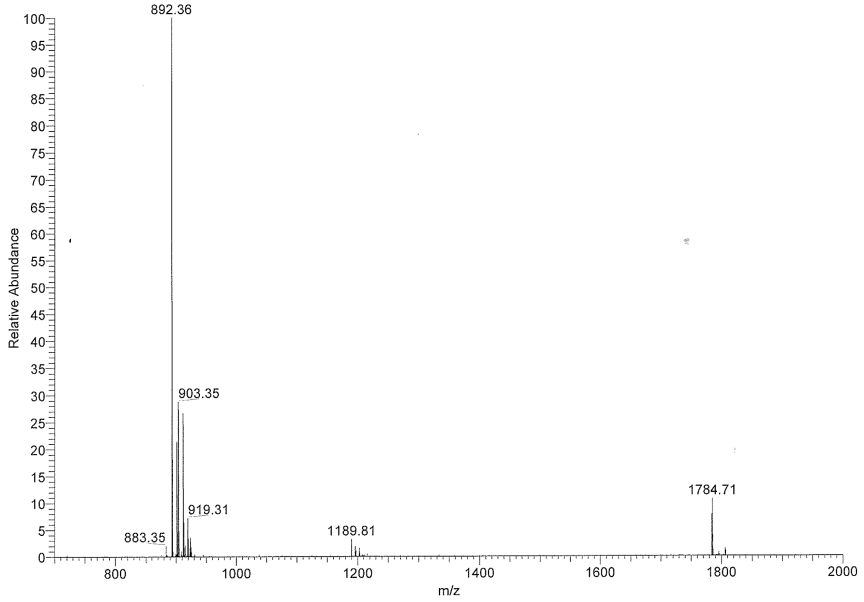

Figure A8. The ESI^{+}-MS of the NBD-Dap is shown. The peaks with m/z = 1784, 892 and1190 correspond to the singly, doubly and triply charged dimer peaks of NBD-Dap.

Chapter 5

The synthesis and purification of myristic acid succiminidyl ester, used in the synthesis of the 14 Carbon - Daptomycin:

The steps for this synthesis were done using the method by Gantner, *et al.*[202] Myristic acid (1.31 mmol) and N, N'-dicyclohexylcarbodimide (1.57 mmol) were added to a round bottom flask in THF (2.62 mL) and stirred at room temperature for 10 minutes. N-hydroxysuccinimide (1.57 mmol in 1.41 mL THF) was added and the reaction was stirred for 22.5 hours at room temperature.

The solvent was removed under reduced pressure, and dry loaded onto a silica gel column. The column had solvent system of 50:1 chloroform:methanol. The product was separated with an R_f = 0.76. The product was concentrated under reduced pressure and lyophilized to produce a white powder (221.33 mg, 51.76% yield). 1H NMR (300 MHz, $CDCl_3$): δ 2.83 (s, 4H), 2.60 (t, J = 7.4 Hz, 2H), 1.74 (p_{app}, J = 6.9 Hz, 2H), 1.26 (m, 20H), 0.88 (t, J = 5.8 Hz, 3H). LRMS (ESI-MS) m/z: 326 $(M+H^+)^+$; HRMS (ESI+-MS) calculated for C18H31N1O4 326.2461; found 326.2359.

The semi-synthesis and purification of the 14C-Daptomycin:

To a solution of Boc-deacyldaptomycin (15.6 mg, 10 μmol) in dry DMF (0.5 ml) was added myristic acid succiminidyl ester (3 mg, 6 μmol, 0.6 eq.). Triethylamine (7 μL, 50 μmol, 5 eq.) was added and the mixture stirred for three days, at room temperature. After this, trifluroacetic acid with 0.2% thioanisole (5 mL) was added and stirred at 0°C for 20 minutes, under argon. Analytic RP-HPLC (Higgins Clipeus, C-18 column, 10 μm) utilizing a mobile phase of 0.1% trifluoroacetic acid with milli-q water and an acetonitrile gradient from 10% to 90% over 60 minutes showed that all of the Boc-deacyldaptomycin was consumed and a single major peak was present (t_r = 44 min) as well as a native Dap peak at t_r = 19 min. The solvent was removed under reduced pressure and the residue dissolved in milli-q water and lyophilized, resulting in a white powder (17.0 mg, 98% yield).

The analytical RP-HPLC chromatogram (Higgins Clipeus, C-18 column, 10 μm) utilizing a mobile phase of 0.1% trifluoroacetic acid with milli-q water and an acetonitrile gradient from 10% to 90% over 60 minutes, gave pure 14C-Dap showing one major peak with a t_r = 17.0 min (See Figure A9). The high-resolution mass spectrometry showed one singly charged peak at 1677.8 $(M + H^+)^+$ (See Figure A10).

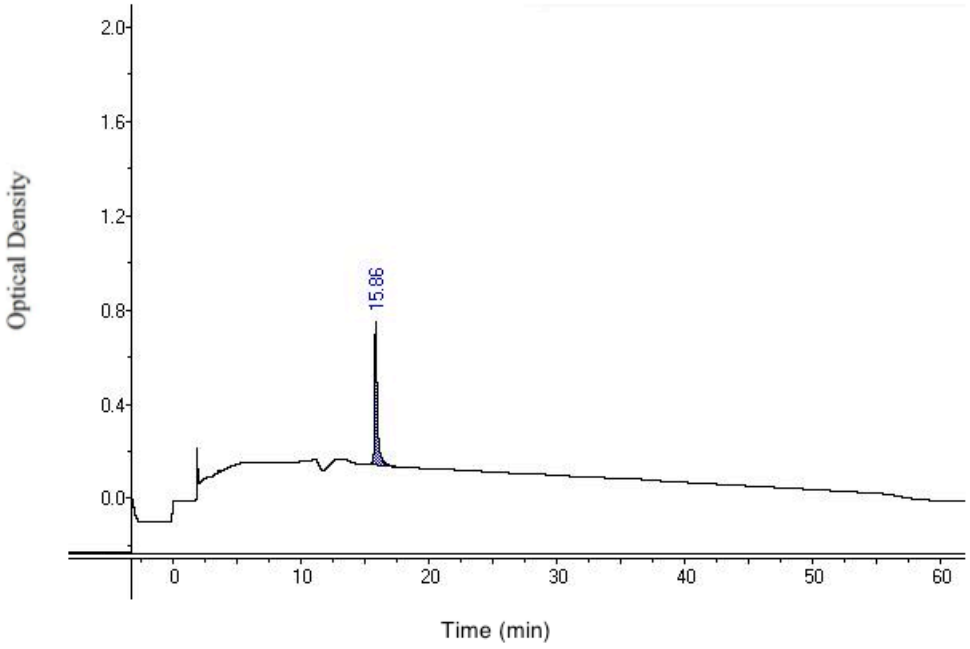

Figure A9. The analytical RP-HPLC chromatogram (at 220 nm) of pure 14C-Dap is shown.

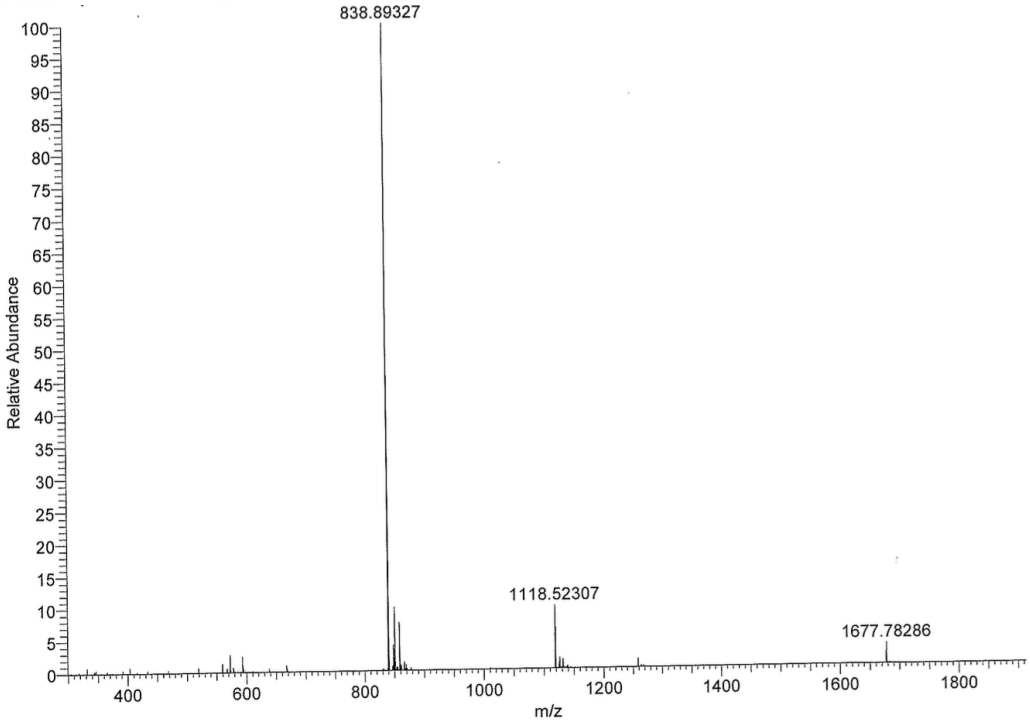

Figure A10. The ESI^{+}-MS of the 14C-Dap is shown. The peaks with m/z = 1677, 838 and1118 correspond to the singly, doubly, triply charged dimer peaks of 14C-Dap.

The individual spectra for the permeabilization results shown in Table 5.1:

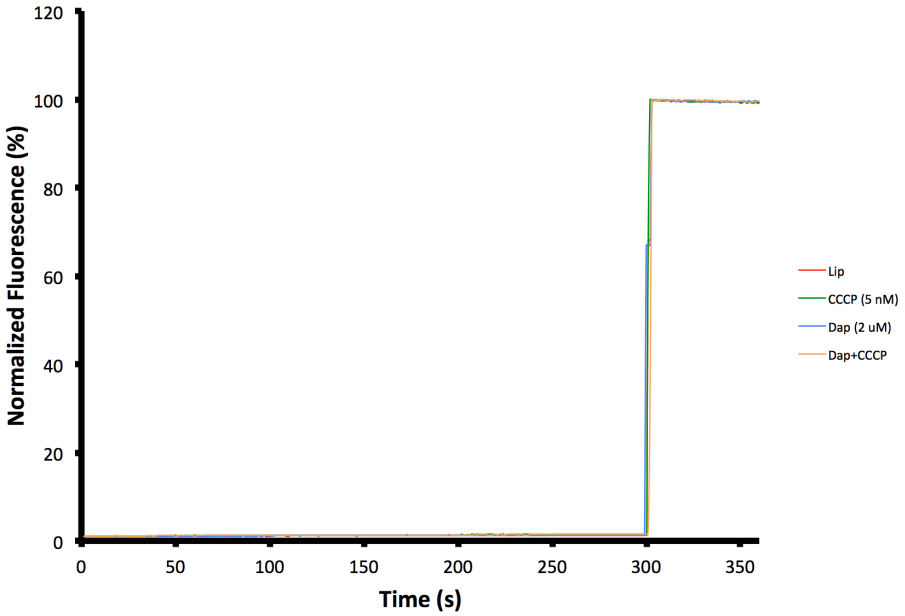

Figure A11. Permeabilization results of Dap on 1/1/2 DOPC/DMPC/DMPG (molar ratio 1/1, PC to PG, 250 μM). LUVs were entrapped with pyranine (1 mM) with a low pH and sodium buffer. Time-based fluorescence was measured (excitation, 470 nm; emission, 510 nm) for 360 seconds. The loaded LUVs were incubated with a calcium (5 mM) pre-mixed buffer, which contained a high pH and increased sodium ions, thus creating a proton/sodium gradient across the bilayer. A proton ionophore carbonyl cyanide m-chlorophenyl hydrazone (CCCP, 5 nM) and Dap (2 and/or 10 μM) were added separately or together. At 300 seconds, Triton X-100 was added (0.1%) to solubilize the membranes. Assays were run in duplicates, at 30^{o}C.

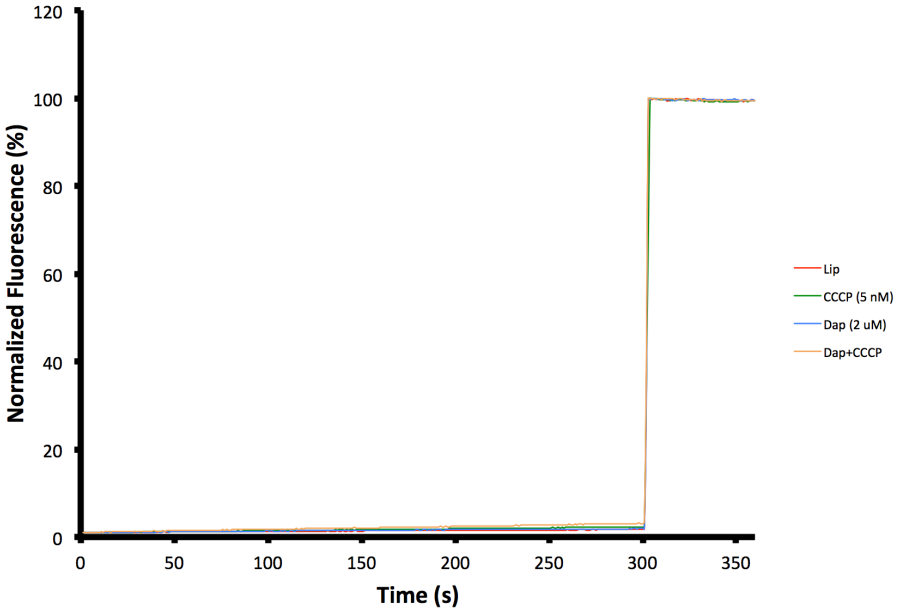

Figure A12. Permeabilization results of Dap on 1/3/4 DOPC/DMPC/DMPG (molar ratio 1/1, PC to PG, 250 μM). The experiment was run with conditions as described in Figure A11. Assays were run in duplicates, at 30°C.

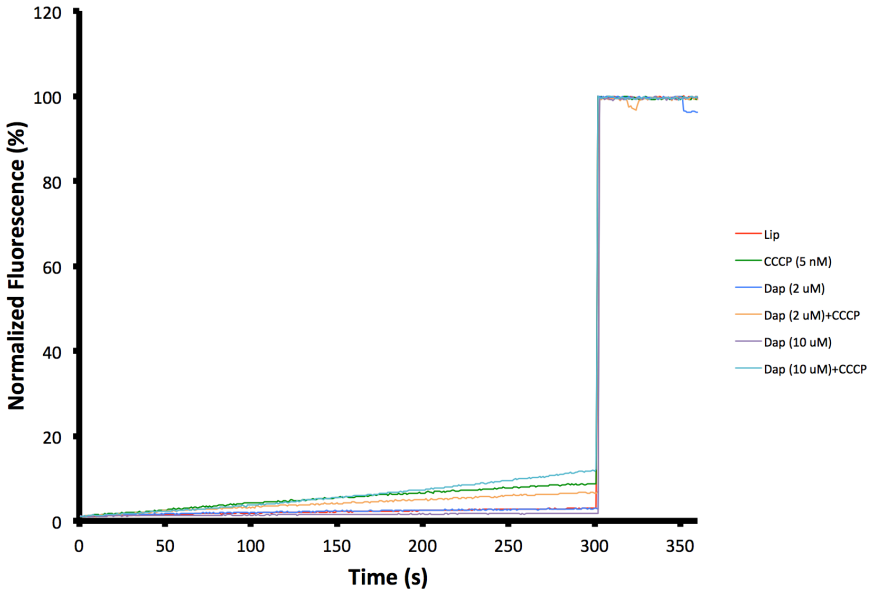

Figure A13. Permeabilization results of Dap on 1/4/5 DOPC/DMPC/DMPG (molar ratio 1/1, PC to PG, 250 μM). The experiment was run with conditions as described in Figure A11. Assays Assays were run in duplicates, at 30°C.

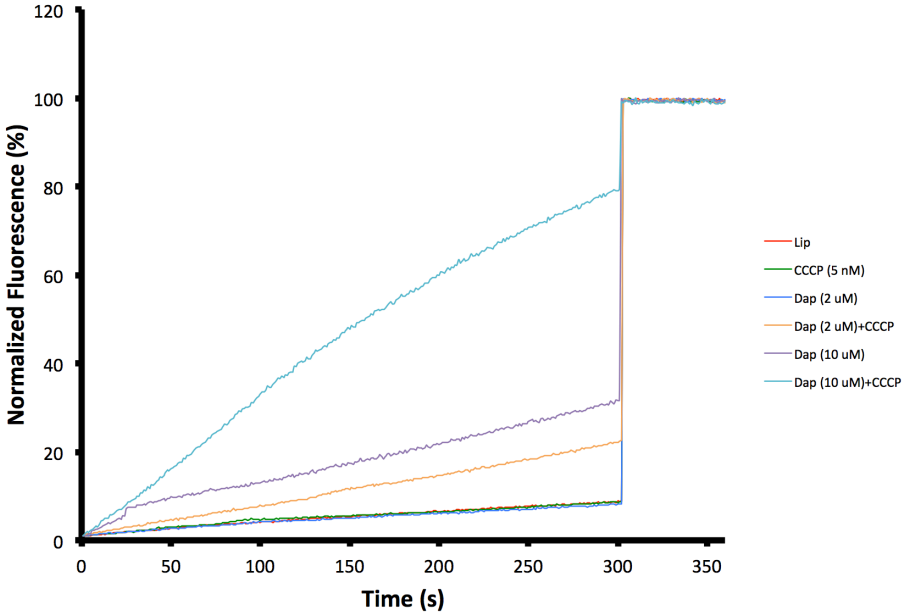

Figure A14. Permeabilization results of Dap on 1/9/10 DOPC/DMPC/DMPG (molar ratio 1/1, PC to PG, 250 μM). The experiment was run with conditions as described in Figure A11. Assays Assays were run in duplicates, at 30°C.

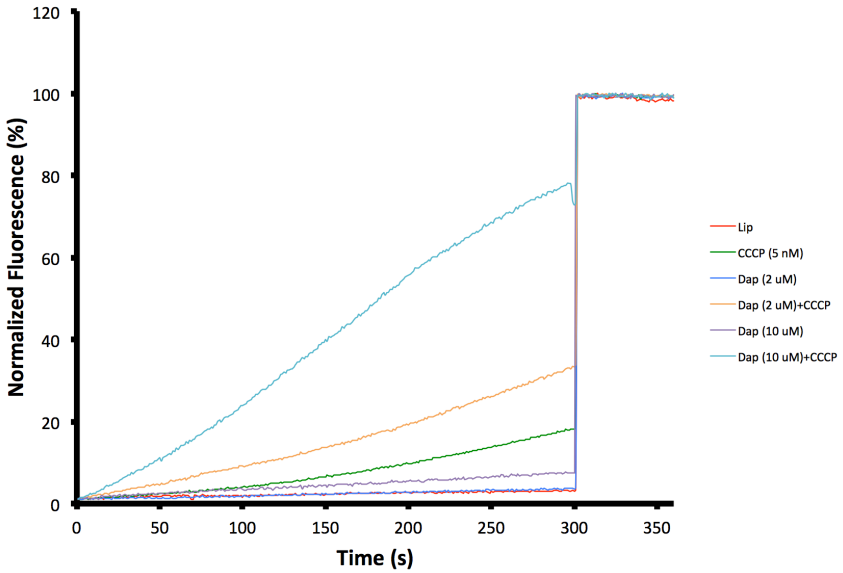

Figure A15. Permeabilization results of Dap on 1/49/50 DOPC/DMPC/DMPG (molar ratio 1/1, PC to PG, 250 μM). The experiment was run with conditions as described in Figure A11. Assays Assays were run in duplicates, at 30°C.

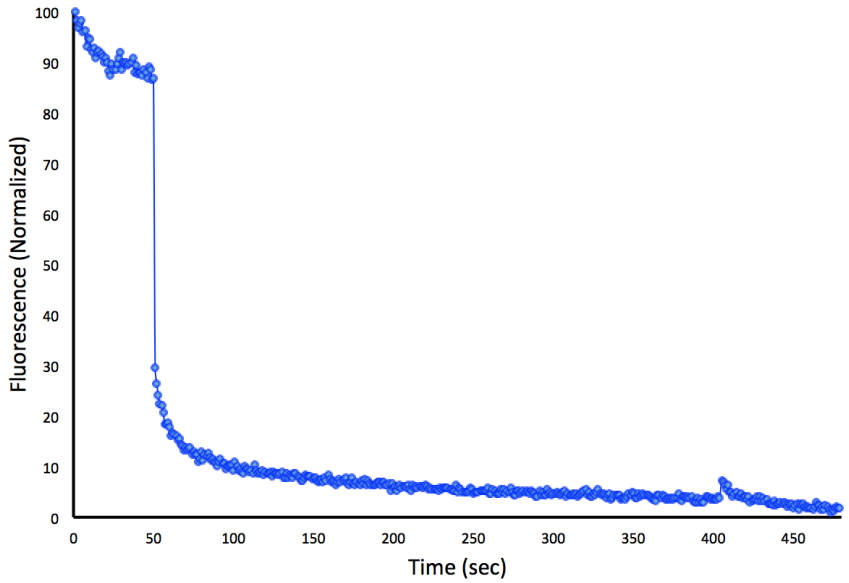

Figure A16. Preliminary translocation results of NBD-Dap across 1/4/5 TMCL/DMPC/DMPG LUVs. The LUVs were incubated with a 2:1 mixture of Dap to NBD-Dap (1 μM total), respectively, at 25 mM calcium. At 50 seconds, dithionite (1 mM) was added to quench the NBD-Dap exposed to the external buffer. At 400 seconds, Triton X-100 (0.1%) was added to solubilize the membrane, exposing any NBD-Dap contained in inner leaflet that has not yet been quenched. NBD fluorescence was measured over time (excitation wavelength, 478 nm; emission wavelength, 520 nm; the assay is a singlet trial). The results presented here show that the TMCL containing membranes mimic the data with a 1/1 DOPC/DOPG composition.

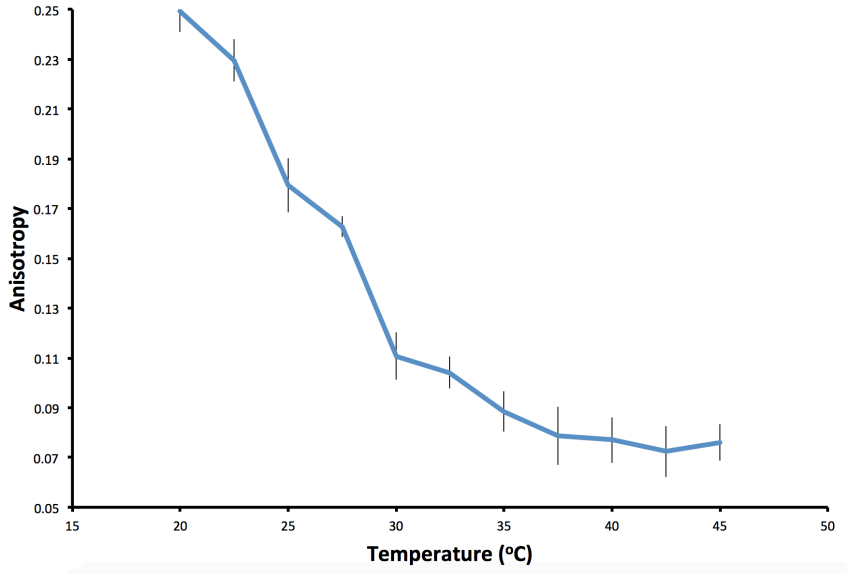

Figure A17. Anisotropy results for 1/4/5 TMCL/DMPC/DMPG LUVs. The experimental protocol was done similar to Thulborn, *et al.*[208] Diphenylhexatriene (DPH, 10 μM) was added to liposomes (250 μM) and the anisotropy monitored over varying temperatures. Each temperature was allowed to stabilize for 10 minutes before measuring sample. The results were repeated in triplicates, with standard deviations shown. From data, the T_m was determined to be ~27°C (mid point of asymptote).